



TECHNISCHE UNIVERSITÄT MÜNCHEN

Wissenschaftszentrum Weihenstephan für Ernährung, Landnutzung und Umwelt

Lehrstuhl für Phytopathologie

Role of barley NADPH oxidases and carbohydrate metabolism enzymes in barley-powdery mildew interactions

Denise Pereira Torres

Vollständiger Abdruck der von der Fakultät Wissenschaftszentrum Weihenstephan für Ernährung, Landnutzung und Umwelt der Technischen Universität München zur Erlangung des akademischen Grades eines

Doktors der Naturwissenschaften (Dr. rer. nat.)

genehmigten Dissertation.

Vorsitzender:

Prof. Dr. Jörg Durner

Prüfer der Dissertation:

1. Prof. Dr. Ralph Hüchelhoven

2. Prof. Dr. Wolfgang Oßwald

Die Dissertation wurde am 17.10.2017 bei der Technischen Universität München eingereicht und durch die Fakultät Wissenschaftszentrum Weihenstephan für Ernährung, Landnutzung und Umwelt am 18.12.2017 angenommen.

PUBLICATIONS

Parts of this work have already been published:

Torres, D.P., Proels, R.K., Schempp, H., and Hüchelhoven, R. (2017) Silencing of RBOHF2 causes leaf age-dependent accelerated senescence, salicylic acid accumulation and powdery mildew resistance in barley. *Molecular Plant-Pathogen Interactions*. DOI: 10.1094/MPMI-04-17-0088-R.

TABLE OF CONTENTS

PUBLICATIONS	i
TABLE OF CONTENTS	ii
ABBREVIATIONS	vi
SUMMARY	viii
ZUSAMMENFASSUNG	ix
1 INTRODUCTION	1
1.1 Plant-pathogen interactions	1
1.2 Preformed defence mechanisms	2
1.3 Pathogen-induced immunity	2
1.3.1 Localized plant immunity	3
1.3.2 Systemic plant immunity	4
1.4 Developmental-induced immunity	4
1.5 Plant NADPH oxidases and immunity	5
1.5.1 Regulation of plant NADPH oxidase during immunity.....	6
1.6 Carbohydrate metabolism and plant defence responses.....	7
1.6.1 Sucrose translocation from photosynthetic active source cells to infected cells .	8
1.6.2 Fates of apoplastic sucrose	8
1.6.3 Fate of cytosolic sugars	9
1.7 Barley-powdery mildew pathosystem and host susceptibility factors	10
1.7.1 Mlo and BI-1 as host susceptibility factors against <i>Bgh</i>	11
1.7.2 LSD1-like proteins.....	12
1.7.3 Other susceptibility factors.....	12
1.8 Objectives.....	14
2 MATERIAL AND METHODS.....	16
2.1 Plant material	16
2.2 Photosynthetic pigment content analysis	16
2.3 Pathogens and inoculation	17
2.3.1 <i>Blumeria graminis</i> f. sp. <i>hordei</i>	17
2.3.2 <i>Fusarium culmorum</i>	17
2.3.3 <i>Bipolaris sorokiniana</i>	17
2.4 Assessment of the powdery mildew infection.....	18
2.4.1 Cytological analysis	18
2.4.2 Powdery mildew disease progression	18

2.5	Gene expression studies	19
2.5.1	Total RNA isolation	19
2.5.2	cDNA synthesis.....	19
2.5.3	Reverse transcription semi-quantitative real-time PCR (RT-sqPCR).....	20
2.5.4	Reverse transcription quantitative real-time PCR (RT-qPCR).....	21
2.6	Salicylic acid quantification	22
2.7	Assessment of the leaf spot blotch disease	23
2.8	Assessment of <i>Fusarium</i> infection.....	23
2.8.1	Extraction of genomic DNA from barley leaves.....	23
2.8.2	Quantification of <i>Fusarium</i> DNA in barley leaves	24
2.9	Sequence alignment and phylogenetic analysis	24
2.10	Transient transformation of barley cells.....	24
2.10.1	Generation of the TIGS vector constructs	25
2.10.2	Generation of overexpression vector constructs.....	26
2.10.3	Transformation of <i>E. coli</i> XL1-blue cells.....	27
2.10.4	Plasmid preparation and selection of positive clones	27
2.10.5	Bioballistic bombardment.....	28
2.10.6	Gene function assessment	28
2.10.7	“Sink” metabolism induction.....	29
2.11	Data analyses	29
3	RESULTS.....	30
3.1	Silencing of <i>HvRBOHF</i> genes leads to premature leaf senescence	30
3.1.1	Characterization of spontaneous cell death in <i>HvRBOHF2</i> KD plants	30
3.1.2	Content of photosynthesis-related pigments in <i>HvRBOHF2</i> KD plants.....	32
3.2	Susceptibility to <i>Bgh</i> in <i>HvRBOHF2</i> KD lines depends on leaf age	36
3.2.1	The <i>HvRBOHF</i> clade modulates susceptibility to penetration by <i>Bgh</i> in a leaf-age and leaf-section dependent manner.....	36
3.2.2	Pre-invasion defence responses in <i>HvRBOHF2</i> KD plants	39
3.2.3	ROS production and pathogen-induced cell death in <i>HvRBOHF2</i> KD plants ...	41
3.2.4	<i>Bgh</i> colonization is also affected in <i>HvRBOHF2</i> KD lines	43
3.3	Differentially expressed genes in <i>HvRBOHF2</i> KD plants during barley powdery mildew interaction.....	48
3.3.1	Expression of <i>HvRBOHF</i> genes	48
3.3.2	Expression of senescence markers and cell death regulatory genes	50
3.3.3	Expression of genes related to carbohydrate catabolism	53
3.3.4	Expression of <i>PR</i> genes	54

3.3.5	SA contents in leaves of <i>HvRBOHF2</i> KD plants	56
3.4	Susceptibility of <i>HvRBOHF2</i> KD plants to other fungal pathogens	58
3.4.1	Susceptibility to <i>B. sorokiniana</i>	58
3.4.2	Susceptibility to <i>F. culmorum</i>	60
3.5	Role of barley NADPH oxidase RBOHD in the susceptibility to <i>Bgh</i>	62
3.5.1	Characterisation of a new <i>HvRBOH</i> gene.....	62
3.5.2	Phylogenetic analysis	64
3.5.3	<i>HvRBOHD</i> expression analysis.....	66
3.5.4	Transient knock-down of <i>HvRBOHD</i> limits penetration by <i>Bgh</i>	67
3.6	Role of carbohydrate metabolism enzymes in the susceptibility to <i>Bgh</i>	69
3.6.1	Expression analysis	69
3.6.2	Transient knock-down of <i>HvCwINV1</i> supports penetration by <i>Bgh</i> in sucrose-treated barley leaves	70
3.6.3	Transient overexpression of <i>HvINVNH1</i> limits penetration by <i>Bgh</i>	72
3.6.4	Transient silencing of <i>HvG6PDH</i> genes does not influence susceptibility to penetration by <i>Bgh</i>	72
4	DISCUSSION	74
4.1	<i>HvRBOHF2</i> KD plants displayed de-regulated PCD processes.....	74
4.1.1	Expression of putative ROS-responsive genes is up-regulated in <i>HvRBOHF2</i> KD plants.....	75
4.1.2	Expression of a <i>LSD1-like</i> gene is down-regulated in <i>HvRBOHF2</i> KD plants ..	76
4.1.3	Expression of <i>ATG</i> genes and <i>Mlo</i> are not affected in KD plants	77
4.2	<i>HvRBOHF2</i> KD leaf age-dependent susceptibility to <i>Bgh</i>	78
4.2.1	Pathogen-triggered ROS burst is affected in <i>HvRBOHF2</i> KD plants	79
4.2.2	Silencing of <i>HvRBOHF</i> genes affect the expression of defence-related and pathogen-induced genes	81
4.2.3	<i>HvRBOHF2</i> KD plants are characterized by an increased SA level.....	82
4.3	Silencing of <i>HvRBOHF</i> genes affects susceptibility to hemibiotrophic fungi.....	83
4.3.1	<i>HvRBOHF2</i> KD plants are less susceptible to spot blotch	84
4.3.2	Susceptibility to <i>F. culmorum</i> is also leaf age-dependent.....	85
4.4	Role of the barley NADPH oxidases RBOHF in susceptibility to pathogens.....	86
4.5	<i>HvRBOHD</i> contributes to penetration resistance towards <i>Bgh</i>	87
4.5.1	<i>HvRBOHD</i> , a previously undescribed barley NADPH oxidase.....	87
4.5.2	<i>HvRBOHD</i> is a possible resistance factor to <i>Bgh</i>	88
4.6	Role of carbohydrate metabolism genes in resistance to <i>Bgh</i>	88

4.6.1	HvCwINV1 is a putative resistance factor to <i>Bgh</i>	89
4.6.2	INVNH1 is another putative resistance factor to <i>Bgh</i>	90
4.7	G6PDH enzymes seems not be involved in modulation of susceptibility to <i>Bgh</i>	91
4.8	Hypothetical model for the role of HvrBOHs and carbohydrate metabolism enzymes in defence responses against <i>Bgh</i>	92
5	REFERENCES	95
6	SUPPLEMENTARY MATERIAL	111
	ACKNOWLEDGEMENTS	132
	<i>CURRICULUM VITAE</i>	133

ABBREVIATIONS

AA	amino acid
ABA	abscisic acid
ADH	alcohol dehydrogenase
APR	adult plant-resistance
AZ	azygous
BC	backcross
<i>Bgh</i>	<i>Blumeria graminis</i> f.sp. <i>hordei</i>
<i>Bs</i>	<i>Bipolaris sorokiniana</i>
Car	carotenoids
Chl	chlorophyll
CI	confidence interval
CK	cytokinins
CPKs	calcium-dependent protein kinases
CSA	conjugated salicylic acid
cv	cultivar
cw	cell wall
CwINV	cell wall invertase
DAB	3,3-diaminobenzidine
dai	days after inoculation
DAMPs	damage associated molecular patterns
das	days after sowing
DHBA	2,3-dihydroxybenzoic acid
ds	double strand
ET	ethylene
ETI	effector-triggered immunity
<i>Fc</i>	<i>Fusarium culmorum</i>
<i>Fg</i>	<i>Fusarium graminearum</i>
FHB	Fusarium head blight
FSA	free-salicylic acid
G6PDH	glucose-6-phosphate dehydrogenase
GFP	green fluorescent protein
hai	hours after inoculation
HR	hypersensitive response
INVNH	invertase inhibitor

ISR	induced systemic resistance
JA	jasmonic acid
KD	knock-down
LB	Luria-Bertani
LMM	lesion-mimic mutants
MAMP	microbe-associated molecular pattern
MLO	mildew resistance locus O
Mub1	monoubiquitin-long-tail fusion 1
OPPP	oxidative pentose phosphate pathway
PA	phosphatidic acid
PCD	programmed cell death
PR	pathogenesis-related
PRR	pattern recognition receptors
<i>Pst</i>	<i>Pseudomonas syringae</i> pv. <i>tomato</i>
PTI	pattern-triggered immunity
qPCR	quantitative PCR
RBOH	Respiratory burst oxidase homologues
RNAi	RNA interference
ROS	reactive oxygen species
RT	reverse transcription
SA	salicylic acid
sqPCR	semi-quantitative PCR
SUS	sucrose synthase
TIGS	transient induced gene silencing
TM	transmembrane
VINV	vacuolar invertase
WT	wild-type

SUMMARY

RBOH (RESPIRATORY BURST OXIDASE HOMOLOGUES)-type NADPH oxidases are prominent sources of superoxide radical anions in plants. RBOHs have a role in developmental processes and in response to environmental challenges, including defence against phytopathogens. Barley *HvRBOHF2* has diverse reported functions in interaction with the biotrophic barley powdery mildew fungus *Blumeria graminis* f.sp. *hordei*. Here I analysed in detail, a transgene-induced leaf age-related resistance phenotype to this pathogen in *HvRBOHF2*-silenced barley plants. This revealed enhanced susceptibility to fungal penetration of young *HvRBOHF2*-silenced leaf tissue but strongly reduced susceptibility of older leaves when compared to controls. Loss of susceptibility in old *HvRBOHF2*-silenced leaves was associated with spontaneous leaf tip necrosis and constitutively elevated levels of free and conjugated salicylic acid. Moreover, these leaves showed altered expression of cell death regulators and more strongly expressed pathogenesis-related genes both constitutively and during interaction with *B. graminis* f.sp. *hordei*. On the other hand, *HvRBOHF2*-silenced plants also displayed a tendency for leaf age-related susceptibility to development of the hemibiotrophic fungus *Fusarium culmorum*. Relative amount of *Fusarium* DNA was higher in old leaves of *HvRBOHF2*-silenced plants than in azygous controls whereas in young leaves it tended to be smaller. Besides that, both old and young leaves of *HvRBOHF2*-silenced plants were less susceptible to foliar spot blotch disease caused by the fungus *Bipolaris sorokiniana*, another hemibiotrophic pathogen. Additionally, a recently identified barley NADPH oxidase, relatively closely related to the *Arabidopsis thaliana* RBOHD, has also a function in resistance to penetration by *B. graminis* f.sp. *hordei*. The expression of *HvRBOHD* was up-regulated in infected barley leaves. Furthermore, transient knock-down of this gene resulted in increased susceptibility to pathogen-penetration.

The activation of plant defence responses has a high metabolic demand and infection with pathogens leads to several alterations in barley primary metabolism. I found that the expression of genes encoding enzymes related to sucrose cleavage was altered in barley leaves infected with *B. graminis* f.sp. *hordei*. Transient knock-down of the barley *HvCwINV1* (CELL WALL INVERTASE 1), responsible for sucrose hydrolyses in the apoplast, resulted in increased susceptibility to *B. graminis* f.sp. *hordei* penetration, when leaves were supplied with sucrose. In the other hand, overexpression of *HvINVNH1* (INVERTASE INHIBITOR 1), a negative regulator of acidic invertases, resulted in reduced penetration.

Taken together, this study showed decisive roles of barley *HvRBOHD/F* type enzymes, *HvCwINV1* and *HvINVNH1* for the interaction outcome of barley and the parasitic fungus *B. graminis* f.sp. *hordei*.

ZUSAMMENFASSUNG

RBOH (RESPIRATORY BURST OXIDASE HOMOLOGUES)-typ NADPH Oxidasen sind eine wichtige Quelle für Superoxidradikalanionen in Pflanzen. RBOHs spielen eine Rolle in Entwicklungsprozessen und bei der pflanzlichen Antwort auf abiotische und biotische Umwelteinflüsse. Für *HvRBOHF2* wurden unterschiedliche Funktionen in der Interaktion von Gerste mit dem biotrophen Mehltaupilz *Blumeria graminis* f.sp. *hordei* berichtet. In der vorliegenden Arbeit beschreibe ich einen Transgen-induzierten, Blattalter-abhängigen Resistenzphänotyp in Gerstenpflanzen mit verringerter *HvRBOHF2* Expression. Blattmaterial dieser Pflanzen zeigte im Vergleich zu azygoten Kontrollpflanzen eine erhöhte Anfälligkeit für Penetration durch *B. graminis* f.sp. *hordei* in jungem Gewebe, und stark verringerte Anfälligkeit in älteren Blättern. Erhöhte Penetrationsresistenz in älteren Blättern war mit spontaner Nekrose in den Blattspitzen und konstitutiv erhöhten Konzentrationen an freier und konjugierter Salizylsäure verbunden. Außerdem konnten in diesem Gewebe Veränderungen in der Expression von Zelltod-Regulatoren beobachtet werden und Pathogen-induzierte Gene wurden sowohl konstitutiv als auch während der Interaktion mit *B. graminis* f.sp. *hordei* stärker exprimiert. Zusätzlich zeigten Pflanzen mit verringerter *HvRBOHF2*-Expression eine tendenziell verstärkte Besiedlung durch den hemibiotrophen Pilz *Fusarium culmorum* in Abhängigkeit vom Blattalter. Die relative Menge an DNA von *F. culmorum* war in älteren Blättern dieser Pflanzen erhöht und in jüngeren Blättern im Vergleich zu einer azygoten Kontrollpflanze eher verringert. Außerdem waren sowohl jüngere als auch ältere Blätter weniger anfällig gegenüber Blattflecken, die durch den hemibiotrophen Pilz *Bipolaris sorokiniana* verursacht wurden. Die Penetrationsresistenz gegen *B. graminis* f.sp. *hordei* war weiter beeinflusst durch transient verringerte Expression von *HvRBOHD*, einer weiteren Isoform von RBOHs, die auch in mit *B. graminis* f.sp. *hordei* infizierten Blättern hochreguliert war.

Die Aktivierung von pflanzlichen Verteidigungsreaktionen führt zu einem erhöhten Metabolismus von Kohlehydraten. Die vorliegende Arbeit zeigt, dass die Expression von Genen, die in Verbindung mit dem Abbau von Saccharose stehen, in *B. graminis* f.sp. *hordei*-infizierten Gerstenblättern verändert ist. Außerdem führt eine transiente Verringerung der Expression von *HvCwINV1* (CELL WALL INVERTASE 1) in Saccharose-versorgten Blättern zu erhöhter Penetrationsrate, während die Überexpression von *HvINVNH1* (INVERTASE INHIBITOR 1), einem negativen Regulator saurer Invertasen, zu einer verringerten Penetrationsrate führt.

Insgesamt zeigt diese Arbeit eine wichtige Funktion von *HvRBOHD/F*-Typ NADPH Oxidasen, *HvCwINV1* und *HvINVNH1* für den Interaktionsausgang von Gerste mit dem parasitischen Pilz *B. graminis* f.sp. *hordei*.

1 INTRODUCTION

1.1 Plant-pathogen interactions

During their lifetime, plants interact with a broad variety of microorganisms including bacteria, fungi, oomycetes and viruses. Some of those interactions are indirect, in which free-living microorganism indirectly modify the plant environment via alteration of nutrient cycling rates and partitioning. In direct interactions, microorganisms establish close symbiotic associations with the plant host. These can be categorised in mutualistic, when both organisms involved are benefited, or parasitic, when only the microorganism is benefited and the association is harmful for the plant (van der Heijden *et al.*, 2008; Schenk *et al.*, 2012).

Phytopathogens, parasitic microorganisms that cause disease in plants, have distinct lifestyles and modes of interaction with their host plants. Biotrophic pathogens like rust fungi, powdery mildew fungi and downy mildew oomycete are obligate parasites that rely on living plant tissue to survive and complete their life cycle. These microorganisms have a limited host range and establish a specific and elaborate association with their plant host (Spanu and Kamper, 2010). Biotrophic pathogens, for instance, often form so called haustoria inside of penetrated plant cells. These specialised infection structures are responsible for the uptake of nutrients from infected host cells and export of effector molecules into host cells (O'Connell and Panstruga, 2006). The genomes of this group of pathogens usually are adapted to rapid evolution as demonstrated by the large percentage of transposable elements in relation to genome size. In addition, the number of genes encoding putative elicitors of host immune responses or responsible for causing damage to the host (see below) like cell wall degrading enzymes is reduced. On the other hand, the number of genes encoding putative secreted effector proteins is increased (Baxter *et al.*, 2010; Spanu *et al.*, 2010; Duplessis *et al.*, 2011; McDowell, 2011). In contrast to biotrophic pathogens, necrotrophs such as the fungal pathogens *Botrytis cinerea* and *Sclerotinia sclerotiorum* have a less complex infection strategy. These pathogens do not have a specialized feeding structure. Instead, they secrete toxins and cell-wall degrading enzymes to kill host cells and release nutrients that can subsequently be taken up by the pathogen (Fernandez *et al.*, 2014). As most of those toxins are host non-specific, necrotrophic pathogens usually have a wide host range and are able to infect different plant tissues (Wen, 2013). In addition, hemibiotrophs are pathogens with a flexible lifestyle that show a combination of characteristics of both biotrophs and necrotrophs (Glazebrook, 2005). This class includes important phytopathogenic fungi like *Magnaporthe oryzae*, which is the causal agent of the rice blast disease and species of the economically important genus *Colletotrichum*. In addition, Kraepiel and Barny (2016) include all gram-negative phytopathogenic bacteria in

this class. All the hemibiotrophs display a biotrophic phase at the beginning of the infection process, in which the host defence responses are avoided or suppressed and the pathogen spreads throughout the infected tissue. At some point, however, the pathogen switches to a necrotrophic phase and secretes toxins that induces host cell death (Koeck *et al.*, 2011).

Despite the extensive number of microorganism of diverse taxonomically groups and lifestyles that can act as putative phytopathogens, only a small fraction of these intruders successfully invade a plant host and cause disease (Hückelhoven, 2005). Both susceptible and resistant plants are able to react to an attempted infection. Thus, the speed and intensity at which the immune responses are activated determines the outcome of the plant-pathogen interactions (Yang *et al.*, 1997). Resistant plants can prevent disease or limit the extent of infection employing a large variety of different preformed or induced defence mechanisms.

1.2 Preformed defence mechanisms

Plants display several pre-existing barriers that slow down or prevent entrance and spreading of a potential pathogen. These constitutive or preformed defences comprise physical protective barriers like wax and cuticle layer in leaves and casparian strips in roots. They also comprise secondary metabolites (phytoanticipins) such as glucosinolates and flavonoids that are produced by healthy plants as part of their normal metabolism and show antimicrobial properties (Bednarek and Osbourn, 2009; De Coninck *et al.*, 2015).

1.3 Pathogen-induced immunity

Detection of pathogens by the plant cell activates immune responses. This comprises two distinct defence strategies, pattern-triggered immunity (PTI) and effector-triggered immunity (ETI; formerly called race-specific resistance following the gene-for-gene model) (Dangl *et al.*, 2013). PTI is a broad spectrum defence mechanism that is crucial to plant defence responses to microbes but also against nematodes, insect herbivores and parasitic plants (Gust *et al.*, 2017). It involves recognition of specific motifs by plant cell surface localised transmembrane receptor-like kinases or receptor-like proteins, called pattern recognition receptors (PRRs). These motifs are conserved structural components of microorganisms (microbe-associated molecular patterns, MAMPs), nematodes or parasitic plants. These immunogenic molecular patterns are usually essential for the pathogen fitness and survival, like for example a peptide of the bacterial flagella, fungal chitin and ascarosides from nematodes (Ranf, 2017). Moreover, plants can perceive endogenous molecules, which are passively released upon host damage (damage-associated molecular patterns, DAMPs) like cutin monomers, extracellular nucleotides and oligogalacturonides. As well plants can perceive signalling peptides (phytocytokines) like plant elicitor peptides (Pep) and rapid

alkalinisation factors (RALFs) that are processed and released in response to tissue damage and other stimuli (Gust *et al.*, 2017). In order to ward off the first layer of plant immunity, adapted pathogens secrete virulence factors, known as effectors, which specifically reprogram plant host cells to avoid or suppress PTI mediated defence responses. In turn, plants have evolved resistance proteins, mostly cytoplasmic nucleotide-binding/leucine-rich-repeat receptors, which are able to perceive these effectors and activate ETI, a highly specific and robust defence response that unlike PTI is limited to a certain species, race or strain of the pathogen (Thomma *et al.*, 2011; Cui *et al.*, 2015). PTI and ETI share many signalling components and together contribute to plant immunity through the activation of defence responses that can additionally result in a localized acquired resistance or systemic plant immunity (Tsuda and Katagiri, 2010).

1.3.1 Localized plant immunity

Localized or local acquired resistance occurs at sites adjacent to an infection attempt and contributes to prevention of microorganism spreading and reduction of disease severity. It comprises a complex defence signalling which includes early defence responses such as reactive oxygen species (ROS) production, elevation of cytosolic calcium ions levels, mitogen-activated protein kinase (MAPK) activation and transcriptional reprogramming. Additionally, localized acquired resistance includes later responses like phytohormones biosynthesis and signalling, metabolic adjustment, and accumulation of phytoalexins. Phytoalexins, in contrast to phytoanticipins, are antimicrobial compounds produced after pathogen recognition (Reimer-Michalski and Conrath, 2016). Although some of these responses can be stronger and/or prolonged in ETI, they are activated in both PTI and ETI pathways (Katagiri and Tsuda, 2010; Cui *et al.*, 2015). For instance, ROS production is triggered by both branches of the plant immune system. However, while PTI results in a monophasic, transient but robust oxidative burst, effectors can trigger a biphasic, stronger and prolonged ROS burst (Torres, 2010; Tsuda and Katagiri, 2010). Localized defence responses also include the hypersensitive response (HR), a rapid and localized pathogen-induced cell death at the site of attempted infection that prevents the spread of the pathogen in the plant tissue. HR is a hallmark of ETI; however, MAMPs from several pathogens and non-pathogens microbes are also able to induce HR in plants (Thomma *et al.*, 2011; Spoel and Dong, 2012). Flagellin from *Pseudomonas syringae* pathovars, a typical bacterial MAMP, triggers HR in nonhost plants like tomato and tobacco (Taguchi *et al.*, 2003). Also, the cell wall glycoprotein CBEL (CELLULOSE-BINDING ELICITOR LECTIN), a MAMP from the oomycete *Phytophthora nicotianae* induces HR-like lesions in both host (tobacco) and nonhost (*Arabidopsis thaliana*) plant species (Khatib *et al.*, 2004).

1.3.2 Systemic plant immunity

Recognition of stress stimulus (e.g. pathogen infection or wounding) by the plant immune system can also trigger immunity in tissues distant from the initial recognition site. For instance, systemic acquired resistance (SAR) and induced systemic resistance (ISR) promotes an increased resistance against reinfection or infection of a broad spectrum of pathogens, respectively, in the whole plant that last from few days to the lifetime of a plant (Reimer-Michalski and Conrath, 2016). SAR is activated by phytopathogens and depends on the systemic accumulation of the lysine catabolite pipecolic acid and the phytohormone salicylic acid (SA). SA is a key signalling component in several physiological and biochemical plant processes, traditionally associated with defence responses against biotrophic pathogens (Glazebrook, 2005; Vlot *et al.*, 2009; Návarová *et al.*, 2012; Spoel and Dong, 2012). In *Arabidopsis*, SAR leads to transcriptional preactivation of genes encoding PRRs, R proteins, MAPK signalling components and transcription factors which are involved in defence signalling (Bernsdorff *et al.*, 2016). Additionally, SAR results in SA-dependent and SA-independent expression of a large number of PATHOGENESIS-RELATED (PR) genes, encoding proteins with antimicrobial activity, and other defence-related genes (Spoel and Dong, 2012; Bernsdorff *et al.*, 2016). On the other hand, ISR is elicited by beneficial root-colonizing growth/yield-promoting bacteria and fungi and depends on the phytohormones ethylene (ET) and jasmonic acid (JA), usually associated with defence against necrotrophic pathogens and insects (Glazebrook, 2005; Reimer-Michalski and Conrath, 2016).

1.4 Developmental-induced immunity

Some elements of plant defence signalling are expressed or activated only in a certain stage of plant development and are therefore triggered by a developmental clue and not by microbe recognition. As a result, the plant or a plant organ become more susceptible (mature tissue susceptibility) or more resistant (adult plant resistance, APR) to a certain pathogen with the progression of the age. Mature tissue susceptibility is a poorly characterized phenomenon and was recently described in the pathosystem barley-*Phytophthora palmivora* (Le Fevre *et al.*, 2016). On the other hand, APR, also known as developmental resistance or age-related resistance, have been described for several plant species (Whalen, 2005; Develey-Riviere and Galiana, 2007). For instance, mature *Arabidopsis* plants are more resistant to the bacteria *Pseudomonas syringae* pv *tomato* (*Pst*) and to the oomycete *Hyaloperonospora arabidopsidis* than young plants (Kus, 2002; Rusterucci *et al.*, 2005). Most importantly, this resistance is related to an increase in the ability of old plants to accumulate SA (Kus, 2002; Carviel *et al.*, 2009; Carviel *et al.*, 2014). In young plants, SA accumulation is

inhibited by the *P. syringae* phytotoxin coronatine. However, in old plants, SHORT VEGETATIVE PHASE (AtSVP), a transcription factor that negatively regulates floral transition, mitigates coronatine-mediated suppression of SA (Carviel *et al.*, 2014). Additionally, the SA derivative 2,3-dihydroxybenzoic acid (DHBA) accumulates in senescent leaves of Arabidopsis (Zhang *et al.*, 2013). Carella *et al.* (2014) suggested that like SA, DHBA could act as an antimicrobial agent in the intercellular space of the Arabidopsis plants.

1.5 Plant NADPH oxidases and immunity

ROS are important signalling molecules that are naturally produced as a consequence of the aerobic metabolism or deliberately generated by enzymatic complexes as part of plant responses to environmental constraints. Plasma membrane-localized NADPH oxidases (RESPIRATORY BURST OXIDASE HOMOLOGUES, RBOHs) constitute a protein family which are prominent sources of apoplastic ROS during plant development and in several biotic and abiotic immune responses (Torres *et al.*, 1998; Mittler *et al.*, 2011). RBOHs have an important role during plant-pathogen interactions. AtRBOHF is a crucial modulator of defence-related metabolism upon pathogen infection and is involved, together with AtRBOHD, in the regulation of basal resistance and HR (Torres *et al.*, 2002; Chaouch *et al.*, 2012; Siddique *et al.*, 2014; Morales *et al.*, 2016). AtRBOHD is the major ROS-generating enzyme that operates in PTI and in systemic stress signalling (Miller *et al.*, 2009; Dubiella *et al.*, 2013). For instance, AtRBOHD functions in abiotic long-distance signalling in response to stimuli such as wounding, heat, cold and salinity (Miller *et al.*, 2009). OsRBOHA is required for HR induction in rice and both OsRBOHA and OsRBOHE are involved in the ROS production in response to a specific elicitor of an avirulent strain of the bacterial pathogen *Acidovorax avenae* (Yoshie *et al.*, 2005). The levels of the wheat *TaRBOHD* and *TaRBOHF* genes are up-regulated upon challenge with the rust fungus *Puccinia triticina* and in the backcross line *TcLR26* the resistance-related oxidative burst response is sensitive to a chemical inhibitor of NADPH oxidases (Dmochowska-Boguta *et al.*, 2013). The barley gene *HvRBOHF2*, a close homologue of Arabidopsis *AtRBOHF* and rice *OsRBOHA*, is involved in defence responses against phytopathogens. The expression of *HvRBOHF2* is enhanced in response to infection by both necrotrophic and biotrophic fungi (Lightfoot *et al.*, 2008).

Like other NADPH oxidases, plant RBOHs possess a core C-terminal region consisting of FAD- and NADPH-binding sites, six transmembrane domains and a functional oxidase domain responsible for superoxide generation. Besides, plant RBOHs have an extended N-terminal region that contains multiple regulatory motifs involved in the posttranslational regulation of their activity (Suzuki *et al.*, 2011). Regulatory elements include ubiquitous calcium-dependent regulatory elements such as two calcium-binding EF hand motifs found in

all described plant RBOHs. Other motifs are for example phosphorylation sites that are distinctly regulated in each RBOH isoform and a phosphatidic acid (PA) binding site described in AtRBOHD and AtRBOHF (Marino *et al.*, 2012; Kadota *et al.*, 2015). Additionally, regulatory elements can include the flanking region of the coiled-coil region at the N-terminus of OsRBOHB, which is responsible for the direct interaction of this protein with the plant RHO-like GTPase (RAC/ROPs) OsRac1 (Wong *et al.*, 2007; Oda *et al.*, 2010; Kosami *et al.*, 2014).

1.5.1 Regulation of plant NADPH oxidase during immunity

Posttranslational regulation of plant NADPH oxidases upon pathogen recognition is well described for AtRBOHD, the main ROS-producing enzyme during both PTI and ETI in Arabidopsis (Kadota *et al.*, 2015). Plant PRRs can be grouped according to structural motifs in their extracellular domains. For instance, receptors such as FLS2 (FLAGELLIN SENSING 2) and EFR (ELONGATION FACTOR THERMO UNSTABLE RECEPTOR) have a leucine-rich repeat (LRR)-type extracellular domain. These receptors perceive proteinaceous elicitors like flg22 or elf18, which are conserved motifs from bacterial flagella and elongation factor thermo unstable (EF-tu), respectively. Extracellular lysine motifs (LysM) like those displayed by LYK5 (LysM-CONTAINING RECEPTOR-LIKE KINASE 5) perceive carbohydrate-based elicitors as for example chitin. On the other hand, LORE (LIPOOLIGOSACCHARIDE-SPECIFIC REDUCED ELICITATION) receptor, crucial for the perception of lipopolysaccharides from some gram negative bacteria, has a lectin-type extracellular domain (Ranf, 2017).

These different classes of PRRs recruit distinct co-receptors to activate immune signalling. For example, the LRR-type PRRs FLS2 and EFR recruit the co-receptor BRI1-ASSOCIATED RECEPTOR KINASE 1 (BAK1). Upon MAMP perception, BAK1 associates with FLS2 and phosphorylates BOTRYTIS-INDUCED KINASE 1 (BIK1), an Arabidopsis receptor-like cytoplasmic kinase from subfamily VII that also interacts with LysM-type PRRs (Silva Couto and Zipfel, 2016). BIK1 subsequently can phosphorylate both BAK1 and FLS2, dissociate from the PRR complex and directly phosphorylate AtRBOHD at the positions Ser39, Ser339 and Ser343 (Kadota *et al.*, 2014; Li *et al.*, 2014). PRR complex activation also result in elevation of cytosolic calcium ions levels. Phosphorylation of AtRBOHD possibly enhanced its affinity to calcium ions binding to the EF-hand motifs and/or sensitivity to subsequent phosphorylation by Ca²⁺-dependent protein kinases (CPKs) at sites Ser133, Ser148 and Ser163 (Fig. 1) (Kadota *et al.*, 2015). Besides BIK1, its closest paralog PBS1 LIKE KINASE (PBL1) is also able to phosphorylate AtRBOHD. Furthermore, fungal chitin and Pep1 perception also seems to lead to AtRBOHD phosphorylation since phospho-dead mutations

in BIK1-mediated sites abolished the ROS burst triggered by these elicitors (Kadota *et al.*, 2014).

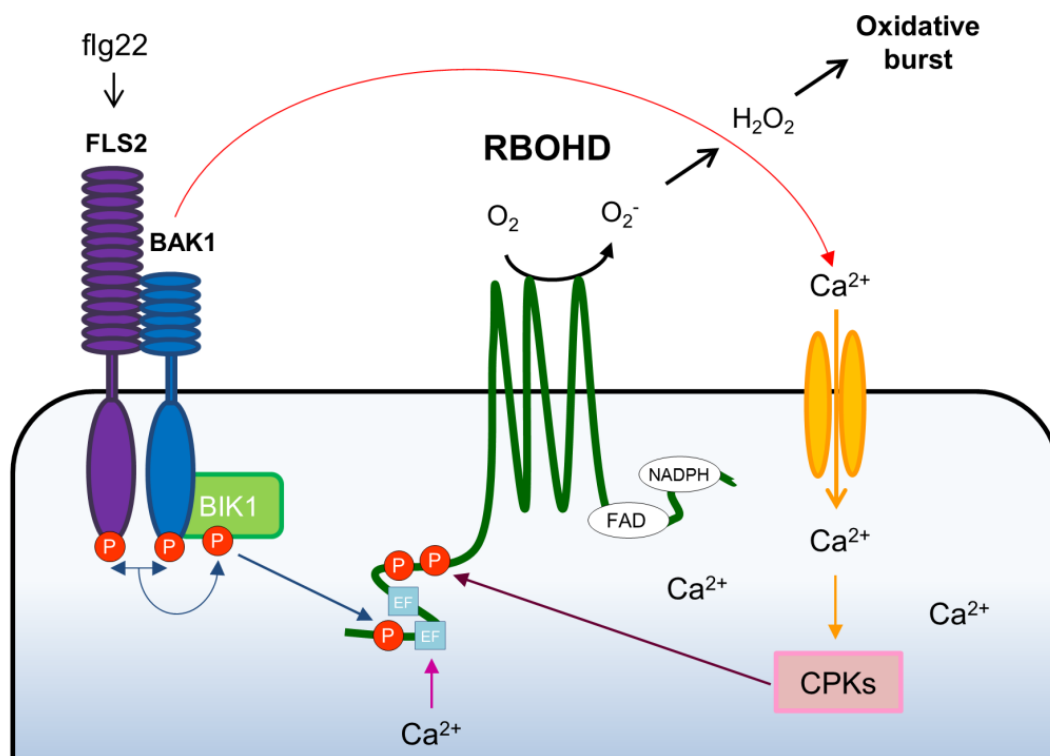


Figure 1: Regulation of RBOHD during PTI in Arabidopsis. Perception of flg22 by FLS2, activates the PRR complex which directly phosphorylates and activates BIK1. Besides, PRR complex activation results in elevation of cytosolic calcium ion levels. Phosphorylated BIK1 dissociates from the PRR complex and directly phosphorylates AtRBOHD at specific sites in a mechanism independent of calcium ions. Additionally, RBOH is activated by Ca²⁺-based regulation, such as Ca²⁺ binding to the EF-hand motif and phosphorylation by Ca²⁺-dependent protein kinases (CPKs). Modified from Kadota *et al.* (2015).

1.6 Carbohydrate metabolism and plant defence responses

The plant defence responses have a high metabolic demand for carbohydrates. Carbohydrates are sources of carbon skeletons, reducing power and energy for biosynthesis of new molecules such as SA, phytoalexins and callose (Bolton, 2009). Moreover, carbohydrates can act as signalling molecule and are involved in the up-regulation of *PR* genes expression and accumulation of anthocyanins, a flavonoid pigment with UV-protecting properties and antimicrobial activity (Bolouri Moghaddam and Van den Ende, 2012). Biotrophic pathogens completely rely on the host for acquisition of sugars (Fernandez *et al.*, 2014). Thus, plants have to regulate metabolic processes in a way that the carbohydrate availability will be restricted for pathogens but sufficient to orchestrate defence responses.

1.6.1 Sucrose translocation from photosynthetic active source cells to infected cells

Sucrose is a major end product of photosynthesis and a key source of carbon for growth, development and defence (Ruan, 2014). In healthy tissues, sucrose is produced in mesophyll cells of photosynthetic tissues, loading to phloem and then exported to different heterotrophic tissues. Although sucrose can move via plasmodesmata between some cells, not all cells are connected by open plasmodesmata, especially at the interface of some organ/tissues, and intercellular transport occurs through the apoplast. Apoplastic transport of sucrose requires at least two types of transporters, efflux carriers and sugar transporters. Efflux carriers such as SUGARS WILL EVENTUALLY BE EXPORTED TRANSPORTERS (SWEET), sucrose effluxer, are responsible for secreting the sugars from cells to the apoplastic space, while sugar transporters are responsible for the reuptake of sugars into adjacent cells (Chen, 2014). In infected leaf tissues, sucrose may be transported from mesophyll cells to the apoplastic space via SWEET sucrose effluxer or directly to the cytoplasm of infected cell via plasmodesmata (Ruan, 2014).

1.6.2 Fates of apoplastic sucrose

In plants, sucrose is cleaved by sucrose synthase (SUS) and invertases. SUS activity is reversible and yields fructose and UDP-glucose. On the contrary, invertase activity is irreversible and produces fructose and glucose (Koch, 2004). Plants possess three types of invertase isoenzymes, vacuolar (VINV), neutral/alkaline and cell wall bound (CwINV) invertases (see Tauzin and Giardina (2014) for a review). CwINVs are responsible for the cleavage of sucrose in the apoplastic space. Therefore, they play a crucial role in metabolic adjustment and sugar signalling during plant-pathogens interactions and in response to other stress stimuli (Roitsch *et al.*, 2003). Phytopathogens of different lifestyles can induce the expression/activity of CwINV in different plant species. As previously mentioned, an increase in hexose levels in infected cells could benefit both pathogens and plant defence mechanisms. Yet, there is increasing evidence suggesting a role of the CwINV in supporting plant defence responses (Proels and Hüchelhoven, 2014; Tauzin and Giardina, 2014).

Beside transcriptional regulation stimulated by several biotic and abiotic stresses, the activity of CwINV is also regulated post-translationally by proteinaceous invertase inhibitors, INVNHs (Proels and Hüchelhoven, 2014). Loss of function of the Arabidopsis CELL WALL/VACUOLAR INHIBITOR OF FRUCTOSIDASE (AtC/VIF1) results in increased CwINV activity and enhanced hexoses levels in germinating seeds. On the other hand, overexpression of AtC/VIF1 results in a reduced activity of CwINV and a delay in seed germination (Su *et al.*, 2016). In addition, the expression and activity of AtC/VIF2 is down-

regulated upon infection with *Pst* or *B. cinerea* while the expression and activity of AtCwINV1 is enhanced. Therefore, it has been suggested that a high AtC/VIF2 activity depressed the CwINV activity in healthy photosynthetic leaves of Arabidopsis while in infected leaves the activity of CwINV is derepressed (Bonfig *et al.*, 2010; Veillet *et al.*, 2016).

1.6.3 Fate of cytosolic sugars

In the cytosol, sucrose can be degraded by SUS or intracellular (neutral/alkaline and vacuolar) invertases. As previously mentioned SUS produces UDP-glucose, a precursor for the synthesis of cellulose and callose, which are important compounds of the plant defence response. Regarding intracellular invertases, some reports have been also implicating these enzymes in plant-pathogen interactions (Tauzin and Giardina, 2014). For instance, the expression and activity of AtCwINV1, AtVIN1 (VACUOLAR INVERTASE 1) and AtVIN2 is induced in Arabidopsis leaves inoculated with *B. cinerea* (Veillet *et al.*, 2016). Furthermore, Liu *et al.* (2015) demonstrated that the knock-down of the wheat cytoplasmic invertase *TaA/N-INV1* enhanced the resistance of the plants to *Puccinia striiformis* f. sp. *tritici*.

Cytosolic hexoses can be used in the glycolysis or enter in to the oxidative pentose phosphate pathway (OPPP) to generate energy and reducing power. OPPP is the source of carbon skeletons for the synthesis of nucleotides, aromatic amino acids, cell wall polymers and phytoalexins. In addition, OPPP is an important source of the reducing agent NADPH in non-photosynthetic cells (Kruger and von Schaewen, 2003). The OPPP pathway is activated during the oxidative burst triggered by the oomycete-derived elicitor cryptogein in tobacco cells and essentially regenerates the NADPH required for ROS production by plant RBOHs (Pugin *et al.*, 1997). OPPP reactions are mainly regulated and limited at the first step, which is catalyzed by glucose-6-phosphate dehydrogenase (G6PDH). Different isoforms of G6PDH occur in plants, and they can be localized in the cytosol, plastids or chloroplasts. The Arabidopsis genome encodes two cytosolic and four plastidic isoforms of G6PDH while barley has two cytosolic and two plastidic isoforms (Wakao and Benning, 2005; Cardi *et al.*, 2011). Interestingly, infection of tobacco leaves with *P. nicotianae* resulted in increased G6PDH activity in a resistant cultivar. This was also associated with an earlier and stronger induction in the expression of cytosolic isoforms of *G6PDH*. Additionally, inhibition of G6PDH activity in leaves of those resistant plants with the competitive inhibitor glucosamine 6-phosphate prevented both ROS production and HR (Scharte *et al.*, 2009). Thus, according to these authors, G6PDH activity is essential for the oxidative burst and therefore a crucial factor in plant defence responses.

1.7 Barley-powdery mildew pathosystem and host susceptibility factors

Powdery mildew fungi are worldwide-distributed ascomycete fungi of the *Erysiphales* order that cause disease in many economically relevant crops and ornamentals plants. Among powdery mildews, *Blumeria graminis* is unique due to its ability to infect grasses such as wheat and barley, which provides a well-established model system to study the interaction of obligate biotrophic fungi with crop plants (Hückelhoven and Panstruga, 2011; Dean *et al.*, 2012). *B. graminis* is separable into several formae speciales distinguishable by their different hosts. The barley powdery mildew *B. graminis* f. sp. *hordei* (*Bgh*) is one of the major pathogens of barley, causing losses that can reach 50% of the yield in conditions favourable for the pathogen (Dreiseitl and Jurečka, 2003; Oerke and Dehne, 2004; Tratwal and Bocianowski, 2014).

Compatible interactions between plants and biotrophic pathogens are very intimate. Besides suppression of plant defence responses, it requires a deep structural and metabolic reprogramming of the host to allow for the accommodation of the haustoria and subsequent pathogen feeding (Hückelhoven *et al.*, 2013). Biotrophic pathogens show a drastic reduction in genes encoding sugar-cleaving enzymes and proteins related to transport and assimilation of inorganic nitrogen and sulphur. For instance, *Blumeria graminis* has lost enzymes for assimilation of nitrate indicating that these pathogens depend on organic nitrogen in the form of host-derived amino acids (Spanu *et al.*, 2010; Duplessis *et al.*, 2011). Thus, according to Hückelhoven *et al.* (2013), loss or dysfunction of host factors involved in pathways that are essential for pathogen accommodation or nutrition can potentially affect susceptibility. Likewise, perturbations of negative regulators of defence response, as for example cell death regulators, also affected plant-pathogen interactions (Hückelhoven *et al.*, 2013). Interestingly, Douchkov *et al.* (2014) showed that 64% of 55 barley genes with a high score of converging evidence for a role in quantitative resistance to *Bgh* actually represent putative host susceptibility factors. Between these high-scored putative host susceptibility genes, more than 10% represent genes related to cell death regulation such as *MILDEW LOCUS O (Mlo)*, *BAX INHIBITOR 1 (BI-1)* and *LESION SIMULATING DISEASE 1 (LSD1)*. These are also involved in non-host susceptibility to the wheat powdery mildew *B. graminis* f. sp. *tritici*. Additionally, characterized barley susceptibility factors and/or genes with a high score of converging evidence include putative receptor-like kinases PRR, WRKY transcription factors, enzymes related to carbohydrate transport or metabolism, RAC/ROP GTPases and ROS producing enzymes (Hückelhoven, 2005; Hückelhoven *et al.*, 2013; Douchkov *et al.*, 2014).

1.7.1 Mlo and BI-1 as host susceptibility factors against *Bgh*

Mlo belongs to a plant specific multigenic family and encodes a calmodulin-binding protein with seven transmembrane domains and unknown function (Büschges *et al.*, 1997; Devoto *et al.*, 1999). Loss-of-function mutations in *Mlo* genes result in powdery mildew resistance in several plant species including barley, Arabidopsis, wheat and tomato (Kusch and Panstruga, 2017). Recessive alleles of barley *mlo* genes promote durable and race- non-specific resistance against the majority if not all *Bgh* isolates by restricting fungal penetration in a mechanism that involve secretion of defence compounds and localized accumulation of hydrogen peroxide (Büschges *et al.*, 1997; Acevedo-Garcia *et al.*, 2014; Kusch and Panstruga, 2017). Moreover, transient expression of *Mlo* in barley single epidermal cells of resistant *mlo*-mutant or susceptible *Mlo* wild-type (WT) leaves leads to the restoration of susceptibility to penetration by *Bgh* and a supersusceptibility phenotype, respectively (Shirasu *et al.*, 1999; Elliott *et al.*, 2002; Kim *et al.*, 2002).

BAX INHIBITOR 1 (BI-1) is another gene involved in penetration resistance to powdery mildew in barley (Hückelhoven *et al.*, 2013). *BI-1* encodes a conserved endoplasmic reticulum-localized protein which negatively regulates stress-induced programmed cell death (PCD) in plants and animals (Watanabe and Lam, 2009). *BI-1* expression is stimulated under multiple stress conditions which potentially trigger ROS-induced PCD such as pathogen infection, high temperature exposure, hydrogen peroxide treatment and also during tissue aging (Hückelhoven, 2004; Watanabe and Lam, 2009). Furthermore, plant BI-1 suppress the cell death triggered by the mammalian proapoptotic BAX protein and other stress stimuli like pathogen elicitors, carbon starvation and SA-treatment (Hückelhoven, 2004). Similar to *HvMlo*, transgenic plants overexpressing or silenced for *HvBI-1* show enhanced susceptibility or resistance to *Bgh* penetration, respectively (Babaeizad *et al.*, 2009; Eichmann *et al.*, 2010). Moreover, transient over expression of *HvBI-1* induces susceptibility of the nonhost barley to the wheat powdery mildew fungus *B. graminis* f. sp. *tritici* (Eichmann *et al.*, 2004).

A role of *Mlo* in the modulation of PCD has been proposed. Arabidopsis and barley *mlo* mutants exhibit senescence-like features like chlorosis, early chlorophyll degradation and spontaneous mesophyll cell death (Wolter *et al.*, 1993; Peterhansel *et al.*, 1997; Piffanelli *et al.*, 2002; Consonni *et al.*, 2006; Consonni *et al.*, 2010). Besides this, transient overexpression of *HvBI-1* induces a breakdown of *mlo*-mediated penetration resistance to *Bgh* in barley *mlo* mutants, indicating that both *HvMlo* and *HvBI-1* may support a survival pathway at sites of fungal attack (Hückelhoven *et al.*, 2003). Moreover, similar to *HvBI-1*, expression of *HvMlo* is also enhanced upon stress stimuli that potentially trigger cell death such as infection with the pathogens *Bgh*, *M. oryzae* and *P. palmivora*, wounding and the

application of the oxidizing agent methyl viologen (Piffanelli *et al.*, 2002; Le Fevre *et al.*, 2016). Likewise expression of a pepper *CaMlo2* were induced by *Xanthomonas campestris* pv. *vesicatoria* and *Phytophthora capsici*, SA, sodium chloride and drought stimuli. Transcripts levels of the rice *OsMlo3* increase in response to *M. oryzae* infection, heat and cold stresses (Kim and Hwang, 2012; Nguyen *et al.*, 2016).

1.7.2 LSD1-like proteins

LSD1-like are a family of genes with conserved zinc finger motifs that are involved in the regulation of ROS-induced plant PCD triggered by biotic and abiotic stresses such as pathogen infection, increased light intensity, treatment with SA-analogues and waterlogging. Arabidopsis LSD1 proteins are negative regulator of plant PCD and their function is antagonized by LSD-ONE-LIKE 1 (LOL1), which, therefore, acts as a positive regulator of oxidative stress-induced cell death (Dietrich *et al.*, 1994; Jabs *et al.*, 1996; Dietrich *et al.*, 1997; Epple *et al.*, 2003; Mateo *et al.*, 2004; Mühlenbock *et al.*, 2007).

Up to now, three barley genes belonging to the *LSD1-like* family were identified and structurally characterized, but the function of these homologues is still unknown. *HvLSD1a* (*HvABC10220*) and *HvLSD1b* (*HvABC06454*) are close homologues of *AtLSD1* whereas *HvCBC04043* is closer to *AtLOL1* (Keisa *et al.*, 2008; Keisa, 2013). Keisa (2013) observed a slight but significant reduction in the expression of all three genes in barley leaves in response to *Bgh* infection. However, neither Douchkov *et al.* (2014) nor Spies *et al.* (2011) found statistically significant changes in the transcript levels of *HvLSD1a* and *HvLSD1b* in *Bgh*-infected barley epidermal cells. Nevertheless, transient knock-down of *HvLSD1a* results in enhanced *Bgh*-penetration resistance while silencing of *HvLSD1b* did not affect the outcome of barley-barley powdery mildew interaction (Spies *et al.*, 2011; Douchkov *et al.*, 2014).

1.7.3 Other susceptibility factors

As previously mentioned, biotrophic pathogens depend on sucrose generated by the plant metabolism. Therefore, it is not surprising that a loss of function of genes related to the transport and metabolism of carbohydrates results in reduced susceptibility to *Bgh*. The transient knock-down of a member of the barley SWEET sugar transporter family lead to a reduction of over 50% in *Bgh*-penetration in barley epidermal cells (Douchkov *et al.*, 2014). Additionally, transient overexpression of ALCOHOL DEHYDROGENASE 1 (*HvADH1*) results in increased *Bgh* penetration success. On the contrary, transient knock-down of this gene or inhibition of ADH activity by the chemical compound pyrazole results in decreased penetration success and delay in *Bgh*-pustule formation (Pathuri *et al.*, 2011). ADH is an

enzyme of the fermentative metabolism responsible for the reversible reduction of aldehydes to their corresponding alcohols. ADH is typically related to response to oxygen deprivation for instance in flooded plants, bulky organs or during seed development (Strommer, 2011). Yet, stress stimuli as for example pathogen infection, low temperature, drought, salt, hormone treatment and hydrogen peroxide also induce ADH expression/activity (Christie et al., 1991; Dolferus et al., 1994; Kim et al., 2009; Pathuri et al., 2011; Proels et al., 2011; Shi et al., 2017). In Arabidopsis, overexpression of the AtADH1 gene results in increased resistance to *Pst*, possible due to the high accumulation of soluble sugars and sucrose, increased expression of PR genes and enhanced callose deposition (Shi et al., 2017). On the other hand, in barley-powdery mildew pathosystem, it is believed that ADH activity supports biotrophy by maintaining *Bgh*-carbohydrate supply (Pathuri et al., 2011).

RAC/ROPs are small GTP-binding proteins that act as molecular switches in signal transduction by cycling between the inactive and cytosolic GDP-bound state and an active membrane-bound GTP-state. RAC/ROPs regulate several cellular processes such as polarized cell growth, cell morphology, cell development and adaptation to biotic and abiotic stresses (Craddock et al., 2012; Kawano et al., 2014). Among all known barley RAC/ROP proteins, HvRAC1, HvRAC3, HvROP6 and HvRACB have been shown to be involved in susceptibility against *Bgh*. Transient or stable overexpression of constitutively active forms of these four proteins leads to increased susceptibility to *Bgh*-penetration. On the other hand, stable knock-down of HvRACB results in reduced *Bgh*-penetration, haustoria development and pustule formation on the surface of transgenic plants (Schultheiss et al., 2003b; Pathuri et al., 2008; Hoefle et al., 2011). HvRACB is involved in polar cell growth. Stable knock-down HvRACB transgenic plants show a dramatic reduction in the number and size of root hairs and a high frequency of defective stomatal subsidiary cells. Plants overexpressing a constitutively activated form of HvRACB show isotropic instead of polar root hair growth (Pathuri et al., 2008; Hoefle et al., 2011; Scheler et al., 2016). In addition, HvRACB did not seem to regulate defence responses. MAMP-triggered responses such as oxidative burst and MAPK activation did not differ between WT and transgenic HvRACB plants and constitutively activated form of HvRACB display constitutive high expression of PR genes (Scheler et al., 2016). Thus, it is likely that *Bgh* exploits HvRACB function in cell polarity to promote its own penetration and haustoria establishment in barley epidermal cells (Hückelhoven et al., 2013).

Rac/Rop GTPases are also involved in the regulation of NADPH oxidase activity (Kawano et al., 2014). Co-expression of a constitutive active form of OsRac1 and OsRBOHB enhanced ROS production. Moreover, mutations in residues critical for interaction between the two enzymes in OsRac1 suppress ROS production in rice cells (Wong et al., 2007; Oda et al.,

2010; Kosami *et al.*, 2014). Barley transgenic plants overexpressing a constitutively activated form of HvRac1, the putative orthologue of OsRac1, display enhanced *Bgh*-induced cell death associated with ROS formation (Pathuri *et al.*, 2008). These data indicate that similar to rice and other plant species, HvrBOHs are possibly regulated by Rac/Rop GTPases.

ROS can act as antimicrobial agent and play a role in lignin cross-linking as a means to reinforce the cell wall to block pathogen entry. Additionally, it acts as local and systemic secondary messenger to trigger further immune responses, such as gene expression, stomata closure and HR (Camejo *et al.*, 2016). At first, ROS were suggested to perform a positive role in the establishment of plant defences and HR. However, mutations in genes encoding proteins related to ROS generation like plants RBOHs and peroxidases show that the effect of ROS on disease resistance and cell death depends of the source of ROS production and the plant-pathogen interaction (Torres, 2010). For instance, the transient overexpression of a CLASS III PEROXIDASE 7 (HvPrx7) in barley single epidermal cells results in enhanced susceptibility to colonization by *Bgh* while the transient overexpression or knock-down of HvPrx40 results in enhanced resistance and supersusceptibility to *Bgh*-penetration (Kristensen *et al.*, 2001; Johrde and Schweizer, 2008). Moreover, knock-down of HvrBOHF2 (previously called HvrBOHA) leads to enhanced fungi-penetration resistance (Trujillo *et al.*, 2006). However, when HvrBOHF2 was stably knocked-down in barley transgenic plants, Proels *et al.* (2010) observed enhanced susceptibility to penetration by *Bgh* in young leaves.

1.8 Objectives

Despite the fact that the role of plant RBOHs during plant-pathogen interactions has been relatively well understood in plants such as *Arabidopsis thaliana*, the contribution of these putative master apoplastic ROS-producers in defence responses in others plants such as barley are still poorly understood. The annotation of barley RBOH gene family revealed six members, HvrBOHB1, B2, E, F1, F2, and J (Lightfoot *et al.*, 2008). Intriguingly, no functional homologue of the Arabidopsis AtRBOHD was described in the barley genome to date. AtRBOHD and orthologue genes in plant species like tobacco, rice and potato encode enzymes that are the primary source of ROS during PTI and ETI (Kadota *et al.*, 2015). Nevertheless, the genes *HvrBOHB2*, *HvrBOHF1* and *HvrBOHF2* are pathogen-responsively expressed and at least *HvrBOHF2* has been proven to be involved in the interaction with the barley powdery mildew fungus *Bgh* (Trujillo *et al.*, 2006; Lightfoot *et al.*, 2008; Persson *et al.*, 2009; Proels *et al.*, 2010). Detached first leaves of barley showed reduced susceptibility to penetration by *Bgh* at the single cell level when HvrBOHF2 was silenced by transient induced gene silencing after biolistic transformation. However, contrary

to the outcome after transient silencing in detached leaves, stable HvrRBOHF2 knock-down (KD) plants displayed enhanced susceptibility to penetration by *Bgh* (Trujillo *et al.*, 2006; Proels *et al.*, 2010). Further investigations revealed that HvrRBOHF2 KD lines become less susceptible to the pathogen with the progression of leaf-age. In addition, RBOH function is associated with the carbohydrate metabolism. As previously described (section 1.5.3), the OPPP is the main supply of reducing power (e.g. NADPH) in non-photosynthetic cells. Thus, it is essential for providing reducing equivalents when RBOHs are active (Scharte *et al.*, 2009). However, sucrose needs to be transported from the photosynthetic cells to the cytosol of the infected cell where it can fuel the OPPP and other pathways necessary for further plant defences. Therefore, enzymes involved in the sucrose transporter/degradation and OPPP potentially play an important role during plant-pathogen interactions.

In this work, the role of barley RBOH-type NADPH oxidases in the outcome of the interaction of barley-barley powdery mildew fungus was studied. The main purpose was to better understand the complex function of HvrRBOHF2 in the interaction of barley and *Bgh*. Most of all, it should be analysed how the silencing of *HvrRBOHF2* resulted in the observed leaf age-related resistance phenotype to *Bgh*. Therefore, the susceptibility to *Bgh*-penetration and the progression of the powdery mildew disease was analysed in different leaves from 11- and 17-day-old barley plants silenced for HvrRBOHF2. Moreover, the contribution of HvrRBOH type F isoforms in the *Bgh*-triggered hydrogen peroxide accumulation was assessed by quantifying the frequency of local cell wall associated diaminobenzidine (DAB) staining and whole cell DAB staining events. Furthermore, because AtRBOHF, a close homologue of *HvrRBOHF2*, is a crucial modulator of defence-related metabolism (Chaouch *et al.*, 2012), SA contents and the transcript levels of pathogen-responsive and defence-related genes were measured in non-challenged and *Bgh*-challenged *HvrRBOHF2* KD plants. Additionally, the function of a putative barley homologue of AtRBOHD, identified in recently published microarray data (Schnepf *et al.*, 2017), in interaction with *Bgh* was also studied. The expression of the gene encoding the new barley RBOH protein was monitored in non-challenged and *Bgh*-challenged barley leaves. Moreover, the role of the new enzyme in the susceptibility to penetration by *Bgh* was tested in a transient induced silencing assay.

A further aim of this thesis was to investigate the function of barley sucrose degradation and OPPP enzymes in susceptibility to *Bgh*. Therefore, the role of some isoforms of barley genes related to the sucrose cleavage and the first enzyme of the OPPP, G6PDH, in the susceptibility to penetration by *Bgh* was also tested in a transient induced silencing assay.

2 MATERIAL AND METHODS

2.1 Plant material

Transgenic barley plants *HvRBOHF2* knock-down (KD) (*Hordeum vulgare* L. cv. Golden Promise) lines 30/2E06 (E06) and 30/2E08 (E08) were used in this study. As a control, the corresponding azygous siblings, offsprings that lost the transgene due to segregation and behaved like the wild type parent plants were used (Proels *et al.*, 2010). In addition, the barley cultivars Golden Promise and Pallas were also used. The seeds were pre-germinated on filter paper soaked with tap water for three days in the dark and the germinated seeds transferred to soil. Plants were grown in a growth chamber at 18 °C with 60% relative humidity and a photoperiod of 16 h with 150 $\mu\text{mol m}^{-2} \text{s}^{-1}$ of photon flux density. Transgenic plants of different growth stages (Zadoks stage 12 to 13) (Zadoks *et al.*, 1974) were used. A schematic representation of the plant stages is shown in the Supplementary Fig. 1.

2.2 Photosynthetic pigment content analysis

The photosynthetic pigment content of barley transgenic lines was measured in whole leaves of 11-day-old plants and leaf sections of 17-day-old plants. For the measurement in whole leaves, first and second leaves were harvested separately, frozen in liquid nitrogen and ground to a fine powder. A pool of 7 to 9 leaves of each genotype was used. One hundred percent methanol was added to the powder resulting in a concentration of 0.1 g ml⁻¹. Pigments were extracted from 1 ml of the homogenate into 2 ml of 100% methanol and the absorbance spectrum of the supernatant was measured in triplicate in a spectrophotometer at 1 nm intervals between 400 nm and 700 nm. Total chlorophyll and total carotenoid content was estimated from the absorption spectra according to the equations of Lichtenthaler and Buschmann (2001).

For the measurement of photosynthetic pigments in leaf sections, leaves were harvested and cut transversally into two sections of equal size. In each section, meristem-distal (tip) and meristem-proximal (base), four leaf discs of 4 mm diameter were taken. The leaf discs from a pool of four leaves of each line were snap frozen in liquid nitrogen and ground to a fine powder using a tissue homogenizer (TissueLyser II, Qiagen) at a frequency of 30 Hz for 2 min. One milliliter of 96% (v/v) ethanol solution was added to the powder and after 5 min of incubation on ice, the solution was centrifuged at 21,100 g for 10 min at 4 °C. The pigment extraction procedure was repeated twice. Absorbance spectra of the pooled supernatants and estimation of total chlorophyll and total carotenoid contents were performed as described above.

2.3 Pathogens and inoculation

The pathosystem barley-barley powdery mildew was the main focus of this study and most of the inoculation experiments were conducted using the fungus *B. graminis* (DC) Speer f. sp. *hordei* Marchal (*Bgh*) race A6. Additionally, an aggressive isolate of *Fusarium culmorum* (W.G.Sm.) Sacc. (*Fc*) strain Fc002 (Linkmeyer *et al.*, 2013) and the hemibiotrophic fungus *Bipolaris sorokiniana* (Sacc.) Shoemaker (*Bs*) were also used.

2.3.1 *Blumeria graminis* f. sp. *hordei*

Bgh was maintained on the cultivar Golden Promise grown in a growth chamber at 18 °C with 60% relative humidity. Inoculations were performed in a settling tower by air current dispersion. For microscopic evaluation and gene expression analysis, the whole plant was inoculated with a spore density of 20 to 50 conidia mm⁻². A spore density of 5 to 15 conidia mm⁻² were used for the evaluation of disease symptom progression and 50 to 60 conidia mm⁻² for SA quantification. In transient expression experiments, detached leaves were inoculated with a spore density of more than 100 conidia mm⁻².

2.3.2 *Fusarium culmorum*

Fc was cultivated on ¼ potato dextrose agar plates in a growth chamber at 20 °C with 60% relative humidity and UV-light with a 12 h day⁻¹ cycle for four to six weeks. Distilled water was added to the plate and conidia were washed off. The spore solution was filtered through a nylon gauze and the conidia suspension adjusted to a concentration of 5 x 10⁻⁵ conidia per ml in 0.02% Tween 20. The conidia suspension was uniformly sprayed onto leaves of 17-day-old barley transgenic plants (Zadoks stage 13) until the spore solution started to run off the leaf blade. The inoculated plants were covered with plastic bags for three days to maintain high humidity and facilitate infection. Plants were kept in a growth chamber at 18 °C with 90% relative humidity and a photoperiod of 16 h of light for seven days.

2.3.3 *Bipolaris sorokiniana*

Bs was isolated from leaves of the winter barley cv. Canberra growing under natural conditions at the field trial "Grünwaldfeld" in Freising, South Germany. A pure culture, named 107/4B, was initiated from a single spore isolate. Conidia from monoconidial cultures were cultivated on potato dextrose agar plates in a growth chamber at 20 °C with 60% relative humidity for two to three weeks. Spore solution preparation and inoculation of the transgenic barley plants were performed as described for *Fc*, with few modifications. Spore solution concentration was adjusted to 2 x 10⁻⁴ conidia per ml. The inoculated plants were covered

with plastic bags and kept in a growth chamber at 18 °C with 60% relative humidity and a photoperiod of 16 h of light for 96 hours.

2.4 Assessment of the powdery mildew infection

2.4.1 Cytological analysis

The outcome of the interaction of barley *HvRBOHF2* KD transgenic lines of different ages with the barley powdery mildew fungus was evaluated in leaf samples harvested 48 h after inoculation (hai). Leaves were destained in ethanol:chloroform solution (3:1 [v/v]) and stored in 50% (v/v) glycerol. Fungal mycelium was stained with acetic ink (10% [v/v] blue ink [Pelikan, Hanover, Germany] in 25% [v/v] acetic acid). The leaves were cut transversally into two sections of equal size. In each section, meristem-distal (tip) and meristem-proximal (base), 50 to 75 interaction sites were evaluated. Four to five leaves per line and experiment were assessed and the experiment was performed three times. In each experiment, a total of 100 to 150 interaction sites per genotype and leaf were scored. Detection of hydrogen peroxide (H₂O₂) accumulation using 3,3-diaminobenzidine (DAB) staining was performed as described by Hüchelhoven et al. (1999). Briefly, leaves of 17-day-old seedlings were inoculated with *Bgh*. Forty-two hours later, leaves were cut and placed in tubes filled with 1 mL of 1 mg mL⁻¹ DAB tetra hydrochloride solution for six hours. Then, the leaves were transferred to the destaining solution and subsequently to a storage solution as describe above. Leaves of 17 day-old-plants were quite long. Therefore, just the base section of the leaves was evaluated to make sure that the analyzed leaf-section had taken up the DAB staining solution properly. Fifty interaction sites per leaf were scored. Four to seven leaves per line and experiment were assessed and the experiment was performed three times. In all experiments, only short cells (cell type A and B) were included in the evaluation as the rate of fungal penetration into different types of epidermal cells varies (Koga et al., 1990).

2.4.2 Powdery mildew disease progression

The progression of the powdery mildew disease in barley transgenic plants was assessed in detached and attached inoculated leaves. For the detached leaf inoculation assay, leaves of about 12 cm length were excised from 17-day-old seedlings, placed on 0.8% water-agar and infected with *Bgh*. For the attached leaf inoculation assay, the whole barley seedlings were infected with the pathogen. Then, seedlings or leaf explants were incubated in a climate chamber for 96 hours. The number of colonies per cm² leaf area was quantified in green tissue under a stereomicroscope at 25x magnification. Leaf segments were destained in ethanol:acetic acid solution (6:1 [v/v]), the fungal structures stained with acetic ink and the

density of colonies quantified again. To measure the colony length, pictures of interaction sites were taken with a Leica MC170 HD digital camera on a Leica MDG41 stereo microscope and the length of oval colonies along the longitudinal leaf axis was measured. Sixty to eighty pustules per treatment were manually sized using the software Leica LAS v4.5. The experiment was performed three times with four to six seedlings per barley line in each experiment.

2.5 Gene expression studies

Gene expression studies in transgenic barley were performed in distinct leaves of 11- and 17-day-old *HvRBOHF2* KD or azygous plants, 48 hai with *Bgh*. Leaves from a pool of three to four seedlings of each line were used.

Gene expression in barley cv. Pallas was performed in *Bgh*-challenged leaves of 12-day-old plants (Zadoks growth stage 12). A pool of six seedlings of each line was harvested from non-inoculated or inoculated seedlings 12, 36 and 48 hours after pathogen inoculation.

2.5.1 Total RNA isolation

Samples were frozen in liquid nitrogen and ground into a fine powder using mortar and pestle. One milliliter of RNA extraction solution (0.8 M guanidinium thiocyanate, 0.4 M ammonium thiocyanate, 0.1 M sodium acetate [pH 5.0], 5% [v/v] glycerol and 50% [v/v] water saturated phenol [Aqua-Phenol, Roti]) and 200 µl of chloroform was added to approximately 200 mg of powder. The solution was vigorously mixed, incubated at room temperature for 10 min in a tube rotator and centrifuged at 17,500 g for 15 min at 4 °C. Then, 850 µl of chloroform was added to the supernatant, and after mixing for 15 sec in a vortex mixer, the samples were centrifuged at 17,500 g for 15 min at 4 °C. The aqueous layer was mixed with 1 ml of isopropanol and incubated overnight at -20 °C to precipitate the RNA. Samples were centrifuged at 17,500 g for 20 min at 4 °C, the RNA-pellet was washed twice with 1 ml of 70% (v/v) ethanol and diluted in sterile RNase-free water. RNA integrity and amount were evaluated by spectrophotometry and/or gel electrophoresis in a 2% non-denaturing agarose gel.

2.5.2 cDNA synthesis

cDNA from barley transgenic plants was synthesized using the Quantitect Reverse Transcription reaction (Qiagen, Hilden, Germany) according to the manufacturer's instructions with some modifications. Genomic DNA contamination was eliminated from the samples in a reaction containing 2 µl gDNA wipeout buffer 7x, 1 µg of total RNA samples and

sterile RNase-free water in a final volume of 14 μ l. Samples were incubated at 42 °C for 7 min and immediately transferred to ice. Then, 1 μ l RT primer mix, 4 μ l 5x Quantiscript RT buffer and 1 μ l Quantiscript Reverse Transcriptase were mixed with the genomic DNA elimination reaction and the mix incubated at 42 °C for 30 min. Transcriptase was inactivated by incubation of the samples for 3 min at 95 °C.

cDNA from barley cv. Pallas was synthesized using the RevertAid First Strand cDNA Synthesis Kit (Thermo Fisher Scientific, St. Leon-Rot, Germany) according to the manufacturer's instructions. Briefly, genomic DNA contamination was eliminated from the samples and RNase inhibited in a reaction containing 5 U DNase, 10x reaction buffer with $MgCl_2$, 50 U RiboLock RNase inhibitor, 10 μ g of total RNA samples and sterile RNase-free water in a final volume of 50 μ l. Following incubation at 37 °C for 30 min, 250 mM EDTA was added and the samples incubated at 65 °C for 10 min. After addition of 5 μ L of 100 μ M random hexamer primer, the samples were incubated at 65 °C for 5 min, spun down and immediately transferred to ice. Finally, 20 μ L of RevertAid reaction buffer 5x, 100 U RiboLock, 100 mM dNTP Mix and 1000 U RevertAid reverse transcriptase were added to the samples and the volume fulfilled to 100 μ l with RNase free water. For reverse transcription, the samples were incubated at 25 °C for 10 min followed by 60 min at 42 °C. Transcriptase was inactivated by incubation of the samples for 10 min at 70 °C.

2.5.3 Reverse transcription semi-quantitative real-time PCR (RT-sqPCR)

RT-sqPCR reactions consisted of 0.5 to 1 μ l of cDNA, 2.5 μ l Taq polymerase 10x reaction buffer, 0.65 U Taq DNA polymerase (SupraTherm, Ares Bioscience GmbH, Köln, Germany), 5 mM dNTP mix, and 400 nM of a gene-specific forward and reverse primer (Table 1) in a total volume of 25 μ l. The barley *MONOUBIQUITIN-LONG-TAIL FUSION 1 (HvMub1)* gene was used as internal control. PCR conditions were 1 min denaturation at 95 °C followed by 32 to 37 cycles of 95 °C for 30 s, 60 °C for 30 s, and 72 °C for 40 s, and a final step at 72 °C for 60 s.

Table 1: Oligonucleotide sequences for gene expression analyses

Gene	Accession number	Primer name	Primer sequence in 5' to 3' orientation
<u>House keeping gene</u>			
<i>HvMub1</i>	M60175	Ubi-kurz-3' Ubi-kurz-5'	ACCCTCGCCGACTACAACAT CAGTAGTGCCGGTCTGAAGTG
<u>Autophagy related genes</u>			
<i>HvATG7</i>	AK367931.1	HvATG7F HvATG7R	CGCTCCTGTTGATTCCGGTCT CAGACGGACCCTCACTGTTC
<i>HvATG8A</i>	BI947475.1	HvATG8AF HvATG8AR	CTGCCGACCTTACTGTTGGC GTGGCAGGCAAGATGGATTAGG

<u>Fusarium DNA quantification</u>			
<i>Fusarium culmorum</i>		FculC561 fwd FculC614 rev	CACCGTCATTGGTATGTTGTCACT CGGGAGCGTCTGATAGTCG
<i>HvEF1α</i>	Z50789	Hor1f Hor2r	TCTCTGGGTTTGAGGGTGAC GGCCCTGTACCAGTCAAGGT
<u>Carbohydrate metabolism genes</u>			
<i>HvADH1</i>	X07774.1	HvADH1-7 HvADH1-8	GTCCTCCCTGTGTTCACTGG ACCGACATGCATGACAGTGT
<i>HvCwINV1</i>	AJ534447.1	HvCwInv1-RNAi CwINV1_qPCR	TGGTTGGATCGGAGCACATG GACGTGGAGGTGAGCTTTGA
<i>HvCwINV3</i>	AK357105.1	HvCwInv3-2 CwINV3-3 qPCR	CAACTTAGGCGCCATTCATC AGGGAAGACCTGCATCCTCT
<i>HvINVNH1</i>	AK361696.1	HvINVNH1-qPCR-3 INVNH1 RNAi1	CTGGCGCTCGTCAACAAGGTC CGCATCCAGAAGAACATGAG
<i>HvSUS1</i>	X65871	HvSuSy1-1 HvSuSy1-2	GTTCTGGAAGTACGTGAGCAACCTG GACAGACGGACCAAATGGAACTACG
<u>Cell death markers genes</u>			
<i>HvBI-1</i>	AJ290421	BI-1 qPCR1 BI-1 qPCR2	GTCCACCTCAAGCTCGTTT ACCCTGTCACGAGGATGCTT
<i>HvCBC04043</i>	EU545230	HvLLO1 qPCR1 HvLLO1 qPCR2	GAGATGGCGCAGCTAGTTTGC CAACTGATGTCACGAACTGCAGAC
<i>HvLsd1a</i>	EU545233	HvLDL1 qPCR1 HvLDL1 qPCR2	CCATACGGAGCATCTTCTGTC AAG GTAACCCCGACTACGACGTTG
<i>HvMlo</i>	Z83834	HvMlo HvMlo	ACAAGCTCGGCCATTGGTT GGATATGAAGCCCACCAGCAT
<i>HvS40</i>	AJ310379.1	HvS40 F HvS40 R	AACTACAACCTCCGAGCACC CTCTTCGCGTCGTTGGTACA
<u>Oxidative pentose phosphate pathway</u>			
<i>HvG6PDH-C1</i>	FJ790424	G6PDH-rev G6PDH-fwd	AGATGTAACCGTGGGTCTGCATG CAACATCGACGCTGGCAAGC
<i>HvG6PDH-C2</i>	MLOC_13014.1	HvG6PDH-B1 HvG6PDH-B2	CTCAATTCCTCAGCAGAGTC TTCCCGGCACTCTTTAACC
<i>HvG6PDH-P2</i>	AM398980.1	HvG6PDH-P2 qPCR-1 HvG6PDH-P2 qPCR-2	CGTACCCTGGATACACTGAAGATAAGA CG CATGTCGGA ACT GCA CTC TAA TCT CAG
<u>Pathogenesis-related genes</u>			
<i>HvPR1b</i>	X74940	HvPR1b PR1b-3'	TGGTATAGAGCAGGCCCATAGAA GTGTTGGAGCCGTAGTCGTAGT
<i>HvPR3</i>	AK364132	PR3_02990_F PR3_02990_R	CTACACGTACGACGCCTTCA GTGGCCTTGCTTATCTCTTCC
<i>HvPR5</i>	AJ001268	PR5_02787_F PR5_02787_R	CACGGACATCACCAAGGATT TTGCCCTTGAAGAACATTGAG
<i>HvPR10</i>	AK360974	PR10_33647_F PR10_33647_R	AGGGCGACAAGGTAAGTGG CATCTTGAGCAGGTCGAGGTA
<u>Respiratory burst oxidase homologues genes</u>			
<i>HvRBOHD</i>	AK366247.1	HvRBOHD RNAi 1 RbohD-2	ACGACGACTACGTGGAGATC TGCGAGACCTGCTTGATC
<i>HvRBOHF1</i>	EU566855	HvRBOH-F1-forw HvRBOH-F1-rev	TTACAACATGGACCTGCGTCCCTACA TGCCTTGGTCAGACACTCAGCTGCAT
<i>HvRBOHF2</i>	EU566859	HvRBOH-F2-forw HvRBOH-F2-rev	TATGCGGAGTCCCGCAGAAAGATG TGTA CTGTACTCCCCCTGCCTGTGT

2.5.4 Reverse transcription quantitative real-time PCR (RT-qPCR)

RT-qPCR was performed in a Mx3005P Cycler (Stratagene, La Jolla, CA, USA). Individual PCR reactions contained 75 to 100 ng of cDNA, 10 μ l Maxima SYBR Green qPCR master mix (2x) (Thermo Fisher Scientific) and 300 nM of a gene-specific forward and reverse

primer (Table 1) in a total volume of 20 μL . The program consisted of an initial step at 95 °C for 3 min followed by 40 cycles of 95 °C for 30 s, 60 °C for 30 s, and 72 °C for 1 min. The specificity of amplification reactions was verified by a melting curve analysis performed at 60 to 95 °C. Relative expression for genes of interest in each sample was calculated using primer efficiency correction as suggested by Pfaffl (2001) and the *HvMub1* gene as normalizer (Ovesna *et al.*, 2012; Pennington *et al.*, 2016). Primer efficiencies were evaluated on a standard curve generated using a two-fold dilution series of a pooled sample over at least four points (5; 2.5; 1.25 and 0.625 ng μL^{-1} of cDNA). The error propagation throughout all calculation steps were taken into account, as recommended by Hellemans *et al.* (2007). In all experiments, three biological replicates of each sample and three technical (PCR) replicates were performed.

2.6 Salicylic acid quantification

Free- and conjugated-SA from the first and third leaves of 17 to 18-days-old seedlings was extracted from a pool of four to five plants of each line and quantified as described by Meuwly and Métraux (1993), with some modifications. Ground leaf powder, corresponding to 200 to 400 mg fresh weight of first leaves and 700 to 1000 mg fresh weight of third leaves, was extracted in 9 ml of 100% methanol and 0.2 ml of internal standard solution (500 μM of o-anisic acid and 250 μM of p-hydroxybenzoic acid in 100% methanol). The methanol leaf powder suspensions were vigorously shaken for 1 min at room temperature and centrifuged at 30,000 g for 15 min at 6 °C. The supernatant was dried under vacuum, resuspended in 2 ml of 5% (w/v) trichloroacetic acid and then extracted twice for SA with 5 ml of ethyl acetate/cyclohexane (1:1, v/v). The organic SA-containing phase was collected after centrifugation at 3,300 g for 5 min. HCl was added (to 3.4 M) to the remaining aqueous trichloroacetic acid phase, again supplemented with 200 μL internal standard, and kept at 80 °C for 1h for acid hydrolysis. The phenolic compounds were resuspended in 1 ml of the mobile phase (Citrate acetate buffer; 30 mM sodium citrate and 27 mM sodium acetate at pH 5). Samples were separated on a Nucleosil ODS 300 column 4.6 x 150 mm, 5 μm , maintained at 30 °C. The mobile phase flow rate was 1 ml min^{-1} and the injection volume was 50 μL . Excitation and emission wavelengths were 298 and 400 nm, respectively. Elution was carried out with citrate acetate buffer for 15 min, followed by a linear 2 min gradient to methanol (100%), isocratic methanol (100%) for 7 min, linear 2 min gradient to citrate acetate buffer and equilibration for 7 min before the next run. The SA content in the samples was corrected according to the amount of internal standard o-anisic acid. The experiment was performed three times.

2.7 Assessment of the leaf spot blotch disease

Disease symptoms caused by *Bs* were analyzed on second and third leaves of 17-day-old barley transgenic plants 96 hai. Leaf levels were individually harvested, destained in ethanol acetic acid solution (6:1 [v/v]) and stored in 50% (v/v) glycerol. The density of *Bs*-lesions per leaf was quantified under a stereomicroscope at 12.5x magnification. To measure lesion length, pictures were taken with a Leica MC170 HD digital camera on a stereo microscope Leica MDG41. Length of the lesion along the longitudinal leaf axis was sized using the Leica LAS v4.5 software. Lesions were grouped based in their length in three classes, small (<1 mm), medium (1-3 mm) and large (> 3 mm). The experiment was performed three times with six plants per barley line in each experiment.

2.8 Assessment of *Fusarium* infection

2.8.1 Extraction of genomic DNA from barley leaves

Genomic DNA was isolated from barley leaves according to Fraaije *et al.* (1999) and modifications suggested by Hofer *et al.* (2016). *Fusarium* inoculated leaves from a pool of four to six seedlings of each line were snap frozen in liquid nitrogen and kept at -80 °C. The samples were ground into a fine powder using mortar and pestle and the powder transferred to a 2 ml reaction tube which was filled to approximately ¼ of its volume. The tubes were filled with an extraction buffer composed of 5mM phenanthroline, 2.1% (w/v) polyvinylpyrrolidone-40, 2% (w/v) SDS, 0,05% (v/v) β-mercaptoethanol and 50% (v/v) TEN buffer (1.4 M NaCl, 0.1 M Tris base [pH 8], 20 mM EDTA [pH 8]). Samples were vigorously mixed and incubated in a water bath at 70 °C for 20 min. They were centrifuged at 16,200 g for 5 min at room temperature and the supernatant transferred to a new reaction tube containing 900 µl of ammonium acetate (7.5 M). Samples were incubated at -4 °C for 20 min and centrifuged at 16,200 g for 15 min at room temperature. Later, 800 µl of the supernatant was mixed with 800 µl of isopropanol and incubated at room temperature for 15 min to precipitate DNA. After centrifugation at 16,200 g for 5 min, the DNA-pellet was washed with 400 µl of 70% (v/v) ethanol and centrifuged for further 5 min at 16,200 g. Finally, the pellet was vacuum-dried at 16,200 g for 25 min at 37 °C in a centrifugal evaporator and re-suspended in 200 µl double distilled autoclaved water. DNA integrity and amount was evaluated by spectrophotometry and the DNA concentration was adjusted to 20 ng/µl with double distilled water.

2.8.2 Quantification of *Fusarium* DNA in barley leaves

Fusarium infection was evaluated via quantification of the relative amount of fungal DNA in first, second and third leaves of barley transgenic plants via RT-qPCR according to Nicolaisen *et al.* (2009) and Linkmeyer *et al.* (2013). Individual PCR reactions contained 100 ng of genomic DNA, 10 µl Maxima SYBR Green qPCR master mix (2x; Thermo Fisher Scientific), 10 µg of bovine serum albumin and 300 nM of *H. vulgare*-specific or *F. culmorum*-specific forward and reverse primers (Table 1) in a total volume of 20 µl. RT-qPCR was performed in a Mx3005P Cyclor (Stratagene, La Jolla, CA, USA). The program consisted of an initial step at 50 °C for 2 min and 95 °C for 10 min, followed by 40 cycles of 95 °C for 15 s and 60 °C for 1 min. Amplification specificity was verified by a melting curve analysis performed at 55 to 95 °C. Absolute quantification of barley and *Fusarium* DNA were calculated from an external standard calibration curve generated using a ten-fold dilution series of pure fungal and barley DNA over five points (100, 10, 1, 0.1 and 0.01 ng of DNA). Fungal DNA was normalized to plant DNA and in all experiments, three biological replicates of each sample and one technical (PCR) replicate were performed.

2.9 Sequence alignment and phylogenetic analysis

Multiple sequence alignments were performed with Clustal Omega (Sievers *et al.*, 2011) using default parameters. For the phylogenetic analysis, full-length amino acid sequences of RBOHs from Arabidopsis, barley, rice and maize were aligned with ClustalW (Thompson *et al.*, 1994) using the BLOSUM 30 protein weight matrix with a gap opening penalty of 10 and a gap-extension penalty of 0.05. Evolutionary analyses were conducted in Molecular Evolutionary Genetics Analysis (MEGA6) (Tamura *et al.*, 2013) using the Maximum Likelihood method based on the JTT matrix-based model and tested with a bootstrap of 1000 replications. Sequences were obtained from NCBI GenBank nucleotide collection (<http://www.ncbi.nlm.nih.gov/genbank/>).

2.10 Transient transformation of barley cells

The function of selected genes in the susceptibility of barley to penetration by the barley powdery mildew fungus was assessed by transient transformation of barley epidermal cells via ballistic delivery of expression vectors, based on a protocol originally developed for wheat (Schweizer *et al.*, 1999). Transient-induced gene silencing (TIGS) and transient overexpression experiments were performed as described by Douchkov *et al.* (2005) and Schweizer *et al.* (1999), with modifications which are briefly described below.

2.10.1 Generation of the TIGS vector constructs

PCR fragments of 400 to 550 bp of the selected genes were amplified from a barley leaf cDNA pool of cv. Pallas inoculated or non-inoculated with *Bgh* using gene-specific primers (Table 2). The reaction consisted of 4 µl 5x Phusion HF buffer, 0.5 to 1µl of cDNA template, 10 mM dNTP mix, 5 µM of forward and reverse primer, 3% [v/v] DMSO and 0.4 U Phusion high-fidelity DNA polymerase (Thermo Fisher Scientific, St. Leon-Rot, Germany) in a total volume of 20 µl. PCR conditions were 1 min denaturation at 98 °C followed by 38 cycles of 98 °C for 10 s, 50 to 60 °C for 30 s, and 72 °C for 30 s, and a final step at 72 °C for 5 min. PCR-fragments were separated electrophoretically in a 0.8% agarose gel, bands were cut out of the gel and PCR products extracted using the NucleoSpin Gel and PCR Clean-up kit (Machery-Nagel GmbH & Co. KG, Düren, Germany).

Table 2: Oligonucleotide sequences for cloning

Gene	Accession number	Primer name	Primer sequence (in 5' to 3' orientation)
<i>HvRbohD</i>	AK366247.1	HvRBOHD RNAi 1	ACGACGACTACGTGGAGATC
		HvRBOHD RNAi 4	CTCCTTCATCCCGATGCAC
<i>HvCwINV1</i>	AJ534447.1	Hv CwInv 1-1	ATGGGCCGGAATCCAGGC
		Hv CwInv 1-2	GCCTGTGAGGTCCGTAGC
<i>HvSUS1</i>	X65871	HvSs1-RNAi-1	CCTGTTCGAATCCGACAAG
		HvSs1-RNAi-2	GAGACCACGAAGGCTCTG
<i>HvG6PDH-C1</i>	FJ790424	G6PDH-rev	AGATGTAACCGTGGGTCTGCATG
		G6PDH-fwd	CAACATCGACGCTGGCAAGC
<i>HvG6PDH-C2</i>	MLOC_13014.1	HvG6PDH-B1	CTCAATTCCTCAGCAGAGTC
		HvG6PDH-B2	TTCCCGGCACTCTTTAACC
<i>HvG6PDH-P2</i>	AM398980.1	HvG6PDHP2 RNAi 1	CTTATCCGTCCT TCGCTTC
		HvG6PDHP2 RNAi 2	CCGAAAGATCCCTTGTAGAG
<i>HvINVNH1</i>	AK361696.1	HvINVNH1 OV1 Sall	Agtcg ACCACTGTGTCTGTACTCAC
		HvINVNH1 qPCR3	GCCATGTTCTCCAGGCAATCG
		HvINVNH1 OV3	AGAACATGG CGGACAGTG
		HvINVNH1 OV2 Sall	tgtcgaCGCATCCAGAAGAACATGAG

The PCR-fragments were ligated into the *Sma*I site of the entry vector pIPKTA38 (Douchkov *et al.*, 2005) in a ligation reaction mix containing 300 ng entry vector, 300 ng PCR-fragment, 2.5 U T4 DNA ligase, 5 U *Sma*I restriction enzyme, 2.5 µl T4 DNA ligase buffer (10x) and double distilled water in a final volume of 10 µl. Following overnight incubation at 25 °C, the ligation reaction was stopped by incubation at 65 °C for 15 min. The reaction was cooled down to RT on ice and re-ligated plasmids were eliminated by further incubation of the reaction at 25 °C for 1 h after addition of 5 U of *Sma*I and 5 µl 10x *Sma*I buffer. After this, the reaction was used to transform chemically competent *Escherichia coli* XL1-blue cells as described below. A correct pIPKTA38-TIGS construct in antisense orientation was subcloned

into the antisense-intron-sense destination vector pIPKTA30N by a LR recombination reaction (Douchkov *et al.*, 2005). In short, 150 ng of pIPKTA38-TIGS construct were mixed with 150 ng of pIPKTA30N, 2 µl LR Clonase mix (Gateway LR Clonase Enzyme mix; Thermo Fisher Scientific, St. Leon-Rot, Germany) and double distilled water in a final volume of 10 µl. The mixture was incubated overnight at 25 °C and later used to transform chemically competent *E. coli* XL1-blue cells.

2.10.2 Generation of overexpression vector constructs

The complete coding sequence of barley *HvINVNH1* was amplified by the overlapping PCR method from a barley leaf cDNA pool of cv. Pallas inoculated or not inoculated with *Bgh* using two out-side and two chimeric primers (Table S2). Two fragments, a C-terminal fragment of 396 bp (amplified with primer pair HvINVINH1 OV1 Sall/HvINVINH1 qPCR3) and a N-terminal fragment of 458 bp (amplified with primer pair HvINVINH1 OV3/HvINVINH1 OV2 Sall) were generated using Phusion polymerase according to the manufacturer's recommendations. Primer HvINVINH1 OV1 Sall (forward) and HvINVINH1 OV2 Sall (reverse) were out-side primers and contained Sall restriction sites at their 5' end each. The other primers were chimeric and shared an overlap of 10 nucleotides. The two PCR-fragments were separated electrophoretically via on an 1% agarose gel, excised and purified as described previously. For the overlap PCR reaction, 68 ng of each fragment were used as template in a second PCR reaction using the out side primers and Phusion polymerase. The PCR-product was subjected to A-tailing of the blunt-end fragment to allow ligation in to the pGEM-T vector (Promega GmbH, Mannheim, Germany) by TA cloning. For the A-tailing, 20 µl of PCR-product were mixed with 250mM of dNTP, 2.5 µl of 10x Taq Polymerase buffer and 5 U of Taq DNA polymerase (SupraTherm, Ares Bioscience GmbH, Köln, Germany) and the mix incubated at 72 °C for 15 min. For the ligation reaction, 1 µl T4 DNA 10x ligase buffer, 5 µl insert, 1 µl pGEM-T and 5 U of T4 DNA ligase (Thermo Fisher Scientific, St. Leon-Rot, Germany) were mixed and incubated overnight at room temperature. The reaction was then used to transform chemically competent *E. coli* XL1-blue cells as described below. After sequence confirmation, the coding sequence of *HvINVINH1* was subcloned into the Sall site of the plant expression vector pGY1 (Schweizer *et al.*, 1999). Before ligation, both destination vector and the pGEM-T-HvINVINH1 plasmid were digested with Sall (Thermo Scientific, Waltham, USA) according to the manufacturer's instructions. Additionally, pGY1 was dephosphorylated by incubation of the digested reaction with 1 U FastAP Thermosensitive Alkaline Phosphatase (Thermo Scientific, USA) at 37 °C for 10 min, followed by enzyme inactivation at 75 °C for 5 min. The ligation reaction, performed as

described in the previous section, was incubated overnight at 25 °C and used to transform chemically competent *E. coli* XL1-blue cells.

2.10.3 Transformation of *E. coli* XL1-blue cells

Chemically competent *E. coli* XL1-blue cells were transformed using the heat shock method. Briefly, 10 µl of the corresponding ligation reaction was added to 100 µl of chemically competent cells and the reaction mixture was gently mixed. After a short incubation on ice, the mixture was placed at 42 °C for 45 s and then transferred back to ice. 500 µl of cold Luria-Bertani (LB) liquid medium (10 g L⁻¹ trypton, 5 g L⁻¹ yeast extract and 10 g L⁻¹ NaCl) was added and the transformed cells were incubated at 37 °C for 1 h with agitation. The transformed cells were plated on LB agar plates supplemented with the appropriate antibiotic (50 µg ml⁻¹ kanamycin for pIPKTA38 or 100 mg ml⁻¹ ampicillin for pIPKTA30N, pGEM-T and pGY1).

2.10.4 Plasmid preparation and selection of positive clones

Plasmid DNA was isolated from a number of recombinant *E. coli* colonies using alkaline lysis. Briefly, single bacterial colonies were inoculated in 2 mL of LB liquid media with the appropriate antibiotic and incubated overnight at 37 °C with agitation. Cells were harvested by centrifugation at room temperature at 20,000 g for 5 min and the pellet was resuspended in 100 µl of Buffer I (50 mM Tris-HCl [pH 8], 100 mM EDTA, and 100 µg mL⁻¹ RNase A). Following addition of 200 µl of alkaline lysis solution (0.2 M NaOH, 1 % SDS), the lysate was gently mixed and incubated for up to 5 min at room temperature. 150 µl of neutralization buffer (3 M K-acetate, 2 M Acetic acid, pH 5.2) were added and the mixture was centrifuged at 4 °C for 20 min to precipitate proteins. After that, plasmid DNA was precipitated by addition of 900 µl of ice-cold ethanol 98% (v/v) to 800 µl of the supernatant and centrifugation at 4 °C for 15 min. The pellet was washed in 100 µl of ice-cold 70% (v/v) ethanol and centrifuged at 4 °C for 10 min. Finally, the supernatant was discarded, the pellets air-dried for about for 30 min at room temperature and resuspended in 30 µl of double distilled water. Putative positive clones were identified by restriction enzyme digestion of the plasmid minipreparation with appropriate restriction enzymes (Thermo Scientific, Waltham, USA) according to the manufacturer's instructions. Subsequently, putative positive plasmid DNA minipreparations were purified with the NucleoSpin Plasmid kit (Machery-Nagel GmbH & Co. KG, Düren, Germany) and sequenced (Eurofins Genomics GmbH, Ebersberg, Germany) to confirm the DNA sequence of the insert and insert orientation. Medium-size scale positive plasmid DNA preparations were carried out, when necessary, using the

Nucleobond Xtra Midi kit (Macherey-Nagel, Düren, Germany) according to the manufacturer's instructions.

2.10.5 Bioballistic bombardment

For the ballistic delivery of expression vectors, 11 μ l of a gold-particle stock solution was coated with 0.5 μ g of pGY1-GFP (transformation marker) (Schweizer *et al.*, 1999) and either 1 μ g of destination vector constructs (pIPKTA30N-TIGS construct or pGY1-*HvINNVNH1*) or empty vector control (pIPKTA30N or pGY1) and mixed with an equal volume of 1 M CaNO_3 (pH 10) per shot. The mixture was incubated at room temperature and mixed from time to time. After 30 min incubation, the mixture was centrifuged at 20 000 g for 30 s and washed with 1 ml of 70 % (v/v) and 100% ethanol. The supernatant was discarded and the coated gold particles were resuspended in 6 μ l 100% ethanol and pipetted on a Biolistic Macrocarrier (Bio-Rad, Hercules, USA). Coated gold particles were bombarded into detached first leaves of 7-day-old barley cv. Golden Promise using the PDS-1000/He Particle Delivery System (Bio-Rad, Hercules, USA) with 900 psi rupture discs and 26 Hg vacuum. Leaf fragments were placed onto petri dishes, containing 0.8% (w/v) water agar with the adaxial epidermis facing up. Seven leaves were used per petri dish and at least two bombardments per construct were performed to ensure a sufficient number of transformed cells. After bombardment, plates were kept in a growth chamber at 18°C with 60% relative humidity and a photoperiod of 16 h.

To prepare the gold-particle stock solution, 27.5 mg of 1.0 μ m Gold Microcarriers (Biorad, Munich, Germany) were mixed with 1 ml double distilled water and incubated for 30 s in an ultrasonic bath. The particles were centrifuged at 20,000 g for 30 s and the supernatant discarded. The process was repeated twice. Afterwards, the particles were washed with 1 ml of 100% ethanol, dried at 50 °C and resuspended in 50 % (v/v) aqueous glycerol. Stock solutions were stored at -20 °C. Before use, the particles were solubilized by incubation for up to 20 min in an ultrasonic bath.

2.10.6 Gene function assessment

To assess the function of the selected genes in the outcome of the interaction of barley-powdery mildew, bombarded barley leaf fragments were inoculated with a high density of *Bgh* spores (> 100 spores mm^{-2}) 6 hours (overexpression assay) or one day (TIGS assay) after the ballistic delivery of coated particles. After inoculation, petri dishes were incubated in a growth chamber at 22 °C with 60% relative humidity and a photoperiod of 10 h. Two days after inoculation, penetration efficiency of *Bgh* in transformed GFP-expressing cells was evaluated by counting the frequency of haustoria-containing cells in relation to total number

of cells attacked by *Bgh*. GFP-expressing cells were detected under blue light excitation in a fluorescence microscope. *Bgh* was detected by light microscopy or by fluorescence staining of the fungal structures with 0.3 % (w/v) calcofluor solution for 30 s in the dark. For each construct, a minimum of three independent experiments were performed. In each experiment, 50 to 80 interactions per construct were evaluated.

2.10.7 “Sink” metabolism induction

The heterotrophic metabolism was induced in bombarded detached leaves of barley by incubation of the bombarded leaf fragments in sucrose solution soon after the bioballistic transformation. Leaf fragments of about 5 cm in length were put upright in 2 ml tubes filled with 1 ml of 10mM sucrose solution to allow for sucrose uptake. Tubes were incubated in a growth chamber at 18 °C with 60% relative humidity and a photoperiod of 16 h. One day later, the leaf fragments were transferred to water agar plate and inoculated with *Bgh* as previously described. After inoculation, leaf fragments were transferred back to the tubes and the volume of sucrose solution in the tube adjusted to 1ml. Tubes were incubated in a growth chamber at 22 °C with 60% relative humidity and a photoperiod of 10 h.

2.11 Data analyses

Data were subjected to either Student's t-tests or one-way analysis of variance followed by Tukey's honest significant difference test at $P = 0.05$. Data of length of *Bgh*-colonies did not meet the assumptions of homogeneity of variance and were subjected to Welch ANOVA followed by Games-Howell post hoc test at $P = 0.05$. Details of the statistical analyses were mentioned in the respective figure legends. No statistical analyses were performed to RT-qPCR data.

Because of the great variability within the independent experiments, only data of one representative experiment is shown in the main text. Data from the other two independent experiments are shown in the supplementary material.

3 RESULTS

3.1 Silencing of *HvRBOHF* genes leads to premature leaf senescence

Barley transgenic plants silenced for the NADPH oxidase gene *HvRBOHF2* (and co-silenced for *HvRBOHF1*) display deregulated cell death processes such as spontaneous mesophyll cell death in fully developed leaves and failure to limit wound-induced cell death (Proels *et al.*, 2010). As mis-regulation of cell death frequently results in alteration of senescence regulation (Lorrain *et al.*, 2003), the physiological status of leaves of *HvRBOHF2* KD plants was investigated.

3.1.1 Characterization of spontaneous cell death in *HvRBOHF2* KD plants

In a first step, I monitored the growth and development of *HvRBOHF2* KD plants from seed sowing until appearance of mesophyll cell death (Fig. 2). Radicle emergence started one to two days after seed imbibition in filter paper soaked with tap water. Germination rate was similar for *HvRBOHF2* KD and azygous seeds, but in general, embryos of the azygous control, which had lost the transgene by segregation, were slightly advanced in development. The first leaf through coleoptile appeared around four days after sowing (DAS) and was unfolded one to two days later (Fig. 2A). The second leaf appeared four to five days later (Fig. 2B), in both *HvRBOHF2* KD and azygous seedlings. Seedlings younger than 11-days (Zadoks stage 12) were macroscopically indistinguishable from the azygous control (Fig. 2C). However, two to three days later (at a plant age of 13 to 14 DAS), necrotic lesions or leaf bleaching were noticeable with the naked eye at the tip of the first leaf in *HvRBOHF2* KD plants (Fig. 2D). During this timeframe the third leaf emerged. Around 16 DAS (Zadoks stage 13) leaf necrosis was also observed in second leaves of *HvRBOHF2* KD plants. Leaf lesions, usually followed by chlorosis, spread quickly throughout the leaf tip and further developed downwards to the leaf base. The appearance of necrotic lesions was age-dependent, and started first in oldest first leaves and then following the order of leaf age. Necrotic lesions were prominent in the tip of first and second leaves of 17-day-old *HvRBOHF2* KD plants but not noticed in the younger third leaf (Fig. 3). When these leaves were fixed and observed under the microscope, I recognized a high level of cell death throughout the leaf tip in the first and second leaves but little cell death in the tip of the third leaf. Azygous control plants, however, showed only a slight induction of cell death at the very tip of all leaves (Supplementary Fig. S2).

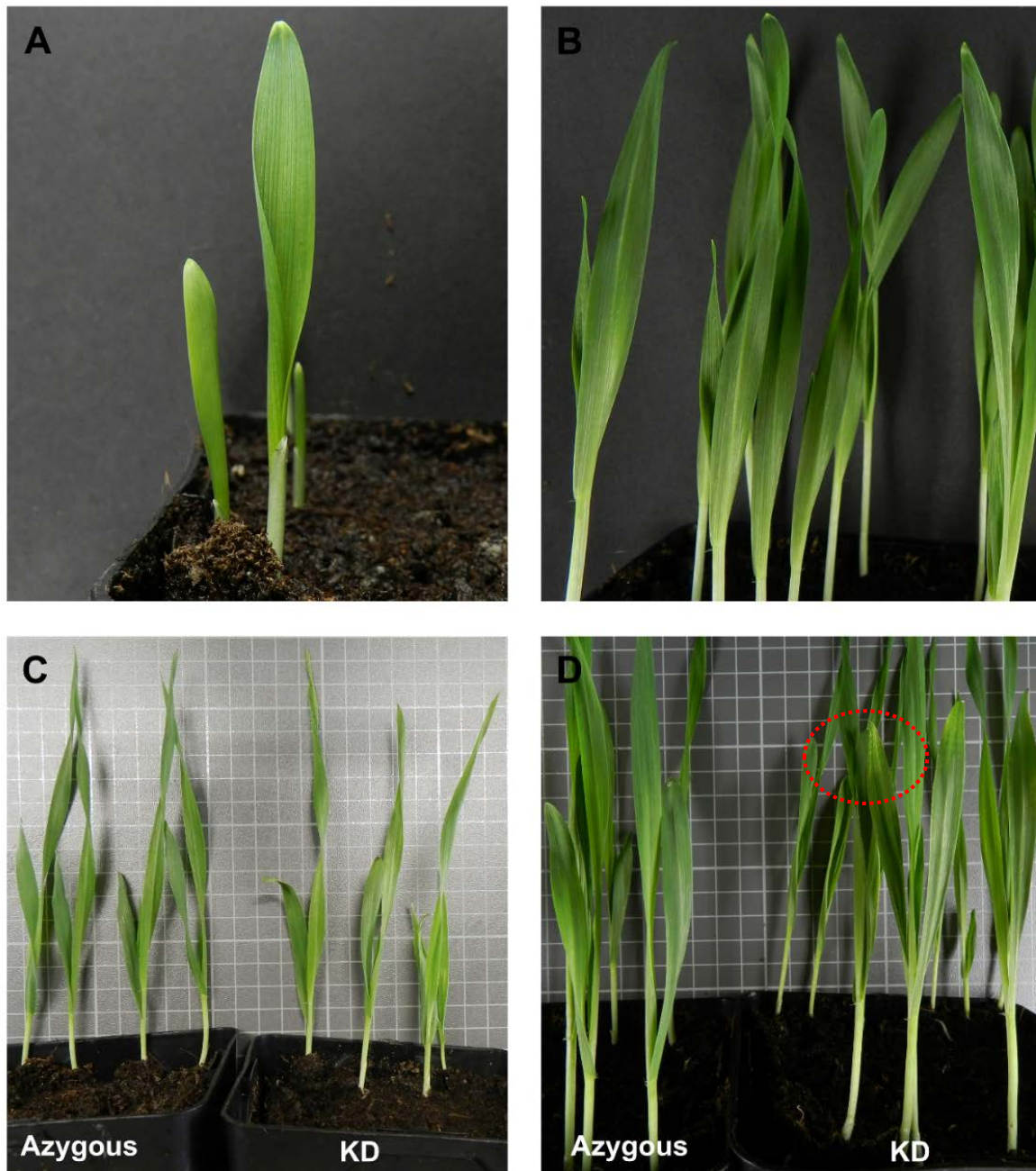


Figure 2: Seedling growth in *HvrBOHF2* KD lines. (A) Five to six days after sowing the first leaf was unfolded (Zadoks stage 11). (B) Approximately two days later the second leaf also appeared (Zadoks stage 11.5). (C) Seedlings younger than 11 days (Zadoks stage 12) do not differ from azygous controls and do not show visible symptoms of spontaneous mesophyll cell-death. (D) Around 13 days after sowing (Zadoks stage 12.5), necrotic spots or leaf bleaching were noticeable with the naked eye at the tip of the first leaf as highlighted with a red broken circle.

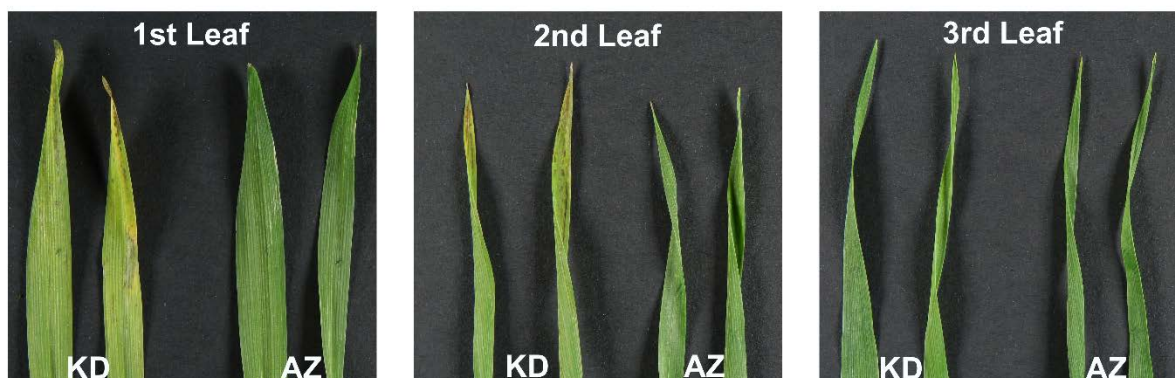


Figure 3: Necrotic spots in 17-day-old plants (Zadoks stage 13). First, second or third leaves of 17-day-old *HvRBOHF2* KD (left) and the azygous control (right) lines were harvested and pictures from the tip leaf section were taken. First and second leaves of *HvRBOHF2* KD plants displayed an early senescence phenotype as evident by spontaneous necrotic lesions and chlorosis in the tip of the leaf.

3.1.2 Content of photosynthesis-related pigments in *HvRBOHF2* KD plants

The chlorophyll content is known to decrease with leaf senescence. Thus, to determine if the spontaneous cell death observed in the leaf tip of *HvRBOHF2* KD plants is associated with premature senescence, I measured the chlorophyll content in leaves of these plants. Photosynthetic pigments (chlorophylls and carotenoids) were extracted into 100% methanol from a whole leaf extract of ground leaves of 11-day-old plants and the absorption spectrum measured in a spectral range between violet and red (400 and 700 nm). The absorption spectra of these leaf extracts were similar to the absorption spectra known from literature (Supplementary Fig. S3). Absorption maxima of chlorophyll (Chl) *a* in red and blue occurred at a wavelength of 665 and 435 nm, respectively. Absorption maxima of Chl *b* and carotenoids (Car) were masked by Chl *a* absorbance, as expected. There was no difference in the absorbance spectrum among any of the leaves tested. Likewise, both total chlorophyll (Chl *a* + *b*) and total carotenoids (xanthophylls and carotenes) content, estimated according to the equations for methanol pure solvent of Lichtenthaler and Buschmann (2001), were very similar among the leaves of *HvRBOHF2* KD and azygous control plants (Table 3). Chl *a* to Chl *b* ratio fluctuated between 2.18 and 2.26 and Chl to Car ratio between 6.79 and 7.53. There was no statistically significant difference between the leaves.

Table 3: Photosynthetic pigment content in whole leaves of 11-day old *HvRBOHF2* KD plants.

Data represent the means of three independent experiments. In each measurement, a pool of 7 to 9 leaves per treatment was used. Values represent the mean \pm 95% confidence interval.

Leaf	Genotype	Chl ^a (mg g ⁻¹ FW)	Car ^b (mg g ⁻¹ FW)	Chl ^c a/b ratio	Chl ^a /Car ^b ratio
1st Leaf	Azygous	1.92 \pm 0.108	0.27 \pm 0.028	2.18 \pm 0.038	7.12 \pm 0.362
	<i>HvRBOHF2</i> KD	1.86 \pm 0.058	0.25 \pm 0.020	2.21 \pm 0.081	7.53 \pm 0.368
2nd Leaf	Azygous	1.87 \pm 0.072	0.26 \pm 0.021	2.19 \pm 0.040	7.13 \pm 0.303
	<i>HvRBOHF2</i> KD	1.96 \pm 0.215	0.29 \pm 0.051	2.26 \pm 0.069	6.79 \pm 0.500

^a Total chlorophyll content (Chl a + b)

^b Total carotenoids content (xanthophylls + carotenes)

^c Chlorophyll

Subsequently, photosynthetic pigments were analysed in 17-day-old plants. As necrotic lesions started to manifest at the tip of older leaves of *HvRBOHF2* KD plants at this age, samples of both tip and base leaf sections were taken. In addition, leaf discs of individual leaves instead of leaf fragments were sampled and the less toxic alcohol ethanol was used as extraction solvent. The leaf disks were ground and the absorption spectrum of the photosynthetic pigments, extracted into ethanol 96% (v/v), was measured as described above. Absorption maxima of Chl a occurred at wavelength 664 in red and 433 nm in blue (Supplementary Fig. S4). Absorbance values were higher in young leaves and lower in old leaves. When the photosynthetic pigments were estimated, no significant difference in total Chl content of third leaves between azygous controls and *HvRBOHF2* KD plants was found. First and second leaves of *HvRBOHF2* KD plants, however, were characterized by significantly reduced Chl content in tip and base compared to azygous controls. In contrast to azygous controls, *HvRBOHF2* KD plants showed a continuous decrease in Chl content from younger third, over the second to the physiologically oldest first leaf (Fig. 4A). The total Car content was similar in tip and base sections of both genotypes in first and third leaves. Yet, there was a tendency of decreased Car content in tip and base leaf sections of the second leaves of *HvRBOHF2* KD plants. Considering the whole leaf, this reduction of approximately 18% in total Car levels was statistically significant (Fig. 4B). Notably, *HvRBOHF2* KD plants also displayed a gradual degradation of carotenoids from younger to older leaves, thus, the chlorophyll to carotenoid ratio did not change within the different leaves. Likewise, the chlorophyll a to chlorophyll b ratio was similar in the leaf sections of all the leaves tested, which indicates a comparable rate of degradation of these two molecules (Table 4).

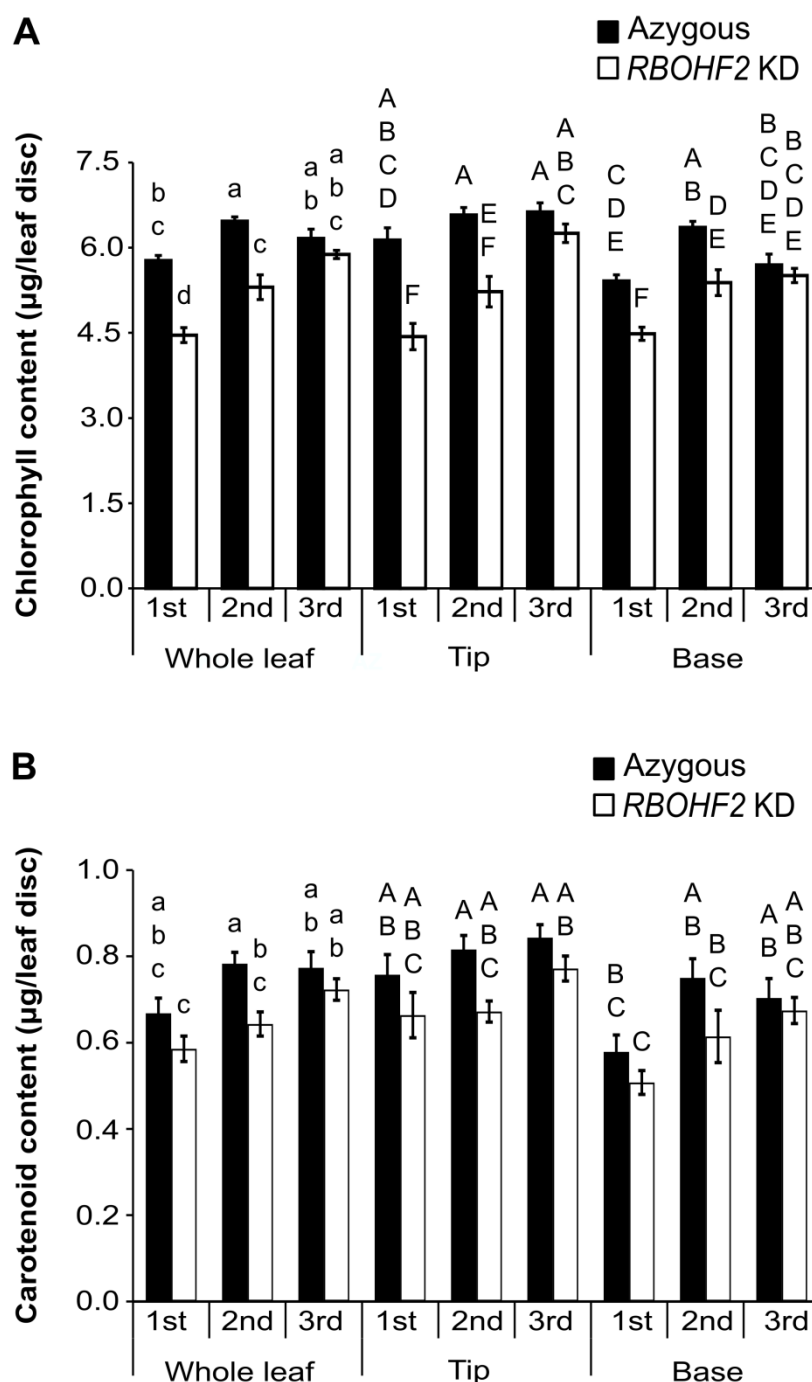


Figure 4: Photosynthetic pigments in leaf sections of 17-day-old *HvRBOHF2* KD plants. Total chlorophyll (A) and total carotenoid (B) content in tip and base leaf sections of 17-day-old barley *HvRBOHF2* knock down (KD) and azygous control lines. Data represent the mean of five independent experiments. In each measurement, a pool of 16 leaf discs from four leaves per treatment were used. Error bars show standard errors of the mean. Lowercase letters show the grouping of datasets relative to the content of photosynthetic pigments in the whole leaf and uppercase in the leaf sections according to Tukey's test at $P = 0.05$.

Table 4: Photosynthetic pigment ratio in leaf sections of 17-day old *HvRBOHF2* KD plants. Data represent the mean of five independent experiments. In each measurement, a pool of 16 leaf discs from four leaves per treatment was used. Values represent the mean \pm 95% confidence interval.

Leaf section	Leaf	Genotype	Chl ^a a/b ratio	Chl ^b /Car ^c ratio
Whole leaf	1st Leaf	Azygous	1.97 \pm 0.122	8.64 \pm 0.804
		<i>HvRBOHF2</i> KD	2.21 \pm 0.081	7.53 \pm 0.368
	2nd Leaf	Azygous	1.98 \pm 0.081	8.24 \pm 0.484
		<i>HvRBOHF2</i> KD	2.10 \pm 0.118	8.26 \pm 0.599
	3rd Leaf	Azygous	2.10 \pm 0.115	7.97 \pm 0.380
		<i>HvRBOHF2</i> KD	2.26 \pm 0.071	6.79 \pm 0.502
Tip	1st Leaf	Azygous	2.09 \pm 0.497	8.09 \pm 0.452
		<i>HvRBOHF2</i> KD	1.88 \pm 0.101	6.68 \pm 1.266
	2nd Leaf	Azygous	2.15 \pm 0.093	8.06 \pm 0.511
		<i>HvRBOHF2</i> KD	1.98 \pm 0.082	7.77 \pm 0.959
	3rd Leaf	Azygous	2.17 \pm 0.111	7.86 \pm 0.361
		<i>HvRBOHF2</i> KD	2.11 \pm 0.109	8.10 \pm 0.510
Base	1st Leaf	Azygous	1.85 \pm 0.171	9.35 \pm 1.465
		<i>HvRBOHF2</i> KD	1.87 \pm 0.060	8.83 \pm 0.525
	2nd Leaf	Azygous	2.03 \pm 0.170	8.47 \pm 0.983
		<i>HvRBOHF2</i> KD	1.99 \pm 0.098	8.76 \pm 1.203
	3rd Leaf	Azygous	2.02 \pm 0.134	8.09 \pm 0.522
		<i>HvRBOHF2</i> KD	2.05 \pm 0.087	8.17 \pm 0.458

^a Chlorophyll

^b Total chlorophyll (Chl a + b)

^c Total carotenoids (xanthophylls + carotenes)

In conclusion, 11-day-old *HvRBOHF2* KD plants did not show any visible indications of spontaneous mesophyll cell-death. In these plants, the content of photosynthetic pigments was very similar between leaves of the same plant and corresponding leaves of the azygous control. Seventeen-day-old *HvRBOHF2* KD plants however, showed spontaneous cell-death in the tip of the first and second leaves. In this case, the total Chl content in older leaves was lower than both in younger leaves of the same plant and first and second leaves of azygous plants. Thus, the reduced Chl content in older leaves coincided with the appearance of spontaneous necrotic lesions in *HvRBOHF2* KD plants.

3.2 Susceptibility to *Bgh* in *HvRBOHF2* KD lines depends on leaf age

Proels *et al.* (2010) showed that young leaves of *HvRBOHF2* KD plants are super-susceptible to penetration by the barley powdery mildew fungus *Bgh*. Interestingly, further inspection of *HvRBOHF2* KD lines revealed that these plants become less susceptible to *Bgh* with the progression of leaf-age (R.K. Proels, TU Munich, personal communication). In this chapter, the susceptibility to *Bgh* was investigated in distinct leaves of transgenic barley lines at two growth stages.

3.2.1 The *HvRBOHF* clade modulates susceptibility to penetration by *Bgh* in a leaf-age and leaf-section dependent manner

Preliminary results suggested that the susceptibility to penetration by *Bgh* differed between different leaves of *HvRBOHF2* KD lines. Thereby physiological older, first leaves were less susceptible than physiological younger leaves (Supplementary Fig. S5). To test whether the susceptibility to *Bgh* differs also in different parts of the leaf blade, the outcome of the interaction in the tip and in the base half sections of barley plants displaying (17-day-old) or not displaying (11-day-old) signs of premature senescence were evaluated. For this, the frequency of successful cell-wall penetration as the percentage of cells with fungal haustoria was quantified, 48 hours after inoculation (hai) with *Bgh*. In whole leaves, when the tip and base leaf sections were analysed together, there was a reduction in the overall haustoria frequency in the first leaf of 11-day-old *HvRBOHF2* KD plants when compared to azygous controls (i.e. siblings that had lost the *HvRBOHF2* silencing cassette due to segregation). On the other hand, in the second, later developing and physiologically younger leaf, the frequency of haustoria formation was slightly but not significantly enhanced in *HvRBOHF2* KD plants (Fig. 5A). This phenotype was similarly visible in 17-day-old plants. In this case, the first and second leaves of the *HvRBOHF2* KD line showed reduced susceptibility, whereas the physiologically younger third leaf showed a tendency of enhanced susceptibility to *Bgh* when compared to the azygous control (Fig. 5B). Thus, during progression of leaf development (between day 11 and day 17), the susceptibility of the second leaves of the *HvRBOHF2* KD line strongly dropped from about 60% penetration rate to less than 35%. In parallel, second leaves of azygous controls retained susceptibility to fungal penetration at a frequency of around 50-55% (Figs. 5A/B). These data support the hypothesis, that leaf age but not leaf type was responsible for this phenotype. In general, susceptibility was higher in physiologically younger leaves of the *HvRBOHF2* KD line (50-60% penetration on second leaves of 11-day-old plants and third leaves of 17-day-old plants), when compared to physiologically older leaves (25-35% penetration on first leaves of 11-day-old plants and

first/second leaves of 17-day-old plants). At the same time, azygous plants did not show a clear leaf-age dependent susceptibility.

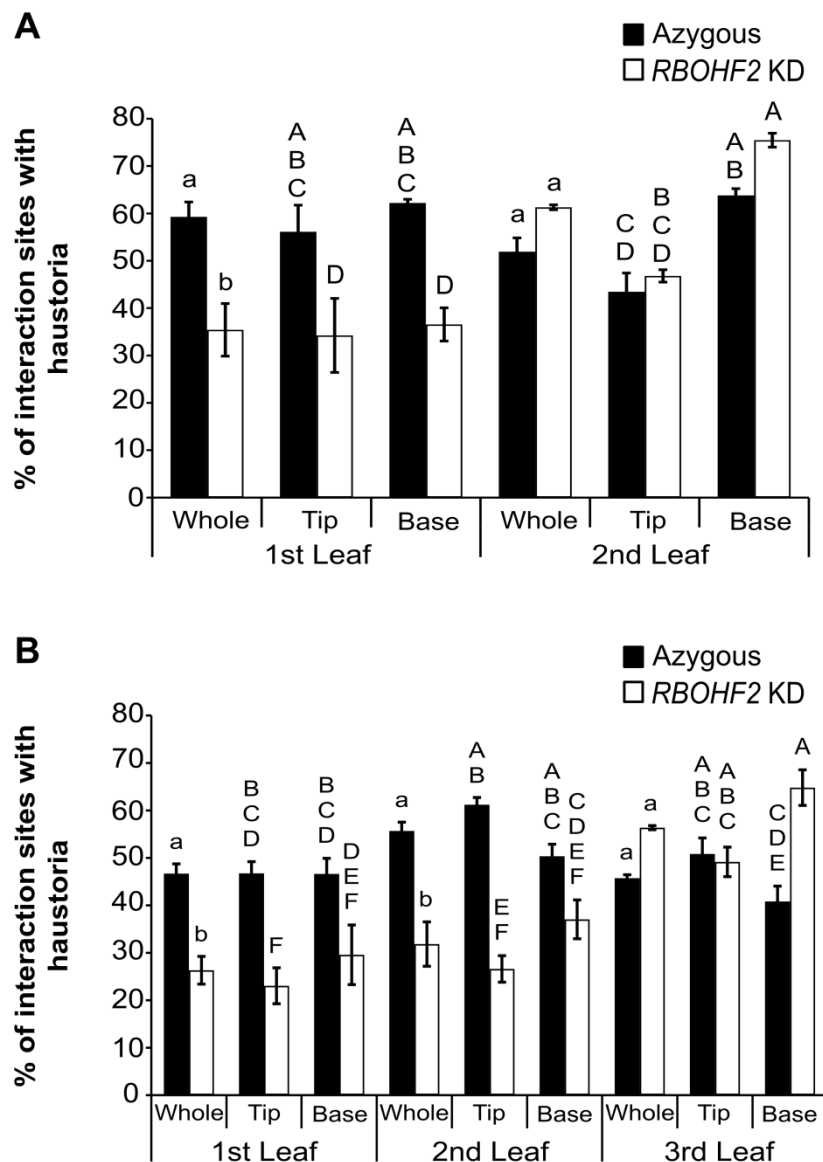


Figure 5: Interaction phenotype of *Bgh* with different leaves of either the *HvRBOHF2* KD line E08 or the azygous control in two growth stages. Frequency of successful cell-wall penetration with formation of visible haustoria at interaction sites in the whole leaf, older meristem-distal (tip) or younger meristem-proximal (base) sections of the leaf in 11-day-old (A) or 17-day-old plants (B). Leaves were fixed 48 hours after inoculation with *Bgh*, and plant and fungal structures were analysed by bright field microscopy. Data represent the average of 110 to 160 interaction sites per leaf of four leaves per line of one representative experiment. Error bars show standard errors of the mean. Lowercase letters show the grouping of data sets relative to successful penetration in the whole leaf and uppercase in the leaf sections according to Tukey's test at $P = 0.05$. The experiment was performed three times with similar results.

Similar finds were observed using a second, independent *HvRBOHF2* KD line, called E06. In this line, reduced and enhanced susceptibility to *Bgh* compared to the azygous control was noticed in first/second and third leaves, respectively. Additionally, the frequency of interaction sites with haustoria in the physiologically younger third leaves were 30% higher than in oldest first leaves of *HvRBOHF2* KD E06 while in azygous E06 the frequency of haustoria formation in both first and third leaves was approximately 46% (Fig. 6).

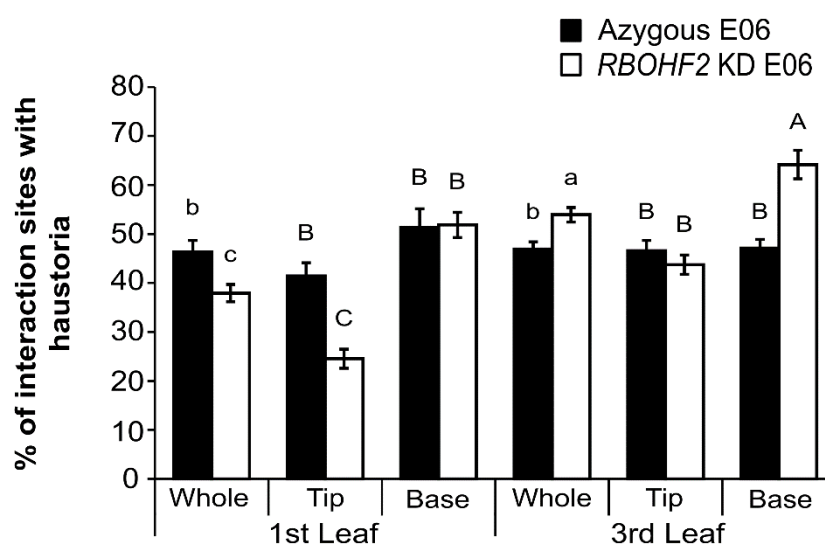


Figure 6: Interaction phenotype of *Bgh* with the *HvRBOHF2* KD line E06. Frequency of successful cell-wall penetration with formation of visible haustoria at interaction sites in the whole leaf, tip or base sections of the leaf in 17-day-old plants. Leaves were fixed 48 hours after inoculation with *Bgh*, and plant and fungal structures were analysed by bright field microscopy. Data represent the average of at least 130 interaction sites per leaf of five leaves per line. Error bars show standard error of the mean and letters the grouping of data sets according to Tukey's test at $P = 0.05$. The experiment was performed three times with similar results.

Growth of grass leaves is limited to the growth zone at the basal meristematic part of the leaf. When entering the elongation zone cells elongate without further cell division until they reach their final length (Kavanová *et al.*, 2006). Therefore, the basal part of the leaf represents the physiologically younger part of the leaf, whereas the distal tip part represents the physiologically older part of the leaf. When the susceptibility of tip and base leaf sections was considered separately, leaf-section-dependent susceptibility phenotypes were observed in 17-day-old *HvRBOHF2* KD lines. In 11-day-old plants, an inconsistent increment in the frequency of haustoria formation in the base section of younger leaves in comparison with the tip section was noticed (Fig. 5A and Supplementary Fig. S6). Nevertheless, in 17-day-old *HvRBOHF2* KD plants, the base section of the young, third leaves were 24% to 31% more susceptible than the tip section of these same leaves in the lines E08 and E06, respectively.

This trend was observed in two out of three independent experiments with line E08 (Fig. 5B and Supplementary Fig. S6) and line E06 (Fig. 6 and Supplementary Fig. S7). Additionally, in 17-day-old *HvRBOHF2* KD plants, the bases of young, third leaves were significantly more susceptible than in azygous controls, whereas the tips of the same leaves were similar to azygous controls. At the same time, older first and second leaves were less susceptible than the controls and this was statistically significant in the tip of the leaves (Fig. 5B and 6). Interestingly, when comparing the susceptibility of the leaf-base and leaf-tip of *HvRBOHF2* KD to that of whole leaves, the tendency of enhanced overall susceptibility in the physiologically younger third leaf of *HvRBOHF2* KD seedlings resulted from a higher susceptibility of the leaf base. Likewise, the reduced overall susceptibility in the physiologically older first and second leaves resulted from a strongly reduced susceptibility of the corresponding leaf tips.

3.2.2 Pre-invasion defence responses in *HvRBOHF2* KD plants

Cell wall appositions at sites of attempted penetration (papilla formation) are a typical pre-invasion defence responses during the barley-*Bgh* interaction, and increased frequencies of papillae are associated with race-specific and race non-specific resistance phenotypes in barley (Hückelhoven and Kogel, 1998; Hückelhoven *et al.*, 1999; Schulze-Lefert and Vogel, 2000). To check if the reduced *Bgh*-susceptibility phenotype as shown by older leaves of *HvRBOHF2* KD seedlings was related to an increase in pre-invasion defence responses, I studied papilla formation in different leaves and leaf-sections of 11- and 17- day-old plants. There was a large variance within individual leaves, especially in the KD lines. No statistical differences in papilla formation were observed between leaves or leaf sections of *HvRBOHF2* KD and azygous controls in 11-day-old seedlings (Fig. 7A). In 17-day-old *HvRBOHF2* KD plants, there was a tendency of an increase in the frequency of non-penetrated cells with papilla formation in the tip section of the first leaf (Fig. 7B and Supplementary Fig. S8). This leaf-section-dependent papilla formation in response to *Bgh*-challenge was also noticed in an independent *HvRBOHF2* KD line E06 (Fig. 8) and was statistically significant in two out of three independent experiments (Supplementary Fig. S9). Besides, a general increase in the frequency of papilla formation with progression of leaf age was also observed.

Thus, the lower frequency of haustoria formation in physiologically older leaf sections (leaf tip) of the first leaf partially correlated with an increase in the frequency of papilla formation (Figs. 5 to 8). In the same way, a high frequency of haustoria formation in physiologically younger leaf sections (leaf base) of the third leaf correlated with a decrease in the frequency

of papilla formation. Therefore, penetration resistance of papilla forming cells did not fully explain enhanced or reduced susceptibility to penetration and haustoria formation by *Bgh*.

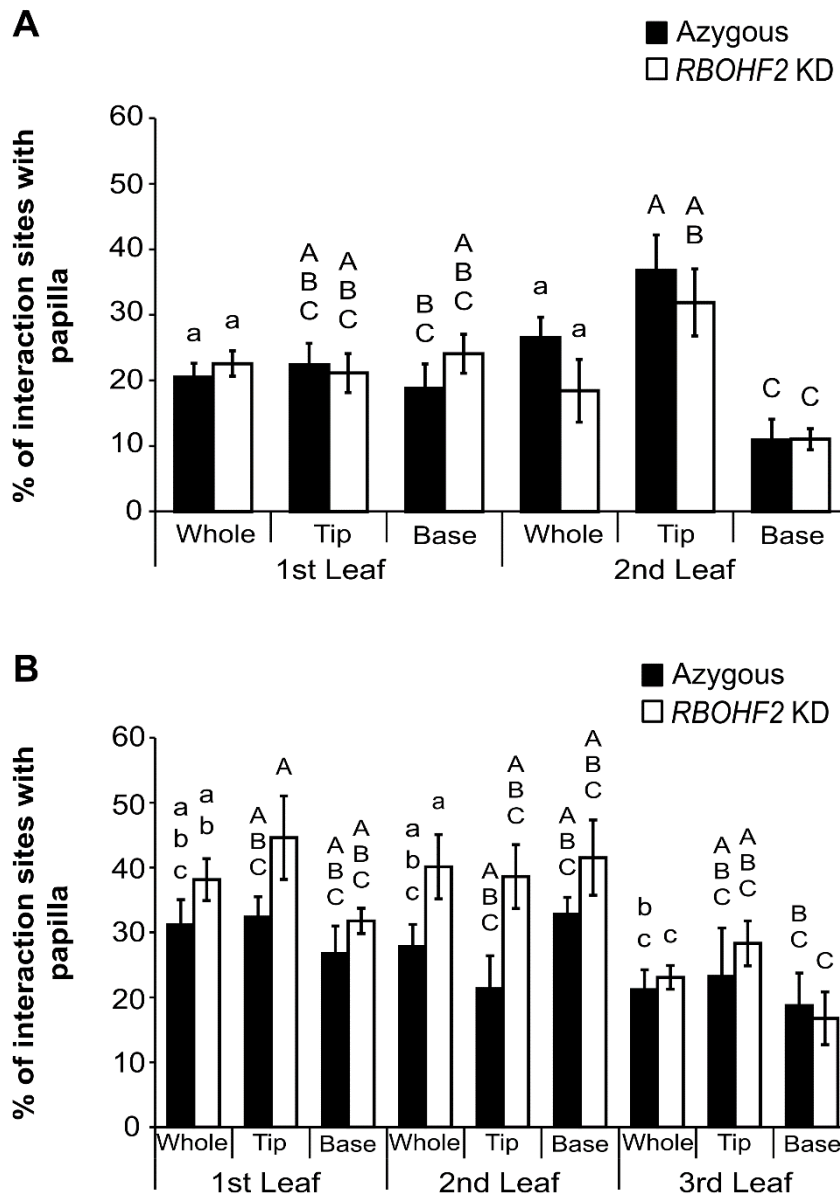


Figure 7: Pre-invasion defence responses in different leaves of *HvRBOHF2* KD line E08 and azygous control plants in two growth stages. Frequency of papilla formation at interaction sites in the whole leaf, older meristem-distal (tip) or younger meristem-proximal (base) sections of the leaf in 11-day-old (A) or 17-day-old plants (B). Leaves were fixed 48 hours after inoculation with *Bgh*, and plant and fungal structures were analysed by bright field microscopy. Data represent the average of 110 to 160 interaction sites per leaf of four leaves per line of one representative experiment. Error bars show standard errors of the mean. Lowercase letters show the grouping of data sets relative to papilla formation whole leaf and uppercase in the leaf sections according to Tukey's test at $P = 0.05$. The experiment was performed three times with similar results.

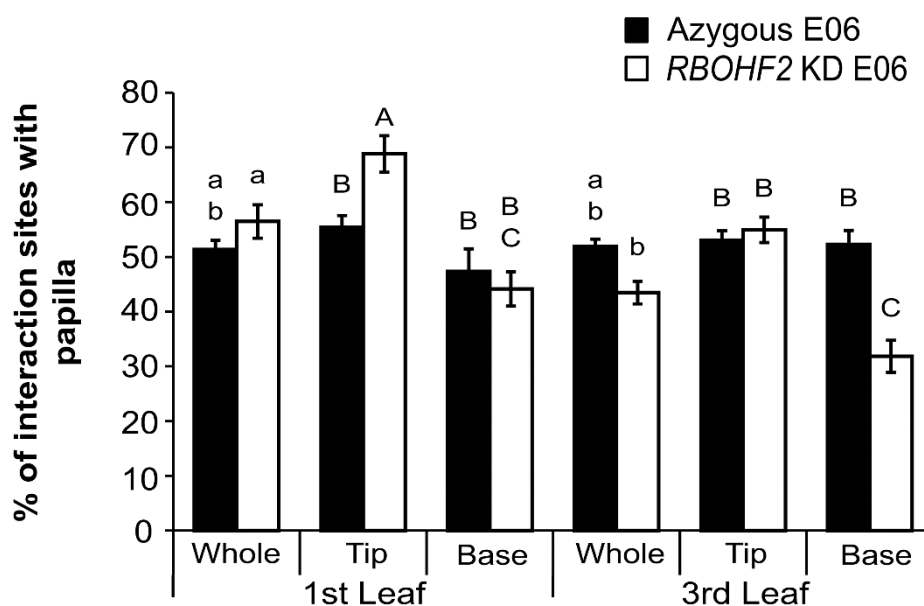


Figure 8: Pre-invasion defence responses in different leaves of *HvRBOHF2* KD line E06.

Frequency of papilla formation at interaction sites in the whole leaf, tip or base sections of the leaf in 17-day-old plants. Leaves were fixed 48 hours after inoculation with *Bgh*, and plant and fungal structures were analysed by bright field microscopy. Data represent the average of at least 130 interaction sites per leaf of five leaves per line. Error bars show standard errors of the mean and letters the grouping of data sets according to Tukey's test at $P = 0.05$. The experiment was performed three times with similar results.

3.2.3 ROS production and pathogen-induced cell death in *HvRBOHF2* KD plants

Because papilla formation frequencies did not fully explain differences in haustoria frequencies, the pathogen-triggered accumulation of hydrogen peroxide, another classical defence response during interaction of powdery mildews and resistant host phenotypes, was analysed (Thordal-Christensen *et al.*, 1997; Hüchelhoven *et al.*, 1999; Hüchelhoven *et al.*, 2000b; Schulze-Lefert and Vogel, 2000). To address this, a 3,3'-diaminobenzidine (DAB) staining of leaves of 17-day-old seedlings, 48 hai with *Bgh* was performed. Initially, tip and base sections of the leaf were scored. However, because the tip of the leaf did not appear to take the DAB solution up as efficiently as the base of the leaf, especially in the *HvRBOHF2* KD leaves, just the base section was further evaluated. As documented in previous studies, DAB staining events were associated with cell wall appositions in non-penetrated cells. DAB staining in penetrated haustoria-containing cells was mainly associated with anticlinal cell walls facing neighbouring epidermal cells. HR-related cell death was evident from whole cell DAB staining (Thordal-Christensen *et al.*, 1997; Hüchelhoven *et al.*, 1999; Hüchelhoven *et al.*, 2000b; Proels *et al.*, 2010). To see whether silencing of *HvRBOHF2* influences the ability

of barley to carry out localized oxidative defence and HR, I counted local cell wall-associated DAB staining and whole cell DAB staining events (Fig. 9).

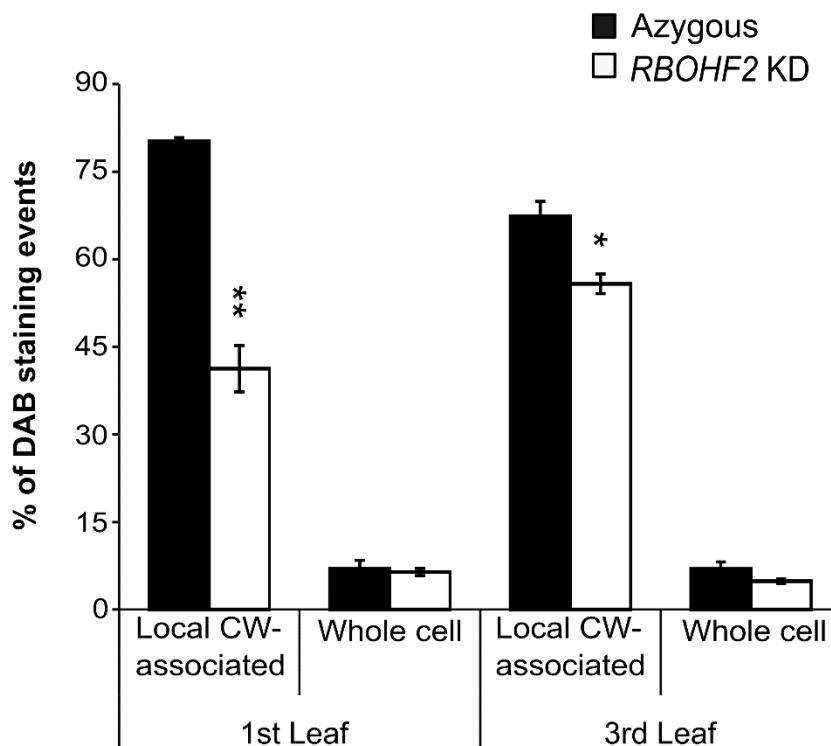


Figure 9: Pathogen-triggered accumulation of hydrogen peroxide in *HvRBOHF2* KD plants.

Frequency of local cell wall (CW)-associated 3,3'-diaminobenzidine (DAB) staining and whole cell DAB staining events in leaves of *HvRBOHF2* KD and azygous control plants. Seventeen-day-old barley plants were inoculated with *Bgh*. Forty-two hours after inoculation the leaves were excised and placed with the cut face in a solution of 1 mg mL⁻¹ DAB for six hours. Then, the leaves were fixed and fungal structures were analysed by bright field microscopy. Bars represent the means of three fully independent experiments. In each experiment, five to seven leaves per line and leaf level were evaluated. Error bars show standard errors of the mean and asterisks indicate significant differences between the genotypes (Student's t test: ** p<0.01, * p<0.05).

First leaves of *HvRBOHF2* KD plants showed overall 49% less DAB staining events compared to azygous controls and third leaves overall 17% less. In addition, in agreement with Proels *et al.* (2010), the frequency of *Bgh*-induced epidermal HR (whole cell DAB staining) was not affected in any leaves of *HvRBOHF2* KD plants. Instead, the percentage of *HvRBOHF2* KD cells with local cell wall-associated DAB staining in papilla or anticlinal cell walls was reduced. Taken together, cellular ROS production as evidenced by DAB staining was reduced in leaves of *HvRBOHF2* KD plants.

3.2.4 *Bgh* colonization is also affected in *HvRBOHF2* KD lines

As shown above, the silencing of *HvRBOHF* genes affected the susceptibility to *Bgh* penetration in a leaf-age dependent manner. To get a better understanding of the role of *HvRBOHF* genes in the post-penetration stages of *Bgh* infection, the powdery mildew disease progression was further analysed. Originally, the number of colonies per leaf area and the size of *Bgh*-colonies were evaluated on detached leaves of 17-day-old plants 96 hpi with *Bgh*. First, the colonies were counted in green leaves. The same leaves were subsequently fixed, destained, and the fungal mycelium was stained with blue ink and the number of developing colonies was again counted, now including microcolonies (elongated secondary hyphae without sporulation). On green tissue, the number of *Bgh* colonies per leaf area was reduced in first and second leaf levels of *HvRBOHF2* KD plants compared to the azygous control (Supplementary Fig. S10). On destained leaves, even though there was a large variability within each leaf, especially in *HvRBOHF2* KD plants, a strong tendency of reduced *Bgh* colonization in leaves of the KD line was also observed. Likewise, in the independent *HvRBOHF2* KD line E06, the number of *Bgh*-colonies per leaf area in fixed first leaves showed a tendency of reduction, but was comparable between the third leaves of both genotypes (Supplementary Fig. S11). Regarding to the size of the colonies, the longitudinal length of *Bgh*-colonies on the surface of *HvRBOHF2* KD leaves was highly variable as noted by the range of the whiskers of the box plots. Despite this, *Bgh*-colony length was significantly smaller on the surface of all tested leaves of both *HvRBOHF2* KD lines E08 and E06 compared to azygous controls (Supplementary Fig. S12).

As previously mentioned *HvRBOHF2* KD plants showed de-regulated PCD processes. Therefore, reduced *Bgh*-development in leaves of *HvRBOHF2* KD plants could result from a cell death phenotype triggered by cutting the leaves for the detached leaf assays. To test if the silencing of *HvRBOHF2* KD has a direct effect on *Bgh* colonization, I also investigated the progression of the disease in intact 17-day-old plants (Fig. 10). Similar to observations from detached leaves, I observed a reduction of over 70% in the number of colonies per leaf area in older first leaf of *HvRBOHF2* KD in comparison with azygous plants (Fig. 10A). Nonetheless, regarding the younger third leaf, no substantial differences in *Bgh*-colonization efficiency between KD and azygous plants was noticeable. However, when I again counted the number of colonies in fixed leaves, now including microcolonies, the differences in colony number in first leaves of *HvRBOHF2* KD compared to the azygous control became smaller (approximately 22%) and statistically insignificant (Fig. 10B).

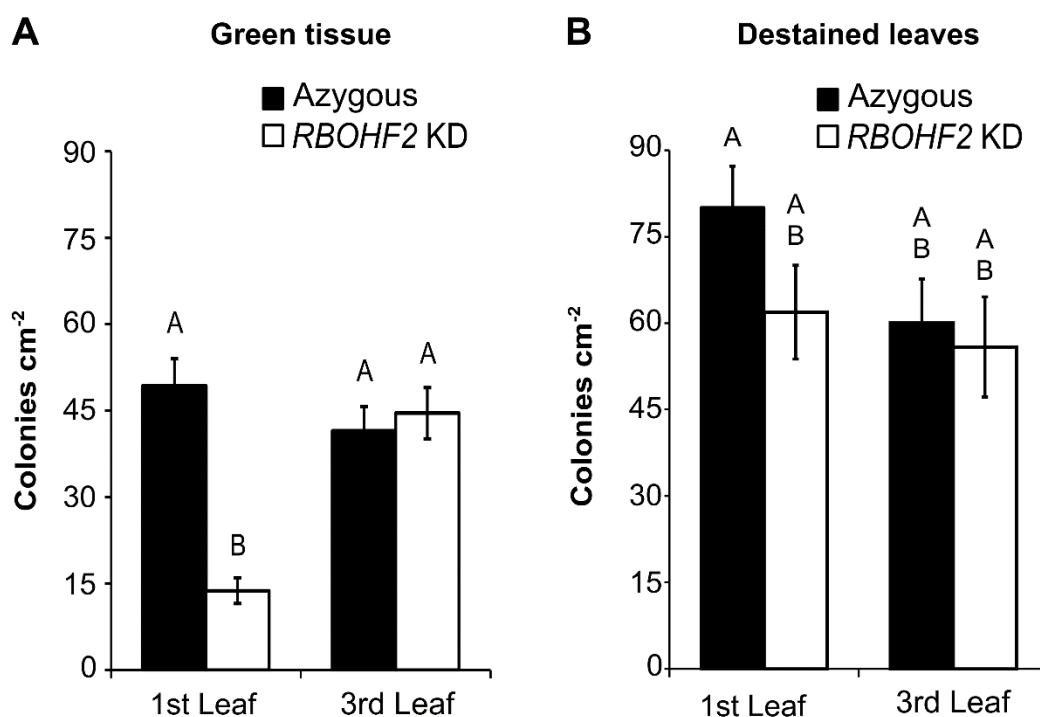


Figure 10: Effect of the silencing of *HvrBOHF* genes on the progression of the powdery mildew disease. Number of developing colonies per leaf area in 17 day-old-barley *HvrBOHF2* KD line E08 and the azygous controls. Colonies were quantified under a stereomicroscope in green tissue (A) or in fixed leaves (B). Plants were infected with *Bgh*, incubated for 96 hours in a climate chamber and individually harvested. Data represent the means of one representative experiment with five leaves per line. Data from the other two independent experiments are shown in Supplementary Fig. S13. Error bars show standard errors of the mean and letters the grouping of data sets according to Tukey's test at $P = 0.05$.

The difference between the counts in green versus fixed tissue could be explained by the fact that the *Bgh* colonies on *HvrBOHF2* leaves were much smaller, had fewer or no conidiophores and reduced hyphal branches compared to the azygous controls (Fig. 11). Therefore, the size of the *Bgh*-colonies was measured. It turned out that similar to detached leaves, colony length was reduced in all tested leaves of *HvrBOHF2* KD plants compared to the azygous controls. Moreover, the length of the *Bgh* colonies decreased from the third to the first leaf in *HvrBOHF2* KD plants but stayed the same in all tested leaves of azygous controls (Fig. 12).

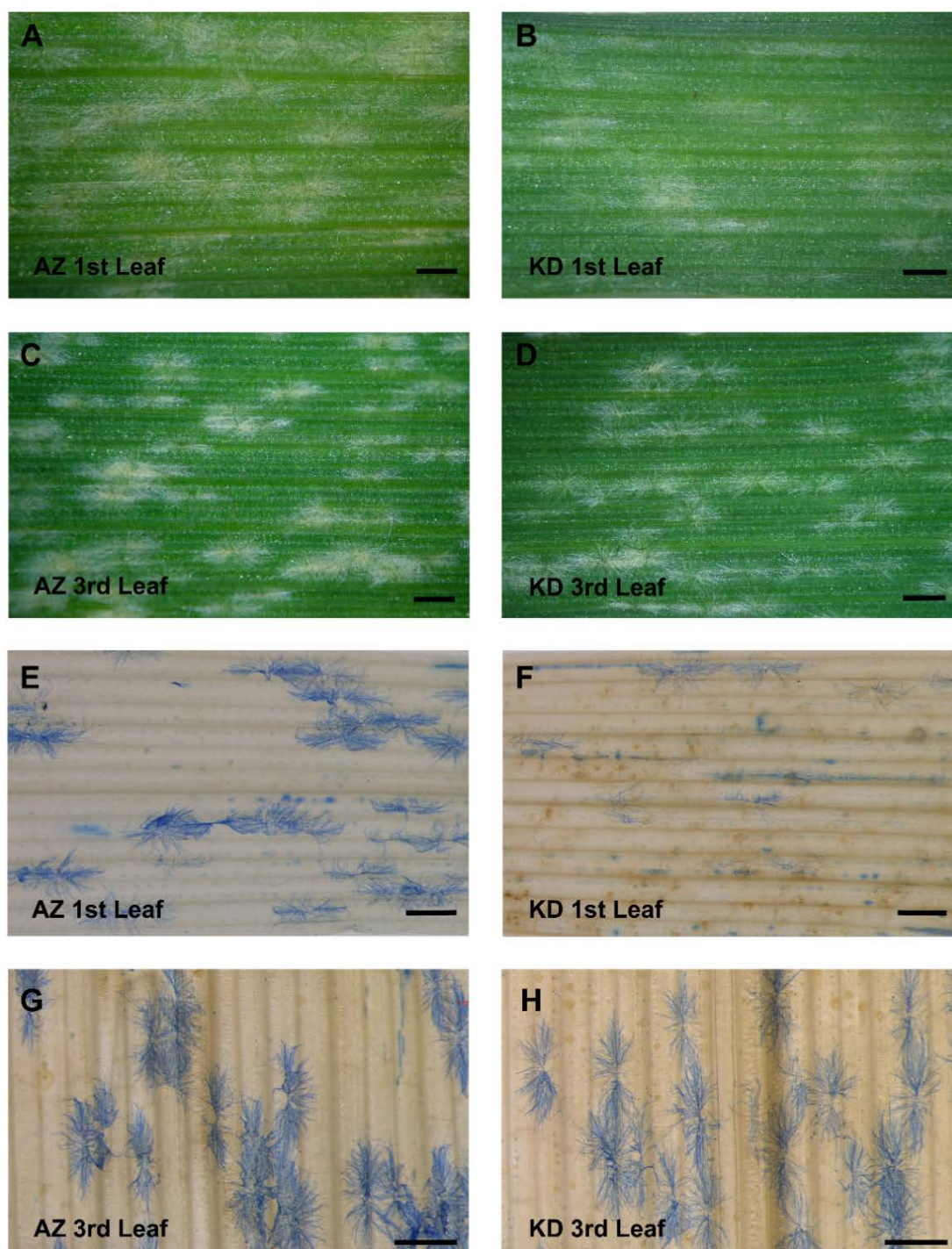


Figure 11: Growth of *Bgh* colonies on leaves of *HvrBOHF2* KD plants. Developing colonies of *Bgh* on the surface of the first leaf of 17 day-old-barley azygous (A) or *HvrBOHF2* KD plants (B). Developing colonies of *Bgh* on the surface of the third leaf of azygous (C) or *HvrBOHF2* KD plants (D). Plants were infected with *Bgh*, incubated for 96 hours in a climate chamber and photographed. Appearance of *Bgh* colonies on the surface of destained first leaf of azygous (E) and *HvrBOHF2* KD plants (F). *Bgh* colonies on the surface of destained third leaf of azygous (G) or *HvrBOHF2* KD plants (H). Leaves were fixed and prepared for inspection under a stereomicroscope. Bars represent 2 mm (A to D) or 1 mm (E to H). AZ, azygous; KD, *HvrBOHF2* KD plants.

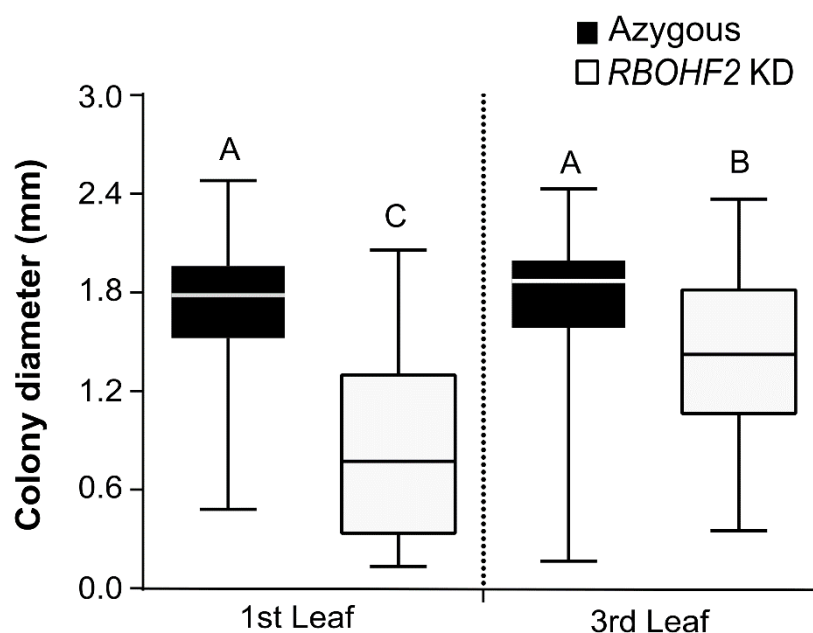


Figure 12: Size of *Bgh* colonies on leaves of *HvRBOHF2* KD plants Length of *Bgh* colonies on the surface of different leaves of 17-day-old barley *HvRBOHF2* KD line E08 and the azygous controls. Colony length was measured using the Leica LAS v4.5 software. Eighty pustules per line and leaf type were evaluated. Box- plots represent the median (horizontal line) and the interquartile range (box). Whiskers show the minimum and maximum measured values and letters the grouping of data sets according to Games-Howell test at $P = 0.05$. Data represent the means of one representative experiment. Data from the other two independent experiments are shown in Supplementary Fig. S14.

Similarly, in a second, independent *HvRBOHF2* KD line, the number of colonies per leaf area in destined first leaves of *HvRBOHF2* KD E6 plants was approximately 30% lower than in first leaves of the azygous control (Fig. 13A). Yet, due to the large variability within each leaf, this reduction was not significant. Besides this, the length of *Bgh*-colonies was also reduced in leaves of *HvRBOHF2* KD E06 plants in an age-dependent manner (Fig. 13B).

In conclusion, the reduction in the frequency of penetration in older leaves of *HvRBOHF2* KD plants did not led to a drastic reduction in the number of *Bgh*-colonies, but was related to a reduced growth of the pathogen on the leaf surface. Therefore, the silencing of *HvRBOHF* genes resulted in a delay in the progression of the powdery mildew disease.

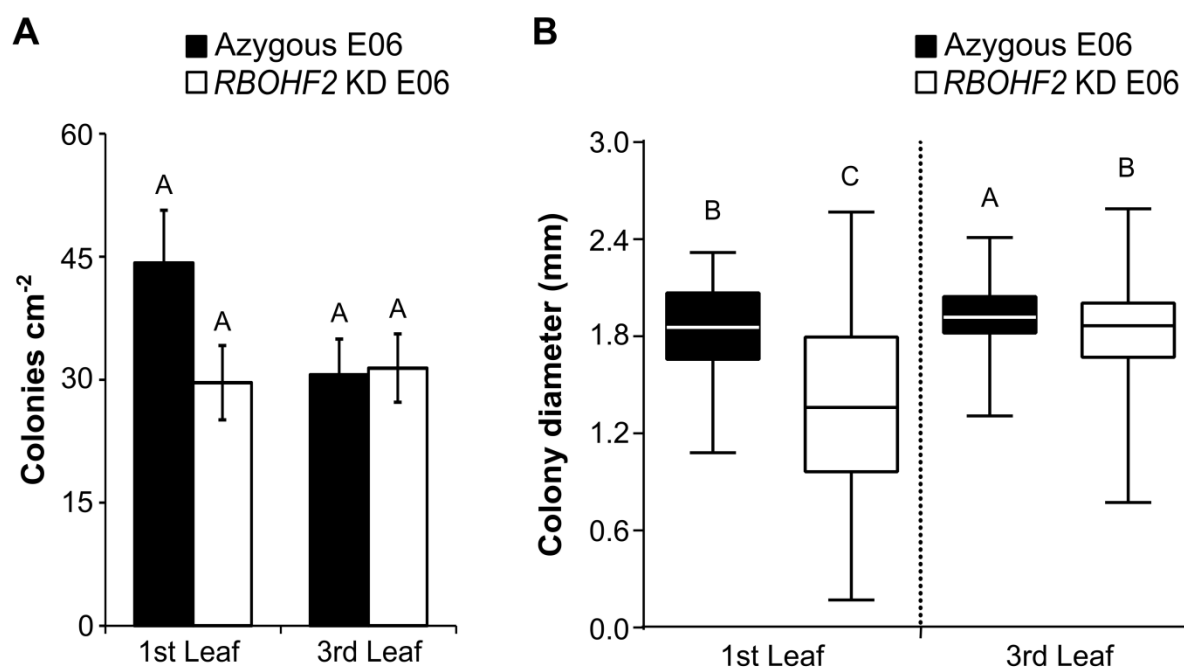


Figure 13: Effect of the silencing of *HvRBOHF2* KD on the progression of the powdery mildew disease in line E06. (A) Number of developing colonies per leaf area on the surface of leaves of 17-day-old-barley *HvRBOHF2* KD line E06 and the azygous control plants. Plants were infected with *Bgh* and incubated for 96 hours in a climate chamber. The leaves were fixed and prepared for inspection under a stereomicroscope. Data represent the means of one representative experiment with four to five leaves per line. Error bars show standard errors of the mean and letters the grouping of data sets according to Tukey's test at $P < 0.05$. (B) Length of *Bgh* colonies on the surface of different leaves of 17 day-old-barley *HvRBOHF2* KD line E06 and the azygous controls. Colony length was sized using the software Leica LAS v4.5. Eighty pustules per line and leaf type were evaluated. Box-plots represent the median (horizontal line) and the interquartile range (box). Whiskers show the minimum and maximum measured values and letters the grouping of data sets according to Games-Howell test at $P = 0.05$. Data from the other two independent experiments are shown in Supplementary Fig. S15.

3.3 Differentially expressed genes in *HvRBOHF2* KD plants during barley powdery mildew interaction

AtRBOHF is a crucial regulator of defence-related metabolism upon pathogen infection and the transcription levels of several genes are differentially regulated under oxidative stress in the *Atrboh* mutant (Chaouch *et al.*, 2012; Willems *et al.*, 2016). As depicted in the previous chapter and elsewhere, typical plant defence response triggered by powdery mildews in a resistant host, such as papilla formation and HR were quite similar between *HvRBOHF2* KD and azygous lines. Yet, *HvRBOHF2* KD plants showed mis-regulated cell death processes. Hence, to better understand the age-dependent susceptibility and spontaneous cell death phenotypes of KD lines, I checked if the expression of genes involved in regulation of PCD and barley defence responses was affected in the leaves of *HvRBOHF2* KD plants. Genes studied include NADPH-oxidase genes, cell death regulators, genes related to carbohydrate metabolism and *PR* genes. The gene expression was studied in different leaves of barley plants 48 hai with the barley powdery mildew fungus via reverse transcription semi-quantitative real-time PCR (RT-sqPCR). Transcript amount of genes with a clear pattern of regulation in *HvRBOHF2* KD plants or where the tendency was not clearly distinguishable in the RT-sqPCR assay were quantitatively assayed via reverse transcription quantitative real-time PCR (RT-qPCR) and the results are presented in the main body of this work. Initially, 11- and 17-day-old plants were sampled. However, obtaining high quality RNA from older leaves of 17-day-old *HvRBOHF2* KD plants turned out to be challenging, likely due to the necrosis shown by these leaves. Despite all attempts, all RNA samples from first leaves of *HvRBOHF2* KD plants obtained from independent experiments displayed a low RNA concentration and poor quality, and were therefore unsuitable for RT-qPCR analyses. For the second leaves it was only possible to obtain high quality RNA from both inoculated and non-inoculated samples in one experiment. For young leaves of *HvRBOHF2* KD plants and all leaves of the azygous line, high quality RNA was extracted of all samples and all experiments. Therefore, gene expression in first and second leaves of 11-day-old *HvRBOHF2* KD plants was alternatively investigated. In addition, the expression of selected genes was also studied in second and third leaves of 17-day-old plants and the results are shown in the supplements because the data from second leaves of *HvRBOHF2* KD plants was not replicated three times.

3.3.1 Expression of *HvRBOHF* genes

Besides a strong reduction in the expression of *HvRBOHF2*, *HvRBOHF2* KD plants also exhibited a decreased expression of *HvRBOHF1*, a closely related isoform that shares 91%

amino acid identity with *HvRBOHF2* (Lightfoot *et al.*, 2008; Proels *et al.*, 2010). To gain a better understanding of the age-regulated susceptibility to barley powdery mildew shown by *HvRBOHF2* KD lines, the expression of *HvRBOHF* genes were studied in different leaves of those barley transgenic plants. A robust reduction in the amount of both *HvRBOHF1* and *HvRBOHF2* transcripts was observed in *HvRBOHF2* KD plants in all leaf samples tested when compared to corresponding azygous controls (Fig. 14 and Supplementary Fig. S16). The basal expression of *HvRBOHF1* seemed higher in older first leaves of both genotypes, but this pattern of regulation was not reproducible (Fig. 14A and Supplementary Fig. S16A). On the other hand, basal expression of *HvRBOHF2* was higher in second, physiologically younger leaves of *HvRBOHF2* KD and the degree of silencing of *HvRBOHF2* was stronger in the first, compared to the second leaf. Hence, younger leaves of 11-day-old *HvRBOHF2* KD plants have a stronger residual expression of *HvRBOHF2* compared to older, less susceptible first leaves (Fig. 14B and Supplementary Fig. S16B).

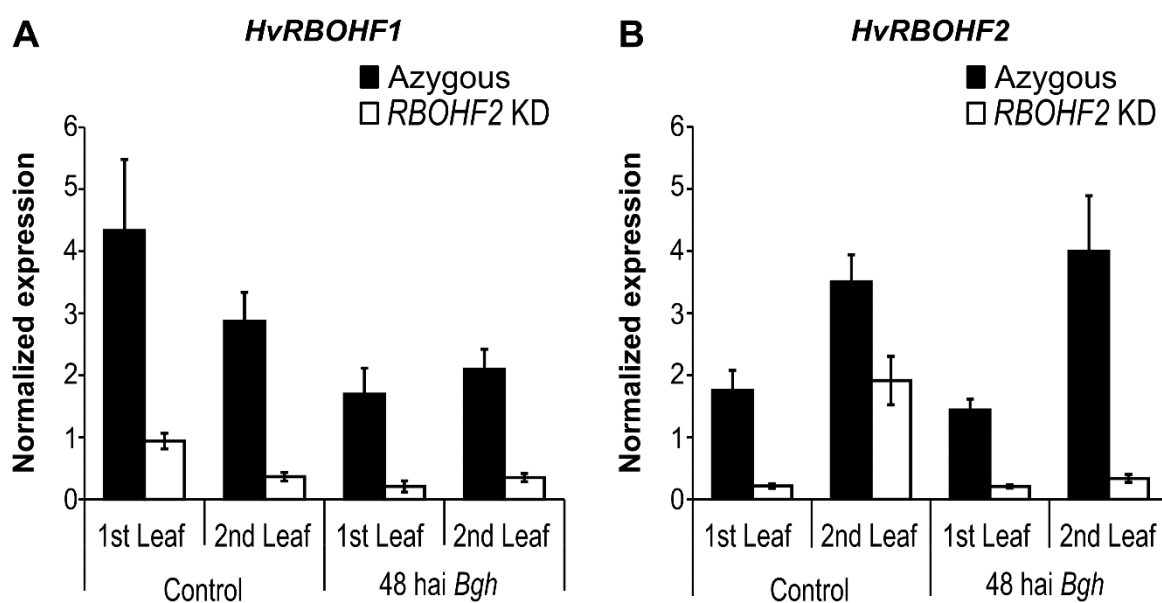


Figure 14: *HvRBOHF2* expression decreases with leaf-age. Relative expression levels of barley *HvRBOHF1* (A) and *HvRBOHF2* (B) in first and second leaves of 11-day-old plants of the *HvRBOHF2* KD line E08 and the corresponding azygous control. Total RNA was extracted from a pool of three to four leaves of barley plants 48 hai from non-inoculated or *Bgh*-inoculated leaves. RNA was reverse transcribed and subjected to real-time PCR analysis. Gene expression was measured relative to the expression of the reference gene barley MONOUBIQUITIN-LONG-TAIL FUSION 1 (*HvMub1*). Data represent the means of three technical repetitions from one representative experiment out of three independent biological experiments with similar results. Error bars show confidence intervals of the means ($n = 3$) at $P = 0.05$.

The expression of *HvRBOHF1* was down-regulated in both first and second leaves of inoculated azygous control plants compared to non-inoculated plants. However, in *HvRBOHF2* KD plants, although a *Bgh*-induced reduction in the residual expression of *HvRBOHF1* was observed in some of the independent experiments, this pattern was not consistent (Fig. 14A and Supplementary Fig. S16A). Likewise, *Bgh*-infection seemed to trigger a down-regulation in the residual *HvRBOHF2* transcript amounts in second leaves of *HvRBOHF2* KD plants. However, this trend was not consistent throughout the three independent experiments. Therefore, it was concluded that there was no *Bgh*-induced differential expression of *HvRBOHF2* in leaves of either barley genotypes at 48 hai (Fig. 14B and Supplementary Fig. S16B).

HvRBOHF2 transcripts were also reduced in 17-day-old *HvRBOHF2* KD plants when compared to corresponding azygous controls (Supplementary Fig. S17). Interestingly, basal transcript level of *HvRBOHF2* in the older second leaf were 1.6-to 3.9-fold lower than in younger third leaves of azygous controls. Moreover, compared to 11-day-old plants, *HvRBOHF2* basal expression in second leaves was down-regulated in 17-day-old of azygous plants. In addition, compared to non-inoculated plants, the expression of *HvRBOHF1* was reduced in the younger third leaf of both genotypes, reaching up to a 76% reduction in *HvRBOHF2* KD plants and 77% in azygous controls.

Taken together, *HvRBOHF* genes showed a robust silencing in all leaves of *HvRBOHF2* KD plants. The expression of *HvRBOHF1* did not differ between the leaves of 11-day-old plants. However, *HvRBOHF2* expression was leaf-age dependent, with the transcript amount of the gene being higher in physiological younger leaves than in physiological older leaves. Furthermore, *Bgh*-infection induced a down-regulation in the expression of *HvRBOHF2* in young leaves of old barley plants at 48 hai.

3.3.2 Expression of senescence markers and cell death regulatory genes

Yellowing or bleaching are the first visible markers of leaf senescence, but by the time this symptom is observed, the majority of senescence processes has already occurred. To have a better understanding of the senescence status in *HvRBOHF2* KD, the expression of barley senescence markers was studied in leaves of these plants via RT-sqPCR (Supplementary Fig. S18). The senescence-associated gene *HvS40* is a nuclear protein with unknown function whose expression is also induced upon pathogen infection in leaf sectors undergoing chlorosis (Krupinska *et al.*, 2002). Basal expression of *HvS40* was prominent in first leaves of 11-day-old *HvRBOHF2* KD plants, while *HvS40* transcript levels were very low and almost undetectable in all tested leaves of azygous control plants and second leaves of *HvRBOHF2* KD plants. *HvS40* transcript abundance increased in response to *Bgh*

inoculation in all tested leaves of both genotypes, but the expression of this gene was stronger in *HvRBOHF2* KD plants. On the other hand, expression of the two AUTOPHAGY-RELATED (ATG) genes *HvATG7* and *HvATG8_2* (*HvATG8A*) did not seem to be affected by the silencing of the *HvRBOHF* genes. *HvATG7* and *HvATG8_2* are part of the Atg8 ubiquitination-like system, involved in phagophore expansion, and therefore, essential for autophagosome formation during autophagy (Avila-Ospina *et al.*, 2014). Basal expression of *HvATG7* was slightly higher in older leaves than in younger leaves of 11-day-old plants but similar between the corresponding leaves of the genotypes. Following *Bgh*-inoculation, the amount of *HvATG7* transcript slightly decreased in first leaves of both *HvRBOHF2* KD and azygous plants, but remains the same in second leaves. Therefore, in inoculated plants the expression of *HvATG7* did not strongly differ between the tested leaves. Additionally, the *HvATG8_2* transcript amount was quite similar among all tested leaves in both non-inoculated and inoculated samples.

PCD requires a fine tuned coordination in the expression of genes involved in activation and regulation of the different types of cell death. Because *HvRBOHF2* KD plants showed de-regulated cell death processes, I checked the expression of barley homologues of genes with a well-known function in the regulation of plant PCD during senescence and in response to biotic and abiotic stresses, namely *HvMlo*, *HvBI-1*, *HvLsd1a* and *HvCBC04043* (Keisa *et al.*, 2008; Eichmann *et al.*, 2010) (Fig.15 and Supplementary Fig. S19). There was no consistent pattern of regulation of *HvMlo* in neither first nor second leaves of non-inoculated 11-day-old *HvRBOHF2* KD plants. Therefore, I assumed that basal transcripts of *HvMlo* did not differ between *HvRBOHF2* KD and azygous control plants. *Bgh*-infection induced an up-regulation in *HvMlo* expression in all leaves tested. Nevertheless, *HvMlo* transcripts amounts were higher in inoculated *HvRBOHF2* KD plants compared to the azygous control (Fig.15A and Supplementary Fig. S19B). On the other hand, basal expression of *HvBI-1* was 3-fold higher in first leaves of non-inoculated 11-day-old *HvRBOHF2* KD plants than in the corresponding leaves of the azygous line. In second leaves, the *HvBI-1* basal expression was similar between the genotypes. Upon *Bgh*-inoculation, a consistent up-regulation of *HvBI-1* was noticed in second leaves of azygous plants, but for the other leaves, no consistent tendency was found (Fig. 15B and Supplementary Fig. S19B). *HvLsd1a* transcript amounts were similar between the corresponding leaves of *HvRBOHF2* KD and azygous plants in both control and inoculated plants (Fig. 15C and Supplementary Fig. S19C). However, *HvCBC04043* transcript amounts in first leaves of *HvRBOHF2* KD plants were lower than in the azygous control. Additionally, despite the basal expression of *HvCBC04043* was higher in the second leaf of KD plants in some of the independent experiments, this pattern was not fully consistent (Fig. 15D and Supplementary Fig. S19D).

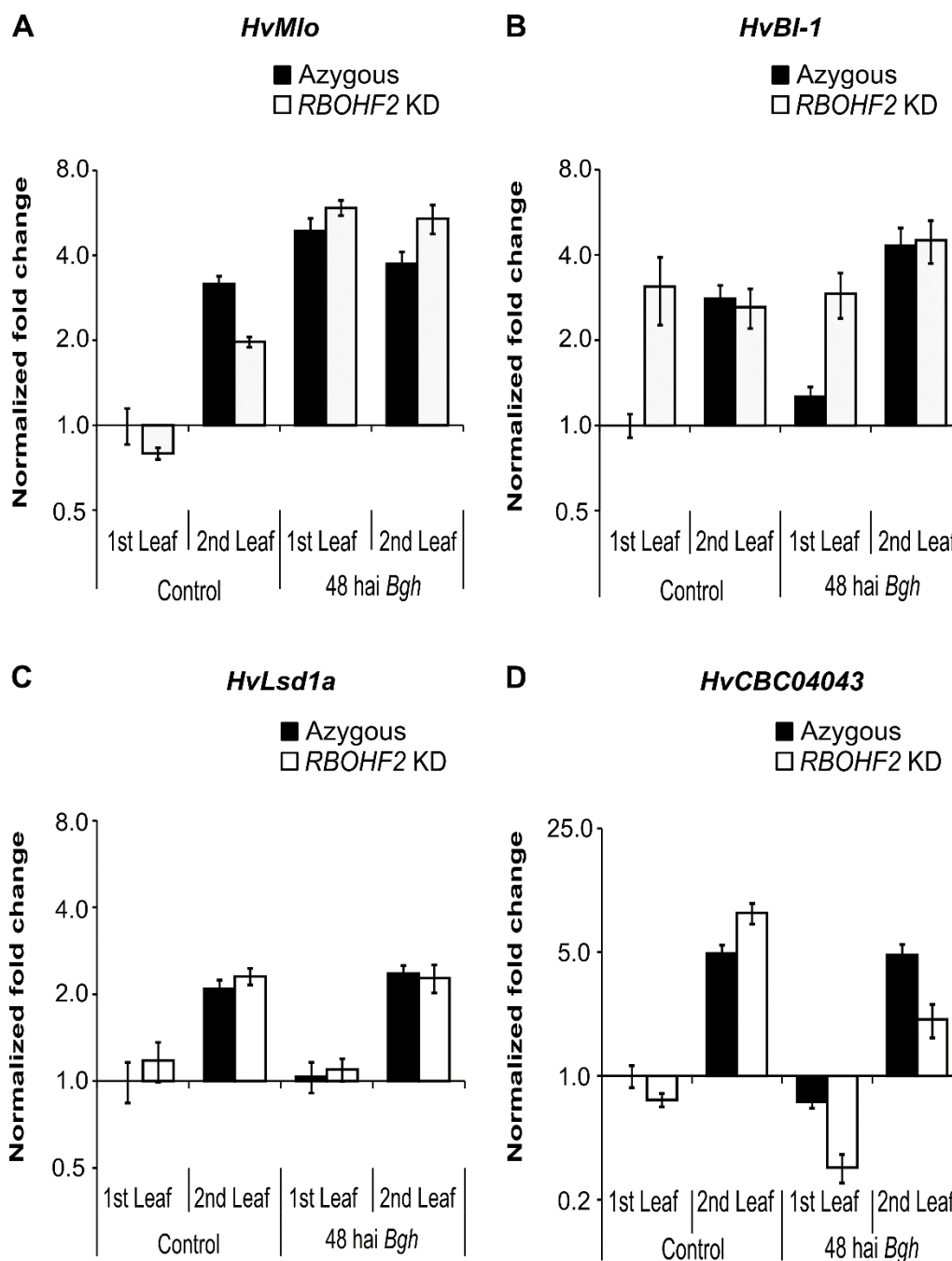


Figure 15: Expression of cell death regulator genes were affected in *HvRBOHF2* KD plants. Relative expression levels of barley (A) *HvMlo*, (B) *HvBI-1*, (C) *HvLsd1a* and (D) *HvCBC04043* in first and second leaves of *HvRBOHF2* KD line E08 and the corresponding azygous control. Total RNA was extracted from a pool of three to four leaves of 11-day-old barley plants 48 hai from non-inoculated or *Bgh*-inoculated leaves. The cDNA was synthesized and afterwards subjected to real-time PCR analysis. Expression of the target genes was measured relative to the expression of the reference gene barley MONOUBIQUITIN-LONG-TAIL FUSION 1 (*HvMub1*) and normalized to the values of the first non-inoculated leaf. Data represent the means of three technical repetitions from a representative experiment out of three independent experiments. Error bars show confidence intervals of the means (n=3) at P= 0.05.

Compared to non-inoculated plants, the expression of *HvCBC04043* was reduced by 58% in first and 75% in second leaves of *HvRBOHF2* KD plants infected with *Bgh*. In azygous plants, a *Bgh*-induced down-regulation of *HvCBC04043* was also observed in first leaves, but in second leaves, the pattern was not consistent (Fig. 15D and Supplementary Fig. S19D).

Taken together, these results show that silencing of *HvRBOHF* genes affects the expression of cell death regulator genes.

3.3.3 Expression of genes related to carbohydrate catabolism

I also studied the expression of genes related to the catabolism of carbohydrates, focusing on genes involved in the hydrolysis of sucrose. The basal transcript amounts of *HvCwINV1* were higher in leaves of *HvRBOHF2* KD plants than in the azygous control. Moreover, after *Bgh*-inoculation, *HvCwINV1* expression was down-regulated in both leaves of the two genotypes (Supplementary Fig. S18). Besides this, the basal expression of *HvCwINV3*, another isoform of cell wall invertase, was higher in second leaves of both non-inoculated and inoculated *HvRBOHF2* KD plants in comparison to second leaves of the azygous line (Fig. 16A and Supplementary Fig. S20A). In contrast to this, expression of the barley *INVERTASE INHIBITOR 1 (HvINVINH1)* did not show any obvious pattern of regulation and seemed similar among all tested leaves (Supplementary Fig. S18).

Similarly, the basal expression of *HvADH1* did not show a clear pattern or was non-reproducible (Fig. 16B and Supplementary Fig. S20B). Despite the basal expression of this gene being lower in first leaves of KD plants in some of the independent experiments, this pattern was not consistent. Besides, in second leaves, the expression of the gene in KD plants did not show any clear trend. *Bgh*-inoculation triggered a consistent up-regulation in the expression of *HvADH1* in second leaves of azygous plants. However, for the other leaves tested this trend was not observed and/or not reproducible.

In short, expression patterns of some genes related to carbohydrate catabolism were altered in *HvRBOHF2* KD plants, especially those genes involved in the degradation of sucrose.

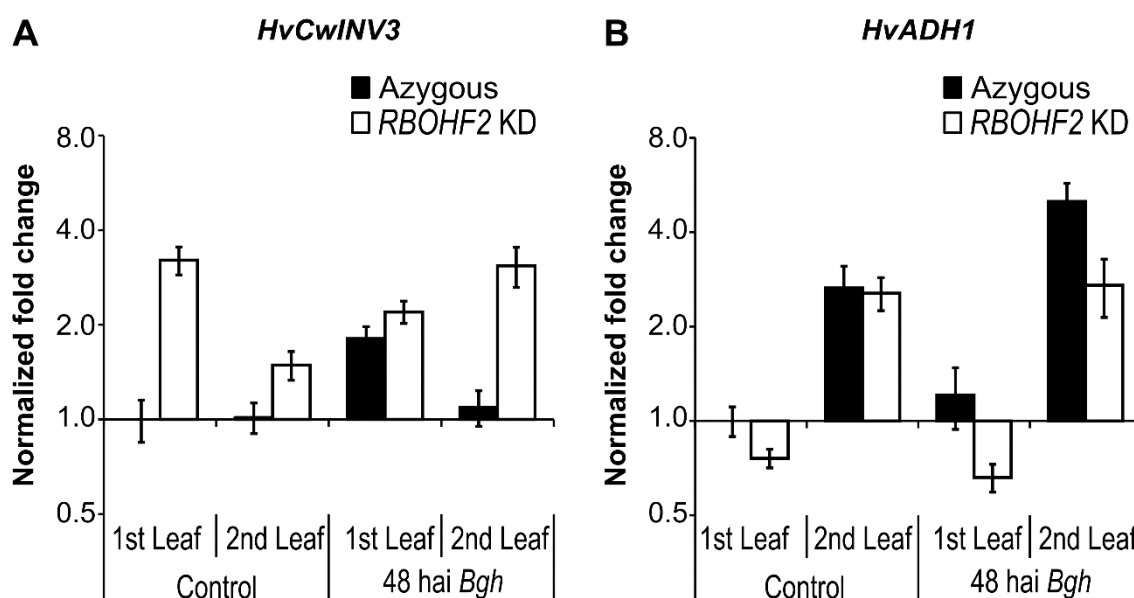


Figure 16: Expression of genes related to carbohydrate catabolism was altered in *HvRBOHF2* KD plants. Relative expression levels of barley (A) *HvCwINV3* and (B) *HvADH1* in first and second leaves of the *HvRBOHF2* KD line E08 and the azygous control. Total RNA was extracted from a pool of three to four leaves of 11-day-old barley plants 48 hai from non-inoculated or *Bgh*-inoculated leaves. The cDNA was synthesized and afterwards subjected to real-time PCR analysis. Expression of the target genes was measured relative to the expression of the reference gene barley MONOUBIQUITIN-LONG-TAIL FUSION 1 (*HvMub1*) and normalized to the values of the first non-inoculated leaf. Data represent the means of three technical repetitions from a representative experiment out of three independent experiments. Error bars show confidence intervals of the means (n=3) at P= 0.05.

3.3.4 Expression of *PR* genes

PR proteins are involved in defence responses during plant pathogen interactions and possibly in leaf senescence-associated cell death, as accumulation of these proteins at advanced stages of development have been reported for some plant species including barley (Tamás *et al.*, 1998; Lim *et al.*, 2007). To check whether the pathogenesis-/early senescence-phenotypes of *HvRBOHF2* KD plants are related to a differential expression of *PR* genes, the expression level of *HvPR1b* was investigated in 11- and 17-day-old plants by RT-qPCR. Additionally, the *PR* genes *HvPR3*, *HvPR5* and *HvPR10* were studied in 11-day-old plants (Fig. 17). A constitutive over-expression of the all tested *PR* genes was noticed in the first leaf of non-inoculated 11-day-old *HvRBOHF2* KD plants in all three independent experiments. This constitutive *PR* gene expression was much less prominent and inconsistent in second leaves of *HvRBOHF2* KD plants, indicating an increase in the *PR* gene expression with the progression of leaf age (Fig. 17 and Supplementary Fig. S21).

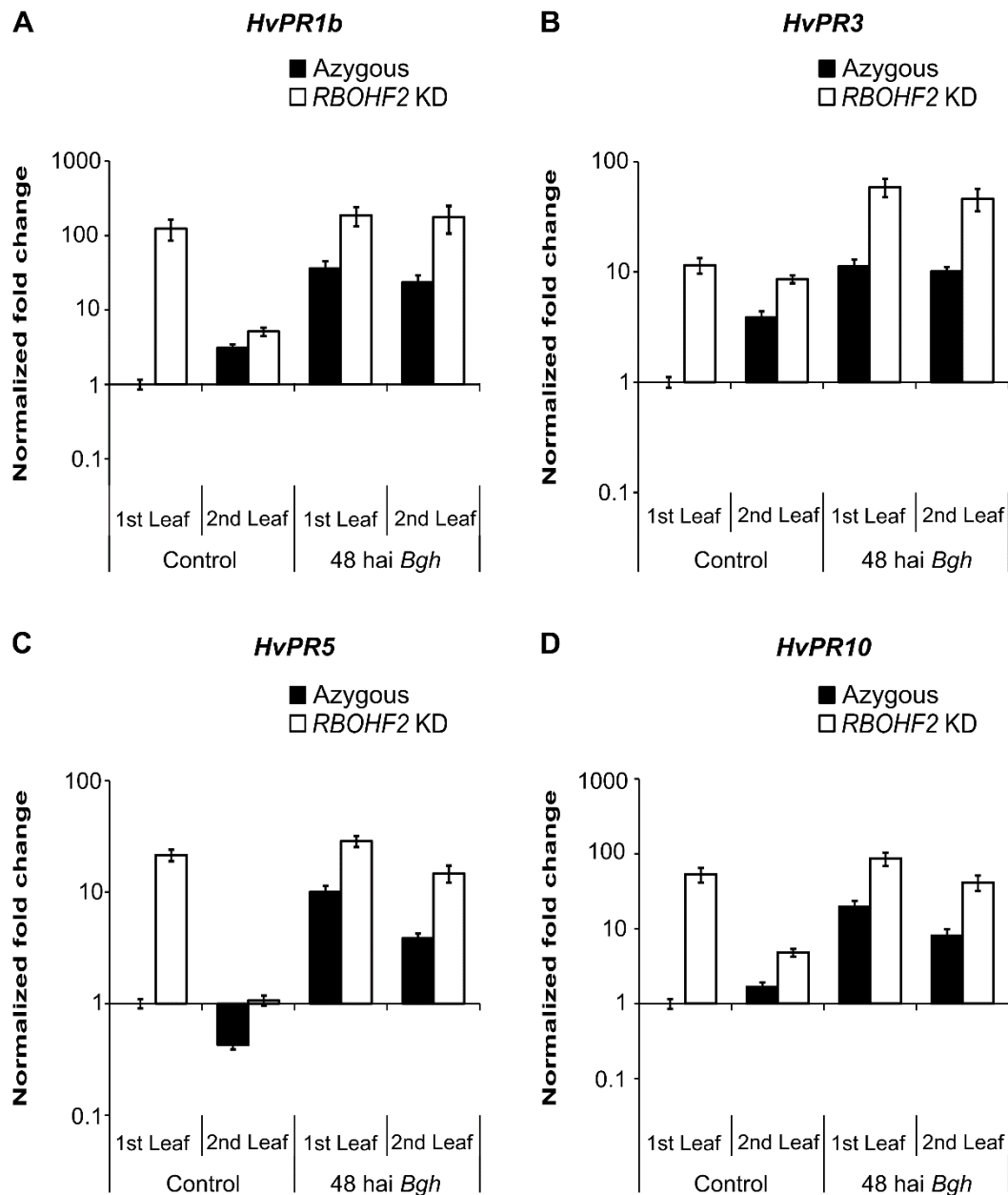


Figure 17: PATHOGENESIS-RELATED (PR) gene expression is enhanced in *HvRBOHF2* KD lines. Relative expression levels of barley *HvPR1b* (A), *HvPR3* (B), *HvPR5* (C) and *HvPR10* (D) in first and second leaves of *HvRBOHF2* KD line E08 and the azygous control. Total RNA was extracted from a pool of three to four leaves of 11-day-old barley plants 48 hai from non-inoculated or *Bgh*-inoculated leaves. The cDNA was synthesized and afterwards subjected to real-time PCR analysis. Expression of the target genes was measured relative to the expression of the reference gene barley MONOUBIQUITIN-LONG-TAIL FUSION 1 (*HvMub1*) and normalized to the values of the first non-inoculated leaf. Data represent the means of three technical repetitions from a representative experiment out of three independent experiments. Error bars show confidence intervals of the means (n = 3) at P = 0.05.

Following inoculation with *Bgh*, the expression of *HvPR3*, *HvPR5* and *HvPR10* was strongly induced in both genotypes and leaves tested. In general, *Bgh*-inoculated *HvRBOHF2* KD plants showed much higher levels of *PR* gene expression compared to corresponding azygous plants. The basal expression of *PR* genes was already very strong in the first leaves of *HvRBOHF2* KD plants in the first independent experiment (20 to over 100-fold constitutive overexpression; Fig. 17) and the level of constitutive *PR* gene expression was not further elevated by *Bgh*-inoculation. It seems in these leaves the expression of *HvPR1b*, *HvPR5* and *HvPR10* has already reached their maxima in non-inoculated leaves. Additionally, no differences were detectable in the expression of *HvPR1b* and *HvPR3* between first and second leaves within each of the genotypes in *Bgh*-infected plants. Hence, the strong *Bgh*-related stimulus overrode developmental differences in *PR* genes expression.

Similarly, *HvPR1b* was constitutively over-expressed in 17-day-old KD plants. Compared to the azygous control, there was a 900-fold increase in second and 2.2- to 19-fold increase in third leaves in the expression of this gene in non-inoculated *HvRBOHF2* KD plants (Supplementary Fig. S22). In addition, the expression of *HvPR1b* was greater in older second leaves than younger third leaves of *HvRBOHF2* KD plants. On the other hand, in azygous plants, *HvPR1b* expression was usually higher in younger third leaves. Furthermore, transcript amounts of *HvPR1b* were higher in *Bgh*-inoculated second and third leaves of *HvRBOHF2* KD plants compared to the azygous control.

These results indicate that the basal expression of *PR* genes was enhanced in *HvRBOHF2* KD plants compared to azygous plants in a leaf-age dependent manner. In addition, transcript abundance of *PR* genes increased in response to *Bgh* inoculation in all tested leaves of both genotypes, but the expression of this gene was stronger in *HvRBOHF2* KD plants.

3.3.5 SA contents in leaves of *HvRBOHF2* KD plants

To determine whether the constitutive expression of *PR* genes and the spontaneous cell death phenotype in older leaves of *HvRBOHF2* KD lines are associated with changes in the content of SA, I analysed the SA content in different leaves of 17-day-old plants. SA was detected by HPLC and fluorescence detection. The retention time was between 8.2 and 8.7 min for SA and between 10.4 and 11.2 min after injection of the internal standard o-anisic acid. SA was found as free (FSA) and conjugated (CSA) forms and their levels were very variable within independent experiments, especially in leaves of KD plants. Surprisingly, an increase in the content of two unknown compounds with a retention time close to SA and to the internal standard was noticed in all samples of the first leaves of *HvRBOHF2* KD (both non-inoculated and inoculated) in the HPLC chromatograms of FSA. These compounds were

not detected in the chromatograms of CSA and their content was considerably lower in the third leaves of the KD line (except for the third biological replicate) and in both leaves of the azygous control (Supplementary Fig. S23).

Only a modest, non-significant, increase in the basal levels of both FSA and conjugated SA (CSA) forms was noticed in young (third) leaves of *HvRBOHF2* KD plants compared to azygous controls (Fig. 18). However, the SA content in older (first) leaves of *HvRBOHF2* KD plants was approximately nine-fold higher for FSA and 48-fold for CSA, compared to azygous controls. Interestingly, basal FSA levels corresponded to 9% of the total SA content in first leaves of *HvRBOHF2* KD plants while in azygous plants this amounted to 31% of the total SA content. In third leaves of both genotypes, basal FSA levels amounted to approximately 16% of the total SA. Moreover, the SA content was higher in older leaves than in younger leaves of *HvRBOHF2* KD plants, while it was similar between leaf levels of azygous plants.

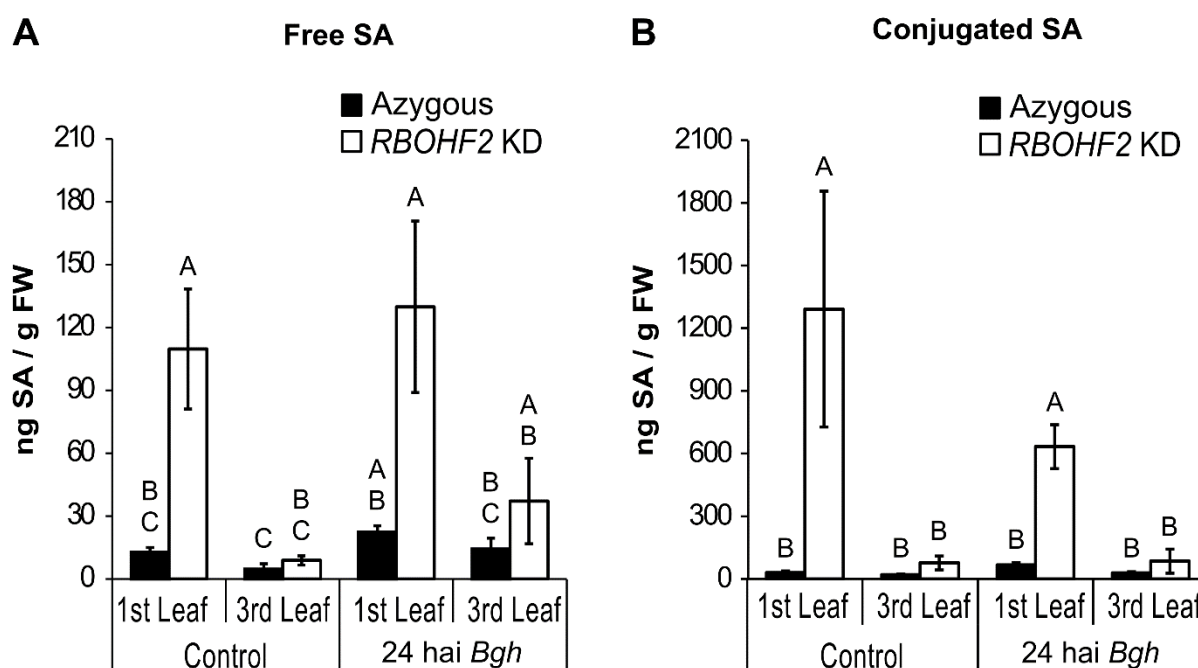


Figure 18: Effect of the silencing of *HvRBOHF2* KD on the endogenous levels of salicylic acid (SA). Free (A) and conjugated (B) levels of SA in first and third leaves of 17-day-old plants of the *HvRBOHF2* KD line E08 and the azygous control. SA was extracted from a pool of four to five leaves of barley plants 24 hai from non-inoculated or *Bgh*-inoculated leaves. SA content was determined by HPLC and fluorescence detection. Data represent the means of three independent experiments. Error bars show standard errors of the mean and letters the grouping of data sets according to Tukey's test at $P = 0.05$. FW, fresh weight; FSA, free salicylic acid; CSA, conjugated salicylic acid.

Bgh infection did not trigger significant SA accumulation in any of the tested leaves or genotypes. These results show a coincidence of higher SA contents in older leaves of *HvRBOHF2* KD barley lines with early senescence-associated cell death, *PR* gene expression and higher resistance to *Bgh*.

3.4 Susceptibility of *HvRBOHF2* KD plants to other fungal pathogens

So far I was concentrating on the pathosystem barley *HvRBOHF2* KD plant-barley powdery mildew. To gain a broader knowledge of the role of barley *RBOHF* genes during disease resistance to fungal pathogens, I studied the outcome of the interaction of *HvRBOHF2* KD plants with two additional pathogens: *B. sorokiniana*, the barley spot blotch fungus, and *F. culmorum*, one of the causal agents of the Fusarium head blight (FHB) and foot diseases (Kumar *et al.*, 2002; Scherm *et al.*, 2013).

3.4.1 Susceptibility to *B. sorokiniana*

The susceptibility to *B. sorokiniana* (*Bs*) was assessed in spray-inoculated leaves of 17-day-old transgenic barley plants 96 hai by the quantification of the number of the *Bs*-induced necrotic lesions. Additionally, lesions were grouped based in their longitudinal length in three classes, small (<1mm), medium (1-3mm) and large (>3mm; Fig. 19). Foliar spot blotches were rare and nearly invisible in first leaves of azygous control plants and indistinguishable from the spontaneous necrotic lesions in first leaves of the *HvRBOHF2* KD lines. Thus, just second and third leaves were examined. I observed a tendency towards a reduced number of lesions per leaf in the *HvRBOHF2* KD line E08 in comparison with the azygous control plants in both second and third leaves. Lesion numbers were 5.1 times lower in second and 6.9 times lower in third leaves of *HvRBOHF2* KD line E06 compared to azygous plants. This reduction was statistically significant (Fig. 19A).

Regarding the size of the lesions, compared with the azygous controls, the frequency of small lesions were slight higher in second and third leaves of *HvRBOHF2* KD line E08. Second leaves of KD plants, however, displayed approximately 30% less large lesions than azygous controls. In the line E06, this difference were even bigger, especially in the second leaves. Sixty-five percent of all necrotic lesions in second leaves of *HvRBOHF2* KD line E06 were small and only 5% were large. On the other hand, in azygous controls, 29% of the lesions were small and 38% were large. In third leaves, the frequency of small lesions was 54% in the KD line and 40% in azygous control plants. The frequency of large lesions very similar between the genotypes (Fig. 19B).

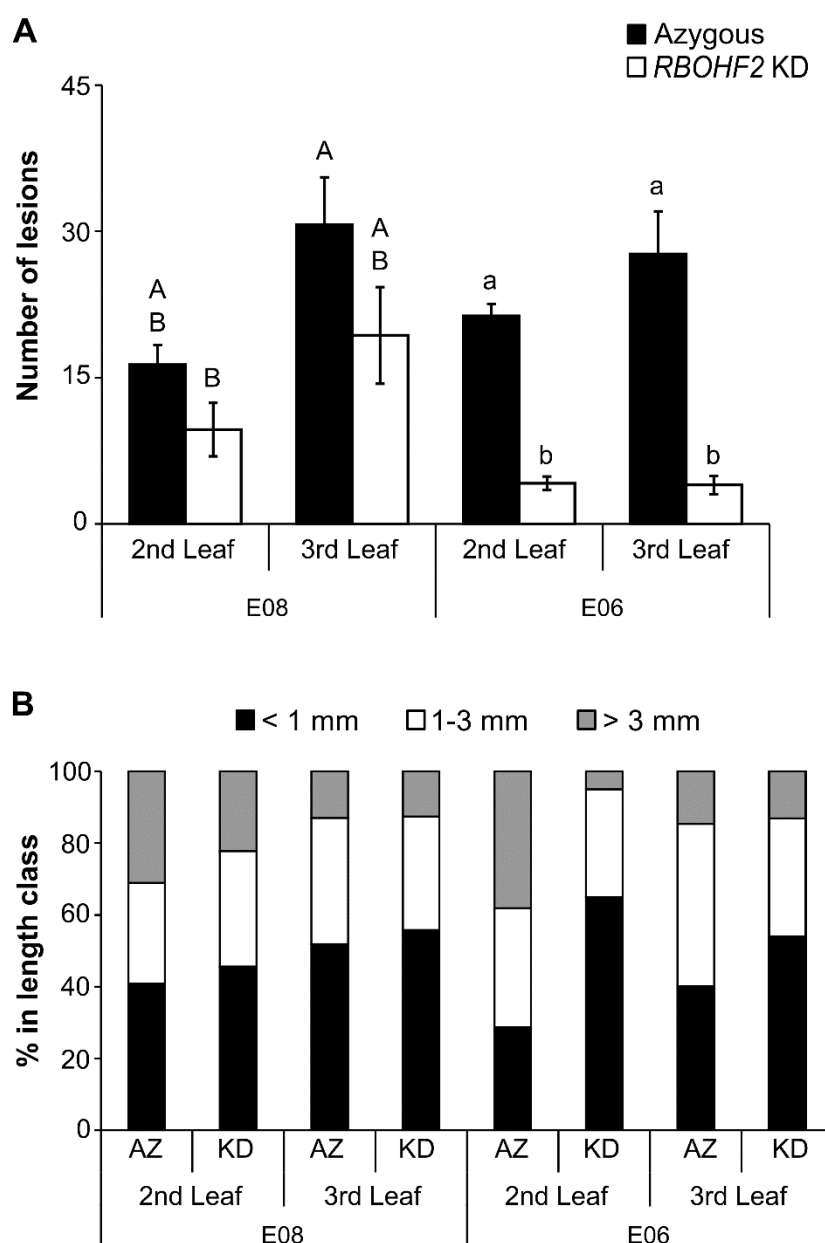


Figure 19: Silencing of *HvrRBOHF2* negatively affects the susceptibility to the hemibiotrophic pathogen *B. sorokiniana*. (A) Number of *Bs*-induced lesions per leaf in 17 day-old-barley *HvrRBOHF2* KD lines E08 and E06 and the azygous controls. Plants were spray-inoculated with *Bs*, incubated for 96 hours in a climate chamber and individually harvested. Lesions were quantified in fixed leaves under a stereomicroscope. Data represent the means of one representative experiment with six leaves per line. Data from the other two independent experiments are shown in Supplementary Fig. S24. Error bars show standard errors of the mean. Uppercase letters show the grouping of data sets relative to line E08 and lowercase to line E06 according to Tukey's test at $P = 0.05$. (B) Size of *Bs*-induced lesions. Lesions length was sized using the software Leica LAS v4.5 and grouped in three classes based on size: lesions smaller than 1 mm, lesions between 1 and 3 mm and lesions bigger than 3 mm. Data are representative of three fully independent experiments. In each experiment, 30 to 80 lesions per line and leaf level were evaluated. AZ: azygous; KD: *HvrRBOHF2* KD.

Interestingly, the number of lesions on second and third leaves of *HvRBOHF2* KD lines was very similar, especially in line E06. Nevertheless, second leaves of *HvRBOHF2* KD E08 had almost twice as many big lesions than third leaves of the same genotype. Intriguingly, in line E06 the opposite was observed. Second leaves had about 60% less big lesions than young third leaves. For azygous plants, a tendency of increased lesion numbers on the older second leaf in comparison with the younger third leaf was found. The number of big lesions was 2-fold higher in second leaves compared to third leaves of the azygous line E08 and 3-fold higher for azygous line E06.

In summary, *HvRBOHF2* KD plants are more resistant to the barley spot blotch disease than azygous controls. Additionally, *HvRBOHF2* KD line E08 and both lines of azygous control plants display a leaf-age dependent susceptibility to *Bs*. Compared to old second leaves, the number of lesions was increased in young third leaves. However, these lesions are much smaller.

3.4.2 Susceptibility to *F. culmorum*

In addition to the hemibiotrophic pathogen *Bs*, I also assessed the effect of silencing *HvRBOHF* genes on the interaction of barley and the hemibiotrophic pathogen *F. culmorum*. Leaves of 17-day-old transgenic barley plants were spray-inoculated with an aggressive strain of the pathogen (Linkmeyer *et al.*, 2013) and the inoculated plants were incubated in a growth chamber with 100% humidity. Seven days after inoculation, azygous plants did not show any symptom of a *Fusarium* infection and potential necrotic *Fc*-lesions in *HvRBOHF2* KD were indistinguishable from the spontaneous necrotic lesions shown by old leaves of those plants. In order to evaluate the susceptibility of KD plants to *Fusarium* infection, I quantified the relative amount of *Fc002* DNA in different leaves of barley via RT-qPCR. Even though the amount of fungal DNA varied between independent experiments, a trend could be observed. In all of the three independent experiments, an increase in the relative amount of *Fc002* DNA was observed in first leaves of *HvRBOHF2* KD plants of two independent lines compared to the corresponding leaves of the azygous controls (Fig. 20). This increased susceptibility to *Fc002* in oldest (first) leaves was even stronger in *HvRBOHF2* KD E06 plants, in which the relative amount of fungal DNA was 15- to over 20-fold higher than in azygous leaves. In second leaves, no tendency was found and the susceptibility to *Fc002* seemed to be similar between *HvRBOHF2* KD and azygous lines. On the other hand, in third leaves, I noticed a tendency of decreased levels of *Fc002* DNA in *HvRBOHF2* KD lines. In these leaves, the relative amount of fungal DNA was reduced by 10 to 50% in the *HvRBOHF2* KD line E08 compared to azygous plants. In line E06, this range for no-reduction at all to up to 80% reduction. Interestingly, an age-dependent

susceptibility to *Fc002* was visible in *HvRBOHF2* KD E06, where the relative fungal DNA amount increased from the third, to the second to the first leaf. However, the relative level of fungal DNA was similar between first and second leaves and lower in third leaves in line E08. Furthermore, the relative amounts of *Fc002* DNA between leaves of both azygous lines E06 and E08 did not show any consistent trend. Together, silencing of *HvRBOHF2* seemed to support susceptibility to *Fc* in older leaves.

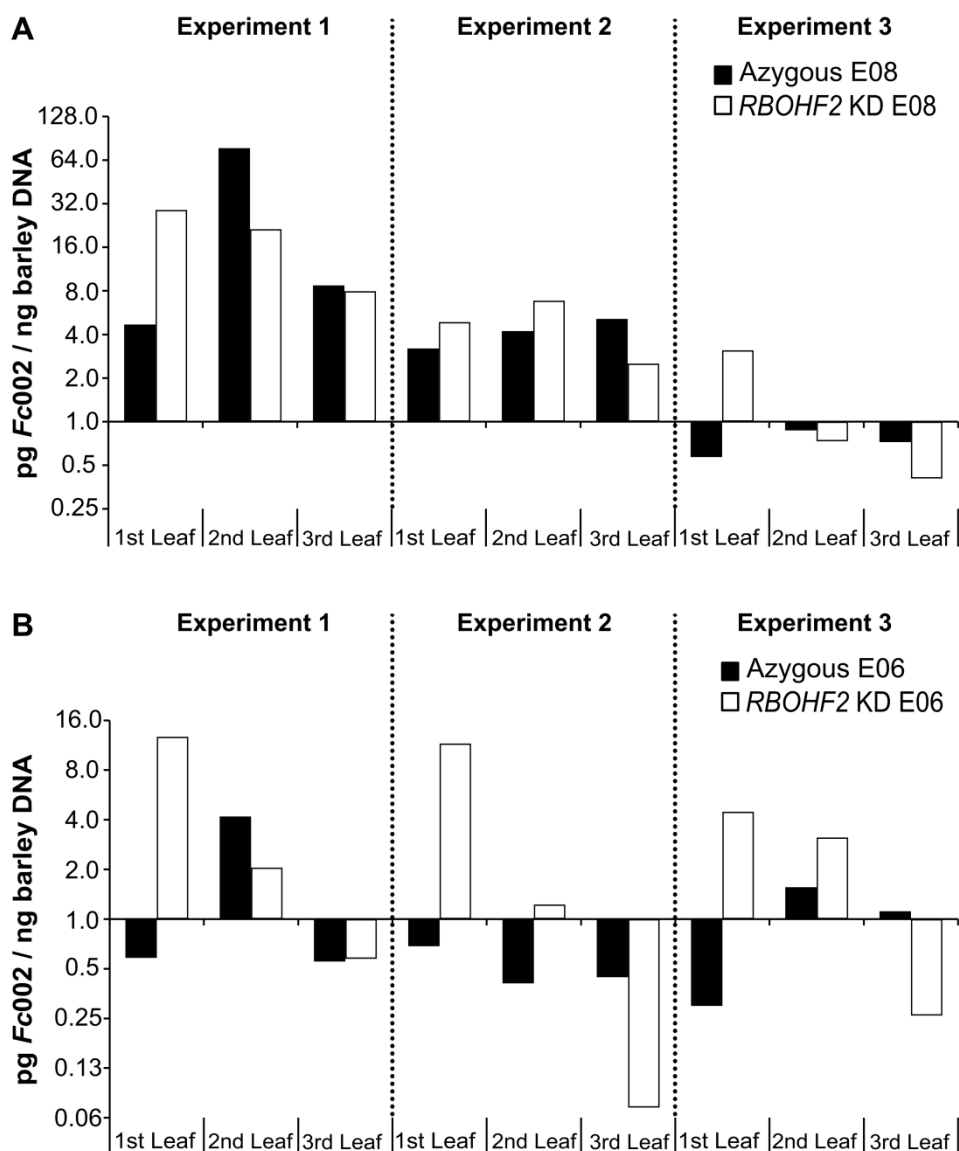


Figure 20: Silencing of *HvRBOHF2* affects the susceptibility to *F. culmorum*. Relative amount of *Fc002* DNA in distinct leaves of barley *HvRBOHF2* KD E08 (A) or E06 (B) and corresponding azygous lines. Plants were spray-inoculated with *Fc002*, incubated for seven days in a climate chamber and individually harvested. Fusarium infection was evaluated via quantification of the relative amount of fungal DNA in leaves of barley transgenic plants via RT-qPCR. Three biological replicates of each sample and one technical (PCR) replicate were performed.

3.5 Role of barley NADPH oxidase RBOHD in the susceptibility to *Bgh*

As previously mentioned, *AtRBOHD*, *AtRBOHF* and their functional homologues in other plant species have important functions during plant pathogen interactions. However, no functional homologue of *AtRBOHD* was found in the barley genome to date. Recently, a microarray dataset with transcriptome profiles of barley transgenic plants silenced or over-expressing a constitutively activated form of the RAC/ROP protein RACB, inoculated or mock inoculated with *Bgh* was published (Schnepf *et al.*, 2017). The data showed a strong expression of an uncharacterized gene (P_35_25908; AK366247) with similarity to a putative RBOH gene from rice in both a *HvRACB* over-expression line and WT plants 12 hai with *Bgh*. Compellingly, further analyses revealed a high similarity between this gene and the gene for RBOH type D of Arabidopsis. In this part of my work, I analysed the expression pattern of the putative *HvRBOHD* upon *Bgh*-infection, and its influence on the outcome of barley-powdery mildew interaction by TIGS (transient-induced gene silencing).

3.5.1 Characterisation of a new *HvRBOH* gene

The predicted amino acid (AA) sequence of the uncharacterized gene (Gene bank accession BAJ97450.1) consists of 916 AA with a molecular weight of 103kD and a pI of 9.29. In order to identify homologues of this gene, the protein sequence was used to perform a BLAST search against protein sequences available from National Center for Biotechnology Information (NCBI) web interface, using the BLASTP algorithm. The search revealed a relatively high similarity between BAJ97450.1 and RBOH isoform D from other plant species, including the well characterized *AtRBOHD* (NP_199602) from Arabidopsis (67% AA identity) and *OsRBOHB* (AAT35117.1) from rice (60% AA identity). When the protein sequence of the putative new *HvRBOH* gene was aligned with these proteins sequences, several conserved features of plant RBOH proteins were identified (Fig. 21).

<i>AtRBOHD</i>	MKMRRGNSSNDHELGLRGANSNTNSD-TEIASDRGAFSGPLGRPKRASKKNARFADDL	59
<i>OsRBOHB</i>	-----MADLEAGMVAATDQGNSTRSQDDAATLIPNSGNLGSNRS-----	41
<i>HvRBOHD</i>	MHNRAGGG-----GAGE-IVEAGERVVPHSGPLGGKRSAMRKSARFAESV	44
 ** * . :	
<i>AtRBOHD</i>	P-----KRSNSVAGGRGDDDEYVEITLDIRDDSVAVHSVQQAAGGGGHLEDP--ELALL	111
<i>OsRBOHB</i>	-----TKTARFKDDDELVEITLDVQRDSVAIQEVRGVDEGGSGHGTGFDGLPLV	90
<i>HvRBOHD</i>	SAPLTAPHGAPRGGGNDDDDDYVEITLDVRRDSSVAVHSVKPAAGGEDSD-----VKLL	98
	. ***: *****: *****:.*: . * . : **	
<i>AtRBOHD</i>	TKKTLESSLNNTTSLSFRRSTSSRIKNASRELRVFSR-----Rp-----SPAVRRFDRT	161
<i>OsRBOHB</i>	SPSSKSGKL-----TSKLRQVTNGLKMKSSSRKAPSPQAQQSAKRVRKRLDRT	138
<i>HvRBOHD</i>	AQT-LEKR-SSSYGQVLRNASTRIKQVSQLRRLASV-----NRRGGGGAGGPGRVDKS	151
	: : : : : : . * *	

			EF-hand-like 1			
AtRBOHD	S	SAAIHALKGLKFIAT--KTAAWPAVDQRFDKLSADSNGLLLSAKFWECLGMNKESKDFA	219			
OsRBOHB	K	SAAVALKGLQFVTAKVGNWGAAVEKRFNQLQ--VDGVLRLSRFGKCIKIGMDG--SDEFA	195			
HvRBOHD	K	SAAHALKGLKFIASRTDGSAGWPAVEKRFDDLA--ENGLLHRSKFGKCIKIGMKE--LAF	207			
	.	*:* *****:*. . * **::**:* :*: * :*:** **				
			EF-hand-like 2	EF-hand 1		
AtRBOHD	D	QLFRALARRNNVSGDAITKEQLRIFWEQISDESFDAKLQVFFDMVDKDEDGRVTEEEVA	279			
OsRBOHB	V	QMFDSLARKRGIVKQVLTkDElKDFYEQLTDQGFDNRLRTFFDMVDKNADGRlTAAEEVK	255			
HvRBOHD	G	ELFDALARRRNlAGDSlSKAEllLEFDWQISDTSFDSRLQTFDDMVdKdADGRITEEEvK	267			
	.	:* :***:.. : :*: * *::*: * * :*:*****: **: * **				
			EF-hand 2			
AtRBOHD	E	IISLSASANKLSNIQKQAKEYAALIMEELDPNAGFIMIENLEMLLLQAPNQSVRMG-D	338			
OsRBOHB	E	IIALSASANKLSIKERADEYtalIMEELDPtNLGYIEMEDLEALLLQSPSEAAARSTT	315			
HvRBOHD	E	ITLSATANNLTkVKDQSEYARlIMEELDPnNLGYIELYNLEMLLLQAPsQsMAIG-T	326			
	.	**:* **:* **:* **:* **:* **:* **:* **:* **:* **:* **:* **:* **:				
			TM1			
AtRBOHD	--	SRIlSQMLsQKLrPAKESNPLVRWSEIKYfILDnWqRLwIMMLWLGICGGLFTYkFI	396			
OsRBOHB	TH	SkLlSKAlSmKlASnKEMSPVrHYwQqfMYfLEENWKRswVMTLWISIClAlFIWkFI	375			
HvRBOHD	TN	SrNlSQMLsQHLrPTAEpNPLRrWYrVSYfLEdNwRRCwVLLlWfCICVGLFTwKfM	386			
	.	* **:* **:* * .*: :: :. **: :*: * *: **:* **:* **:* **:* **:				
			Ferric oxidoreductase			
			TM2	TM3		
AtRBOHD	Q	YKNKAAYGVMGYCVCVAKGGAETLKFNMALILLPVCrNTITWLRNKTKLGTVPFDDSL	456			
OsRBOHB	Q	YRNRAVFGIMGYCVTTAKGAAETLKFNMALVLLPVCrNTITWIRSKTQVGAVVPFNdNI	435			
HvRBOHD	Q	YRERAVfKVMGYCVCVAKGGAEMlKFNMALILLPVCrNTITWfRNrTAAGRfVpFDDNI	446			
	.	**::*:.. : ***** .***.* *****:*****:*.:* * .***:..:				
			TM3			
AtRBOHD	N	fhKvIAsGIVvGvllhAgAhLTCDfPrllAAEDTYePMekYFGD-QPTsYwWfVKGvE	515			
OsRBOHB	N	fhKvIaAgvAvGvAlhAgAhLTCDfPrllhASDAQYELMKPFfGekRPPNYWfVKGTE	495			
HvRBOHD	N	fhKvIaAGISvGAGLHIIShLTCDfPrllRAtEEYePMKRFfGEEQPPNYWfVKGTE	506			
	.	*****:*. ** .** :*****: * : ** * : **:* **:* **:* **:				
			TM4	TM5		
AtRBOHD	G	WTGIVMVVLMAlAfTLATpWfFRNKLnlPnflKkLTGFNAfWYTHHLfIIVYAlLIVHG	575			
OsRBOHB	G	WTGvVmvVlMAIAfTLAQpWfFRNKLKdSNPlKkMTGFNAfWfTHHLfVIvYtLlFvHG	555			
HvRBOHD	G	WTGLVMLVLMAlAfTLATpWfFRGRlSlPKPlNRLTGFNAfWYSHHLfIIVYAlLIVHG	566			
	.	***:***:***** ***:.* : :*:*****:***:***:***:***:***:				
			TM5	TM6		
AtRBOHD	I	KLYLTKIwYqTtwMyLAvPIllyASerllRAfRssIKPvKMIKvAVyPGNvLSLhMTK	635			
OsRBOHB	T	CLYLsrKWyKkTtwMyLAvPvVlyVserIlRlRfRsh-DAVGIQKvAVyPGNvLAlYMSK	614			
HvRBOHD	H	FLYLtKkWqKkStwMyLAvPMIlYAcERlTRAlRssVRpVkiLkVAVyPGNvLSLhFSK	626			
	.	***: * :*:*****:*.**:* * :** * : *****:***:***:				
			FAD BS			
AtRBOHD	P	QGFkyKSGQfMLvNCRAVSPfEWHPFsITsAPGDdYlSVHIRTlGDwTRKLRtVfSEVC	695			
OsRBOHB	P	PgFRYrSGQYIFIKtAVSPYEWHPFSITsAPGDdYlSVHIRTlRDWTSrLRtVfSEAc	674			
HvRBOHD	P	QGFryKSGQYIFVNCaAvSPfQWHPFSITsAPQdYvSVHIRTlGDwTRELKNVfSKVC	686			
	.	* **:* **:* **:* **:* **:* **:* **:* **:* **:* **:* **:* **:				
			NADH-ribose BS			
AtRBOHD	K	PPTAgKSGLLRAD---GGDGNlPFPkVlIdGPyGAPAQDYkKYDVLLVGLGIGATPM	751			
OsRBOHB	R	PpTEGESGLLRADlSKGITDEKARfPKLLVDGPYGAPAQDYREYDVLlIGLIGATPl	734			
HvRBOHD	R	PpTEGKSGLLRAEYDRdGAMSNPSPkVlIdGPyGAPAQDYKQYDlVLLVGLGIGATPM	746			
	.	:** *:*****: : *****:*****:***:***:*****:				

AtRBOHD	ISILKDIINNMKGPDRDSDIE-NNNSNNNSKGFKTRKAYFYWVTREQGSFEWFKGIMDEI	810
OsRBOHB	ISIVKDVLNHIQEGSVGTTEPESSKAKKKPFMTKRAYFYWVTREEGSFEWFRGVMNEV	794
HvRBOHD	ISILKDIINNMKRLLEGDVESG-NPGDASTSTSFRTRRAYFYWVTREQGSFEWFRGVMDEI	805
	::***: : : * *:*****:*****:***:***:	
AtRBOHD	SELDEEGIIELHNYCTSVYEEGDARVALIAMLQSLQHAKNGVDVVSQTRVKSHFAKPNWR	870
OsRBOHB	SEKDKDGVIELHNHCSSVYQEGDARSALIVMLQELQHAKKGV DILSGTSVKTHFARPNWR	854
HvRBOHD	AESDKKGVIELHNYCTSVYEDGDARSALIAMLQSLNHAKNGVDIVSGTRVKTHFARPNWR	865
	: * * : . * :*****:***:***:*** * * . * * . * :*****:*** * * :***:***	
NADH-adenine BS		
AtRBOHD	QVYKKIADVQHPGKRIGVIFYCGMPGMIKELKNLALDFSRKTTTKFDFHKENF	921
OsRBOHB	SVFKKVAVSHENQRVGVIFYCGEPVLPQLRQLSADFTHKTNTRFDFHKENF	905
HvRBOHD	NVYKRIALNHRERQVGVIFYCGAPVLTKELELAQDFSRKTNTKFEFHKENF	916
	. * :***:*** * : * :***: * * :***:*** * :***:***	

Figure 21: Multiple sequence alignment was performed with Clustal Omega (Sievers et al., 2011) using default parameters. Identified conserved features are highlighted and include two EF-hand and two EF-hand-like motifs, several putative transmembrane domains (TM) and sites known for binding (BS) of FAD, NADPH-ribose and NADPH-adenine in the C-terminal region. A functional ferric oxidoreductase domain is show in green. Conserved phosphorylation sites (Ser39, Ser148, Ser163, Ser339, Ser343 and Ser347) in the N-terminal region are show in red and putative phosphatidic acid- (PA) binding sites (R157) in blue. Amino acids responsible for the hydrophobic core in the EF-hand-like motifs are highlighted in boldface.

3.5.2 Phylogenetic analysis

In order to infer the evolutionary relationship of the RBOH protein family, the deduced amino acid sequence of HvRBOHD was also compared with the sequence of other already characterized barley isoforms and with divergent RBOHs from Arabidopsis, maize, rice, tobacco and tomato. The full sequences were aligned with ClustalW (Thompson *et al.*, 1994) and evolutionary analyses were conducted in MEGA6 (Tamura *et al.*, 2013) using the Maximum Likelihood algorithm. In accordance with Li *et al.* (2015), five groups of orthologs were identified (Fig. 22). Clade I is consisting of distinct isoforms of RBOHs from dicot and monocot plants, including the new RBOH protein from barley. This clade includes proteins with specific functions in root hair formation like AtRBOHC. It also includes AtRBOHD, which is a multi-task protein mediating diverse functions ranging from stomatal closure and root hair formation to pathogen response or abiotic stress signalling (Miller *et al.*, 2009; Suzuki *et al.*, 2011; Marino *et al.*, 2012; Jiao *et al.*, 2013).

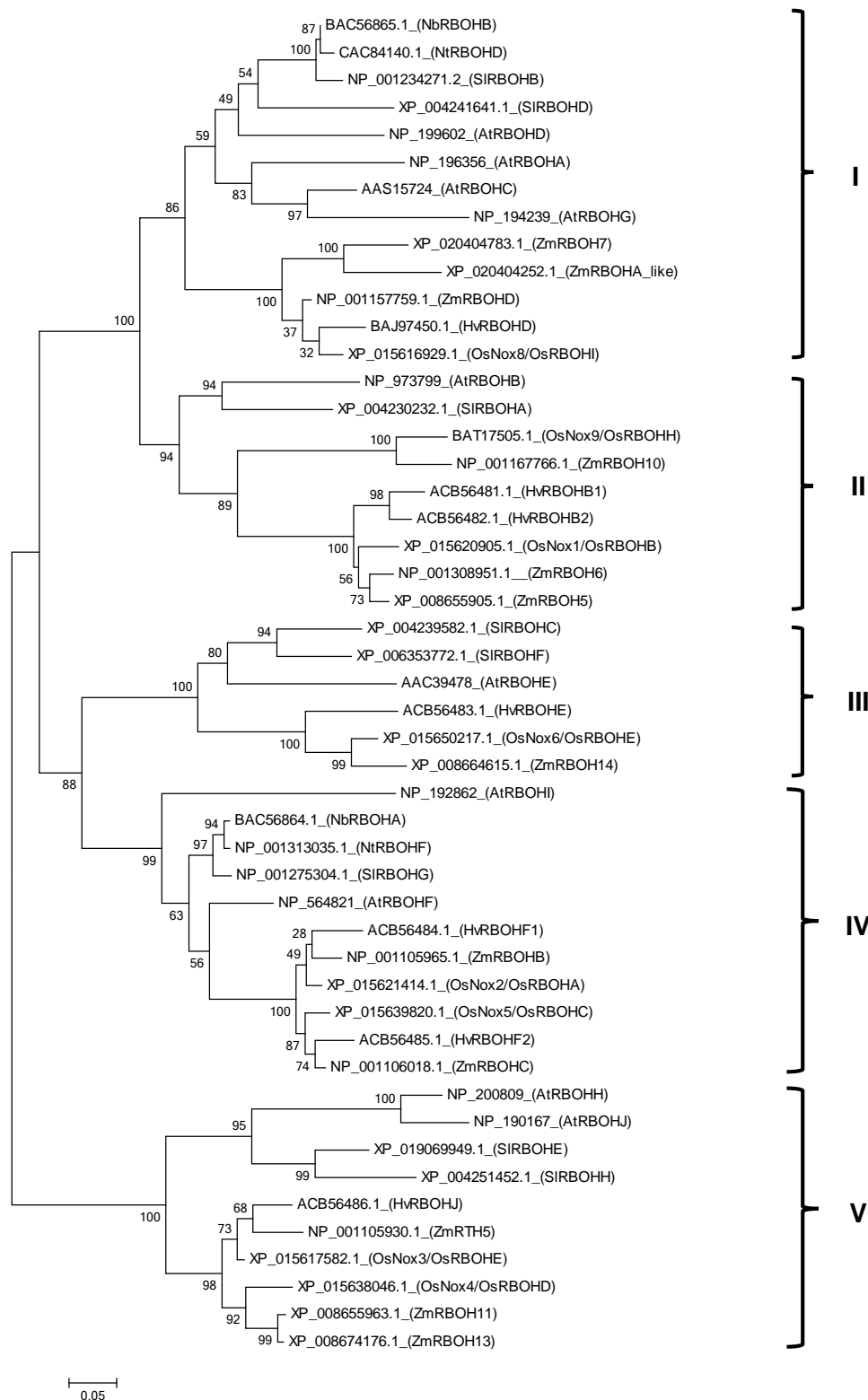


Figure 22: Phylogenetic analysis of plants RBOHs. The full-length amino acid sequences of RBOHs from *Arabidopsis thaliana* (At), barley (Hv), maize (Zm), tobacco (*Nicotiana benthamiana* Nb; *N. tabacum*, Nt), tomato (Sl) and rice (Os) were aligned with ClustalW (Thompson *et al.*, 1994) using the BLOSUM 30 protein weight matrix with a gap opening penalty of 10 and a gap-extension penalty of 0.05. Evolutionary analyses were conducted in MEGA6 (Tamura *et al.*, 2013) using the Maximum

Likelihood method based on the JTT matrix-based model and tested with a bootstrap of 1000 replications. Gene nomenclature according to Simon-Plas *et al.* (2002); Yoshioka *et al.* (2003); Torres and Dangl (2005); Lightfoot *et al.* (2008); Wang *et al.* (2013); Nestler *et al.* (2014); Li *et al.* (2015). For accession numbers, see figure.

Clade II is comprised of protein homologues to AtRBOHB, which is implicated in seed after-ripening (Müller *et al.*, 2009). Clade III contains proteins with unknown function that are homologues to OsRBOHE, a protein implicated in late ROS production in response to an avirulent strain of the bacteria *Acidovorax avenae* subsp. *avenae* (Yoshie *et al.*, 2005). Clade IV is composed of proteins with well-known functions in regulation of defence responses, such as HvrBOHF2, AtRBOHF and OsRBOHA (Torres *et al.*, 2002; Yoshie *et al.*, 2005; Trujillo *et al.*, 2006; Proels *et al.*, 2010). Additionally, clade VI included AtRBOHI, a protein recently reported to be involved in drought-stress response (He *et al.*, 2017). Finally, clade V contains proteins involved in ROS-mediated polar root hair growth (AtRBOHH, AtRBOHJ and ZmRTH5) and pollen tube growth (AtRBOHH and AtRBOHJ) (Kaya *et al.*, 2014; Nestler *et al.*, 2014; Mangano *et al.*, 2017).

The new barley RBOH isoform grouped into clade I with several known RBOH isoforms. Based on the AA identity, the closest homologue was OsRBOHI (OsNox8; 87% identity), followed by ZmRBOHD (85% identity). Among the AtRBOHs, isoform D was the closest homologue, followed by AtRBOHB (67% identity) and AtRBOHC (63% identity). Based on this evolutionary relationship with the Arabidopsis RBOHs, the gene was named *HvrBOHD*.

3.5.3 *HvrBOHD* expression analysis

Bgh infection triggers the expression of barley *HvrBOH* genes like *HvrBOHB2* and *HvrBOHF2* (Trujillo *et al.*, 2006) (R. Hüchelhoven, personal communication). To check if the expression of *HvrBOHD* was also induced by *Bgh*-inoculation, I studied the expression of this gene in leaves of the barley cv. Pallas. Whole barley plants were inoculated in the morning with approximately 50 spores mm⁻² and the leaves harvested at specific time points from inoculated and non-inoculated plants. Expression of *HvrBOHD* was slightly up-regulated at 12 hai and dropped back to the same level of non-inoculated plants at 24 hai (Fig. 23). As powdery mildew fungi infect the epidermis of plant leaves, I next tested if *HvrBOHD* was expressed in this specific tissue. The expression of this gene was quantified in abaxial epidermal peels of barley leaves and in the remaining leaf tissue of first leaves of 9-day-old Golden Promise plants. *HvrBOHD* transcripts were detected equally in both epidermis and remaining leaf tissue (Supplementary Fig. S25).

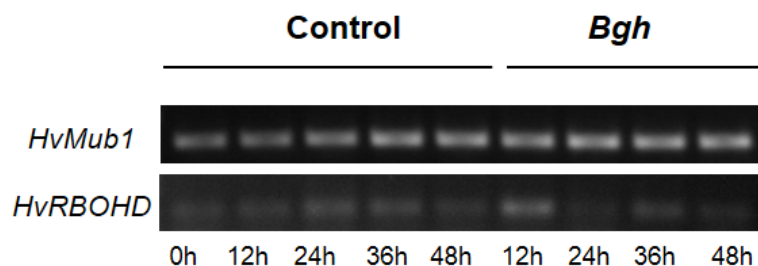


Figure 23: *HvrBOHD* expression is slightly induced upon *Bgh*-infection. Total RNA was extracted from *Bgh*-inoculated or non-inoculated leaves that were harvested 0, 12, 36 and 48 hai with the pathogen. The barley MONOUBIQUITIN-LONG-TAIL FUSION 1 (*HvMub1*) gene as used as internal control. Pictures show inverted photographs of ethidium-bromide-stained 1% agarose-gels after electrophoresis of RT-PCR products. Three independent experiments lead to similar results.

3.5.4 Transient knock-down of *HvrBOHD* limits penetration by *Bgh*

In addition, I assessed the function of *HvrBOHD* during the interaction between barley and powdery mildew. *HvrBOHD* was transiently silenced by expression of a double strand (ds) RNA construct delivered in single epidermal cells of barley cv. Golden Promise by particle bombardment (Schweizer *et al.*, 2000; Douchkov *et al.*, 2005). To assure specificity, the 419 bp fragment for dsRNA synthesis was amplified from the 5'-end of *HvrBOHD* (nucleotide position 371-789), corresponding to the AA position 64-203 in the N-terminal domain, the most variable region of the plant NADPH oxidases (Trujillo *et al.*, 2006). Bombarded leaf fragments were inoculated with *Bgh* and two days later, the frequency of haustoria formation in *Bgh*-attacked pIPKTA30N-*HvrBOHD*-transformed cells was quantified and compared with the frequency of haustoria formation in cells transformed with pIPKTA30N (empty vector control). Expression of the green fluorescent protein (GFP) was used as a marker to identify transformed single epidermis cells. In five independent TIGS experiments, the average frequency of successful cell penetration (haustoria formation) in cells transformed with the empty vector control, pIPKTA30N-*HvrBOHD* TIGS and pIPKTA30N-*HvMlo* TIGS were $35.6 \pm 2.0\%$ (mean \pm SE), $47.1 \pm 3.0\%$ and $13.8 \pm 1.3\%$, respectively (Fig. 26). On average, TIGS of *HvrBOHD* resulted therefore in a significant increase of 34% in the susceptibility of barley to penetration by *Bgh*. *Mlo* TIGS was used as a positive control. According to Schweizer *et al.* (2000) and Douchkov *et al.* (2014), transient silencing of *HvMlo* results in a reduction of at least 50% in the frequency of successful cell penetration by *Bgh* compared to an empty vector control. Here, the reduction of about 60% in the frequency of haustoria formation in pIPKTA30N-*HvMlo* TIGS construct bombarded leaf cells confirmed the general efficiency of the TIGS experiments.

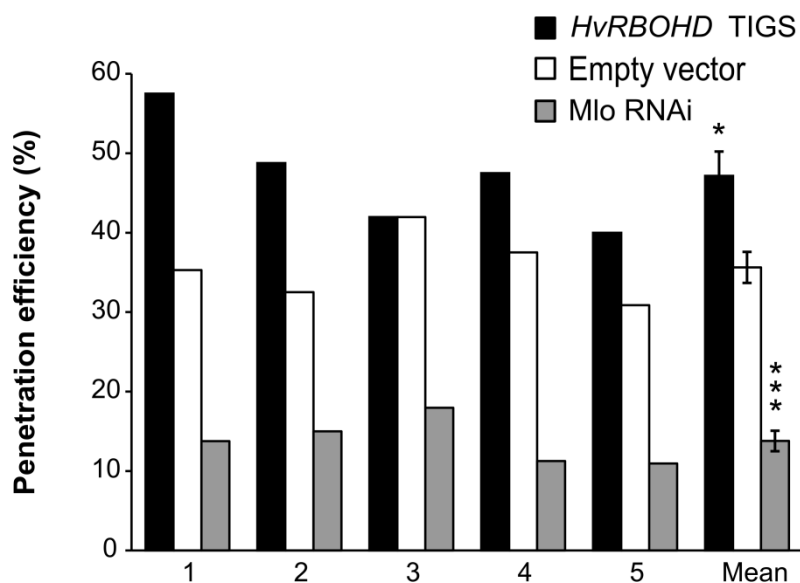


Figure 24: Transient induced silencing of *HvrBOHD* resulted in increased susceptibility to *Bgh*. Detached first leaves of 7-day-old barley cv. Golden Promise were ballistically co-transformed with the transformation marker construct pGY1-GFP together with pIPKTA30N-*HvrBOHD*, pIPKTA30N-Mlo or empty vector control pIPKTA30N. One day after bombardment, leaf fragments were inoculated with a high density of *Bgh* spores and two days later *Bgh*-penetration efficiency was evaluated under a microscope. Individual results of five independent experiments and means with standard errors are shown. Asterisks indicate significant differences (Student's *t* test: *** $p < 0.001$, * $p < 0.05$).

In short, changes in expression of *HvrBOHD* upon *Bgh* inoculation and the results of the TIGS experiments suggest a role of *HvrBOHD* as a resistance factor to the barley powdery mildew fungus *Bgh*.

3.6 Role of carbohydrate metabolism enzymes in the susceptibility to *Bgh*

The activation of plant defence responses has a high metabolic demand for carbohydrates. It is therefore believed that enzymes related to carbohydrate synthesis, transport and cleavage play a crucial role during plant-pathogen interactions. In this part of my work, I tested the involvement of selected barley genes encoding enzymes related to sucrose hydrolysis (CwINV, SUS and INVNH) and OPPP (G6PDH) in the susceptibility to the barley powdery mildew fungus.

3.6.1 Expression analysis

In order to identify genes related to carbohydrate metabolism that could have a role in the susceptibility to *Bgh*, I studied the expression of selected genes in inoculated and non-inoculated barley leaves. Two groups of genes were selected. The first group contained one isoform of SUS (*HvSUS1*) and one isoform of CwINV (*HvCwINV1*). These enzymes are responsible for the cleavage of intracellular and extracellular sucrose into hexoses, respectively. Additionally, it includes *HvINVNH1*, which encodes a putative inhibitor of acidic invertases. I observed that transcript levels of *HvSUS1* were enhanced upon *Bgh*-infection while transcript levels of *HvCwINV1* were slightly down-regulated (Fig. 25). On the other hand, transcript levels of *HvINVNH1* seem not be affected by *Bgh*-infection.

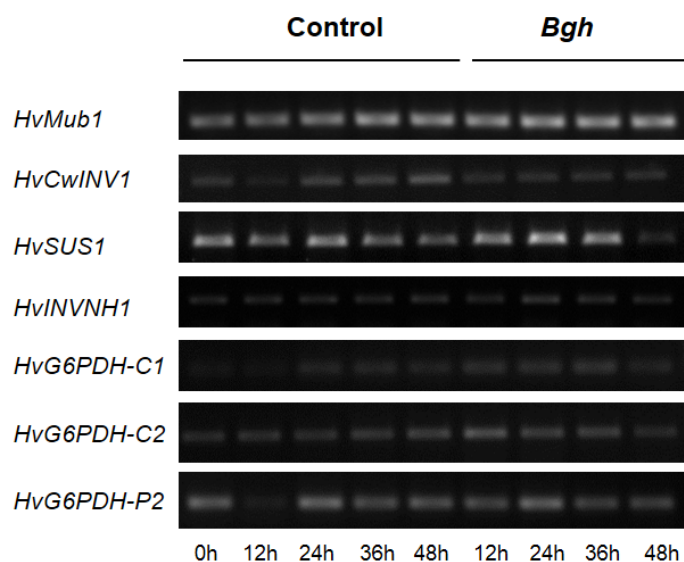


Figure 25: Expression of genes related to sucrose cleavage and OPPP upon *Bgh*-infection. Total RNA was extracted from *Bgh*-inoculated or non-inoculated leaves that were harvested 0, 12, 36 and 48 hai with the pathogen. The barley MONOUBIQUITIN-LONG-TAIL FUSION 1 (*HvMub1*) gene was used as internal control. Pictures show inverted photographs of ethidium-bromide-stained 1% agarose-gels after electrophoresis of RT-PCR products. Independent experiments leads to similar results.

The second group consists of isoforms of G6PDH (*HvG6PDH-C1*, *HvG6PDH-C2* and *HvG6PDH-P2*), which is the first enzyme of the oxidative reactions of OPPP. In this case, I observed a slight induction of all three *HvG6PDH* genes after the infection with *Bgh*.

I tested if genes of the two groups were expressed in epidermal cells (Supplementary Fig. S25). All the genes were constitutively expressed in both abaxial epidermal peels of barley leaves and in the remaining leaf tissue. Expression of *HvSUS1*, *HvINVNH1* and *HvG6PDH-C1* did not differ between the tissues. However, expression of *HvCwINV1*, *HvG6PDH-C2* and *HvG6PDH-P2* were stronger in remaining leaf tissues, that is, mesophyll cells and adaxial epidermal peels.

3.6.2 Transient knock-down of *HvCwINV1* supports penetration by *Bgh* in sucrose-treated barley leaves

Next, I used TIGS to evaluate the influence of *HvSUS1* and *HvCwINV1* on susceptibility of barley to the barley powdery mildew. Surprisingly, neither the knock-down of *HvSUS1* nor *HvCwINV1* resulted in statistically significant changes in susceptibility to *Bgh* (Fig. 26A). Nevertheless, there was a tendency of enhanced susceptibility to *Bgh*-penetration when *HvCwINV1* was transiently silenced.

Activity of both *SUS1* and *CwINV* are related to heterotrophic tissues (Koch, 2004) and *Bgh*-infection induces heterotrophic metabolism in infected leaves (Swarbrick *et al.*, 2006). However, it is possible that the pathogen did not induce heterotrophic metabolism in all infected cells. Therefore, in order to promote a homogenous induction of those enzymes, we treated the leaf fragments with sucrose solution directly after ballistic transformation and kept the plant material in this solution until evaluation. In this case, compared with the empty vector control, the average frequency of haustoria formation were increased by 35% in cells transformed with the TIGS constructs *pipkta30N-HvSUS1* and 49% in cells transformed with *pipkta30N-HvCwINV1* (Fig. 26B). In conclusion, the result of this TIGS experiment in leaves supplemented with sucrose supports a role of *HvCwINV1* in defence responses against *Bgh*. Additionally, the data also suggests a possible contribution of *HvSUS1*, albeit on a smaller scale.

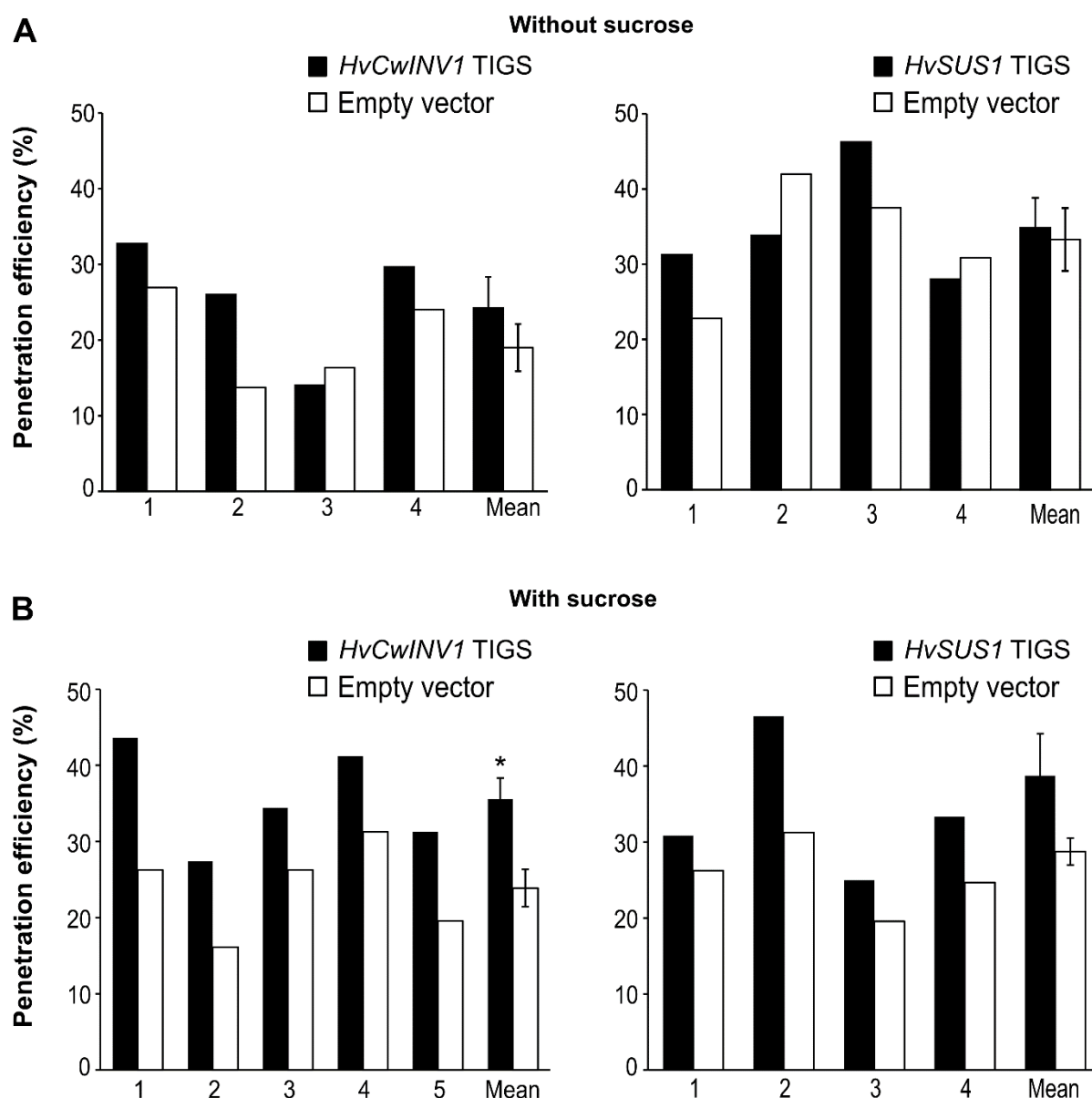


Figure 26: Role of sucrose cleavage enzymes in susceptibility to *Bgh*. Transient induced silencing of *HvCwINV1* and *HvSUS1* in leaf fragments (A) non-supplemented or (B) supplemented with 10mM sucrose solution. Detached first leaves of 7-day-old barley cv. Golden Promise were ballistically co-transformed with the transformation marker construct pGY1-GFP together with vector constructs of pIPKTA30N-*HvSUS1*, pIPKTA30N-*HvCwINV1* or empty vector control pIPTKTA30N. In (B) leaf fragments were transferred to 2 ml tubes filled with 1ml of 10mM sucrose soon after bombardment. One day after bombardment, leaf fragments were inoculated with a high density of *Bgh* spores and two days later *Bgh*-penetration efficiency evaluated under a microscope. Individual results of independent experiments and their means with standard errors are shown. Asterisks indicate significant differences (Student's test: * $p < 0.05$).

3.6.3 Transient overexpression of *HvINVNH1* limits penetration by *Bgh*

Transient overexpression (OE) of *HvINVNH1* resulted in decreased susceptibility to *Bgh* (Fig. 27). On average, the frequency of haustoria formation in cells transformed with pGY1-INVNH1 OE was nearly 40% less than in cells transformed with the empty vector control pGY1.

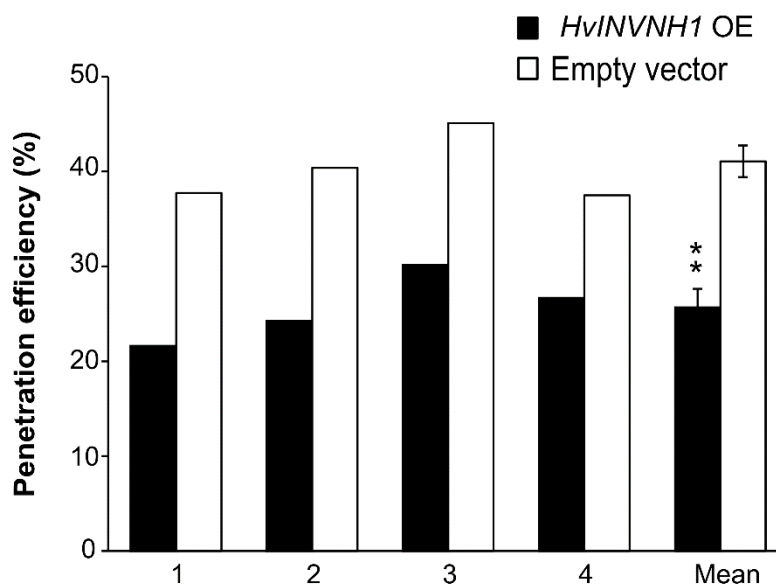


Figure 27: Transient overexpression (OE) of *HvINVNH1* leads to reduced susceptibility to *Bgh*.

Detached first leaves of 7-day-old barley cv. Golden Promise were ballistically co-transformed with the transformation marker construct pGY1-GFP together with pGY1-*HvINVNH1* or empty vector pGY1. One day after bombardment, leaf fragments were inoculated with a high density of *Bgh* spores and two days later *Bgh*-penetration efficiency evaluated under a microscope. Individual results of five independent experiments and means with standard errors are shown. Asterisks indicate significant differences between the constructs (Student's t test: ** $p < 0.01$).

3.6.4 Transient silencing of *HvG6PDH* genes does not influence susceptibility to penetration by *Bgh*

Besides several genes of sucrose cleaving enzymes, I also studied the effect of silencing the three different isoforms of G6PDH. The results of the transient knock-down indicate that neither *HvG6PDH-C1* nor *HvG6PDH-P2* modulate susceptibility of barley to barley powdery mildew (Fig. 28). In all three independent experiments, the frequency of haustoria formation was very similar between cells transformed with the *HvG6PDH-C1* TIGS construct or empty vector. Transient expression of the *HvG6PDH-P2* TIGS construct however, resulted in variable outcomes. KD of *HvG6PDH-C2* leads to a clear but not statistically significant tendency towards enhanced susceptibility of barley to *Bgh* penetration.

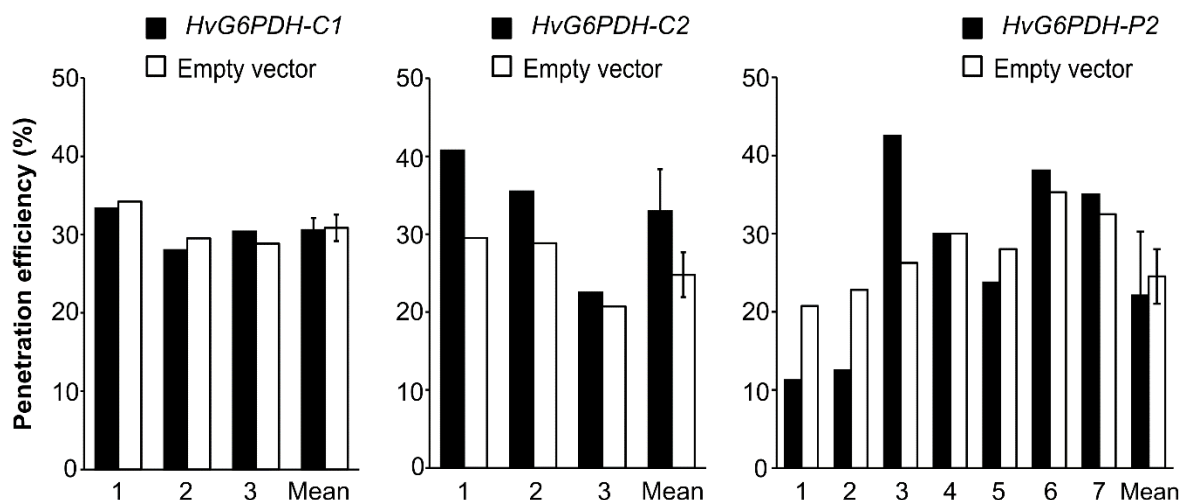


Figure 28: TIGS of G6PDH seems not to affect susceptibility to *Bgh*. Detached first leaves of 7-day-old barley cv. Golden Promise were ballistically co-transformed with the transformation marker construct pGY1-GFP and with TIGS constructs pIPKTA30N-HvG6PDH-C1, pIPKTA30N-HvG6PDH-C2, pIPKTA30N-HvG6PDH-P2 or empty vector pIPTKTA30N. One day after bombardment, leaf fragments were inoculated with a high density of *Bgh* spores and two days later *Bgh*-penetration efficiency was evaluated under a microscope. Individual results of independent experiments and means with standard errors are shown.

4 DISCUSSION

Here, I studied the role of the barley NADPH oxidase *HvRBOHF2* in the leaf-age dependent modulation of susceptibility to the biotrophic fungus *Bgh* and two hemibiotrophic fungal pathogens, *Bs* and *Fc*. I noticed that the expression of *HvRBOHF2* decreases with the progression of the leaf age in barley transgenic plants. In old leaves of *HvRBOHF2* KD lines, hyper-reduction in the *HvRBOHF2* residual expression results in constitutive expression of defence-related genes, SA accumulation and spontaneous cell death. Consequently, compared to azygous controls, these old leaves are less susceptible to the powdery mildew fungus whereas young leaves are more susceptible. Furthermore, *HvRBOHF2* KD plants are less susceptible to the hemibiotrophic fungus *Bs*. On the other hand, old leaves of *HvRBOHF2* KD lines are more susceptible to colonization by *Fc* but young leaves tend to be less susceptible.

In addition, I showed that the NADPH oxidase *HvRBOHD*, the cell wall invertase *HvCwINV1* and the invertase inhibitor *HvINVNH1* are putatively involved in resistance against *Bgh*-penetration.

4.1 *HvRBOHF2* KD plants displayed de-regulated PCD processes

PCD is a highly organized cellular self-destruction process mediated through an active genetic program that occurs during plant development or in response to stresses (Greenberg, 1996; Lim *et al.*, 2007). For instance, processes like the development of tracheary elements in the xylem of vascular plants, root cap cell formation, plant senescence and HR are classic examples of PCD (Pennell and Lamb, 1997). Interestingly, mis-regulation of these PCD processes or alterations in metabolic pathways, can result in so-called lesion-mimic mutants (LMM) that display spontaneous cell death or HR-like lesions in the absence of a pathogen (Dangl *et al.*, 1996). Initiation mutants are affected in the regulation of PCD induction and propagation mutants in suppression of cell death (Lorrain *et al.*, 2003). *HvRBOHF2* KD lines show both classes of LMM phenotypes. Fully developed leaves of 17-day-old *HvRBOHF2* KD plants show spontaneous mesophyll cell death and a runaway cell death phenotype (cell death propagation) appears when leaves are wounded by cutting the leaf blade (Proels *et al.*, 2010). I analysed the spontaneous cell death initiation LMM phenotype in *HvRBOHF2* KD plants. With progression of leaf-age, silencing of *HvRBOHF2* results in patches of necrotic mesophyll cells starting in the tip of fully developed older leaves. Older leaves of *HvRBOHF2* KD plants showed also typical features of a premature leaf senescence phenotype as for examples leaf yellowing or bleaching (Figs. 2 and 3) and a decrease in chlorophyll content (Fig. 4). In this context, Chl to Car ratio did not change within

the different leaves of either KD or azygous plants. This feature is a hallmark of barley leaves in which Chl and Car decrease with similar rates while in most of the plants the photosynthetic pigments are degraded differentially during leaf senescence (Biswal, 1995). Additionally, older leaves of *HvRBOHF2* KD plants display increased basal expression of *HvS40* (Fig. S18), a gene with unknown function, the expression of which is associated with senescence-like processes (Krupinska *et al.*, 2002). Moreover, RNA isolated from first and second leaves of 17-day-old seedlings were usually low yield, impure and degraded which could indicate an increased RNase activity (data not shown). According to Lim *et al.* (2007), a quick decrease in total RNA level due to an increased activity of several RNases is a hallmark of leaf senescence.

Plant premature senescence can be triggered by several biotic and abiotic stresses such as pathogen infection, drought, nutrient deprivation, and wounding. However, it is still unknown if stress is causing the onset of senescence, or if the senescence itself is inducing stress responses (Buchanan-Wollaston *et al.*, 2003). Some progress in the identification and characterization of genes related to senescence and other types of PCD have been made in the past years (Pontier *et al.*, 1999; Swidzinski *et al.*, 2002; Buchanan-Wollaston *et al.*, 2005; Lim *et al.*, 2007; Olvera-Carrillo *et al.*, 2015). It resulted in the discovery of genes that share common regulatory mechanisms or are differentially regulated in distinct PCD types. Curiously, the expression of genes frequently associated with senescence is also increased in leaves subjected to different stresses. The expression of the *Brassica napus* metallothionine gene *BnLSC54*, for example, is induced upon pathogen infection and in response to several types of oxidative stress (Butt *et al.*, 1998; Navabpour *et al.*, 2003). Likewise, the transcript levels of HR gene markers such as *B. napus BnPR1a* and tobacco *HARPIN INDUCED GENE (NtHIN1)* are also upregulated during leaf senescence (Hanfrey *et al.*, 1996; Pontier *et al.*, 1999). Consistent with these findings, old leaves of *HvRBOHF2* KD plants displaying a senescence-like phenotype also had an enhanced constitutive expression of defence-associated and pathogen-induced genes (Figs. 15 and 17 and Supplementary Fig. S18).

4.1.1 Expression of putative ROS-responsive genes is up-regulated in *HvRBOHF2* KD plants

Transcript levels of *HvBI-1* and *HvS40* accumulate to higher levels in older leaves of *HvRBOHF2* KD plants than in the azygous control. Interestingly, the expression of these genes has been associated with oxidative stress (Krupinska *et al.*, 2002; Hüchelhoven, 2004; Krupinska *et al.*, 2014). For instance, hydrogen peroxide and SA treatment, which lead to ROS accumulation through the inhibition of catalase activity, induce the expression of the

Arabidopsis *AtBI-1* and the barley *HvS40* genes (Durner *et al.*, 1997; Horváth *et al.*, 2002; Krupinska *et al.*, 2002; Metwally *et al.*, 2003; Kawai-Yamada *et al.*, 2004; Krupinska *et al.*, 2014). Barley LMM *NECROTIC LEAF SPOT1* (*nec1*) and *nec8* are thought to have mutations in genes involved in the regulation of intracellular fluxes of calcium ions. Interestingly, both *nec1* and *nec8*, characterized by enhanced ROS accumulation, show constitutive enhanced expression of *HvBI-1* (Rostoks *et al.*, 2006; Zhang *et al.*, 2009a; Keisa *et al.*, 2011; McGrann *et al.*, 2015). Besides this, expression of several *PR* genes, most notably *HvPR1b* whose expression can be triggered by ROS (Schultheiss *et al.*, 2003a), was enhanced in *HvRBOHF2* KD plants. Despite the fact that transcripts of these genes accumulated already in young leaves of KD plants in some of the independent biological replicates, the basal expression of these genes was much higher in old leaves of *HvRBOHF2* KD, reaching levels usually only measured after *Bgh*-infection (Fig. 17, Supplementary Figs. S21 and S22).

4.1.2 Expression of a *LSD1-like* gene is down-regulated in *HvRBOHF2* KD plants

The expression of *HvRBOHF2* reduced strongly with the progression of the leaf age, especially in leaves undergoing senescence (Fig. 14 and Supplementary Fig. S17). In 11-day-old *HvRBOHF2* KD plants, the transcript amount of *HvRBOHF2* was about 9-fold lower in old leaves compared to young leaves of the same plant. Moreover, hyper-reduction in the expression of *HvRBOHF2* in old leaves was associated with decreased expression of *HvCBC04043*, an *AtLSD1* homologue (Fig. 15D; Supplementary Fig. S19D). Similar to *HvRBOHF2* KD plants, both Arabidopsis *Atlsd1* mutants and old leaves of rice silenced for *OsLOL1* display a lesion mimic phenotype in absence of a pathogen, elevated expression of the *PR-1* gene and increased resistance against pathogens with a biotrophic or hemibiotrophic life style (Dietrich *et al.*, 1994; Aviv *et al.*, 2002; Wang *et al.*, 2005).

Curiously, it seems that in monocot plants, LOL1-like proteins instead of LSD1 homologues act as negative regulator of PCD in leaves. Despite the fact that both *OsLOL1* and *TaLOL1* encode proteins that negatively regulate PCD in leaves of rice and wheat, based on sequence homology and gene exon-intron structure these genes are evolutionary closer to *AtLOL1* than to *AtLSD1* (Wang *et al.*, 2005; Guo *et al.*, 2013). Additionally, *HvLsd1b*, showing 55% of AA identity with *AtLSD1*, failed in complementing the runaway cell death phenotype of *Atlsd1* mutants (Keisa, 2013). Concerning the opposite roles of LOL1 in dicots and monocots, the nomenclature of monocot LSD1-like proteins in literature is confusing because sometimes the protein is named based on its functional characterization instead of sequence homology. For instance, *OsLOL1* and *TaLOL1* were originally referred to as *OsLSD1* and *TaLSD1*. Therefore, to avoid misunderstandings in the nomenclature,

I performed a phylogenetic analysis using AA sequences of LSD1-like genes of some plants, including the well characterized proteins of Arabidopsis and rice and re-assigned unique names to them (Supplementary Fig. S26). As expected, HvLsd1a and HvLsd1b grouped with AtLSD1. HvCBC04043 grouped with AtLOL1 and from now on will be referred to as *HvLOL1*.

Barley *HvRBOHF2* KD plants displayed a reduced expression of *HvLOL1* in old leaves and a tendency of higher expression in young leaves. Reduction in *HvLOL1* transcript levels in the first biological replicate (reduced by approximately 30% of the expression of the control) was not as dramatic as in the following experiments. However, Epple *et al.* (2003) showed that a reduction of 25% in the expression of *AtLOL1* in Arabidopsis *Atlsd1/Atlol1*-double mutants was enough to partially complement the run-away cell death phenotype of *Atlsd1* mutants triggered by the SA-analog benzothiadiazole (BTH) or by the necrotrophic pathogen *B. cinerea*. Moreover, although *OsLOL1* antisense RNAs accumulate to high levels in transgenic *OsLOL1* rice antisense plants and the antisense expression of this gene causes lesion mimic and increased HR phenotypes, endogenous transcript levels of *OsLOL1* were similar between transgenic lines and WT plants (Wang *et al.*, 2005). Thus, it seems that even very small changes in the expression of genes of the LSD1 family are enough to induce cell death phenotypes.

Based on the high sequence similarity with functional orthologous of LSD1 in monocots and the failure of *HvLSD1b* to restore AtLSD1 function, I propose, that *HvLOL1* is possibly a functional homologue of LSD1 in barley. However, further experiments are required to prove this hypothesis. Reduced expression of *HvLOL1* was also reported for another barley LMM mutant, which also points to a role of this gene in the negative regulation of barley PCD. The expression of *HvLSD1a* is higher in the *nec1* mutant than in the parental lines, but the transcript levels of *HvLOL1* are reduced (Keisa *et al.*, 2008). On the other hand, *HvLSD1b* expression was not affected. Similar to *HvRBOHF2* KD lines, visible cell death occurs in *nec1* in the first few weeks after germination and is visible as small dark brown spots, which rarely coalesce (Keisa, 2013). Yet, spontaneous cell death in *nec1* mutants is unlikely to be under the control of *HvRBOHF2*, as the expression of this gene is not affected by a *nec1* mutation (Keisa *et al.*, 2011).

4.1.3 Expression of ATG genes and *Mlo* are not affected in KD plants

Autophagy is a typical eukaryotic cell catabolic process that allows for the degradation and recycling of cytoplasmic constituents or toxic compounds during development or under stress conditions (Pérez-Pérez *et al.*, 2012). The expression of several ATG genes, including *HvATG7* and *HvATG8_2*, is up-regulated during barley natural leaf senescence (Christiansen and Gregersen, 2014; Avila-Ospina *et al.*, 2016). In this study, I did not see

differences in the basal expression of these *ATG* genes between 11-day-old *HvRBOHF2* KD plants and azygous controls (Fig. S18). This might be due the fact that plants of this age do not display visible symptoms of leaf senescence. According to Avila-Ospina *et al.* (2014) autophagy genes are induced after the up-regulation of *SAG* genes and possibly, autophagy is induced by leaf senescence and not the other way around. Alternatively, autophagy may not play a role during the premature senescence of *HvRBOHF2* KD mutants.

Likewise, the basal expression of *HvMlo* did not seem to differ between 11-day-old *HvRBOHF2* KD and azygous plants (Fig. 15A). Similar to *HvRBOHF2* KD plants, Arabidopsis and barley *mlo* mutants display an early leaf senescence phenotype (Kusch and Panstruga, 2017). Piffanelli *et al.* (2002) observed that *HvMlo* expression gradually increases in barley leaves soon after the leaves reach their final size (about 10 DAS) and maximum transcript levels are detected around the time of the onset of leaf senescence. Although the Chl content of 11-day-old *HvRBOHF2* KD and azygous plants did not differ, there was a tendency of reduced Chl content in KD plants, indicating that in these plants leaf senescence could have already started. In agreement with this, approximately two days later senescence-like symptoms became visible. The simultaneous lack of *HvMlo* up-regulation suggests that usual developmental-induced expression of *HvMlo* is de-regulated in *HvRBOHF2* KD plants. Taken together, premature leaf senescence in *HvRBOHF2* KD plants seems to be different from natural senescence.

4.2 *HvRBOHF2* KD leaf age-dependent susceptibility to *Bgh*

HvRBOHF2 KD lines showed age-dependent reduced susceptibility to both penetration and growth of *Bgh* on the leaf surface (Figs. 5, 6, 10 and 13). Furthermore, I observed a difference in susceptibility of different sections of the leaf blade, in which physiologically older leaf tips of *HvRBOHF2* KD lines were less susceptible to *Bgh* penetration than younger leaf sections near the leaf base. This developmental resistance is reminiscent of APR described by plant breeders for cereals. A shift from susceptibility to resistance to various diseases, such as bacterial leaf blight, rusts and powdery mildews is observed with the progression of the plant or leaf age (Sunderwirth and Roelfs, 1980; Douglas *et al.*, 1984; Century *et al.*, 1999; Ellis *et al.*, 2014). APR to *Bgh* has been identified in some barley cultivars both in laboratory and in field conditions (Lin and Edwards, 1974; Wright and Heale, 1984; Gupta *et al.*, 2015). Wright and Heale (1984) reported a reduction in the density of *Bgh*-colonies on later-formed leaves of Athos, Porthos and Golden Promise cultivars. According to these authors, the reduction in the number of colonies per leaf area and *Bgh*-sporulation in older leaves were related to an accelerated rate of leaf-senescence in the cultivar Athos (Wright and Heale, 1984). In wheat, PR and other defence gene transcripts accumulate during

different types of APR (Chen *et al.*, 2013; Guo *et al.*, 2013; Hao *et al.*, 2016). PR proteins also accumulate in the intercellular space of barley primary leaves during leaf senescence (Tamás *et al.*, 1998) and this gradual PR protein accumulation, possibly correlates with the barley APR against *Bgh*.

Here, the reduced susceptibility to *Bgh* I observed in old leaves of *HvRBOHF2* KD lines was also associated with a premature leaf senescence-phenotype (chapter 4.1), up-regulated expression of *PR* genes and increased accumulation of SA in older leaves. In agreement with Hüchelhoven *et al.* (2001) who reported the expression of *HvRBOHF2* to be developmentally controlled with higher levels of expression in youngest plants, I observed a lower expression of *HvRBOHF2* in older versus younger leaves of 11-day-old *HvRBOHF2* KD plants. Remarkably, in the azygous control, this leaf age-dependent expression of *HvRBOHF2* was consistent only in 17-day-old plants (Supplementary Fig. S17). Although no data exist that would support a direct function of *HvRBOHF2* in regulation of naturally occurring APR, it might be worth measuring *RBOHF* expression levels in APR of *Triticeae*.

My results suggested that leaf-age and physiological stage are critical parameters in the *HvRBOHF2* KD-powdery mildew interactions. This could also explain previous contradicting results regarding a lower susceptibility to *Bgh* following a transient silencing of *HvRBOHF2* (Trujillo *et al.*, 2006) and a higher susceptibility to *Bgh* in young leaves of stable transgenic *HvRBOHF2* KD lines (Proels *et al.*, 2010). The resistance phenotype in transiently silenced leaf explants (Trujillo *et al.*, 2006) could have resulted from the fact, that in this assay first leaves are cut off from the plant, transiently transformed via particle bombardment, left on agar plates for 24 hours before *Bgh* inoculation and evaluated for resistance 40 h later. During the course of this experiment, the leaf explants might have changed to a physiological older status, resulting in higher resistance to *Bgh* when *HvRBOHF2* is silenced.

4.2.1 Pathogen-triggered ROS burst is affected in *HvRBOHF2* KD plants

A prominent decrease in the frequency of cell wall-associated hydrogen peroxide formation in papilla and in anticlinal cell walls of cells adjacent to penetrated cells was observed in first leaves of *HvRBOHF2* KD plants (Fig. 9). According to previous studies (Hüchelhoven *et al.*, 1999; Hüchelhoven *et al.*, 2000a; Hüchelhoven *et al.*, 2000b), non-penetrated papilla are usually associated with hydrogen peroxide formation, whereas penetrated cells are often free of detectable H₂O₂ or show H₂O₂ formation in anticlinal cell walls facing neighbouring cells. Therefore, the reduced DAB staining in leaves of *HvRBOHF2* KD plants seems to indicate a contribution of the *HvRBOHF2* oxidase to H₂O₂ formation in interaction with *Bgh*. However, transient silencing of *HvRBOHF2* (Trujillo *et al.*, 2006) or silencing in young leaves (Proels *et al.*, 2010) did not support this because no consistent reduction of H₂O₂ formation was

observable. Taken together, I speculate that the progression of leaf senescence rather than the direct lack of *HvRBOHF2* protein was responsible for the reduced DAB staining in older leaves of *HvRBOHF2* KD plants. This is supported by the fact that the frequency of DAB staining did not strongly differ between younger third leaves of *HvRBOHF2* KD and azygous control plants (Fig. 9). On the other hand, *HvRBOHF* genes seem to be involved in the ROS-burst triggered by MAMPs. The amount of ROS is strongly reduced in leaf discs from distinct leaves of the *HvRBOHF2* KD plants after treatment with the elicitors flg22, chitin or laminarin. Moreover, in discs from the second leaf, the oxidative burst was almost completely abolished (Torres *et al.*, 2017). However, because the current methods to determine the ROS burst rely on leaf discs that are cut from leaves with tissue punchers, wound-related phenotypes of *HvRBOHF2* KD lines might have interfered with the ability of leaf discs to respond to MAMPs. As previously mentioned, *HvRBOHF2* KD lines are unable to stop the spreading of the leaf cell death triggered by the cutting of the leaf so that leaf necrosis progresses until the entire leaf is necrotic (Proels *et al.*, 2010). Thus, although leaf discs did not show clear signs of tissue necrosis, it cannot be ruled out that the reduction in ROS burst is a consequence of a de-regulated wound response rather than a direct effect of silencing *HvRBOHF1* and *HvRBOHF2*.

Taken together, it is necessary to carefully interpret these data because the contribution of *HvRBOHF2* to the MAMP- and *Bgh*-triggered ROS formation may be less prominent than data suggest. Nevertheless, a role of *HvRBOHF* genes in ROS production during the immune responses is plausible, since putative orthologues of these genes in plant species such as *Arabidopsis* and *N. benthamiana* have been proven to trigger, at least partially, PAMP-/pathogen-dependent ROS accumulation. For instance, the ROS burst triggered by the bacterial elicitor flg22 was partly dependent on a functional *AtRBOHF* gene in a study performed by Zhang *et al.* (2007). Hydrogen peroxide accumulation in response to avirulent strains of *Pst* and the necrotrophic fungi *Alternaria brassicicola* and *S. sclerotiorum* is not affected in an *AtrbohF* mutant, but is partially reduced after inoculation with the *Arabidopsis* powdery mildew fungus *Golovinomyces cichoracearum* (Torres *et al.*, 2002; Pogány *et al.*, 2009; Berrocal-Lobo *et al.*, 2010; Perchepped *et al.*, 2010; Ma *et al.*, 2016). Silencing of the *HvRBOHF2*-related *N. benthamiana* NADPH oxidase *NbRBOHA* completely abolishes the *Phytophthora infestans* triggered hydrogen peroxide accumulation and also the silencing of the *HvRBOHF2*-related rice gene *OsRBOHA* affects a PAMP-induced oxidative burst (Yoshioka *et al.*, 2003; Yoshie *et al.*, 2005).

Curiously, the number of cells undergoing *Bgh*-induced local cell death was not different between the leaves of the *HvRBOHF2* KD plants and the azygous controls (Fig. 9; Proels *et al.*, 2010). Therefore, *HvRBOHF2*, unlike its close homologues *AtRBOHF* and *OsRBOHA*

(Torres *et al.*, 2002; Yoshie *et al.*, 2005) might not be involved in the regulation of pathogen-triggered cell death. However, since virulent *Bgh* is not a strong trigger of cell death, further studies are necessary come to a final conclusion.

4.2.2 Silencing of *HvRBOHF* genes affect the expression of defence-related and pathogen-induced genes

Bgh-infection triggered an increase in transcripts of *PR* genes in leaves of both *HvRBOHF2* KD and azygous plants (Fig. 17, Supplementary Figs. S21 and S22). Nevertheless, the total expression of genes coding for PR1b (unknown function), PR3 (endochitinase), PR5 (thaumatin-like) and PR10 (ribonuclease-like) were much higher in *HvRBOHF2* KD plants, especially *HvPR1b*. Enhanced resistance to pathogens in monocot LMM often is related to constitutive expression of *PR* genes (Yin *et al.*, 2000; Wright *et al.*, 2013; McGrann *et al.*, 2015; Wang *et al.*, 2016). For instance, ectopic expression of the wheat APR gene *LR34* in barley leads to resistance to *Bgh* and other pathogens in the seedling stage and this resistance was associated with constitutive expression of defence-associated genes, including several *PR* genes (Risk *et al.*, 2013; Chauhan *et al.*, 2015). The *PR* proteins consist of 17 families of small, secreted proteins with antimicrobial properties (Sels *et al.*, 2008). PR1b is a basic protein that belongs to the class 1 of *PR* proteins family, an abundant group of *PR* proteins with unknown function and frequently associated with SAR in dicot plants (Van Loon and Van Strien, 1999). Remarkably, *HvPR-1b* expression is associated with *Bgh*-resistance. *Bgh* induced *HvPR-1b* expression is stronger in resistant than in susceptible barley lines. Furthermore, transient silencing of *HvPR-1b* by dsRNAi renders barley cells slightly more susceptible to *Bgh* penetration (Hückelhoven *et al.*, 2000a; Schultheiss *et al.*, 2003a). Additionally, the expression of *HvCwINV3* was also higher in inoculated *HvRBOHF2* KD plants compared to the azygous control (Fig. 16, Supplementary Fig. S20). Invertases are regulated by several abiotic and biotic stress stimuli, including pathogen infection. According to Roitsch *et al.* (2003), cell wall invertases are an important part of the plant defence response against phytopathogens and can thus be considered as pathogenesis-related proteins.

Finally, expression of *HvS40* was also enhanced in both leaves of *HvRBOHF2* KD plants (Supplementary Fig. S18). Krupinska *et al.* (2002) showed that expression of this gene is induced in *P. teres* infected barley leaves at the sites of necrotic lesions surrounded by chlorotic tissue but not in sectors of the same leaf without infection sites. Additionally, just a weak and rather late accumulation of *HvS40* was observed in leaves of the resistant barley cv. Sultan 5 inoculated with *Bgh*. Therefore, the authors conclude that expression of this gene is most likely not related to the defence against pathogens (Krupinska *et al.*, 2002).

Thus, increased expression of *HvS40* in inoculated KD plants appears due to de-regulated senescence in those plants.

4.2.3 *HvRBOHF2* KD plants are characterized by an increased SA level

In contrast to the relatively well-understood role of SA during immune responses of tobacco and Arabidopsis, its role in the barley-*Bgh* pathosystem is still unknown. Exogenous application of SA or synthetic analogues of SA induces disease resistance against *Bgh* (Kogel *et al.*, 1994; Beßer *et al.*, 2000; Dey *et al.*, 2014). In addition, barley transgenic plants silenced for the gene *NON-EXPRESSOR OF PATHOGENESIS RELATED GENES1* (*HvNPR1*), a critical SA signal transducer, displayed enhanced susceptibility to *Bgh*, also suggesting a role of *HvNPR1* in barley immunity (Dey *et al.*, 2014). However, although *Bgh* inoculation triggered typical defence responses such as hydrogen peroxide accumulation, HR and induction of *PR* gene expression, these responses were not associated with an increase in the SA content (Vallélian-Bindschedler *et al.*, 1998; Hückelhoven *et al.*, 1999). Likewise, I did not observe a statistically significant increase in the SA content after *Bgh*-inoculation (Fig. 18). On the other hand, I found strongly increased constitutive FSA and CSA levels in the first, older leaf of *HvRBOHF2* KD plants.

The majority of the SA produced in planta is converted via glycosylation, methylation or amino acid conjugation to biological inactive derivatives (Gao *et al.*, 2015). SA O- β -glucoside (SAG) is the most abundant of these derivatives and is produced by the activity of a pathogen-inducible SA glucosyltransferase (Vlot *et al.*, 2009). The exact role of SAG during SA-signalling is still unknown, but it has been proposed that SAG acts as a large inactive SA storage that progressively releases free active SA and keeps the pathway signalling over time (Lee *et al.*, 1995). Thus, CSA possibly has a role in mediating barley defence responses and in direct limitation of pathogen development. In addition, plants also accumulate a hydroxylated form of SA that seems play important roles in defence responses and in the control of leaf senescence. The levels of 2,5-dihydroxybenzoic acid (DHBA) or gentisic acid increase in leaves of tomato infected with citrus exocortis viroid or tomato mosaic virus and this compound specifically induces the expression of *PR* genes that are not induced by SA (Bellés *et al.*, 1999). Glycosylated 2,5-DHBA and 2,3-DHBA accumulate in both infected leaves and Arabidopsis mature leaves and the conversion of SA to 2,3-DHBA by the activity of SA 3-hydroxylase regulates the leaf longevity by the regulation of the SA levels (Bartsch *et al.*, 2010; Zhang *et al.*, 2013). I observed a positive correlation between the SA content and the levels of two unknown compounds with retention time close to SA (Fig. S23). Considering the high levels of SA found in leaves of the KD plants showing advanced symptoms of premature senescence, it is reasonable to assume a possible role of these compounds in the

regulation of barley SA levels in senescent leaves. However, additional experiments are necessary to reveal the contribution of these compounds in the SA-signalling.

SA has been described as *in-vitro* antimicrobial agent against the Gram-negative bacterium *Pst*, the vascular fungi *Eutypa lata*, *Ophiostoma ulmi* and *O. novo-ulmi* and several other soilborne phytopathogens (Prithiviraj *et al.*, 1997; Georgiou *et al.*, 2000; Amborabé *et al.*, 2002; Cameron and Zaton, 2004; Martín *et al.*, 2009). Besides the reduction in haustoria formation at 48 hai, I also observed a reduced development of *Bgh* colonies on the leaf surface of *HvRBOHF2* KD lines at 96 hai (Fig. 10-13). Thereby, the effect of a reduced colony length in *HvRBOHF2* KD lines was more pronounced in older leaves, which might be additionally caused by a reduced metabolic activity in those tissues characterized by spontaneous cell death. Since *Bgh* follows an obligate biotrophic lifestyle, accelerated senescence and cell death should strongly limit its development. In addition, considering the high content of FSA found in older leaves of *HvRBOHF2* KD plants, the arrest in *Bgh*-growth also could be a result of a possible antifungal activity of SA or of SA-induced defence compounds.

Interestingly, there are further reports about RBOH functions in support of disease progression. Torres *et al.* (2002) reported that the reproductive success of *H. arabidopsidis* isolate Emco5 was reduced on *AtrbohF* mutant leaves and plants showed enhanced HR. In interaction with cyst nematodes *AtrbohD/AtrbohF*-double mutants showed enhanced cell death in response to nematode infection, and feeding site formation was limited on the mutants. Further genetic disruption of *SID2*, which is required for salicylic acid biosynthesis, led to an increased size of nematodes in *sid2/rbohD/rbohF* mutant plants, but did not eliminate the cell death reaction (Siddique *et al.*, 2014). Thus, NADPH oxidases modulate the amount of cell death and control salicylic acid-induced defence responses in diverse plant tissues and under diverse physiological situations.

4.3 Silencing of HvRBOHF genes affects susceptibility to hemibiotrophic fungi

PCD is usually associated with defence responses against biotrophic/hemibiotrophic pathogens as necrotrophic pathogens can benefit from dead host cells (Glazebrook, 2005). Nevertheless, the picture is not very clear as monocot LMM show contradictory responses to pathogens of different lifestyles, especially hemibiotrophic ones. Barley LMM mutants necrotic leaf spot *nec8.3550* (former *BIPOLARIS SOROKINIANA TOLERANT 1*, *bst1*) and mottled leaf *mtt8.1661* are more resistant to the barley leaf rust *P. hordei* and more susceptible to the necrotrophic fungus *P. teres*, compared with the parental line Bowman

Rph3.c (Wright *et al.*, 2013). Barley *nec8* mutants show increased resistance against *Puccinia graminis* and facultative pathogens with a hemibiotrophic lifestyle such as *Ramularia collo-cygni*, *F. culmorum* and *Oculimacula yallundae*, but not against *P. striiformis* f. sp. *hordei* (Zhang *et al.*, 2009a; McGrann *et al.*, 2015). In contrast, barley *mlo*-mutants are supersusceptible to the hemibiotrophic pathogens *M. oryzae* and *Ramularia collo-cygni* and more sensitive to the toxic culture filtrate of *B. sorokiniana* (Jarosch *et al.*, 1999; Kumar *et al.*, 2001; McGrann *et al.*, 2014). Here, I found that, besides an altered susceptibility to *Bgh* penetration and colonization, barley LMM *HvRBOHF2* KD mutants also showed altered outcomes during the interaction with pathogens with a hemibiotrophic lifestyle.

4.3.1 *HvRBOHF2* KD plants are less susceptible to spot blotch

Both young and old leaves of *HvRBOHF2* KD plants were more resistant to *Bs*-induced necrosis than the azygous control (Fig. 21). *Bs* is a severe soil-born pathogen of barley and wheat and causes economically important diseases such as foliar spot blotch and common root rot in warmer and humid growing areas (Kumar *et al.*, 2002). *Bs* is a hemibiotrophic pathogen that displays a short biotrophic growth phase in which well-developed pathogen hyphae were visualized in barley living epidermal cells. Following this, a necrotrophic growth phase occurs, in which host cell death is triggered, probably by toxin secretion, and *Bs*-hyphae spread into the mesophyll tissue (Schäfer *et al.*, 2004). Interestingly, H₂O₂ accumulation during the *Bs* necrotrophic growth phase seems to play a key role in the susceptibility to spot blotch in barley. This fact could explain, at least partially, the resistance phenotype of the *HvRBOHF2* KD plants, characterized by reduced pathogen-induced oxidative burst. H₂O₂ levels strongly increase in collapsing mesophyll cells of barley plants inoculated with *Bs* and in *Bs* culture filtrate-infiltrated leaf areas, especially in the *mlo*-mutant (Kumar *et al.*, 2001). On other hand, in the barley LMM mutant *nec8.3550*, which is tolerant to *Bs*, the pathogen-induced generation of H₂O₂ in leaves is greatly reduced in comparison to the moderately susceptible parental line Bowman Rph3 (Persson *et al.*, 2009). Additionally, a reduction in the number and size of *Bs*-induced lesions may be associated with the enhanced SA-related defence responses in *HvRBOHF2* KD plants. It was shown recently that resistance to *Bs* in wheat is linked to accumulation of SA and phenolic compounds (Sahu *et al.*, 2016). Moreover, tolerance to spot blotch in *nec8.3550* leaves was also associated with high constitutive expression of *PR* genes (that was not further increased upon *Bs*-infection) and reduced expression of the NADPH oxidase *HvRBOHB* both in inoculated and mock-inoculated plants (Persson *et al.*, 2009).

4.3.2 Susceptibility to *F. culmorum* is also leaf age-dependent

In contrast to susceptibility to *Bgh*, old leaves of *HvrRBOHF2* KD lines were more susceptible to development of the aggressive *Fusarium* strain *Fc002* while young leaves were rather more resistant (Fig. 20). *Fc* is another soil-borne fungal pathogen and is associated with important diseases in wheat, barley and other cereals in northern, central, western and recently in the Mediterranean regions of Europe (Scherm *et al.*, 2013). *Fc* together with *F. graminearum* (*Fg*) are the main species of the *Fusarium* complex causing FHB, a worldwide spreading, devastating disease of small grain cereal crops (Walter *et al.*, 2010). *Fc*, as well as the close relative *Fg*, display a hemibiotroph lifestyle in floral tissue, with a very brief biotrophic phase (Boddu *et al.*, 2006; Linkmeyer *et al.*, 2013). *Fusarium* complex fungi normally do not cause foliar infection in barley or wheat. However, (detached) leaf infection assays have been used to study the interaction of these cereals with *Fusarium* spp. and/or identify resistant sources to FHB, as resistance detected in foliar tissues correlates well with resistance to the pathogen in floral tissues (Browne, 2007; Chen *et al.*, 2009; Barna *et al.*, 2011; McGrann *et al.*, 2015). Furthermore, both *Fc* and *Fg* are able to colonize and cause symptoms in intact foliar tissues of the wild grass *Brachypodium distachyon* and infection of these tissues is very similar (Peraldi *et al.*, 2011). In this study, I could not observe *Fc002*-induced lesions in intact leaves of the azygous control in any of the independent biological experiments. In KD plants, if there were symptoms they were not distinguishable from the spontaneous cell death phenotype. However, fungal DNA was detected in all the leaves of the inoculated plants. *Fusarium* asymptomatic infections are quite common. *Fusarium* spp. DNA and mycotoxins are detectable in both symptomatic and asymptomatic barley kernels (Geißinger *et al.*, 2017). Ali and Francl (2001) were able to isolate *Fusarium* spp. from asymptomatic leaves of wheat and the authors suggested that FHB pathogens can survive parasitically and saprophytically on leaves throughout the season.

Intriguing, old leaves of *HvrRBOHF2* KD plants, characterized by enhanced accumulation of SA, displayed enhanced colonization by *Fc002*. SA have been implicated in resistance against FHB. Expression of genes related to SA-signalling pathways is strongly up-regulated in wheat spikes infected with *Fg*. Moreover, SA levels increase in *Fg*-inoculated wheat spikes and treatment with SA-analogues enhanced resistant to FHB (Ding *et al.*, 2011; Makandar *et al.*, 2012). Additionally, ectopic expression of the *Arabidopsis thaliana AtNPR1* gene in wheat leads to enhanced basal resistance to *Fg* (Makandar *et al.*, 2006).

Susceptibility to FHB may be associated with PCD. DELLA are nuclear plant proteins involved in repression of growth and promotion of plant survival upon stress stimulus through the regulation of ROS levels (Achard *et al.*, 2006; 2008; Navarro *et al.*, 2008). Wheat and

barley DELLA gain-of-function mutants display enhanced resistance to cell death following wound-inoculation of leaves with *Fg*. Furthermore, wheat DELLA gain-of-function mutants are more tolerant to the Fusarium mycotoxin deoxynivalenol (Saville *et al.*, 2011). In addition, over-expression of the negative cell death regulator *HvBI-1* in barley transgenic plants results in reduced susceptibility to *Fg* (Babaeizad *et al.*, 2009). As discussed previous (chapter 4.1), old leaves of 17-day-old *HvRBOHF2* KD plants displayed enhanced signs of spontaneous cell death. Therefore, increased susceptibility to *Fc* colonization in older first leaves of KD plants may be associated with PCD. However, this did not completely explain supersusceptibility phenotype of *HvRBOHF2* KD, as the level of *Fc*-DNA in second leaves did not differ between the two genotypes.

4.4 Role of the barley NADPH oxidases RBOHF in susceptibility to pathogens

RBOH-derived ROS production appears to be essential in the signalling pathways leading to plant defence (Marino *et al.*, 2012). Yet, the exact function of these molecules in plant disease resistance against pathogens is very complex because of the multiplicity of signals that are affected by RBOH enzymes. *HvRBOHF2* KD plants seem to display reduced levels of pathogen/MAMP-induced ROS burst (Fig. 9, Torres *et al.*, 2017). Although these data have to be interpreted carefully, one could speculate that a reduced ability to mount an early oxidative burst could have contributed to enhanced susceptibility to penetration by *Bgh* of young *HvRBOHF2* KD leaves. Additionally, inoculated leaves of KD plants display enhanced expression of the susceptibility factor *HvMlo*, especially in young leaves. It has been shown, that transient overexpression of *HvMlo* in the *Mlo* background further increased the frequency of *Bgh*-penetration, indicating that the *HvMlo*-promoted susceptibility to powdery in WT plants is incomplete (Kim *et al.*, 2002). Although an increase in the number and size of papilla has been described as a hallmark of the *mlo*-resistance (Kusch and Panstruga, 2017), the mechanism that promotes supersusceptibility to *Bgh* in plants overexpressing *Mlo* is unknown. Thus, it is reasonable to suggest that the enhanced *HvMlo* expression may contribute to enhanced susceptibility to *Bgh*-penetration in young leaves of *HvRBOHF2* KD plants, even though the frequency of papilla formation was not altered in KD lines (Fig. 9 and Supplementary Fig. S9). In older leaves, the effect of a reduced ROS burst and enhanced *Mlo* expression might have then been over-compensated by the spontaneous cell death phenotype, as biotrophic pathogens need living tissue to survive. Besides, alternative defence responses associated with functions of PR proteins and SA could contribute to resistance in old leaves of KD plants.

Similarly, enhanced expression of *PR* genes and accumulation of SA could explain the increased resistance to the hemibiotrophic fungal pathogen *Bs* in second leaves of

HvRBOHF2 KD lines. However, as the third leaves of KD plants were also more resistant to the spot blotch disease, it is reasonable to suggest that a reduction in the pathogen/MAMP-triggered oxidative burst may contribute for this phenotype. Regarding the susceptibility to *Fc*, enhanced accelerated senescence and cell death possible support the increased colonization by *Fc002* in old leaves of *HvRBOHF2* KD lines.

4.5 *HvRBOHD* contributes to penetration resistance towards *Bgh*

4.5.1 *HvRBOHD*, a previously undescribed barley NADPH oxidase

Based on results of a recently published microarray (Schnepf *et al.*, 2017), a new barley NADPH oxidase was characterized here. Phylogenetic analyzes revealed a high similarity of the protein with AtRBOHD and putative RBOHD orthologs in plant species such as maize (ZmRBOHD), rice (OsRBOHB-like [OsNox8]), tomato (SIRBOHB and SIRBOHD) and tobacco (NtRBOHD and NbRBOHB) and the gene was named *HvRBOHD* (Fig. 22). *HvRBOHD* showed all conserved features of plant RBOH proteins such as the core C-terminal region and the multiple regulatory motifs such as the two calcium-binding EF in the N-terminal region (Suzuki *et al.*, 2011). Curiously, the publication of the crystal structure of the N-terminal region of OsRBOHB, revealed the existence of two additional EF-hand-like motifs not predicted from a sequence analysis (Oda *et al.*, 2010). Interestingly, the AA involved in the formation of the hydrophobic core and backbone hydrogen bonds necessary to form the anti-parallel β -sheet in the EF-hand-like domain (Oda *et al.*, 2010), are conserved in *HvRBOHD* (Fig. 21). Additionally, serine residues, proven to be phosphorylated by Arabidopsis AtCPK5 and/or AtBIK1 in AtRBOHD, are also highly conserved (Dubiella *et al.*, 2013; Kadota *et al.*, 2014; Li *et al.*, 2014). To my knowledge, there is no ortholog of BIK1 characterized in barley. However, recently, Cieřla *et al.* (2016) identified 24 barley putative CPKs, including HvCPK5a (BAJ96062) a predicted barley orthologue of AtCPK5.

Regulation of NADPH oxidase proteins by PA has been also reported. PA is key lipid signal in plants whose formation is triggered in response to stress such as pathogen infection, drought, salinity, wounding and cold (Testerink and Munnik, 2005). Zhang *et al.* (2009b) showed that the PHOSPHOLIPASE D α 1(PLD α 1)-derived PA interacts directly with AtRBOHD and enhances ABA-induced ROS production in Arabidopsis guard cells, thus, suggesting a role of PA in the regulation of RBOHD orthologues. Curiously, just one PA-binding site was found in the *HvRBOHD* sequence. In Arabidopsis, arginine residues R149, R150, R156 and R157 of AtRBOHD have been shown to be important for the PA binding to this protein (Zhang *et al.*, 2009b). However, despite basic residues (His, Lys and Arg) are usually implicated in PA binding, no consensus AA sequence or structural fold involved in

these processes has been identified so far (Wang *et al.*, 2006). Thus, a possible regulation of HvrBOHD by PA cannot be ruled out.

4.5.2 *HvrBOHD* is a possible resistance factor to *Bgh*

HvrBOHD expression in barley leaves was usually weak but got up-regulated upon *Bgh*-infection (Fig. 23). Likewise, transcript levels of *HvrBOHF2* slightly accumulate in infected leaves in the first hours after *Bgh*-inoculation, dropping back to control levels at 48 hai (Hückelhoven *et al.*, 2001; Trujillo *et al.*, 2006). According to Trujillo *et al.* (2006) the data suggested that post-transcriptional regulation may be more important for the activity of these enzymes than transcriptional regulation. As described above, HvrBOHD possess most or even all the conserved multiple regulatory motifs of the N-terminal region. Alternatively, the expression of *HvrBOHD* could be induced strongest at very early time points, because it is directly after the pathogen is recognized by the plant immune system. In fact, Arabidopsis AtRBOHD is related to early immune responses. Recently, Morales *et al.* (2016) reported on the generation of Arabidopsis transgenic lines expressing the promoters of *AtRBOHD* and *AtRBOHF* fused to β -glucuronidase and luciferase reporters. The authors showed that activation of the AtRBOHD promoter can be detected already 15 min after elicitation with different MAMPs. In addition, the expression of AtRBOHD in WT plants treated with flg22 is approximately 5-fold higher than in mock-treated plants 90 min after elicitation (Morales *et al.*, 2016).

Despite the *Bgh*-induced *HvrBOHD* expression at 12 hai, my results indicate that this gene contributes to resistance against the barley powdery mildew fungus. Plants RBOH type D are the primary source of ROS during PTI and ETI (Kadota *et al.*, 2015). Tomato plants silenced for *SIRBOHB* inoculated with the necrotrophic fungus *B.cinerea* display a reduced pathogen-induced ROS accumulation and attenuated expression of defence response genes (Li *et al.*, 2015). In Arabidopsis, *AtRBOHD* modulates susceptibility to several classes of pathogens with different lifestyles, including the powdery mildew fungus *G. cichoracearum* (Marino *et al.*, 2012).

4.6 Role of carbohydrate metabolism genes in resistance to *Bgh*

Infection with pathogens leads to several alterations in host sugar metabolism. For instance, barley plants infected with *Bgh* display a lower rate of photosynthesis, increased ADH activity and accumulation of glucose and fructose in cells which *Bgh* attempts to penetrate. The latter is related to a progressive increase in the activity of sucrose cleaving enzymes, invertases and to a less extent, SUS (Swarbrick *et al.*, 2006; Pathuri *et al.*, 2011). Here, silencing of barley HvSUS1 did not significantly alter fungal penetration success. However, more

comprehensive studies would be required to conclude on possible functions of barley sucrose synthases in interaction with *Bgh*.

4.6.1 HvCwINV1 is a putative resistance factor to *Bgh*

Enhanced foliar activity of HvCwINV is observed in both resistant and susceptible barley lines inoculated with the barley powdery mildew fungus. However, it starts earlier and is much stronger in resistant genotypes, suggesting a role of barley CwINVs in resistance against *Bgh* (Swarbrick *et al.*, 2006). Here, I observed that *HvCwINV1* expression was slightly reduced during *Bgh*-infection (Fig. 25). TIGS of this gene results in a small and not fully reproducible increase in susceptibility to penetration by *Bgh*. However, when the leaves were kept in sucrose solution after the particle bombardment, a statistically significant increase in the susceptibility was noticed in cells transformed with the *HvCwINV1* TIGS construct (Fig. 26).

The majority of the phytopathogens express hexose transporters for the uptake of host sugar molecules, indicating that sucrose must be hydrolysed in the host before it can be taken up by the pathogen. However, some phytopathogens such as the biotrophic corn smut fungus *Ustilago maydis* express sucrose transporters instead (Fernandez *et al.*, 2014; Ruan, 2014). Interestingly, the *B. graminis* genome has two sucrose transporter genes with similarities to the sucrose transporter of *U. maydis* UmSrt1, suggesting that *Bgh* does not depend on hexoses released from host CwINV activity (Spanu and Kamper, 2010). Taken together, these data suggests that CwINV may act as a resistance factor against *Bgh*. A role of the CwINV in supporting plant defence responses is also suggested by other studies (Proels and Hückelhoven, 2014; Tausin and Giardina, 2014). For instance, Sonnewald *et al.* (2012) showed that type three effectors from the phyto-bacteria *Xanthomonas euvesicatoria* negatively regulates the activity of pepper cell wall invertases, suppressing sugar-enhanced defence responses during the pathogen infection. Additionally, rice *GRAIN INCOMPLETE FILLING 1* (*gif1*) mutants have a loss-of-function mutation in the *OsCWIN2* gene. *gif1* mutants are supersusceptible to postharvest fungal pathogens like *Alternaria* sp. and *Rhizopus* sp. On the contrary, mutants constitutively overexpressing the *OsCWIN2* gene show constitutively activated immune responses and are more resistant to both the bacterial pathogen *Xanthomonas oryzae* pv. *oryzae* and the rice blast fungal pathogen *M. oryzae* (Sun *et al.*, 2014).

The phenotype of barley single cells which are transiently silenced for *HvCwINV1* was rather weak and dependent on sucrose supplementation. This indicates perhaps, that other isoforms of CwINV also contribute to *Bgh* resistance in barley. Weschke *et al.* (2003) identified three putative CwINV genes (*HvCwINV1*, *HvCwINV2* and *HvCwINV3*) in the barley

genome. However, a BLASTP search at the NCBI GenBank against the *H. vulgare* database using the protein sequences of HvCwINV1 revealed five further putative CwINV genes besides the three mentioned ones (Supplementary Fig. S27). Surprisingly, among the eight putative genes, half of them, including HvCwINV2, showed a mutated Asp-239 residue. The Asp-239 residue has a critical role in both binding and hydrolysis of sucrose, therefore it is essential to CwINV activity. It is believed that enzymes lacking this amino acid residue are unable to hydrolyse sucrose and these enzymes are called defective invertases (Le Roy *et al.*, 2007; Van den Ende *et al.*, 2009). Defective invertases are described in several plant species such as Arabidopsis, maize, potato, rice, tobacco and tomato (Li *et al.*, 2017). Interestingly, they also seem to be involved in the regulation of CwINV activity. Recently, Le Roy *et al.* (2013) showed that the tobacco Nin88, a previously presumed functional CwINV involved in pollen development, lacks the crucial amino acids Asp-239 and Trp-47. Surprisingly, the activity of the tobacco NtCwINV1 is enhanced in the presence of Nin88. The authors suggested that Nin88 competitively binds to the pollen cell wall matrix, which results in increased levels of free NtCwINV1, which is able to hydrolyse apoplastic sucrose. On the other hand, Nin88 potentially enhances the effect of NtCIF, the specific INVNH of NtCwINV1, by competition with the binding on the cell wall matrix or by increasing the level of NtCwINV1 available for NtCIF binding (Le Roy *et al.*, 2013).

Both *SUS* and *CwINV* genes are sugar responsive, meaning their expression is modulated by sugar (Koch, 1996). The sugar supplementation was performed to induce the expression of these genes homogeneously in single cells of the detached barley leaves. However, several defence-related genes are also sugar responsive and sugars haven been reported as inductors of plant resistance (Gómez-Ariza *et al.*, 2007; Kano *et al.*, 2013). Therefore, an effect of sucrose on induction of disease resistance against *Bgh* cannot be ruled out. Further studies are necessary to uncover the role of sucrose supplementation in *HvCwINV1* KD-mediated susceptibility to *Bgh*. Nevertheless, *HvCwINV1* apparently plays a role, either directly or indirectly, in barley resistance against *Bgh*.

4.6.2 INVNH1 is another putative resistance factor to *Bgh*

INVNHs compete with sucrose for the binding site of acidic invertases (CwINV and VINV) and negatively regulated the activity of these enzymes in a pH-dependent manner (reviewed by Proels and Hüchelhoven, 2014). INVNHs can be highly specific such as the tobacco NtVIF, which specifically inhibits VINV or non-specific such as NtCIF, which shows an activity against a broad range of different plant CwINV and VINV preparations. However, this protein family is not well conserved and a prediction of the function based only on sequence information is very difficult and can be unreliable (Rausch and Greiner, 2004). Here I showed

that transient overexpression of HvINVNH1 led to enhanced resistance against *Bgh*-penetration (Fig. 26). This result suggests that at least one isoform of barley acidic invertases could be a putative susceptibility factor towards *Bgh*. However, there is no information available about the function of HvINVNH1. Thus, it is not possible to determine if CwINV and/or VINV is the target of this enzyme.

Contrasting with the well-established link between plant response against pathogen and CwINVs, the role of VINVs during plant-pathogens interactions is poorly understood (Tauzin and Giardina, 2014). Veillet *et al.* (2016) showed that VINV activity is higher than the activity of CwINV and cytoplasmatic invertase in both non-inoculated and *B. cinerea* infected Arabidopsis leaves. Moreover, although expression and activity of AtCwINV1 is up-regulated in infected leaves, susceptibility to *B. cinerea* is not affected in the loss of function *Atcwinv1* mutant. According to the authors, intracellular invertase activity was probably sufficient to maintain sugar homeostasis in host cells and to fuel plant defences (Veillet *et al.*, 2016). On the other hand, infection of tobacco leaves with oomycete *P. nicotianae* did not lead to increase in the VINV activity. Moreover, the VINV activity in tobacco source leaves was not affected by the repression of NtCwINV in neither *P. nicotianae*-infected nor non-infected leaves (Essmann *et al.*, 2008a; 2008b).

4.7 G6PDH enzymes seems not be involved in modulation of susceptibility to *Bgh*

G6PDH enzymes catalyse the first step of the OPPP, therefore, they play an important role in the generation of the reducing agent NADPH in non-photosynthetic cells. NADPH is necessary in several reductive metabolic pathways (e.g. biosynthesis of fatty acids and carotenoids) and is essential for the activity of antioxidative enzymes (e.g. glutathione reductase and NADPH-dependent thioredoxin reductases) and plant NADPH oxidase enzymes (Kruger and von Schaewen, 2003; Corpas and Barroso, 2014). G6PDH enzymes is involved in resistance to biotic and abiotic stresses (Esposito, 2016). Both the expression and activity of the sugarcane ScG6PD enzyme are induced upon stress stimulus such as salt, drought, heavy metal and low temperature treatments (Yang *et al.*, 2014). ROS burst and HR triggered by INF1 elicitor from *P. infestans* are compromised in *N. benthamiana* plants silenced for *NbG6PDH-P2* and this plants are more susceptible to this oomycete (Asai *et al.*, 2011). In addition, there are evidences of a role of the OPP pathway in resistance against *Bgh* in barley. 6-Phosphocluconolactonase (6PGL) catalyses the second enzymatic reaction of the OPPP, which also generates NADPH. Interestingly, the expression of barley *Hv6PGL* is down regulated in *Bgh*-infected barley epidermal peels. Moreover, the transient knock-down of *Hv6PGL* results in enhanced susceptibility to *Bgh*-penetration (Douchkov *et*

al., 2014). Here, I did not find clear evidence that *Bgh*-infection results in induction of the expression of *HvG6PDH* isogenes (Fig 25). Additionally, according to the results of my TIGS experiments results, only G6PDH-C2 is potentially involved in modulation of susceptibility to *Bgh* (Fig. 28). Nevertheless, the effect of TIGS of *HvG6PDH-C2* was rather weak and statistically not significant.

4.8 Hypothetical model for the role of HvRBOHs and carbohydrate metabolism enzymes in defence responses against *Bgh*

Based on the results shown here and elsewhere, I propose a model for the role of barley NADPH oxidases, CwINV1 and INVNH1 enzymes in regulation of barley defence responses against *Bgh* (Fig. 29). Barley RBOHF acts as a negative regulator of PCD processes possibly via regulation of expression of genes involved in the control of cell death and suppression of SA biosynthesis and/or signalling. In dicots plants, SA accumulates during leaf senescence and play a positive role in senescence-associated cell death. Arabidopsis transgenic plants defectives in SA-signalling display extended leaf longevity whereas plants accumulating high levels of this hormone undergo leaf senescence early (Morris *et al.*, 2000; Bartsch *et al.*, 2010; Zhang *et al.*, 2013; Zhao *et al.*, 2016). I suggest that a threshold reduction in expression/activity of HvRBOHF2 triggered either by developmental or stress stimuli alters the expression of genes related to PCD regulation or execution. Moreover, it directly or indirectly results in de-repression or stimulation of SA accumulation. Collectively these modifications culminate in cell death. As a biotrophic pathogen, *Bgh* needs living tissue to survive. Thus, PCD indirectly contribute to resistance against the barley powdery mildew fungus in leaves where the HvRBOHF2 threshold reduction was reached. Besides, SA possible also supports resistance against *Bgh*. SA plays a crucial role in the genetic reprogramming, being responsible for transcriptional control of several defence related genes as for instance those encoding PR proteins (Vlot *et al.*, 2009; Herrera-Vásquez *et al.*, 2015). The expression of several *PR* genes was constitutively up-regulated in HvRBOHF2 KD plants, including *HvPR1b*, proven to be involved in resistance to *Bgh* (Schultheiss *et al.*, 2003a). Additionally, SA or SA-derivatives may have an antimicrobial activity against *Bgh* and other pathogens.

Besides its role in regulation of cell death, HvRBOHF enzymes are also involved, together with RBOHD, in defence responses. Upon *Bgh* recognition by the barley immune system, HvRBOHD/F are activated through an unknown mechanism. HvRBOHD/F-produced ROS can contribute to plant defence responses directly, for example as an antimicrobial agent against *Bgh*. In addition, it can act as secondary messenger to trigger or hamper further immune responses.

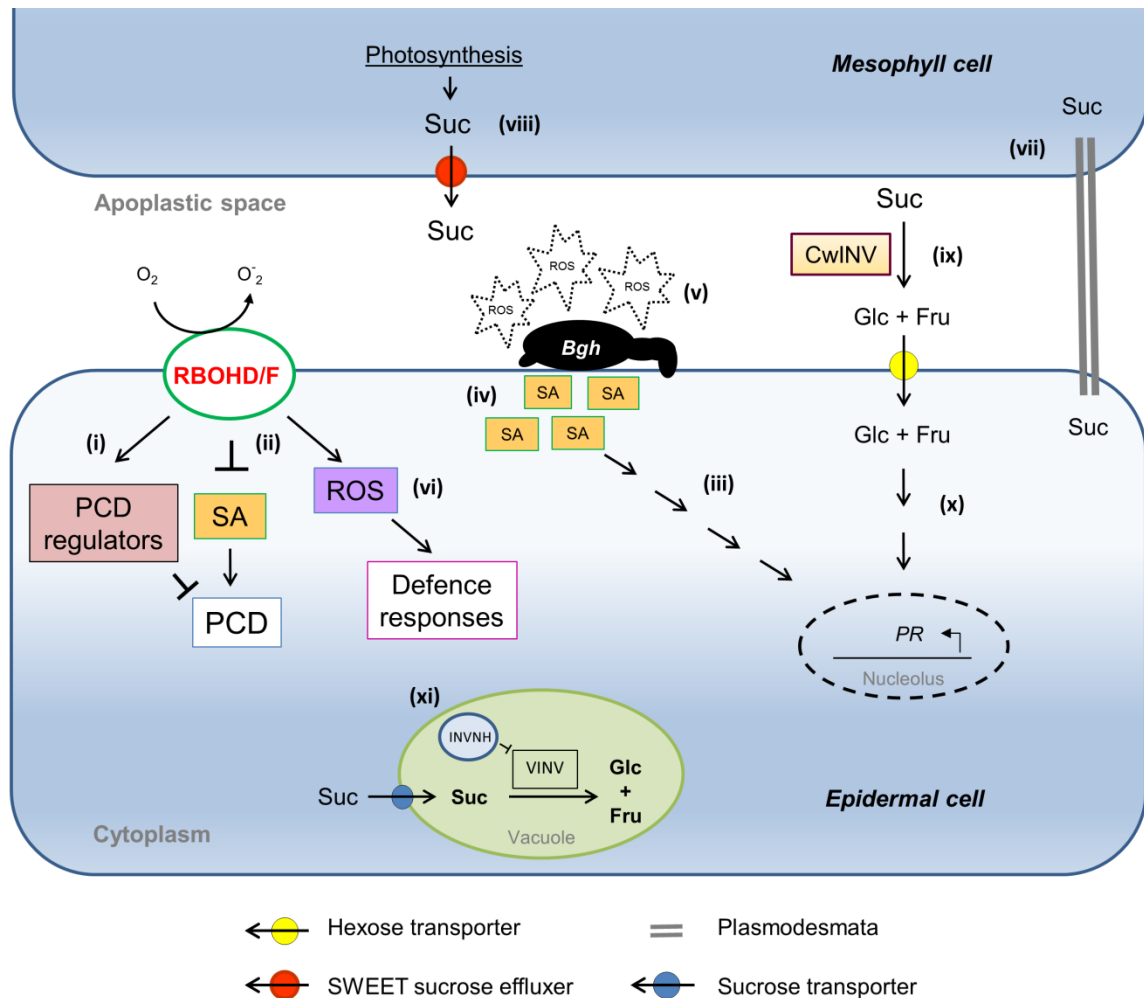


Figure 29: Hypothetical model for the role of HvrBOHs and sucrose metabolism in barley defence responses against *Bgh*. A threshold reduction in expression/activity of HvrBOHF2 triggers PCD, possible via down-regulation of the expression of PCD negative regulators genes (i) and stimulation of SA accumulation (ii). SA accumulation results in induction of expression of defence genes related genes such as *PR* genes (iii). Additionally, SA or SA-derivatives may have an antimicrobial activity against *Bgh* (iv). Upon *Bgh* recognition by the barley immune system, HvrBOHD/F is activated through an unknown mechanism. HvrBOHD/F-produced ROS can act as an antimicrobial agent against *Bgh* (v). Or it can act as secondary messenger to trigger or hamper further immune responses (vi). Besides ROS accumulation, *Bgh*-infection also triggers changes in the barley carbohydrate metabolism. Sucrose (Suc) produced in the photosynthetic active source cells is transported from mesophyll cells directly into the cytoplasm of the infected cell (vii) or to the apoplastic space (viii). Apoplastic sucrose can be degraded into hexoses by cell wall invertase (CwINV) and then transferred to the cytoplasm of the infected cell (ix). In the cytoplasm, hexoses fuel defence related processes. Hexoses can also act as signalling molecule to activate expression of defence-related genes such as *PR* genes (x). Invertase inhibitor (INVNH) directly interacts with acidic invertase (CwINV and VINV), keeping the activity of the enzyme at low levels (xi). Fru, fructose; Glc, glucose; SA, salicylic acid; RBOH, respiratory burst oxidase; *PR*, pathogenesis-related.

Bgh infection also triggers a deep reorganization in barley sugar metabolism. Carbohydrates are necessary to fuel defence related processes and are sources of carbon skeletons, reducing power and energy for biosynthesis of new molecules (Bolton, 2009). Sucrose produced in photosynthetic tissues may be transported from mesophyll cells to the apoplastic space (via SWEET sucrose effluxers) or directly into the cytoplasm of the infected cell (via plasmodesmata). Apoplastic sucrose can be degraded into hexoses by CwINV and then transferred to the cytoplasm via hexose transporters. In fact, there are several reports of concomitant enhanced expression of CwINV genes and hexose transporters (reviewed by Proels and Hüchelhoven, 2014; Tauzin and Giardina, 2014). In the cytosol, hexoses can possibly act as signalling molecule to activate expression of defence-related genes such as *PR* genes. INVNH directly interacts with the acidic invertase (CwINV and VINV), keeping the activity of the enzyme at low levels. Overexpression of INVNH1 results in reduced susceptibility to *Bgh*-penetration, suggesting the involvement of VINV in susceptibility to *Bgh*. However, more experiments are necessary to make reliable conclusions about this.

5 REFERENCES

- Acevedo-Garcia J, Kusch S, Panstruga R.** 2014. Magical mystery tour: MLO proteins in plant immunity and beyond. *New Phytologist* **204**, 273-281.
- Achard P, Cheng H, De Grauwe L, Decat J, Schoutteten H, Moritz T, Van Der Straeten D, Peng J, Harberd NP.** 2006. Integration of plant responses to environmentally activated phytohormonal signals. *Science* **311**, 91-94.
- Achard P, Renou J-P, Berthomé R, Harberd NP, Genschik P.** 2008. Plant DELLAs restrain growth and promote survival of adversity by reducing the levels of reactive oxygen species. *Current Biology* **18**, 656-660.
- Ali S, Franci L.** 2001. Progression of Fusarium species on wheat leaves from seedlings to adult stages in North Dakota. *Anais, National Fusarium Head Blight Forum, Erlanger, KY, USA*, 99.
- Amborabé B-E, Fleurat-Lessard P, Chollet J-F, Roblin G.** 2002. Antifungal effects of salicylic acid and other benzoic acid derivatives towards *Eutypa lata*: structure-activity relationship. *Plant Physiology and Biochemistry* **40**, 1051-1060.
- Asai S, Yoshioka M, Nomura H, Tone C, Nakajima K, Nakane E, Doke N, Yoshioka H.** 2011. A plastidic glucose-6-phosphate dehydrogenase is responsible for hypersensitive response cell death and reactive oxygen species production. *Journal of General Plant Pathology* **77**, 152-162.
- Avila-Ospina L, Marmagne A, Soulay F, Masclaux-Daubresse C.** 2016. Identification of barley (*Hordeum vulgare* L.) autophagy genes and their expression levels during leaf senescence, chronic nitrogen limitation and in response to dark exposure. *Agronomy* **6**, 15.
- Avila-Ospina L, Moison M, Yoshimoto K, Masclaux-Daubresse C.** 2014. Autophagy, plant senescence, and nutrient recycling. *Journal of Experimental Botany*, eru039.
- Aviv DH, Rustérucchi C, Iii BFH, Dietrich RA, Parker JE, Dangl JL.** 2002. Runaway cell death, but not basal disease resistance, in *Isd1* is SA- and NIM1/NPR1-dependent. *The Plant Journal* **29**, 381-391.
- Babaeizad V, Imani J, Kogel K-H, Eichmann R, Hückelhoven R.** 2009. Over-expression of the cell death regulator BAX inhibitor-1 in barley confers reduced or enhanced susceptibility to distinct fungal pathogens. *Theoretical and Applied Genetics* **118**, 455-463.
- Barna B, Jansen C, Kogel KH.** 2011. Sensitivity of barley leaves and roots to fusaric acid, but not to H₂O₂, is associated with susceptibility to Fusarium infections. *Journal of Phytopathology* **159**, 720-725.
- Bartsch M, Bednarek P, Vivancos PD, Schneider B, von Roepenack-Lahaye E, Foyer CH, Kombrink E, Scheel D, Parker JE.** 2010. Accumulation of isochlorogenic acid-derived 2,3-dihydroxybenzoic 3-O-β-D-xyloside in *Arabidopsis* resistance to pathogens and ageing of leaves. *Journal of Biological Chemistry* **285**, 25654-25665.
- Baxter L, Tripathy S, Ishaque N, Boot N, Cabral A, Kemen E, Thines M, Ah-Fong A, Anderson R, Badejoko W.** 2010. Signatures of adaptation to obligate biotrophy in the *Hyaloperonospora arabidopsidis* genome. *Science* **330**, 1549-1551.
- Bednarek P, Osbourn A.** 2009. Plant-microbe interactions: chemical diversity in plant defense. *Science* **324**, 746-748.
- Bellés JM, Garro R, Fayos J, Navarro P, Primo J, Conejero V.** 1999. Gentisic acid as a pathogen-inducible signal, additional to salicylic acid for activation of plant defenses in tomato. *Molecular Plant-Microbe Interactions* **12**, 227-235.
- Bernsdorff F, Döring A-C, Gruner K, Schuck S, Bräutigam A, Zeier J.** 2016. Pipecolic acid orchestrates plant systemic acquired resistance and defense priming via salicylic acid-dependent and independent pathways. *Plant Cell* **28**, 102-129.
- Berrocal-Lobo M, Stone S, Yang X, Antico J, Callis J, Ramonell KM, Somerville S.** 2010. ATL9, a RING zinc finger protein with E3 ubiquitin ligase activity implicated in chitin- and NADPH oxidase-mediated defense responses. *PLoS One* **5**, e14426.

- Beßer K, Jarosch B, Langen G, Kogel KH.** 2000. Expression analysis of genes induced in barley after chemical activation reveals distinct disease resistance pathways. *Molecular Plant Pathology* **1**, 277-286.
- Biswal B.** 1995. Carotenoid catabolism during leaf senescence and its control by light. *Journal of Photochemistry and Photobiology B: Biology* **30**, 3-13.
- Boddu J, Cho S, Kruger WM, Muehlbauer GJ.** 2006. Transcriptome analysis of the barley-*Fusarium graminearum* interaction. *Molecular Plant-Microbe Interactions* **19**, 407-417.
- Bolouri Moghaddam MR, Van den Ende W.** 2012. Sugars and plant innate immunity. *Journal of Experimental Botany* **63**, 3989-3998.
- Bolton MD.** 2009. Primary metabolism and plant defense-fuel for the fire. *Molecular Plant-Microbe Interactions* **22**, 487-497.
- Bonfig KB, Gabler A, Simon UK, Luschin-Ebengreuth N, Hatz M, Berger S, Muhammad N, Zeier J, Sinha AK, Roitsch T.** 2010. Post-translational derepression of invertase activity in source leaves via down-regulation of invertase inhibitor expression is part of the plant defense response. *Molecular Plant* **3**, 1037-1048.
- Browne R.** 2007. Components of resistance to *Fusarium* head blight (FHB) in wheat detected in a seed-germination assay with *Microdochium majus* and the relationship to FHB disease development and mycotoxin accumulation from *Fusarium graminearum* infection. *Plant Pathology* **56**, 65-72.
- Buchanan-Wollaston V, Earl S, Harrison E, Mathas E, Navabpour S, Page T, Pink D.** 2003. The molecular analysis of leaf senescence—a genomics approach. *Plant Biotechnology Journal* **1**, 3-22.
- Buchanan-Wollaston V, Page T, Harrison E, Breeze E, Lim PO, Nam HG, Lin JF, Wu SH, Swidzinski J, Ishizaki K.** 2005. Comparative transcriptome analysis reveals significant differences in gene expression and signalling pathways between developmental and dark/starvation-induced senescence in *Arabidopsis*. *The Plant Journal* **42**, 567-585.
- Büschges R, Hollricher K, Panstruga R, Simons G, Wolter M, Frijters A, van Daelen R, van der Lee T, Diergaarde P, Groenendijk J.** 1997. The barley Mlo gene: a novel control element of plant pathogen resistance. *Cell* **88**, 695-705.
- Butt A, Mousley C, Morris K, Beynon J, Can C, Holub E, Greenberg JT, Buchanan-Wollaston V.** 1998. Differential expression of a senescence-enhanced metallothionein gene in *Arabidopsis* in response to isolates of *Peronospora parasitica* and *Pseudomonas syringae*. *The Plant Journal* **16**.
- Camejo D, Guzman-Cedeno A, Moreno A.** 2016. Reactive oxygen species, essential molecules, during plant-pathogen interactions. *Plant Physiology and Biochemistry* **103**, 10-23.
- Cameron RK, Zaton K.** 2004. Intercellular salicylic acid accumulation is important for age-related resistance in *Arabidopsis* to *Pseudomonas syringae*. *Physiological and Molecular Plant Pathology* **65**, 197-209.
- Cardi M, Chibani K, Cafasso D, Rouhier N, Jacquot J-P, Esposito S.** 2011. Abscisic acid effects on activity and expression of barley (*Hordeum vulgare*) plastidial glucose-6-phosphate dehydrogenase. *Journal of Experimental Botany* **62**, 4013-4023.
- Carella P, Wilson DC, Cameron RK.** 2014. Some things get better with age: differences in salicylic acid accumulation and defense signaling in young and mature *Arabidopsis*. *Frontiers in Plant Science* **5**, 775.
- Carviel JL, Al-Daoud F, Neumann M, Mohammad A, Provart NJ, Moeder W, Yoshioka K, Cameron RK.** 2009. Forward and reverse genetics to identify genes involved in the age-related resistance response in *Arabidopsis thaliana*. *Molecular Plant Pathology* **10**, 621-634.
- Carviel JL, Wilson DC, Isaacs M, Carella P, Catana V, Golding B, Weretilnyk EA, Cameron RK.** 2014. Investigation of intercellular salicylic acid accumulation during compatible and incompatible *Arabidopsis-pseudomonas syringae* interactions using a fast neutron-generated mutant allele of EDS5 identified by genetic mapping and whole-genome sequencing. *PLoS One* **9**, e88608.
- Century KS, Lagman RA, Adkisson M, Morlan J, Tobias R, Schwartz K, Smith A, Love J, Ronald PC, Whalen MC.** 1999. Developmental control of Xa21-mediated disease resistance in rice. *The Plant Journal* **20**, 231-236.

- Chaouch S, Queval G, Noctor G.** 2012. AtRbohF is a crucial modulator of defence-associated metabolism and a key actor in the interplay between intracellular oxidative stress and pathogenesis responses in Arabidopsis. *The Plant Journal* **69**, 613-627.
- Chauhan H, Boni R, Bucher R, Kuhn B, Buchmann G, Sucher J, Selter LL, Hensel G, Kumlehn J, Bigler L.** 2015. The wheat resistance gene Lr34 results in the constitutive induction of multiple defense pathways in transgenic barley. *The Plant Journal* **84**, 202-215.
- Chen LQ.** 2014. SWEET sugar transporters for phloem transport and pathogen nutrition. *New Phytologist* **201**, 1150-1155.
- Chen X, Coram T, Huang X, Wang M, Dolezal A.** 2013. Understanding molecular mechanisms of durable and non-durable resistance to stripe rust in wheat using a transcriptomics approach. *Current Genomics* **14**, 111-126.
- Chen X, Steed A, Travella S, Keller B, Nicholson P.** 2009. *Fusarium graminearum* exploits ethylene signalling to colonize dicotyledonous and monocotyledonous plants. *New Phytologist* **182**, 975-983.
- Christiansen MW, Gregersen PL.** 2014. Members of the barley NAC transcription factor gene family show differential co-regulation with senescence-associated genes during senescence of flag leaves. *Journal of Experimental Botany*, eru046.
- Christie PJ, Hahn M, Walbot V.** 1991. Low-temperature accumulation of alcohol dehydrogenase-1 mRNA and protein activity in maize and rice seedlings. *Plant Physiology* **95**, 699-706.
- Cieśla A, Miśtuła F, Misztal L, Fedorowicz-Strońska O, Janicka S, Tajdel-Zielińska M, Marczak M, Janicki M, Ludwików A, Sadowski J.** 2016. A role for barley calcium-dependent protein kinase CPK2a in the response to drought. *Frontiers in Plant Science* **7**.
- Consonni C, Bednarek P, Humphry M, Francocci F, Ferrari S, Harzen A, van Themaat EVL, Panstruga R.** 2010. Tryptophan-derived metabolites are required for antifungal defense in the Arabidopsis mlo2 mutant. *Plant Physiology* **152**, 1544-1561.
- Consonni C, Humphry ME, Hartmann HA, Livaja M, Durner J, Westphal L, Vogel J, Lipka V, Kemmerling B, Schulze-Lefert P, Somerville SC, Panstruga R.** 2006. Conserved requirement for a plant host cell protein in powdery mildew pathogenesis. *Nature Genetics* **38**, 716-720.
- Corpas FJ, Barroso JB.** 2014. NADPH-generating dehydrogenases: their role in the mechanism of protection against nitro-oxidative stress induced by adverse environmental conditions. *Frontiers in Environmental Science* **2**, 55.
- Craddock C, Lavagi I, Yang Z.** 2012. New insights into Rho signaling from plant ROP/Rac GTPases. *Trends in Cell Biology* **22**, 492-501.
- Cui H, Tsuda K, Parker JE.** 2015. Effector-triggered immunity: from pathogen perception to robust defense. *Annual Review of Plant Biology* **66**, 487-511.
- Dangl JL, Dietrich RA, Richberg MH.** 1996. Death don't have no mercy: cell death programs in plant-microbe interactions. *Plant Cell* **8**, 1793.
- Dangl JL, Horvath DM, Staskawicz BJ.** 2013. Pivoting the plant immune system from dissection to deployment. *Science* **341**, 746-751.
- De Coninck B, Timmermans P, Vos C, Cammue BP, Kazan K.** 2015. What lies beneath: belowground defense strategies in plants. *Trends in Plant Science* **20**, 91-101.
- Dean R, Van Kan JA, Pretorius ZA, Hammond-Kosack KE, Di Pietro A, Spanu PD, Rudd JJ, Dickman M, Kahmann R, Ellis J, Foster GD.** 2012. The Top 10 fungal pathogens in molecular plant pathology. *Molecular Plant Pathology* **13**, 414-430.
- Develey-Riviere MP, Galiana E.** 2007. Resistance to pathogens and host developmental stage: a multifaceted relationship within the plant kingdom. *New Phytologist* **175**, 405-416.
- Devoto A, Piffanelli P, Nilsson I, Wallin E, Panstruga R, von Heijne G, Schulze-Lefert P.** 1999. Topology, subcellular localization, and sequence diversity of the Mlo family in plants. *Journal of Biological Chemistry* **274**, 34993-35004.
- Dey S, Wenig M, Langen G, Sharma S, Kugler KG, Knappe C, Hause B, Bichlmeier M, Babaeizad V, Imani J, Janzik I, Stempffl T, Huckelhoven R, Kogel KH, Mayer KF, Vlot AC.** 2014. Bacteria-

- triggered systemic immunity in barley is associated with WRKY and ETHYLENE RESPONSIVE FACTORS but not with salicylic acid. *Plant Physiology* **166**, 2133-2151.
- Dietrich RA, Delaney TP, Uknes SJ, Ward ER, Ryals JA, Dangl JL.** 1994. Arabidopsis mutants simulating disease resistance response. *Cell* **77**, 565-577.
- Dietrich RA, Richberg MH, Schmidt R, Dean C, Dangl JL.** 1997. A novel zinc finger protein is encoded by the Arabidopsis LSD1 gene and functions as a negative regulator of plant cell death. *Cell* **88**, 685-694.
- Ding L, Xu H, Yi H, Yang L, Kong Z, Zhang L, Xue S, Jia H, Ma Z.** 2011. Resistance to hemibiotrophic *Fusarium graminearum* infection is associated with coordinated and ordered expression of diverse defense signaling pathways. *PLoS One* **6**, e19008.
- Dmochowska-Boguta M, Nadolska-Orczyk A, Orczyk W.** 2013. Roles of peroxidases and NADPH oxidases in the oxidative response of wheat (*Triticum aestivum*) to brown rust (*Puccinia triticina*) infection. *Plant Pathology* **62**, 993-1002.
- Dolferus R, Jacobs M, Peacock WJ, Dennis ES.** 1994. Differential interactions of promoter elements in stress responses of the Arabidopsis *Adh* gene. *Plant Physiology* **105**, 1075-1087.
- Douchkov D, Lück S, Johrde A, Nowara D, Himmelbach A, Rajaraman J, Stein N, Sharma R, Kilian B, Schweizer P.** 2014. Discovery of genes affecting resistance of barley to adapted and non-adapted powdery mildew fungi. *Genome biology* **15**, 518.
- Douchkov D, Nowara D, Zierold U, Schweizer P.** 2005. A high-throughput gene-silencing system for the functional assessment of defense-related genes in barley epidermal cells. *Molecular Plant-Microbe Interactions* **18**, 755-761.
- Douglas S, Sherwood R, Lukezic F.** 1984. Effect of adult plant resistance on primary penetration of oats by *Erysiphe graminis* f. sp. *avenae*. *Physiological plant pathology* **25**, 219-228.
- Dreiseitl A, Jurečka D.** 2003. Severity of powdery mildew on spring barley in the Czech Republic in 1971–2000. *Plant Protection Science* **39**, 39-51.
- Dubiella U, Seybold H, Durian G, Komander E, Lassig R, Witte C-P, Schulze WX, Romeis T.** 2013. Calcium-dependent protein kinase/NADPH oxidase activation circuit is required for rapid defense signal propagation. *Proceedings of the National Academy of Sciences* **110**, 8744-8749.
- Duplessis S, Cuomo CA, Lin Y-C, Aerts A, Tisserant E, Veneault-Fourrey C, Joly DL, Hacquard S, Amselem J, Cantarel BL.** 2011. Obligate biotrophy features unraveled by the genomic analysis of rust fungi. *Proceedings of the National Academy of Sciences* **108**, 9166-9171.
- Durner J, Shah J, Klessig DF.** 1997. Salicylic acid and disease resistance in plants. *Trends in Plant Science* **2**, 266-274.
- Eichmann R, Bischof M, Weis C, Shaw J, Lacomme C, Schweizer P, Douchkov D, Hensel G, Kumlehn J, Hükelhoven R.** 2010. BAX INHIBITOR-1 is required for full susceptibility of barley to powdery mildew. *Molecular Plant-Microbe Interactions* **23**, 1217-1227.
- Eichmann R, Schultheiss H, Kogel K-H, Hükelhoven R.** 2004. The barley apoptosis suppressor homologue BAX inhibitor-1 compromises nonhost penetration resistance of barley to the inappropriate pathogen *Blumeria graminis* f. sp. *tritici*. *Molecular Plant-Microbe Interactions* **17**, 484-490.
- Elliott C, Zhou F, Spielmeier W, Panstruga R, Schulze-Lefert P.** 2002. Functional conservation of wheat and rice Mlo orthologs in defense modulation to the powdery mildew fungus. *Molecular Plant-Microbe Interactions* **15**, 1069-1077.
- Ellis JG, Lagudah ES, Spielmeier W, Dodds PN.** 2014. The past, present and future of breeding rust resistant wheat. *Frontiers in Plant Science* **5**, 641.
- Epple P, Mack AA, Morris VR, Dangl JL.** 2003. Antagonistic control of oxidative stress-induced cell death in Arabidopsis by two related, plant-specific zinc finger proteins. *Proceedings of the National Academy of Sciences* **100**, 6831-6836.
- Esposito S.** 2016. Nitrogen assimilation, abiotic stress and glucose 6-phosphate dehydrogenase: the full circle of reductants. *Plants* **5**, 24.

- Essmann J, Bones P, Weis E, Scharte J.** 2008a. Leaf carbohydrate metabolism during defense: intracellular sucrose-cleaving enzymes do not compensate repression of cell wall invertase. *Plant Signaling & Behavior* **3**, 885-887.
- Essmann J, Schmitz-Thom I, Schön H, Sonnewald S, Weis E, Scharte J.** 2008b. RNA interference-mediated repression of cell wall invertase impairs defense in source leaves of tobacco. *Plant Physiology* **147**, 1288-1299.
- Fernandez J, Marroquin-Guzman M, Wilson RA.** 2014. Mechanisms of nutrient acquisition and utilization during fungal infections of leaves. *Annual Review of Phytopathology* **52**, 155-174.
- Fraaije B, Lovell D, Rohel E, Hollomon D.** 1999. Rapid detection and diagnosis of *Septoria tritici* epidemics in wheat using a polymerase chain reaction/PicoGreen assay. *Journal of Applied Microbiology* **86**, 701-708.
- Gao Q-M, Zhu S, Kachroo P, Kachroo A.** 2015. Signal regulators of systemic acquired resistance. *Frontiers in Plant Science* **06**.
- Geißinger C, Hofer K, Habler K, Heß M, Hückelhoven R, Rychlik M, Becker T, Gastl M.** 2017. Fusarium Species on Barley Malt: Is Visual Assessment an Appropriate Tool for Detection? *Cereal Chemistry*, CCHEM-08-16-0212-R.
- Georgiou CD, Tairis N, Sotiropoulou A.** 2000. Hydroxyl radical scavengers inhibit lateral-type sclerotial differentiation and growth in phytopathogenic fungi. *Mycologia*, 825-834.
- Glazebrook J.** 2005. Contrasting mechanisms of defense against biotrophic and necrotrophic pathogens. *Annual Review of Phytopathology* **43**, 205-227.
- Gómez-Ariza J, Campo S, Rufat M, Estopà M, Messeguer J, Segundo BS, Coca M.** 2007. Sucrose-mediated priming of plant defense responses and broad-spectrum disease resistance by overexpression of the maize pathogenesis-related PRms protein in rice plants. *Molecular Plant-Microbe Interactions* **20**, 832-842.
- Greenberg JT.** 1996. Programmed cell death: a way of life for plants. *Proceedings of the National Academy of Sciences* **93**, 12094-12097.
- Guo J, Bai P, Yang Q, Liu F, Wang X, Huang L, Kang Z.** 2013. Wheat zinc finger protein TaLSD1, a negative regulator of programmed cell death, is involved in wheat resistance against stripe rust fungus. *Plant Physiology and Biochemistry* **71**, 164-172.
- Gupta R, Lee SE, Agrawal GK, Rakwal R, Park S, Wang Y, Kim ST.** 2015. Understanding the plant-pathogen interactions in the context of proteomics-generated apoplastic proteins inventory. *Frontiers in Plant Science* **6**, 352.
- Gust AA, Pruitt R, Nürnberger T.** 2017. Sensing Danger: Key to Activating Plant Immunity. *Trends in Plant Science*.
- Hanfrey C, Fife M, Buchanan-Wollaston V.** 1996. Leaf senescence in *Brassica napus*: expression of genes encoding pathogenesis-related proteins. *Plant Molecular Biology* **30**, 597-609.
- Hao Y, Wang T, Wang K, Wang X, Fu Y, Huang L, Kang Z.** 2016. Transcriptome Analysis Provides Insights into the Mechanisms Underlying Wheat Plant Resistance to Stripe Rust at the Adult Plant Stage. *Plos One* **11**, e0150717.
- He H, Yan J, Yu X, Liang Y, Fang L, Scheller HV, Zhang A.** 2017. The NADPH-oxidase AtRbohI plays a positive role in drought-stress response in *Arabidopsis thaliana*. *Biochemical and Biophysical Research Communications*.
- Hellemans J, Mortier G, De Paepe A, Speleman F, Vandesompele J.** 2007. qBase relative quantification framework and software for management and automated analysis of real-time quantitative PCR data. *Genome biology* **8**, R19.
- Herrera-Vásquez A, Salinas P, Holuigue L.** 2015. Salicylic acid and reactive oxygen species interplay in the transcriptional control of defense genes expression. *Frontiers in Plant Science* **6**.
- Hoefle C, Huesmann C, Schultheiss H, Bornke F, Hensel G, Kumlehn J, Hückelhoven R.** 2011. A barley ROP GTPase ACTIVATING PROTEIN associates with microtubules and regulates entry of the barley powdery mildew fungus into leaf epidermal cells. *Plant Cell* **23**, 2422-2439.

- Hofer K, Barmeier G, Schmidhalter U, Habler K, Rychlik M, Hückelhoven R, Hess M.** 2016. Effect of nitrogen fertilization on Fusarium head blight in spring barley. *Crop Protection* **88**, 18-27.
- Horváth E, Janda T, Szalai G, Páldi E.** 2002. In vitro salicylic acid inhibition of catalase activity in maize: differences between the isozymes and a possible role in the induction of chilling tolerance. *Plant Science* **163**, 1129-1135.
- Hückelhoven R.** 2004. BAX Inhibitor-1, an ancient cell death suppressor in animals and plants with prokaryotic relatives. *Apoptosis* **9**, 299-307.
- Hückelhoven R.** 2005. Powdery mildew susceptibility and biotrophic infection strategies. *FEMS Microbiology Letters* **245**, 9-17.
- Hückelhoven R, Dechert C, Kogel KH.** 2003. Overexpression of barley BAX inhibitor 1 induces breakdown of mlo-mediated penetration resistance to *Blumeria graminis*. *Proceedings of the National Academy of Sciences* **100**, 5555-5560.
- Hückelhoven R, Dechert C, Trujillo M, Kogel K-H.** 2001. Differential expression of putative cell death regulator genes in near-isogenic, resistant and susceptible barley lines during interaction with the powdery mildew fungus. *Plant Molecular Biology* **47**, 739-748.
- Hückelhoven R, Eichmann R, Weis C, Hoefle C, Proels R.** 2013. Genetic loss of susceptibility: a costly route to disease resistance? *Plant Pathology* **62**, 56-62.
- Hückelhoven R, Fodor J, Preis C, Kogel K-H.** 1999. Hypersensitive cell death and papilla formation in barley attacked by the powdery mildew fungus are associated with hydrogen peroxide but not with salicylic acid accumulation. *Plant Physiology* **119**, 1251-1260.
- Hückelhoven R, Fodor J, Trujillo M, Kogel K-H.** 2000a. Barley Mla and Rar mutants compromised in the hypersensitive cell death response against *Blumeria graminis* f. sp. *hordei* are modified in their ability to accumulate reactive oxygen intermediates at sites of fungal invasion. *Planta* **212**, 16-24.
- Hückelhoven R, Kogel K-H.** 1998. Tissue-specific superoxide generation at interaction sites in resistant and susceptible near-isogenic barley lines attacked by the powdery mildew fungus (*Erysiphe graminis* f. sp. *hordei*). *Molecular Plant-Microbe Interactions* **11**, 292-300.
- Hückelhoven R, Panstruga R.** 2011. Cell biology of the plant-powdery mildew interaction. *Current Opinion in Plant Biology* **14**, 738-746.
- Hückelhoven R, Trujillo M, Kogel KH.** 2000b. Mutations in Ror1 and Ror2 genes cause modification of hydrogen peroxide accumulation in mlo-barley under attack from the powdery mildew fungus. *Molecular Plant Pathology* **1**, 287-292.
- Jabs T, Dietrich RA, Dangl JL.** 1996. Initiation of runaway cell death in an Arabidopsis mutant by extracellular superoxide. *Science* **273**, 1853-1855.
- Jarosch B, Kogel K-H, Schaffrath U.** 1999. The ambivalence of the barley Mlo locus: mutations conferring resistance against powdery mildew (*Blumeria graminis* f. sp. *hordei*) enhance susceptibility to the rice blast fungus *Magnaporthe grisea*. *Molecular Plant-Microbe Interactions* **12**, 508-514.
- Ji X, Van den Ende W, Van Laere A, Cheng S, Bennett J.** 2005. Structure, evolution, and expression of the two invertase gene families of rice. *Journal of Molecular Evolution* **60**, 615-634.
- Jiao Y, Sun L, Song Y, Wang L, Liu L, Zhang L, Liu B, Li N, Miao C, Hao F.** 2013. AtrbohD and AtrbohF positively regulate abscisic acid-inhibited primary root growth by affecting Ca²⁺ signalling and auxin response of roots in Arabidopsis. *Journal of Experimental Botany* **64**, 4183-4192.
- Johrde A, Schweizer P.** 2008. A class III peroxidase specifically expressed in pathogen-attacked barley epidermis contributes to basal resistance. *Molecular Plant Pathology* **9**, 687-696.
- Kadota Y, Shirasu K, Zipfel C.** 2015. Regulation of the NADPH Oxidase RBOHD During Plant Immunity. *Plant and Cell Physiology* **56**, 1472-1480.
- Kadota Y, Sklenar J, Derbyshire P, Stransfeld L, Asai S, Ntoukakis V, Jones JD, Shirasu K, Menke F, Jones A.** 2014. Direct regulation of the NADPH oxidase RBOHD by the PRR-associated kinase BIK1 during plant immunity. *Molecular Cell* **54**, 43-55.

- Kano A, Fukumoto T, Ohtani K, Yoshihara A, Ohara T, Tajima S, Izumori K, Tanaka K, Ohkouchi T, Ishida Y.** 2013. The rare sugar d-allose acts as a triggering molecule of rice defence via ROS generation. *Journal of Experimental Botany* **64**, 4939-4951.
- Katagiri F, Tsuda K.** 2010. Understanding the plant immune system. *Molecular Plant-Microbe Interactions* **23**, 1531-1536.
- Kavanová M, Lattanzi FA, Grimoldi AA, Schnyder H.** 2006. Phosphorus deficiency decreases cell division and elongation in grass leaves. *Plant Physiology* **141**, 766-775.
- Kawai-Yamada M, Ohori Y, Uchimiya H.** 2004. Dissection of Arabidopsis Bax inhibitor-1 suppressing Bax-, hydrogen peroxide-, and salicylic acid-induced cell death. *The Plant Cell* **16**, 21-32.
- Kawano Y, Kaneko-Kawano T, Shimamoto K.** 2014. Rho family GTPase-dependent immunity in plants and animals. *Frontiers in Plant Science* **5**.
- Kaya H, Nakajima R, Iwano M, Kanaoka MM, Kimura S, Takeda S, Kawarazaki T, Senzaki E, Hamamura Y, Higashiyama T.** 2014. Ca²⁺-activated reactive oxygen species production by Arabidopsis RbohH and RbohJ is essential for proper pollen tube tip growth. *Plant Cell* **26**, 1069-1080.
- Keisa A.** 2013. Regulation of hypersensitive response in barley. Doctoral thesis, University of Latvia.
- Keisa A, Kanberga-Silina K, Nakurte I, Kunga L, Rostoks N.** 2011. Differential disease resistance response in the barley necrotic mutant nec1. *BMC Plant Biology* **11**, 66.
- Keisa A, Kanberga K, Gill U, Kleinhofs A, Rostoks N.** 2008. Cloning and characterization of barley homologues of the Arabidopsis LSD1 gene: putative regulators of hypersensitive response. *Acta Universitatis Latviensis* **745**, 87-101.
- Khatib M, Lafitte C, Esquerré-Tugayé MT, Bottin A, Rickauer M.** 2004. The CBEL elicitor of *Phytophthora parasitica* var. *nicotianae* activates defence in Arabidopsis thaliana via three different signalling pathways. *New Phytologist* **162**, 501-510.
- Kim DS, Hwang BK.** 2012. The pepper MLO gene, CaMLO2, is involved in the susceptibility cell-death response and bacterial and oomycete proliferation. *The Plant Journal* **72**, 843-855.
- Kim MC, Panstruga R, Elliott C, Müller J, Devoto A, Yoon HW, Park HC, Cho MJ, Schulze-Lefert P.** 2002. Calmodulin interacts with MLO protein to regulate defence against mildew in barley. *Nature* **416**, 447-451.
- Kim Y-J, Shim J-S, Lee J-H, Jung D-Y, Sun H, In J-G, Yang D-C.** 2009. Isolation and characterization of a novel short-chain alcohol dehydrogenase gene from *Panax ginseng*. *BMB reports* **42**, 673-678.
- Koch K.** 1996. Carbohydrate-modulated gene expression in plants. *Annual Review of Plant Biology* **47**, 509-540.
- Koch K.** 2004. Sucrose metabolism: regulatory mechanisms and pivotal roles in sugar sensing and plant development. *Current Opinion in Plant Biology* **7**, 235-246.
- Koeck M, Hardham AR, Dodds PN.** 2011. The role of effectors of biotrophic and hemibiotrophic fungi in infection. *Cellular Microbiology* **13**, 1849-1857.
- Kogel K-H, Beckhove U, Dreschers J, Munch S, Romme Y.** 1994. Acquired resistance in barley (the resistance mechanism induced by 2, 6-dichloroisonicotinic acid is a phenocopy of a genetically based mechanism governing race-specific powdery mildew resistance). *Plant Physiology* **106**, 1269-1277.
- Kosami K-i, Ohki I, Nagano M, Furuita K, Sugiki T, Kawano Y, Kawasaki T, Fujiwara T, Nakagawa A, Shimamoto K.** 2014. The crystal structure of the plant small GTPase OsRac1 reveals its mode of binding to NADPH oxidase. *Journal of Biological Chemistry* **289**, 28569-28578.
- Kraepiel Y, Barny M-A.** 2016. Gram-negative phytopathogenic bacteria, all hemibiotrophs after all? *Molecular Plant Pathology* **17**, 313-316.
- Kristensen BK, Ammitzbøll H, Rasmussen SK, Nielsen KA.** 2001. Transient expression of a vacuolar peroxidase increases susceptibility of epidermal barley cells to powdery mildew. *Molecular Plant Pathology* **2**, 311-317.

- Kruger NJ, von Schaewen A.** 2003. The oxidative pentose phosphate pathway: structure and organisation. *Current Opinion in Plant Biology* **6**, 236-246.
- Krupinska K, Dähnhardt D, Fischer-Kilbiński I, Kucharewicz W, Scharrenberg C, Trösch M, Buck F.** 2014. Identification of WHIRLY1 as a factor binding to the promoter of the stress-and senescence-associated gene HvS40. *Journal of Plant Growth Regulation* **33**, 91-105.
- Krupinska K, Haussuhl K, Schafer A, van der Kooij TA, Leckband G, Lorz H, Falk J.** 2002. A novel nucleus-targeted protein is expressed in barley leaves during senescence and pathogen infection. *Plant Physiology* **130**, 1172-1180.
- Kumar J, Hüchelhoven R, Beckhove U, Nagarajan S, Kogel K-H.** 2001. A compromised Mlo pathway affects the response of barley to the necrotrophic fungus *Bipolaris sorokiniana* (teleomorph: *Cochliobolus sativus*) and its toxins. *Phytopathology* **91**, 127-133.
- Kumar J, Schäfer P, Hüchelhoven R, Langen G, Baltruschat H, Stein E, Nagarajan S, Kogel KH.** 2002. *Bipolaris sorokiniana*, a cereal pathogen of global concern: cytological and molecular approaches towards better control. *Molecular Plant Pathology* **3**, 185-195.
- Kus JV.** 2002. Age-related resistance in Arabidopsis is a developmentally regulated defense response to *Pseudomonas syringae*. *The Plant Cell Online* **14**, 479-490.
- Kusch S, Panstruga R.** 2017. mlo-Based Resistance: An Apparently Universal “Weapon” to Defeat Powdery Mildew Disease. *Molecular Plant-Microbe Interactions* **30**, 179-189.
- Lammens W, Le Roy K, Schroeven L, Van Laere A, Rabijns A, Van den Ende W.** 2009. Structural insights into glycoside hydrolase family 32 and 68 enzymes: functional implications. *Journal of Experimental Botany* **60**, 727-740.
- Le Fevre R, O'Boyle B, Moscou MJ, Schornack S.** 2016. Colonization of barley by the broad-host hemibiotrophic pathogen *Phytophthora palmivora* uncovers a leaf development-dependent involvement of Mlo. *Molecular Plant-Microbe Interactions* **29**, 385-395.
- Le Roy K, Lammens W, Verhaest M, De Coninck B, Rabijns A, Van Laere A, Van den Ende W.** 2007. Unraveling the difference between invertases and fructan exohydrolases: a single amino acid (Asp-239) substitution transforms Arabidopsis cell wall invertase1 into a fructan 1-exohydrolase. *Plant Physiology* **145**, 616-625.
- Le Roy K, Vergauwen R, Struyf T, Yuan S, Lammens W, Mátrai J, De Maeyer M, Van den Ende W.** 2013. Understanding the role of defective invertases in plants: tobacco Nin88 fails to degrade sucrose. *Plant Physiology* **161**, 1670-1681.
- Lee H-I, León J, Raskin I.** 1995. Biosynthesis and metabolism of salicylic acid. *Proceedings of the National Academy of Sciences* **92**, 4076-4079.
- Li J, Wu L, Foster R, Ruan YL.** 2017. Molecular regulation of sucrose catabolism and sugar transport for development, defence and phloem function. *Journal of Integrative Plant Biology* **59**, 322-335.
- Li L, Li M, Yu L, Zhou Z, Liang X, Liu Z, Cai G, Gao L, Zhang X, Wang Y.** 2014. The FLS2-associated kinase BIK1 directly phosphorylates the NADPH oxidase RbohD to control plant immunity. *Cell Host & Microbe* **15**, 329-338.
- Li X, Zhang H, Tian L, Huang L, Liu S, Li D, Song F.** 2015. Tomato SIRbohB, a member of the NADPH oxidase family, is required for disease resistance against *Botrytis cinerea* and tolerance to drought stress. *Frontiers in Plant Science* **6**.
- Lichtenthaler HK, Buschmann C.** 2001. Chlorophylls and carotenoids: Measurement and characterization by UV-VIS spectroscopy. *Current Protocols in Food Analytical Chemistry*. New York: John Wiley and Sons.
- Lightfoot DJ, Boettcher A, Little A, Shirley N, Able AJ.** 2008. Identification and characterisation of barley (*Hordeum vulgare*) respiratory burst oxidase homologue family members. *Functional Plant Biology* **35**, 347-359.
- Lim PO, Kim HJ, Gil Nam H.** 2007. Leaf senescence. *Annual Review of Plant Biology* **58**, 115-136.
- Lin MR, Edwards H.** 1974. Primary penetration process in powdery mildewed barley related to host cell age, cell type, and occurrence of basic staining material. *New Phytologist* **73**, 131-137.

- Linkmeyer A, Götz M, Hu L, Asam S, Rychlik M, Hausladen H, Hess M, Hüchelhoven R.** 2013. Assessment and introduction of quantitative resistance to Fusarium head blight in elite spring barley. *Phytopathology* **103**, 1252-1259.
- Liu J, Han L, Huai B, Zheng P, Chang Q, Guan T, Li D, Huang L, Kang Z.** 2015. Down-regulation of a wheat alkaline/neutral invertase correlates with reduced host susceptibility to wheat stripe rust caused by *Puccinia striiformis*. *Journal of Experimental Botany* **66**, 7325-7338.
- Lorrain S, Vaillau F, Balagué C, Roby D.** 2003. Lesion mimic mutants: keys for deciphering cell death and defense pathways in plants? *Trends in Plant Science* **8**, 263-271.
- Ma X, Wang W, Bittner F, Schmidt N, Berkey R, Zhang L, King H, Zhang Y, Feng J, Wen Y.** 2016. Dual and opposing roles of xanthine dehydrogenase in defense-associated reactive oxygen species metabolism in Arabidopsis. *The Plant Cell* **28**, 1108-1126.
- Makandar R, Essig JS, Schapaugh MA, Trick HN, Shah J.** 2006. Genetically engineered resistance to Fusarium head blight in wheat by expression of Arabidopsis NPR1. *Molecular Plant-Microbe Interactions* **19**, 123-129.
- Makandar R, Nalam VJ, Lee H, Trick HN, Dong Y, Shah J.** 2012. Salicylic acid regulates basal resistance to Fusarium head blight in wheat. *Molecular Plant-Microbe Interactions* **25**, 431-439.
- Mangano S, Denita-Juarez SP, Choi H-S, Marzol E, Hwang Y, Ranocha P, Velasquez SM, Borassi C, Barberini ML, Aptekmann AA.** 2017. Molecular link between auxin and ROS-mediated polar growth. *Proceedings of the National Academy of Sciences*, 201701536.
- Marino D, Dunand C, Puppo A, Pauly N.** 2012. A burst of plant NADPH oxidases. *Trends in Plant Science* **17**, 9-15.
- Martín JA, Solla A, Witzell J, Gil L, García-Vallejo MC.** 2009. Antifungal effect and reduction of Ulmus minor symptoms to Ophiostoma novo-ulmi by carvacrol and salicylic acid. *European Journal of Plant Pathology* **127**, 21-32.
- Mateo A, Mühlenbock P, Rustérucci C, Chang CC-C, Miszalski Z, Karpinska B, Parker JE, Mullineaux PM, Karpinski S.** 2004. LESION SIMULATING DISEASE 1 is required for acclimation to conditions that promote excess excitation energy. *Plant Physiology* **136**, 2818-2830.
- McDowell JM.** 2011. Genomes of obligate plant pathogens reveal adaptations for obligate parasitism. *Proceedings of the National Academy of Sciences* **108**, 8921-8922.
- McGrann GR, Stavrinides A, Russell J, Corbitt MM, Booth A, Chartrain L, Thomas WT, Brown JK.** 2014. A trade off between mlo resistance to powdery mildew and increased susceptibility of barley to a newly important disease, Ramularia leaf spot. *Journal of Experimental Botany* **65**, 1025-1037.
- McGrann GR, Steed, Andrew, Burt C, Nicholson P, Brown JK.** 2015. Differential effects of lesion mimic mutants in barley on disease development by facultative pathogens. *Journal of Experimental Botany* **66**, 3417-3428.
- Metwally A, Finkemeier I, Georgi M, Dietz K-J.** 2003. Salicylic acid alleviates the cadmium toxicity in barley seedlings. *Plant Physiology* **132**, 272-281.
- Meuwly P, Métraux J-P.** 1993. Ortho-anisic acid as internal standard for the simultaneous quantitation of salicylic acid and its putative biosynthetic precursors in cucumber leaves. *Analytical Biochemistry* **214**, 500-505.
- Miller G, Schlauch K, Tam R, Cortes D, Torres MA, Shulaev V, Dangl JL, Mittler R.** 2009. The plant NADPH oxidase RBOHD mediates rapid systemic signaling in response to diverse stimuli. *Science Signaling* **2**, ra45-ra45.
- Mittler R, Vanderauwera S, Suzuki N, Miller G, Tognetti VB, Vandepoele K, Gollery M, Shulaev V, Van Breusegem F.** 2011. ROS signaling: the new wave? *Trends in Plant Science* **16**, 300-309.
- Morales J, Kadota Y, Zipfel C, Molina A, Torres M-A.** 2016. The Arabidopsis NADPH oxidases RbohD and RbohF display differential expression patterns and contributions during plant immunity. *Journal of Experimental Botany* **67**, 1663-1676.
- Morris K, Mackerness SAH, Page T, John CF, Murphy AM, Carr JP, Buchanan-Wollaston V.** 2000. Salicylic acid has a role in regulating gene expression during leaf senescence. *The Plant Journal* **23**, 677-685.

- Mühlenbock P, Plaszczyca M, Plaszczyca M, Mellerowicz E, Karpinski S. 2007. Lysigenous aerenchyma formation in Arabidopsis is controlled by LESION SIMULATING DISEASE1. *The Plant Cell* **19**, 3819-3830.
- Müller K, Carstens AC, Linkies A, Torres MA, Leubner-Metzger G. 2009. The NADPH-oxidase AtrbohB plays a role in Arabidopsis seed after-ripening. *New Phytologist* **184**, 885-897.
- Navabpour S, Morris K, Allen R, Harrison E, A-H-Mackerness S, Buchanan-Wollaston V. 2003. Expression of senescence-enhanced genes in response to oxidative stress. *Journal of Experimental Botany* **54**, 2285-2292.
- Návarová H, Bernsdorff F, Döring A-C, Zeier J. 2012. Pipecolic acid, an endogenous mediator of defense amplification and priming, is a critical regulator of inducible plant immunity. *The Plant Cell* **24**, 5123-5141.
- Navarro L, Bari R, Achard P, Lisón P, Nemri A, Harberd NP, Jones JD. 2008. DELLAs control plant immune responses by modulating the balance of jasmonic acid and salicylic acid signaling. *Current Biology* **18**, 650-655.
- Nestler J, Liu S, Wen TJ, Paschold A, Marcon C, Tang HM, Li D, Li L, Meeley RB, Sakai H. 2014. Roothairless5, which functions in maize (*Zea mays* L.) root hair initiation and elongation encodes a monocot-specific NADPH oxidase. *The Plant Journal* **79**, 729-740.
- Nguyen VN, Vo KT, Park H, Jeon J-S, Jung K-H. 2016. A systematic view of the MLO family in rice suggests their novel roles in morphological development, diurnal responses, the light-signaling pathway, and various stress responses. *Frontiers in Plant Science* **7**.
- Nicolaisen M, Supronienė S, Nielsen LK, Lazzaro I, Spliid NH, Justesen AF. 2009. Real-time PCR for quantification of eleven individual Fusarium species in cereals. *Journal of Microbiological Methods* **76**, 234-240.
- O'Connell RJ, Panstruga R. 2006. Tete a tete inside a plant cell: establishing compatibility between plants and biotrophic fungi and oomycetes. *New Phytologist* **171**, 699-718.
- Oda T, Hashimoto H, Kuwabara N, Akashi S, Hayashi K, Kojima C, Wong HL, Kawasaki T, Shimamoto K, Sato M. 2010. Structure of the N-terminal regulatory domain of a plant NADPH oxidase and its functional implications. *Journal of Biological Chemistry* **285**, 1435-1445.
- Oerke E-C, Dehne H-W. 2004. Safeguarding production—losses in major crops and the role of crop protection. *Crop Protection* **23**, 275-285.
- Olvera-Carrillo Y, Van Bel M, Van Hautegeem T, Fendrych M, Huysmans M, Simaskova M, Van Durme M, Buscaill P, Rivas S, Coll NS. 2015. A conserved core of programmed cell death indicator genes discriminates developmentally and environmentally induced programmed cell death in plants. *Plant Physiology* **169**, 2684-2699.
- Ovesna J, Kučera L, Vaculová K, Štryplová K, Svobodova I, Milella L. 2012. Validation of the β -amy1 transcription profiling assay and selection of reference genes suited for a RT-qPCR assay in developing barley caryopsis. *PLoS One* **7**, e41886.
- Pathuri IP, Reitberger IE, Hückelhoven R, Proels RK. 2011. Alcohol dehydrogenase 1 of barley modulates susceptibility to the parasitic fungus *Blumeria graminis* f. sp. hordei. *Journal of Experimental Botany*, err017.
- Pathuri IP, Zellerhoff N, Schaffrath U, Hensel G, Kumlehn J, Kogel K-H, Eichmann R, Hückelhoven R. 2008. Constitutively activated barley ROPs modulate epidermal cell size, defense reactions and interactions with fungal leaf pathogens. *Plant Cell Reports* **27**, 1877.
- Pennell RI, Lamb C. 1997. Programmed cell death in plants. *Plant Cell* **9**, 1157.
- Pennington HG, Li L, Spanu PD. 2016. Identification and selection of normalization controls for quantitative transcript analysis in *Blumeria graminis*. *Molecular Plant Pathology* **17**, 625-633.
- Peraldi A, Beccari G, Steed A, Nicholson P. 2011. *Brachypodium distachyon*: a new pathosystem to study Fusarium head blight and other Fusarium diseases of wheat. *BMC Plant Biology* **11**, 100.
- Perchepped L, Balagué C, Riou C, Claudel-Renard C, Rivière N, Grezes-Besset B, Roby D. 2010. Nitric oxide participates in the complex interplay of defense-related signaling pathways controlling

- disease resistance to *Sclerotinia sclerotiorum* in *Arabidopsis thaliana*. *Molecular Plant-Microbe Interactions* **23**, 846-860.
- Pérez-Pérez ME, Lemaire SD, Crespo JL.** 2012. Reactive oxygen species and autophagy in plants and algae. *Plant Physiology* **160**, 156-164.
- Persson M, Falk A, Dixelius C.** 2009. Studies on the mechanism of resistance to *Bipolaris sorokiniana* in the barley lesion mimic mutant *bst1*. *Molecular Plant Pathology* **10**, 587-598.
- Peterhansel C, Freialdenhoven A, Kurth J, Kolsch R, Schulze-Lefert P.** 1997. Interaction analyses of genes required for resistance responses to powdery mildew in barley reveal distinct pathways leading to leaf cell death. *The Plant Cell* **9**, 1397-1409.
- Pfaffl MW.** 2001. A new mathematical model for relative quantification in real-time RT-PCR. *Nucleic Acids Research* **29**, e45-e45.
- Piffanelli P, Zhou F, Casais C, Orme J, Jarosch B, Schaffrath U, Collins NC, Panstruga R, Schulze-Lefert P.** 2002. The barley MLO modulator of defense and cell death is responsive to biotic and abiotic stress stimuli. *Plant Physiology* **129**, 1076-1085.
- Pogány M, von Rad U, Grün S, Dongó A, Pintye A, Simoneau P, Bahnweg G, Kiss L, Barna B, Durner J.** 2009. Dual roles of reactive oxygen species and NADPH oxidase RBOHD in an *Arabidopsis-Alternaria* pathosystem. *Plant Physiology* **151**, 1459-1475.
- Pontier D, Gan S, Amasino RM, Roby D, Lam E.** 1999. Markers for hypersensitive response and senescence show distinct patterns of expression. *Plant Molecular Biology* **39**, 1243-1255.
- Prithiviraj B, Singh UP, Manickam M, Ray AB.** 1997. Antifungal activity of anacardic acid, a naturally occurring derivative of salicylic acid. *Canadian Journal of Botany* **75**, 207-211.
- Proels RK, Hückelhoven R.** 2014. Cell-wall invertases, key enzymes in the modulation of plant metabolism during defence responses. *Molecular Plant Pathology* **15**, 858-864.
- Proels RK, Oberhollenzer K, Pathuri IP, Hensel G, Kumlehn J, Hückelhoven R.** 2010. RBOHF2 of barley is required for normal development of penetration resistance to the parasitic fungus *Blumeria graminis* f. sp. *hordei*. *Molecular Plant-Microbe Interactions* **23**, 1143-1150.
- Proels RK, Westermeier W, Hückelhoven R.** 2011. Infection of barley with the parasitic fungus *Blumeria graminis* f. sp. *hordei* results in the induction of HvADH1 and HvADH2. *Plant Signaling & Behavior* **6**, 1584-1587.
- Pugin A, Frachisse J-M, Tavernier E, Bligny R, Gout E, Douce R, Guern J.** 1997. Early events induced by the elicitor cryptogein in tobacco cells: involvement of a plasma membrane NADPH oxidase and activation of glycolysis and the pentose phosphate pathway. *The Plant Cell* **9**, 2077-2091.
- Ranf S.** 2017. Sensing of molecular patterns through cell surface immune receptors. *Current Opinion in Plant Biology* **38**, 68-77.
- Rausch T, Greiner S.** 2004. Plant protein inhibitors of invertases. *Biochimica et Biophysica Acta (BBA)-Proteins and Proteomics* **1696**, 253-261.
- Reimer-Michalski E-M, Conrath U.** 2016. Innate immune memory in plants. *Seminars in Immunology*, Vol. 28: Elsevier, 319-327.
- Risk JM, Selter LL, Chauhan H, Krattinger SG, Kumlehn J, Hensel G, Viccars LA, Richardson TM, Buesing G, Troller A.** 2013. The wheat Lr34 gene provides resistance against multiple fungal pathogens in barley. *Plant Biotechnology Journal* **11**, 847-854.
- Roitsch T, Balibrea M, Hofmann M, Proels R, Sinha A.** 2003. Extracellular invertase: key metabolic enzyme and PR protein. *Journal of Experimental Botany* **54**, 513-524.
- Rostoks N, Schmierer D, Mudie S, Drader T, Brueggeman R, Caldwell DG, Waugh R, Kleinhofs A.** 2006. Barley necrotic locus *nec1* encodes the cyclic nucleotide-gated ion channel 4 homologous to the *Arabidopsis* HLM1. *Molecular Genetics and Genomics* **275**, 159-168.
- Ruan Y-L.** 2014. Sucrose metabolism: gateway to diverse carbon use and sugar signaling. *Annual Review of Plant Biology* **65**, 33-67.

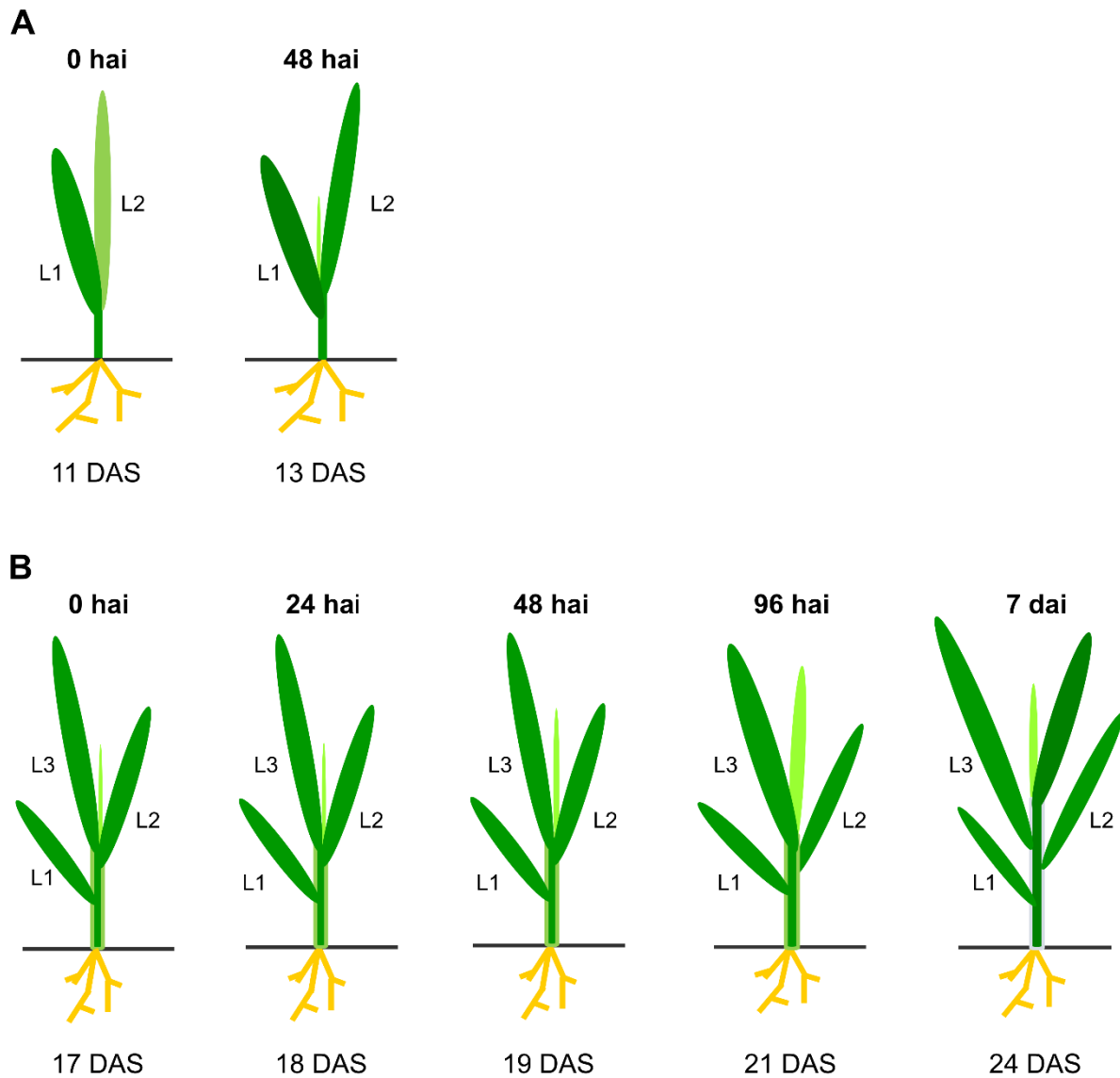
- Rusterucci C, Zhao Z, Haines K, Mellersh D, Neumann M, Cameron RK.** 2005. Age-related resistance to *Pseudomonas syringae* pv. *tomato* is associated with the transition to flowering in *Arabidopsis* and is effective against *Peronospora parasitica*. *Physiological and Molecular Plant Pathology* **66**, 222-231.
- Sahu R, Sharaff M, Pradhan M, Sethi A, Bandyopadhyay T, Mishra VK, Chand R, Chowdhury AK, Joshi AK, Pandey SP.** 2016. Elucidation of defense-related signaling responses to spot blotch infection in bread wheat (*Triticum aestivum* L.). *The Plant Journal* **86**, 35-49.
- Saville R, Gosman N, Burt C, Makepeace J, Steed A, Corbitt M, Chandler E, Brown J, Boulton M, Nicholson P.** 2011. The 'Green Revolution' dwarfing genes play a role in disease resistance in *Triticum aestivum* and *Hordeum vulgare*. *Journal of Experimental Botany* **63**, 1271-1283.
- Schäfer P, Hückelhoven R, Kogel K-H.** 2004. The white barley mutant *Albostrians* shows a supersusceptible but symptomless interaction phenotype with the hemibiotrophic fungus *Bipolaris sorokiniana*. *Molecular Plant-Microbe Interactions* **17**, 366-373.
- Scharte J, Schön H, Tjaden Z, Weis E, von Schaewen A.** 2009. Isoenzyme replacement of glucose-6-phosphate dehydrogenase in the cytosol improves stress tolerance in plants. *Proceedings of the National Academy of Sciences* **106**, 8061-8066.
- Scheler B, Schnepf V, Galgenmüller C, Ranf S, Hückelhoven R.** 2016. Barley disease susceptibility factor RACB acts in epidermal cell polarity and positioning of the nucleus. *Journal of Experimental Botany*, erw141.
- Schenk PM, Carvalhais LC, Kazan K.** 2012. Unraveling plant-microbe interactions: can multi-species transcriptomics help? *Trends in Biotechnology* **30**, 177-184.
- Scherm B, Balmas V, Spanu F, Pani G, Delogu G, Pasquali M, Migheli Q.** 2013. *Fusarium culmorum*: causal agent of foot and root rot and head blight on wheat. *Molecular Plant Pathology* **14**, 323-341.
- Schnepf V, Vlot AC, Kugler K, Hückelhoven R.** 2017. Barley susceptibility factor RACB modulates transcript levels of signalling protein genes in compatible interaction with *Blumeria graminis* f. sp. *hordei*. *Molecular Plant Pathology*.
- Schultheiss H, Dechert C, Király L, Fodor J, Michel K, Kogel K-H, Hückelhoven R.** 2003a. Functional assessment of the pathogenesis-related protein PR-1b in barley. *Plant Science* **165**, 1275-1280.
- Schultheiss H, Dechert C, Kogel KH, Hückelhoven R.** 2003b. Functional analysis of barley RAC/ROP G-protein family members in susceptibility to the powdery mildew fungus. *The Plant Journal* **36**, 589-601.
- Schulze-Lefert P, Vogel J.** 2000. Closing the ranks to attack by powdery mildew. *Trends in Plant Science* **5**, 343-348.
- Schweizer P, Pokorný J, Abderhalden O, Dudler R.** 1999. A transient assay system for the functional assessment of defense-related genes in wheat. *Molecular Plant-Microbe Interactions* **12**, 647-654.
- Schweizer P, Pokorný J, Schulze-Lefert P, Dudler R.** 2000. Double-stranded RNA interferes with gene function at the single-cell level in cereals. *The Plant Journal* **24**, 895-903.
- Sels J, Mathys J, De Coninck BM, Cammue BP, De Bolle MF.** 2008. Plant pathogenesis-related (PR) proteins: a focus on PR peptides. *Plant Physiology and Biochemistry* **46**, 941-950.
- Shi H, Liu W, Yao Y, Wei Y, Chan Z.** 2017. Alcohol dehydrogenase 1 (ADH1) confers both abiotic and biotic stress resistance in *Arabidopsis*. *Plant Science*.
- Shirasu K, Nielsen K, Piffanelli P, Oliver R, Schulze-Lefert P.** 1999. Cell-autonomous complementation of mlo resistance using a biolistic transient expression system. *The Plant Journal* **17**, 293-299.
- Siddique S, Matera C, Radakovic ZS, Hasan MS, Gutbrod P, Rozanska E, Sobczak M, Torres MA, Grundler FM.** 2014. Parasitic worms stimulate host NADPH oxidases to produce reactive oxygen species that limit plant cell death and promote infection. *Science Signaling* **7**, ra33-ra33.

- Sievers F, Wilm A, Dineen D, Gibson TJ, Karplus K, Li W, Lopez R, McWilliam H, Remmert M, Söding J.** 2011. Fast, scalable generation of high-quality protein multiple sequence alignments using Clustal Omega. *Molecular Systems Biology* **7**, 539.
- Silva Couto D, Zipfel C.** 2016. Regulation of pattern recognition receptor signalling in plants. *Nature Reviews Immunology* **16**, 537-552.
- Simon-Plas F, Elmayer T, Blein JP.** 2002. The plasma membrane oxidase NtrbohD is responsible for AOS production in elicited tobacco cells. *The Plant Journal* **31**, 137-147.
- Sonnewald S, Priller JP, Schuster J, Glickmann E, Hajirezaei M-R, Siebig S, Mudgett MB, Sonnewald U.** 2012. Regulation of cell wall-bound invertase in pepper leaves by *Xanthomonas campestris* pv. *vesicatoria* type three effectors. *PLoS One* **7**, e51763.
- Spanu P, Kamper J.** 2010. Genomics of biotrophy in fungi and oomycetes-emerging patterns. *Current Opinion in Plant Biology* **13**, 409-414.
- Spanu PD, Abbott JC, Amselem J, Burgis TA, Soanes DM, Stüber K, van Themaat EVL, Brown JK, Butcher SA, Gurr SJ.** 2010. Genome expansion and gene loss in powdery mildew fungi reveal tradeoffs in extreme parasitism. *Science* **330**, 1543-1546.
- Spies A, Korzun V, Bayles R, Rajaraman J, Himmelbach A, Hedley PE, Schweizer P.** 2011. Allele mining in barley genetic resources reveals genes of race-non-specific powdery mildew resistance. *Frontiers in Plant Science* **2**.
- Spoel SH, Dong X.** 2012. How do plants achieve immunity? Defence without specialized immune cells. *Nature Reviews Immunology* **12**, 89-100.
- Strommer J.** 2011. The plant ADH gene family. *The Plant Journal* **66**, 128-142.
- Su T, Wolf S, Han M, Zhao H, Wei H, Greiner S, Rausch T.** 2016. Reassessment of an Arabidopsis cell wall invertase inhibitor AtCIF1 reveals its role in seed germination and early seedling growth. *Plant Molecular Biology* **90**, 137-155.
- Sun L, Yang DI, Kong Y, Chen Y, Li XZ, Zeng LJ, Li Q, Wang ET, He ZH.** 2014. Sugar homeostasis mediated by cell wall invertase GRAIN INCOMPLETE FILLING 1 (GIF1) plays a role in pre-existing and induced defence in rice. *Molecular Plant Pathology* **15**, 161-173.
- Sunderwirth S, Roelfs A.** 1980. Greenhouse evaluation of the adult plant resistance of Sr2 to wheat stem rust. *Phytopathology* **70**, 634-637.
- Suzuki N, Miller G, Morales J, Shulaev V, Torres MA, Mittler R.** 2011. Respiratory burst oxidases: the engines of ROS signaling. *Current Opinion in Plant Biology* **14**, 691-699.
- Swarbrick PJ, Schulze-Lefert P, Scholes JD.** 2006. Metabolic consequences of susceptibility and resistance (race-specific and broad-spectrum) in barley leaves challenged with powdery mildew. *Plant, Cell & Environment* **29**, 1061-1076.
- Swidzinski JA, Sweetlove LJ, Leaver CJ.** 2002. A custom microarray analysis of gene expression during programmed cell death in Arabidopsis thaliana. *The Plant Journal* **30**, 431-446.
- Taguchi F, Shimizu R, Nakajima R, Toyoda K, Shiraishi T, Ichinose Y.** 2003. Differential effects of flagellins from *Pseudomonas syringae* pv. *tabaci*, tomato and glycinea on plant defense response. *Plant Physiology and Biochemistry* **41**, 165-174.
- Tamás L, Čiamporová M, Luxová M.** 1998. Accumulation of pathogenesis-related proteins in barley leaf intercellular spaces during leaf senescence. *Biologia Plantarum* **41**, 451-460.
- Tamura K, Stecher G, Peterson D, Filipowski A, Kumar S.** 2013. MEGA6: molecular evolutionary genetics analysis version 6.0. *Molecular Biology and Evolution* **30**, 2725-2729.
- Tauzin AS, Giardina T.** 2014. Sucrose and invertases, a part of the plant defense response to the biotic stresses. *Frontiers in Plant Science* **5**.
- Testerink C, Munnik T.** 2005. Phosphatidic acid: a multifunctional stress signaling lipid in plants. *Trends in Plant Science* **10**, 368-375.
- Thomma BP, Nurnberger T, Joosten MH.** 2011. Of PAMPs and effectors: the blurred PTI-ETI dichotomy. *Plant Cell* **23**, 4-15.

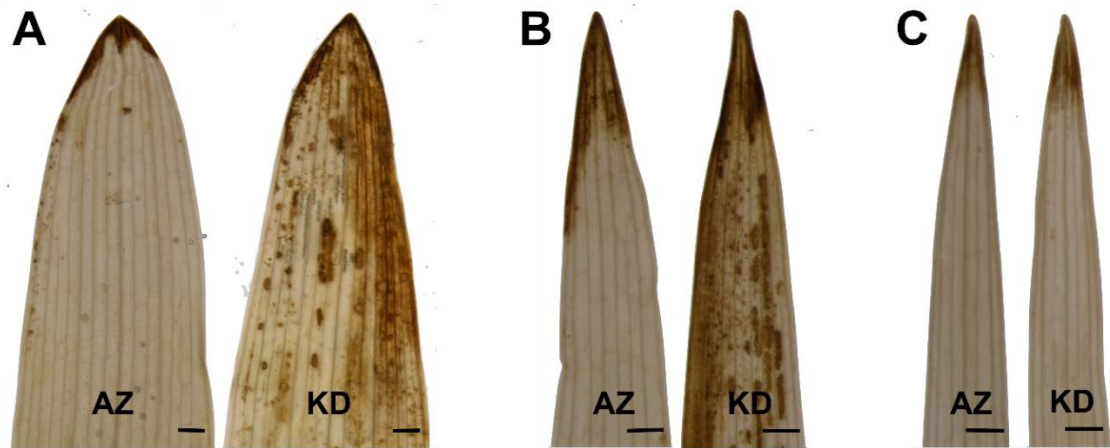
- Thompson JD, Higgins DG, Gibson TJ.** 1994. CLUSTAL W: improving the sensitivity of progressive multiple sequence alignment through sequence weighting, position-specific gap penalties and weight matrix choice. *Nucleic Acids Research* **22**, 4673-4680.
- Thordal-Christensen H, Zhang Z, Wei Y, Collinge DB.** 1997. Subcellular localization of H₂O₂ in plants. H₂O₂ accumulation in papillae and hypersensitive response during the barley—powdery mildew interaction. *Plant Journal* **11**, 1187-1194.
- Torres DP, Proels RK, Schempp H, Huckelhoven R.** 2017. Silencing of RBOHF2 causes leaf age-dependent accelerated senescence, salicylic acid accumulation and powdery mildew resistance in barley. *Molecular Plant-Microbe Interactions*.
- Torres MA.** 2010. ROS in biotic interactions. *Physiologia Plantarum* **138**, 414-429.
- Torres MA, Dangl JL.** 2005. Functions of the respiratory burst oxidase in biotic interactions, abiotic stress and development. *Current Opinion in Plant Biology* **8**, 397-403.
- Torres MA, Dangl JL, Jones JD.** 2002. Arabidopsis gp91phox homologues AtrbohD and AtrbohF are required for accumulation of reactive oxygen intermediates in the plant defense response. *Proceedings of the National Academy of Sciences* **99**, 517-522.
- Torres MA, Onouchi H, Hamada S, Machida C, Hammond-Kosack KE, Jones JD.** 1998. Six Arabidopsis thaliana homologues of the human respiratory burst oxidase (gp91phox). *The Plant Journal* **14**, 365-370.
- Tratwal A, Bocianowski J.** 2014. *Blumeria graminis* f. sp. *hordei* virulence frequency and the powdery mildew incidence on spring barley in the Wielkopolska province. *Journal of Plant Protection Research* **54**, 28-35.
- Trujillo M, Altschmied L, Schweizer P, Kogel KH, Huckelhoven R.** 2006. Respiratory burst oxidase homologue A of barley contributes to penetration by the powdery mildew fungus *Blumeria graminis* f. sp. *hordei*. *Journal of Experimental Botany* **57**, 3781-3791.
- Tsuda K, Katagiri F.** 2010. Comparing signaling mechanisms engaged in pattern-triggered and effector-triggered immunity. *Current Opinion in Plant Biology* **13**, 459-465.
- Vallélian-Bindschedler L, Métraux J-P, Schweizer P.** 1998. Salicylic acid accumulation in barley is pathogen specific but not required for defense-gene activation. *Molecular Plant-Microbe Interactions* **11**, 702-705.
- Van den Ende W, Lammens W, Van Laere A, Schroeven L, Le Roy K.** 2009. Donor and acceptor substrate selectivity among plant glycoside hydrolase family 32 enzymes. *The FEBS journal* **276**, 5788-5798.
- van der Heijden MG, Bardgett RD, van Straalen NM.** 2008. The unseen majority: soil microbes as drivers of plant diversity and productivity in terrestrial ecosystems. *Ecology Letters* **11**, 296-310.
- Van Loon L, Van Strien E.** 1999. The families of pathogenesis-related proteins, their activities, and comparative analysis of PR-1 type proteins. *Physiological and Molecular Plant Pathology* **55**, 85-97.
- Veillet F, Gaillard C, Coutos-Thévenot P, La Camera S.** 2016. Targeting the AtCWIN1 Gene to explore the role of invertases in sucrose transport in roots and during *Botrytis cinerea* infection. *Frontiers in Plant Science* **7**.
- Vlot AC, Dempsey DMA, Klessig DF.** 2009. Salicylic acid, a multifaceted hormone to combat disease. *Annual Review of Phytopathology* **47**, 177-206.
- Wakao S, Benning C.** 2005. Genome-wide analysis of glucose-6-phosphate dehydrogenases in Arabidopsis. *The Plant Journal* **41**, 243-256.
- Walter S, Nicholson P, Doohan FM.** 2010. Action and reaction of host and pathogen during Fusarium head blight disease. *New Phytologist* **185**, 54-66.
- Wang F, Wu W, Wang D, Yang W, Sun J, Liu D, Zhang A.** 2016. Characterization and genetic analysis of a novel light-dependent lesion mimic mutant, Im3, showing adult-plant resistance to powdery mildew in common wheat. *PLoS One* **11**, e0155358.

- Wang G-F, Li W-Q, Li W-Y, Wu G-L, Zhou C-Y, Chen K-M.** 2013. Characterization of rice NADPH oxidase genes and their expression under various environmental conditions. *International Journal of Molecular Sciences* **14**, 9440-9458.
- Wang L, Pei Z, Tian Y, He C.** 2005. OsLSD1, a rice zinc finger protein, regulates programmed cell death and callus differentiation. *Molecular Plant-Microbe Interactions* **18**, 375-384.
- Wang X, Devaiah SP, Zhang W, Welti R.** 2006. Signaling functions of phosphatidic acid. *Progress in Lipid Research* **45**, 250-278.
- Watanabe N, Lam E.** 2009. Bax inhibitor-1, a conserved cell death suppressor, is a key molecular switch downstream from a variety of biotic and abiotic stress signals in plants. *International Journal of Molecular Sciences* **10**, 3149-3167.
- Wen L.** 2013. Cell death in plant immune response to necrotrophs. *Journal of Plant Biochemistry & Physiology* **2013**.
- Weschke W, Panitz R, Gubatz S, Wang Q, Radchuk R, Weber H, Wobus U.** 2003. The role of invertases and hexose transporters in controlling sugar ratios in maternal and filial tissues of barley caryopses during early development. *The Plant Journal* **33**, 395-411.
- Whalen MC.** 2005. Host defence in a developmental context. *Molecular Plant Pathology* **6**, 347-360.
- Willems P, Mhamdi A, Simon S, Storme V, Kerchev PI, Noctor G, Gevaert K, Van Breusegem F.** 2016. The ROS wheel: refining ROS transcriptional footprints in Arabidopsis. *Plant Physiology*, pp. 00420.02016.
- Wolter M, Hollricher K, Salamini F, Schulze-Lefert P.** 1993. The mlo resistance alleles to powdery mildew infection in barley trigger a developmentally controlled defence mimic phenotype. *Molecular and General Genetics MGG* **239**, 122-128.
- Wong HL, Pinontoan R, Hayashi K, Tabata R, Yaeno T, Hasegawa K, Kojima C, Yoshioka H, Iba K, Kawasaki T.** 2007. Regulation of rice NADPH oxidase by binding of Rac GTPase to its N-terminal extension. *The Plant Cell* **19**, 4022-4034.
- Wright AJ, Heale J.** 1984. Adult plant resistance to powdery mildew (*Erysiphe graminis*) in three barley cultivars. *Plant Pathology* **33**, 493-502.
- Wright SA, Azarang M, Falk A.** 2013. Barley lesion mimics, supersusceptible or highly resistant to leaf rust and net blotch. *Plant Pathology* **62**, 982-992.
- Yang Y, Fu Z, Su Y, Zhang X, Li G, Guo J, Que Y, Xu L.** 2014. A cytosolic glucose-6-phosphate dehydrogenase gene, ScG6PDH, plays a positive role in response to various abiotic stresses in sugarcane. *Scientific reports* **4**.
- Yang Y, Shah J, Klessig DF.** 1997. Signal perception and transduction in plant defense responses. *Genes & Development* **11**, 1621-1639.
- Yin Z, Chen J, Zeng L, Goh M, Leung H, Khush GS, Wang G-L.** 2000. Characterizing rice lesion mimic mutants and identifying a mutant with broad-spectrum resistance to rice blast and bacterial blight. *Molecular Plant-Microbe Interactions* **13**, 869-876.
- Yoshie Y, Goto K, Takai R, Iwano M, Takayama S, Isogai A, Che F-S.** 2005. Function of the rice gp91phox homologs OsrbhA and OsrbhE genes in ROS-dependent plant immune responses. *Plant Biotechnology* **22**, 127-135.
- Yoshioka H, Numata N, Nakajima K, Katou S, Kawakita K, Rowland O, Jones JD, Doke N.** 2003. *Nicotiana benthamiana* gp91phox homologs NbrbohA and NbrbohB participate in H₂O₂ accumulation and resistance to *Phytophthora infestans*. *The Plant Cell* **15**, 706-718.
- Zadoks JC, Chang TT, Konzak CF.** 1974. A decimal code for the growth stages of cereals. *Weed Research* **14**, 415-421.
- Zhang J, Shao F, Li Y, Cui H, Chen L, Li H, Zou Y, Long C, Lan L, Chai J.** 2007. A *Pseudomonas syringae* effector inactivates MAPKs to suppress PAMP-induced immunity in plants. *Cell Host & Microbe* **1**, 175-185.

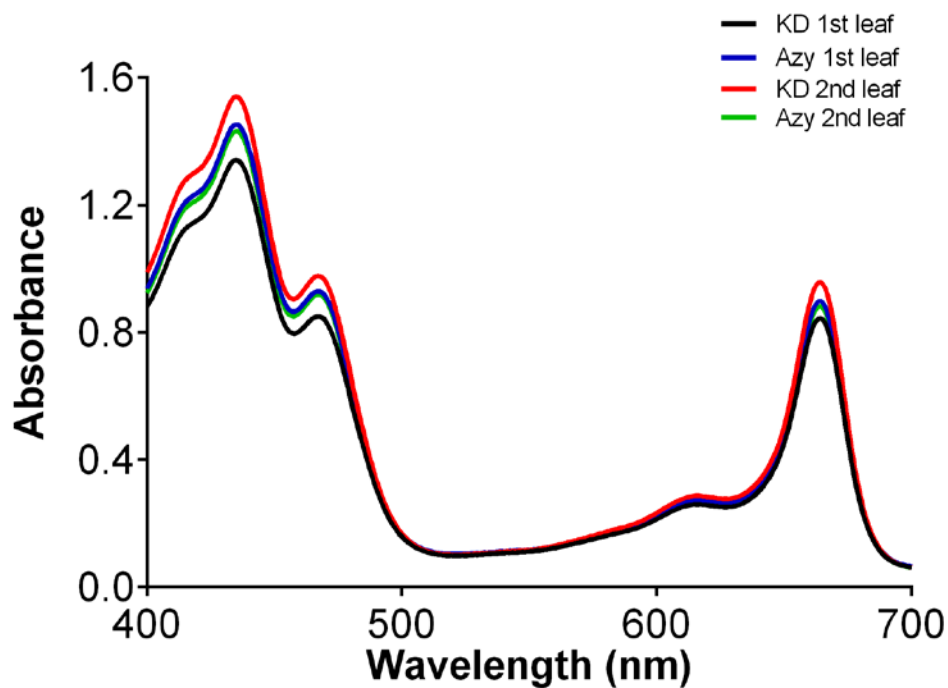
-
- Zhang K, Halitschke R, Yin C, Liu CJ, Gan SS.** 2013. Salicylic acid 3-hydroxylase regulates Arabidopsis leaf longevity by mediating salicylic acid catabolism. *Proceedings of the National Academy of Sciences* **110**, 14807-14812.
- Zhang L, Lavery L, Gill U, Gill K, Steffenson B, Yan G, Chen X, Kleinhofs A.** 2009a. A cation/proton-exchanging protein is a candidate for the barley NecS1 gene controlling necrosis and enhanced defense response to stem rust. *Theoretical and Applied Genetics* **118**, 385-397.
- Zhang Y, Zhu H, Zhang Q, Li M, Yan M, Wang R, Wang L, Welti R, Zhang W, Wang X.** 2009b. Phospholipase D α 1 and phosphatidic acid regulate NADPH oxidase activity and production of reactive oxygen species in ABA-mediated stomatal closure in Arabidopsis. *The Plant Cell* **21**, 2357-2377.
- Zhao X-Y, Wang J-G, Song S-J, Wang Q, Kang H, Zhang Y, Li S.** 2016. Precocious leaf senescence by functional loss of PROTEIN S-ACYL TRANSFERASE14 involves the NPR1-dependent salicylic acid signaling. *Scientific reports* **6**.

6 SUPPLEMENTARY MATERIAL

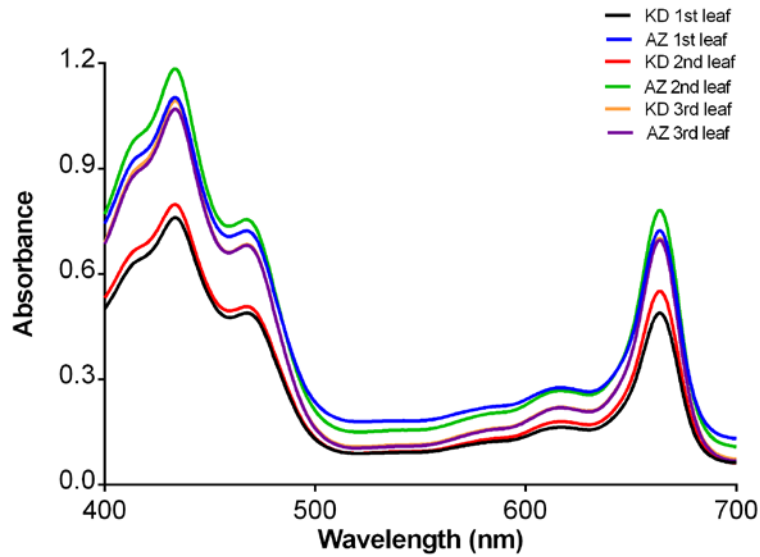
Supplementary Fig. S1: Schematic representation of the growth stage of transgenic plants used in this study. 11 day-old (A) and 17 day-old (B) barley plants. DAS: days after sowing; L1: first leaf; L2: second leaf; L3: third leaf. Just the leaves indicated were harvested and used for further analysis.



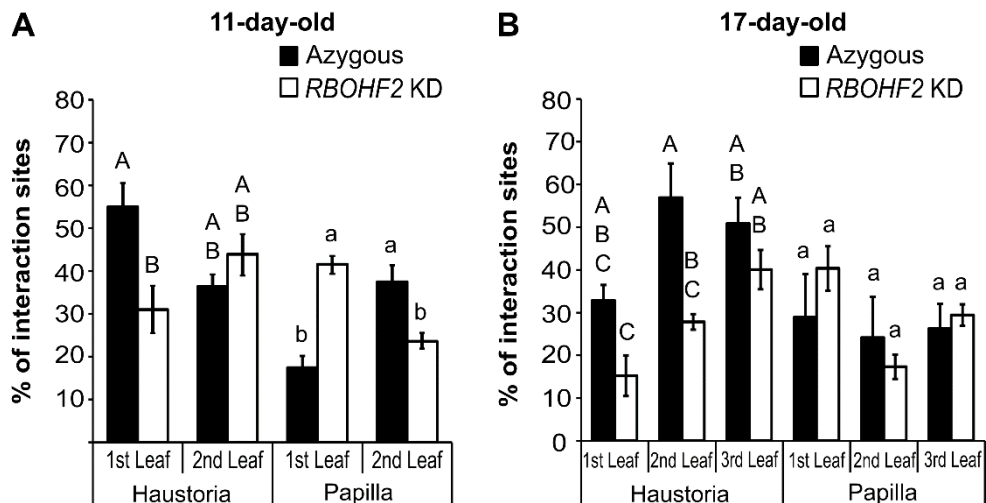
Supplementary Fig. S2: Silencing of *HvrBOHF2* results in spontaneous leaf tip necrosis. First (A), second (B) or third (C) leaves of 19-day-old barley *HvrBOHF2* knock down (KD) and the azygous (AZ) control lines were fixed and photographed. Pictures are representative for three independent experiments. Bars = 1 mm.



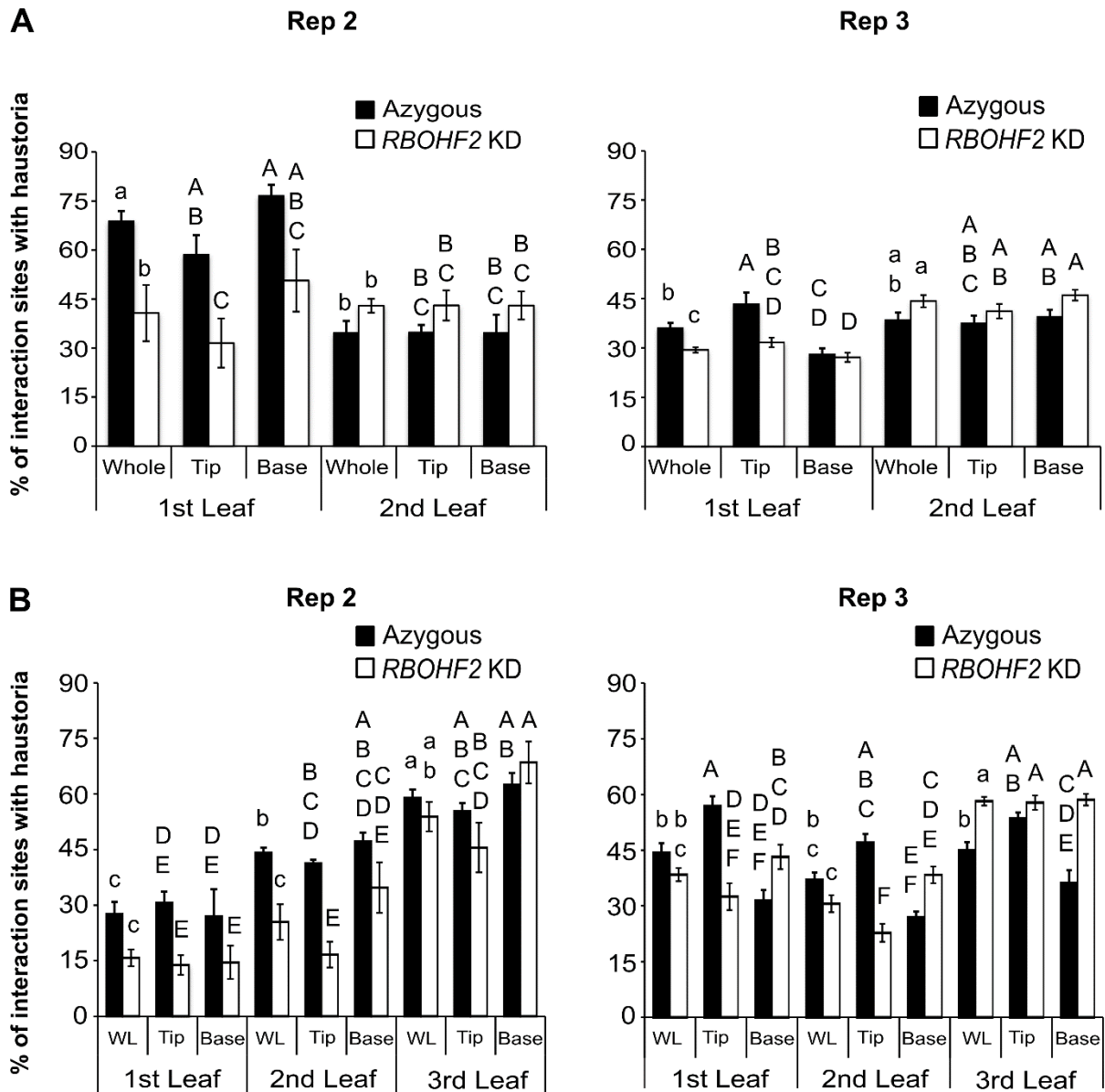
Supplementary Fig. S3: Absorption spectrum of pigments from leaf extracts of 11-day-old plants. A pool of 7 to 9 first and second leaves of each genotype were harvested, frozen in liquid nitrogen and ground to a fine powder. Methanol 100% was added to the powder to a concentration of 0.1 g ml⁻¹. Pigments were extracted from 1 ml of the homogenate into 2 ml of 100% methanol and the absorbance spectrum of the supernatant was measured at 1 nm intervals between 400 nm and 700 nm. Data represent the mean of photosynthetic pigments absorbance from one representative experiment measured in triplicates.



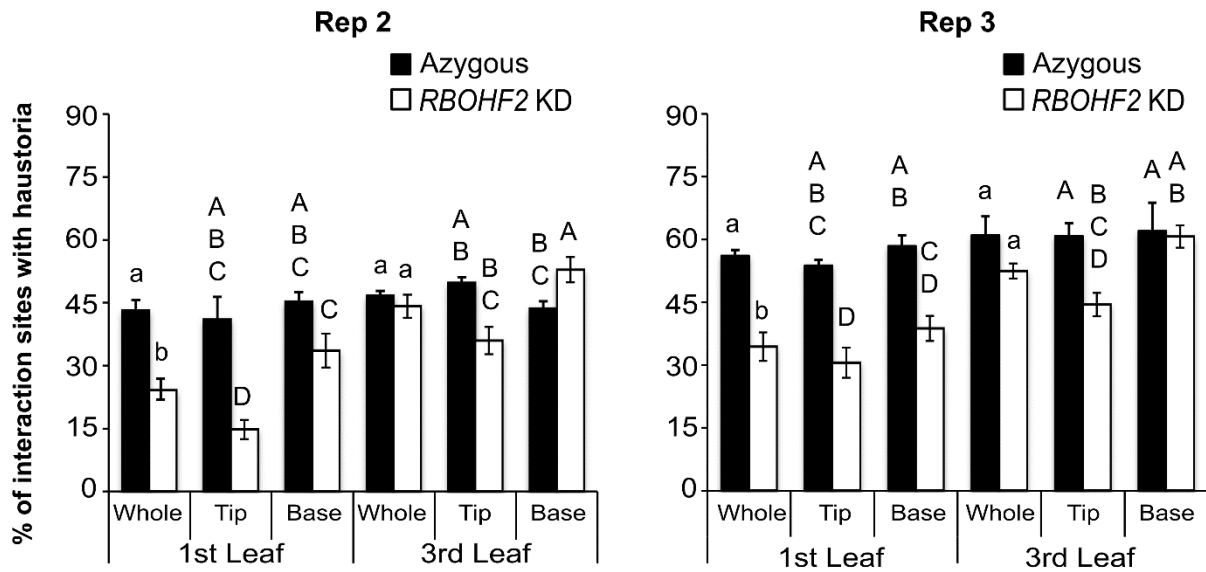
Supplementary Fig. S4: Absorption spectra of pigments from leaf discs of 17-day-old plants. Discs from the base leaf section from different leaves were taken. The leaf discs were snap frozen in liquid nitrogen and ground to a fine powder using a tissue homogenizer. The pigments were extracted into 2 ml of 96% (v/v) ethanol solution and the absorbance spectrum of the supernatant was measured at 1 nm intervals between 400 nm and 700 nm. Data represent the mean of photosynthetic pigments absorbance from one representative experiment measured in triplicates.



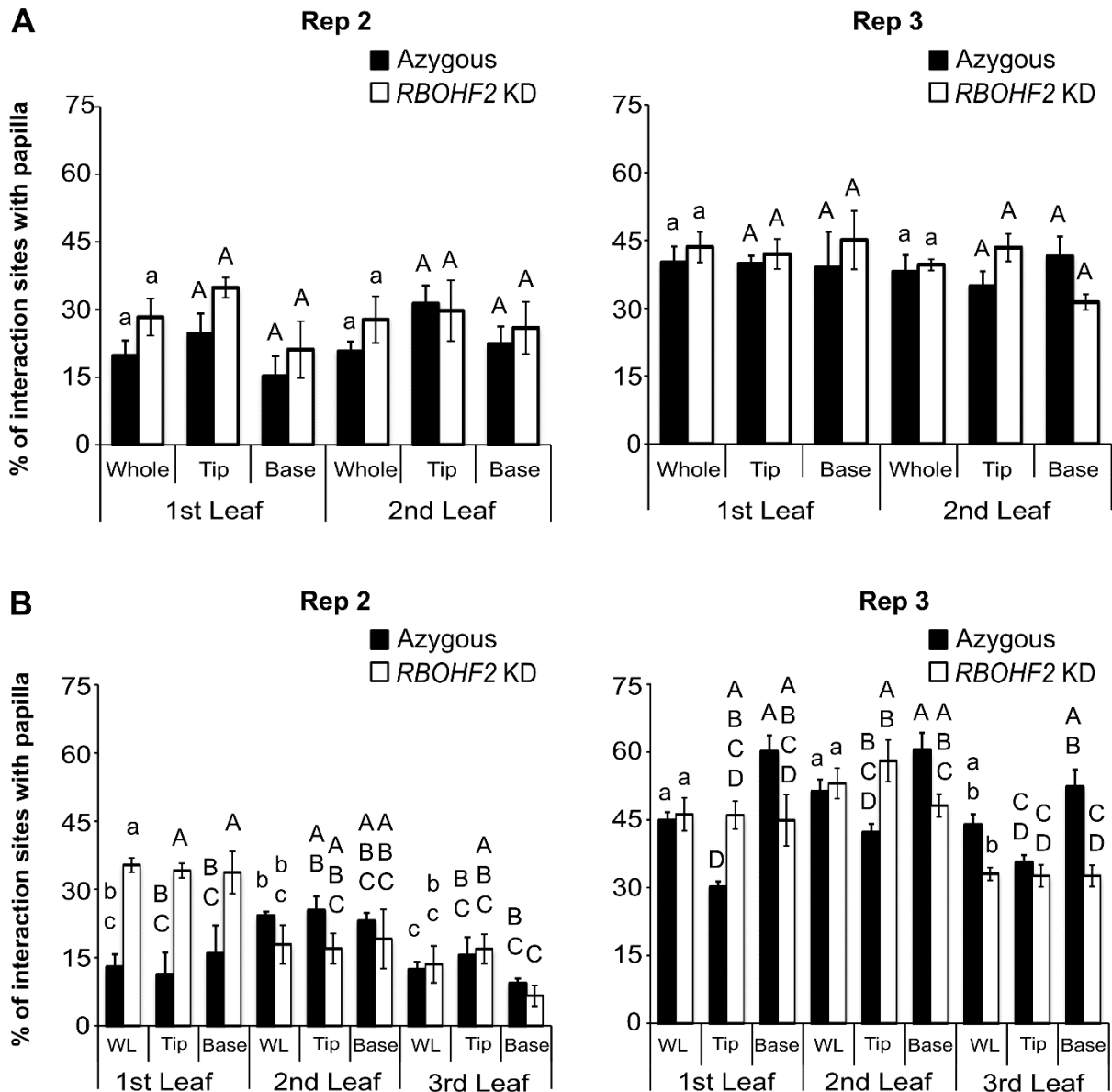
Supplementary Fig. S5: Pre-experiment age-dependent susceptibility. Frequency of successful cell-wall penetration with formation of visible haustoria and papilla formation at interaction sites in leaves of 11-day-old (A) or 17-day-old plants (B). Leaves were fixed 48 hours after inoculation with *Bgh*, and plant and fungal structures were analysed by bright field microscopy. Data represent the average of 120 (A) or 10 to 50 (B) interaction sites per leaf of three to four leaves per line of one experiment. Error bars show standard errors of the mean. Uppercase letters show the grouping of data sets relative to successful penetration and lowercase papilla formation according to Tukey's test at $P = 0.05$. Error bars show confidence intervals of the means at $P = 0.05$.



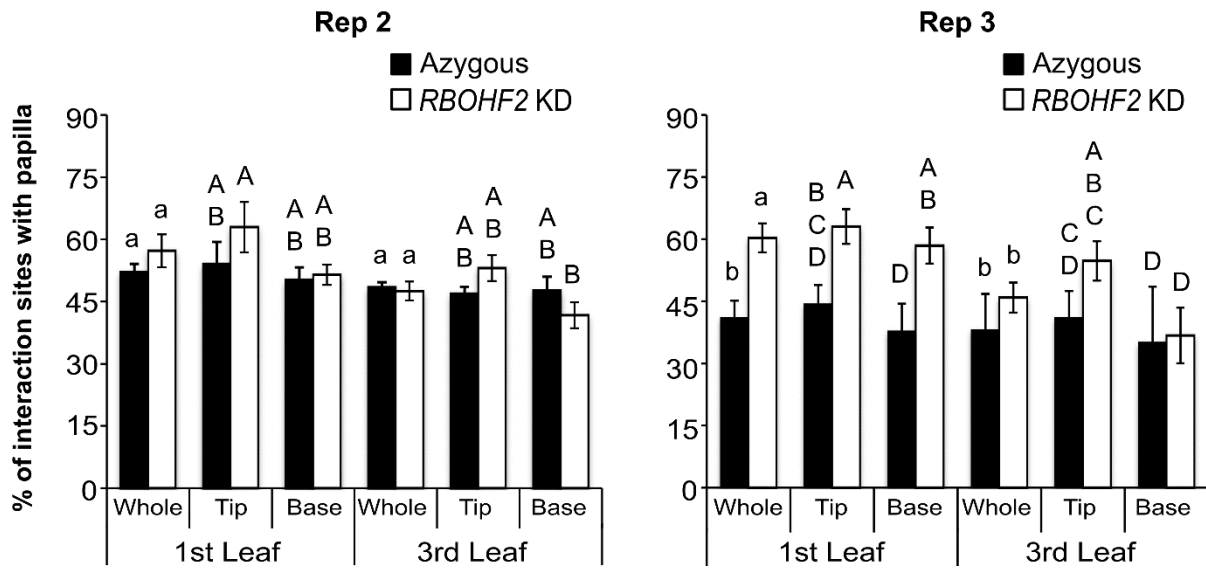
Supplementary Fig. S6: Interaction phenotype of *Bgh* with the *HvRBOHF2* KD line E08 in two further independent experiments. Frequency of successful cell-wall penetration with formation of visible haustoria at interaction sites in the whole leaf (WL), older meristem-distal (tip) or younger meristem-proximal (base) sections of the leaf in 11-day-old (A) or 17-day-old plants (B). Leaves were fixed 48 hours after inoculation with *Bgh*, and plant and fungal structures were analysed by bright field microscopy. Data represent the average of 115 to 160 interaction sites per leaf of four leaves per line. Error bars show standard errors of the mean. Lowercase letters show the grouping of data sets relative to successful penetration in the whole leaf and uppercase in the leaf sections according to Tukey's test at $P = 0.05$.



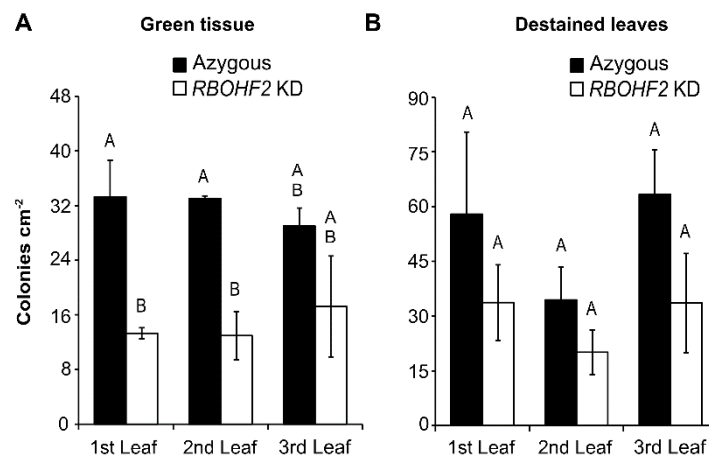
Supplementary Fig. S7: Interaction phenotype of *Bgh* with the *HvRBOHF2* KD line E06 in two further independent experiments. Frequency of successful cell-wall penetration with formation of visible haustoria at interaction sites in the whole leaf and tip or base sections of the leaf in 17-day-old plants. Leaves were fixed 48 hours after inoculation with *Bgh*, and plant and fungal structures were analysed by bright field microscopy. Data represent the average of at least 100 interaction sites per leaf of five leaves per line. Error bars show standard errors of the mean. Lowercase letters show the grouping of data sets relative to successful penetration in the whole leaf and uppercase in the leaf sections according to Tukey's test at $P = 0.05$.



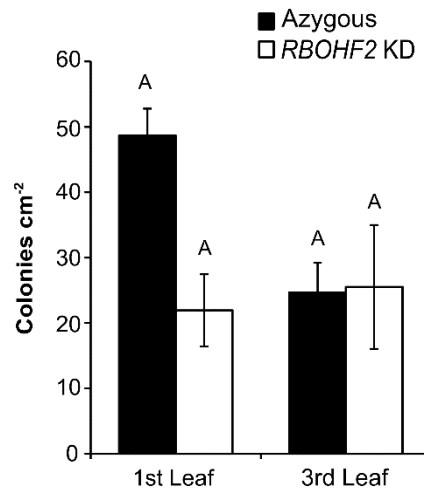
Supplementary Fig. S8: Pre-invasion defence responses in leaves of *HvRBOHF2* knock down (KD) line E08 and azygous control plants in two further independent experiments. Frequency of papilla formation at interaction sites in the whole leaf (WL), older meristem-distal (tip) or younger meristem-proximal (base) sections of the leaf in 11-day-old (A) or 17-day-old plants (B). Leaves were fixed 48 hours after inoculation with *Bgh*, and plant and fungal structures were analysed by bright field microscopy. Data represent the average of 115 to 160 interaction sites per leaf of four leaves per line. Error bars show standard errors of the mean. Lowercase letters show the grouping of data sets relative to successful penetration in the whole leaf and uppercase in the leaf sections according to Tukey's test at $P = 0.05$.



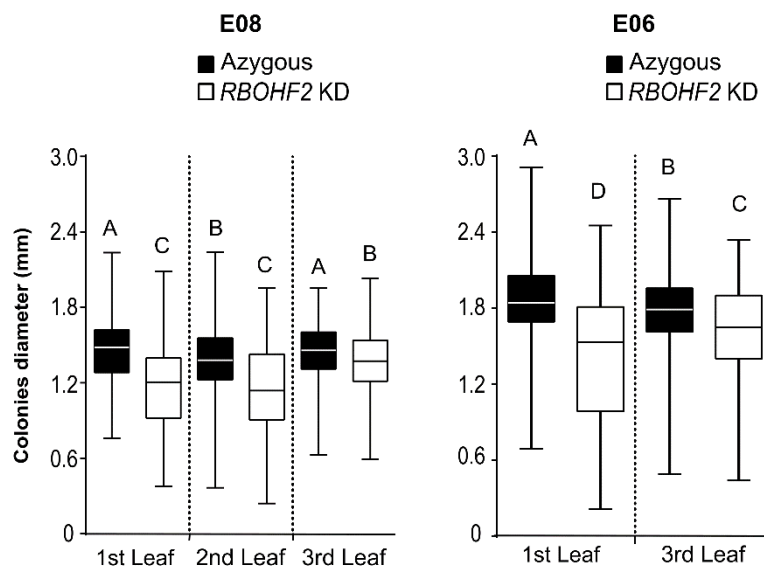
Supplementary Fig. S9: Pre-invasion defence responses in different leaves of HvRBOHF2 KD line E06 in two further experiments. Frequency of papilla formation at interaction sites in the whole leaf and tip or base sections of the leaf in 17-day-old plants. Leaves were fixed 48 hours after inoculation with *Bgh* and plant and fungal structures were analysed by bright field microscopy. Data represent the average of at least 100 interaction sites per leaf of five leaves per line. Error bars show standard errors of the mean. Lowercase letters show the grouping of data sets relative to successful penetration in the whole leaf and uppercase in the leaf sections according to Tukey's test at P = 0.05.



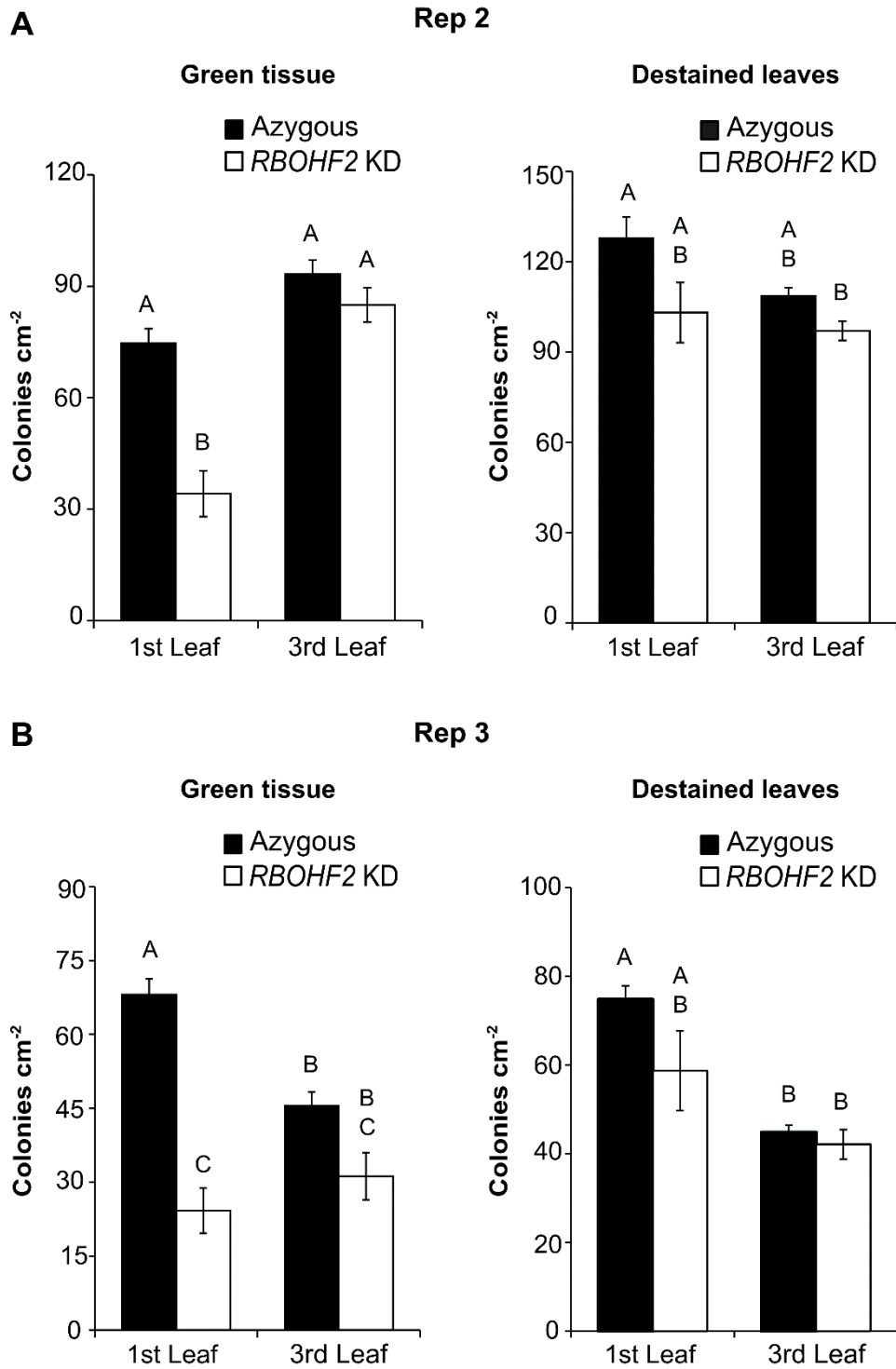
Supplementary Fig. S10: Effect of the silencing of *HvRBOHF* genes on the progression of the powdery mildew disease on detached leaves of the line E08. Number of developing colonies per leaf area in 17 day-old barley plants. Colonies were quantified under a stereomicroscope in green tissue (A) or in fixed leaves (B). Leaves explants of about 12 cm length were excised, placed on 0.8% water-agar and infected with *Bgh*. Inoculated leaf explants were incubated for 96 hours in a climate chamber. Bars represent the means of three fully independent experiments. In each experiment, four leaves per line and leaf level were evaluated. Error bars show standard errors of the mean and letters the grouping of data sets according to Tukey's test at P = 0.05.



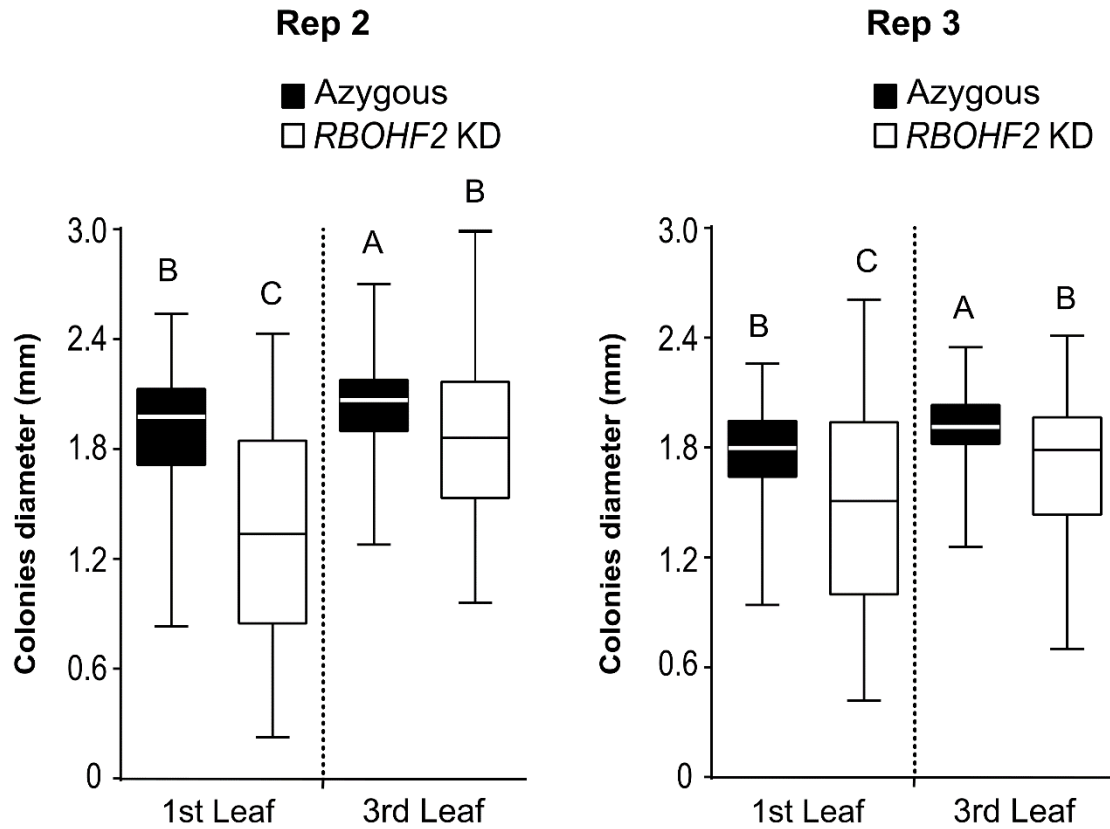
Supplementary Fig. S11: Effect of the silencing of *HvRBOHF* genes on the progression of the powdery mildew disease on detached leaves of the line E06. Number of developing colonies per leaf area in 17 day-old barley plants. Leaves explants of about 12 cm length were excised, placed on 0.8% water-agar and infected with *Bgh*. Inoculated leaf explants were incubated for 96 hours in a climate chamber. Then, the leaves were fixed and prepared for inspection under a stereomicroscope. Bars represent the means of three fully independent experiments. In each experiment, five to six leaves per line and leaf level were evaluated. Error bars show standard errors of the mean and letters the grouping of data sets according to Tukey's test at P = 0.05.



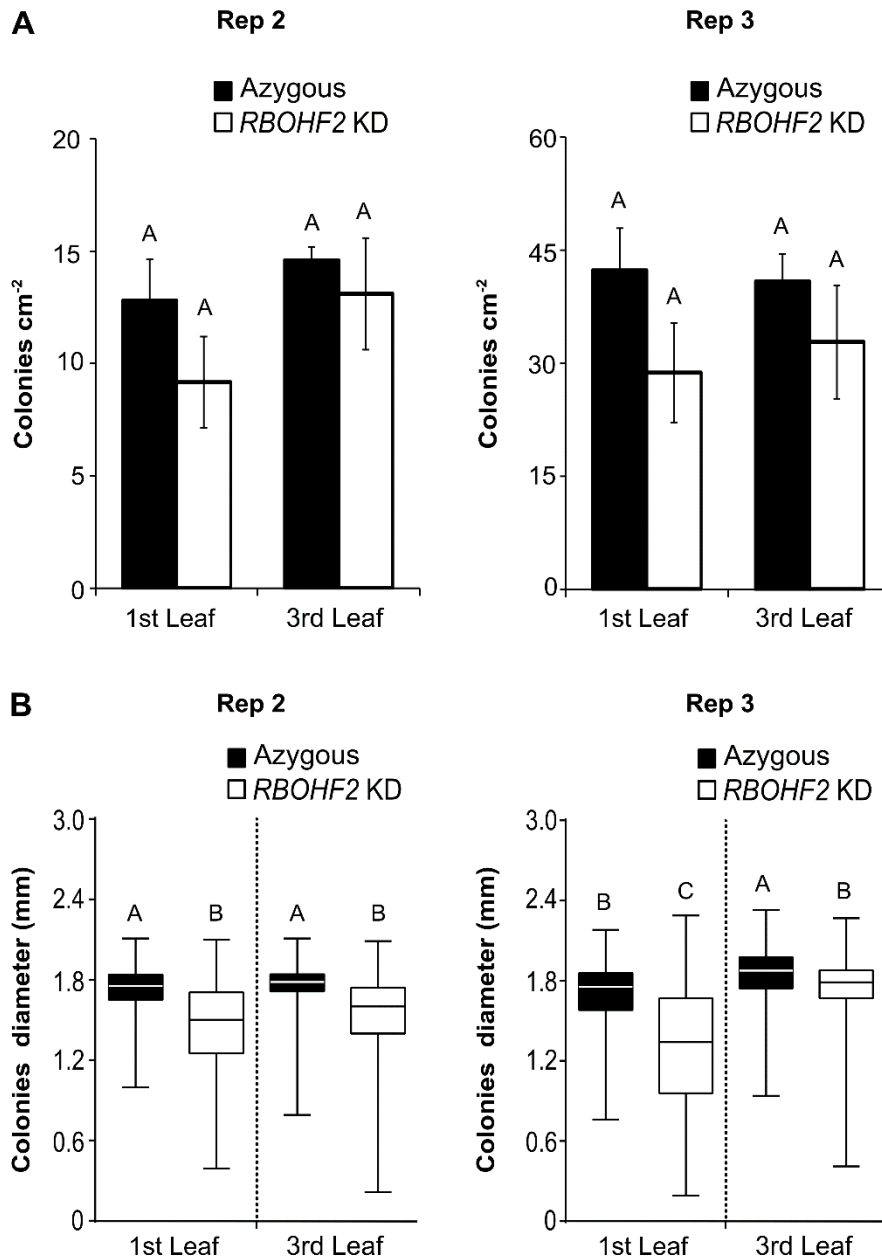
Supplementary Fig. S12: Size of *Bgh* colonies on detached leaves of *HvRBOHF2* KD lines. Length of *Bgh* colonies on the surface of explant leaves of 17 day-old-barley *HvRBOHF2* KD line E08 (A) or E06 (B) and the respective azygous controls. Colony length was sized using the software Leica LAS v4.5. Data represent the means of three fully independent experiments. In each experiment sixty to eighty pustules per line and leaf type were evaluated. Box- plots represent the median (horizontal line) and the interquartile range (box). Whiskers show the minimum and maximum measured values and letters the grouping of data sets according to Games-Howell test at P = 0.05.



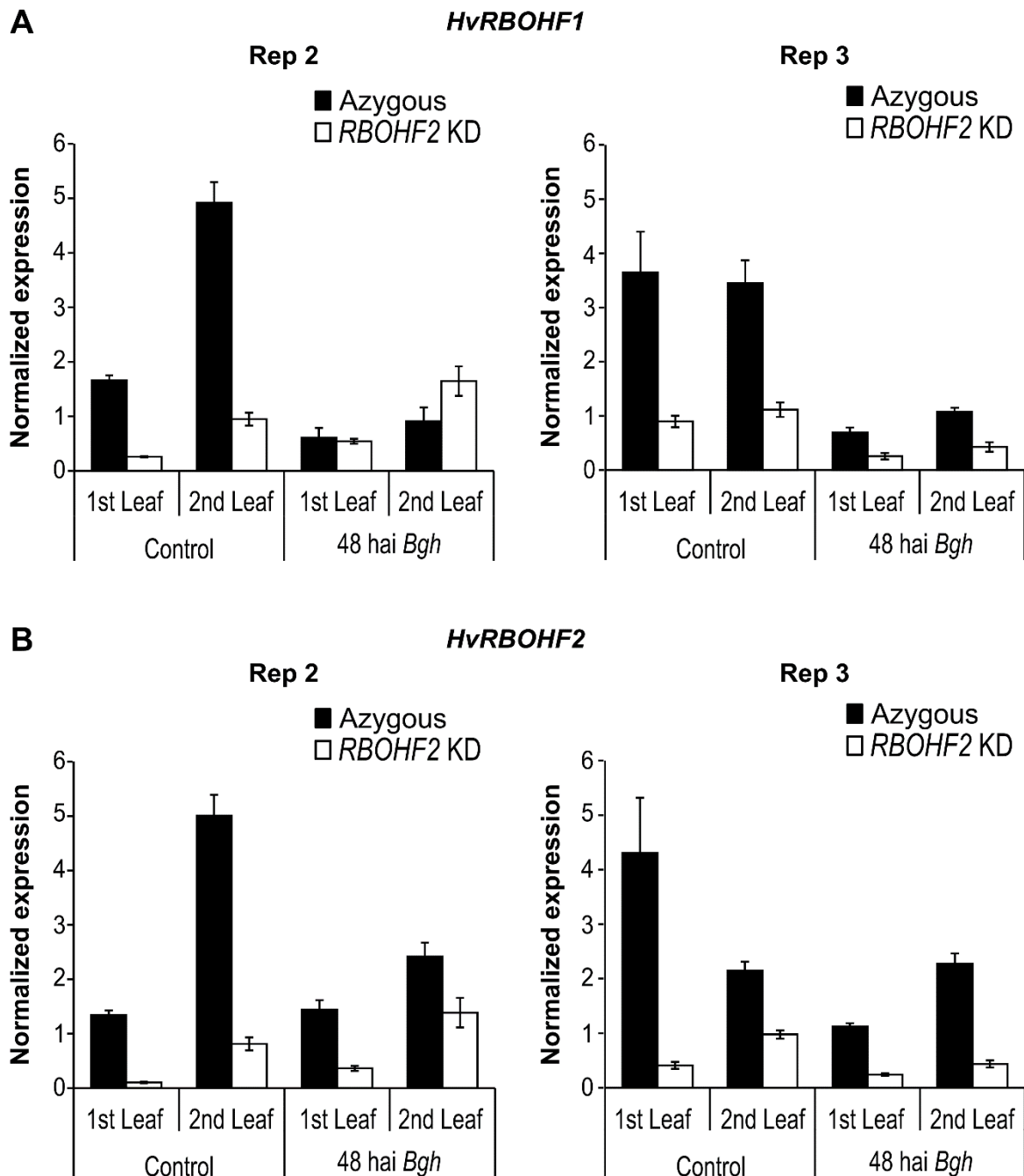
Supplementary Fig. S13: Effect of the silencing of *HvRBOHF* genes on the progression of the powdery mildew disease in two further independent experiments. Number of developing colonies per leaf area in 17 day-old-barley *HvRBOHF2* KD line E08 and the azygous controls. Colonies were quantified in green tissue or in fixed leaves under a stereomicroscope. Plants were infected with *Bgh*, incubated for 96 hours in a climate chamber and individually harvested. Error bars show standard errors of the mean of six leaves per line. Letters show the grouping of data sets according to Tukey's test at P = 0.05.



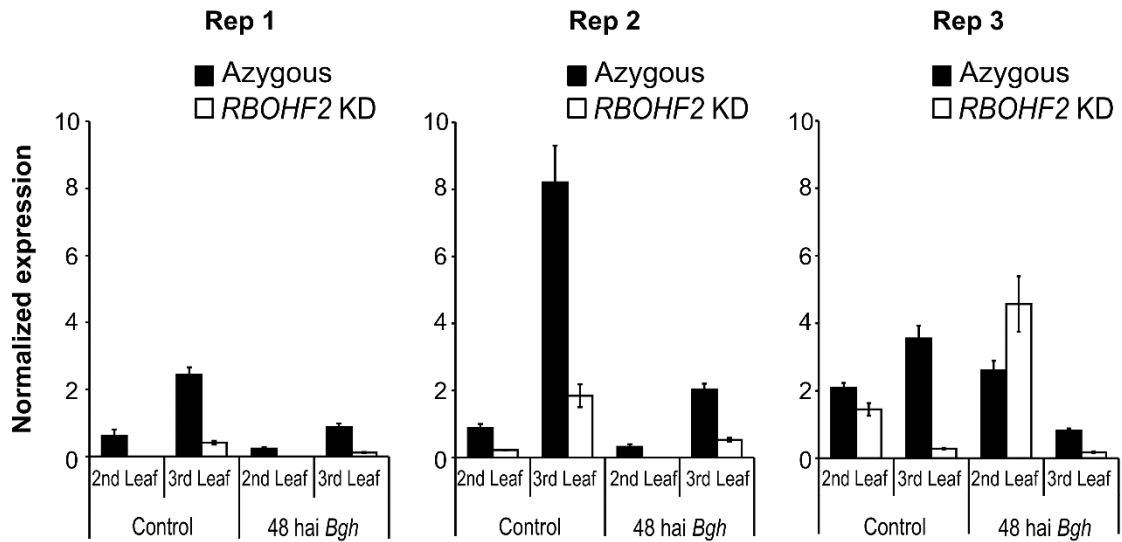
Supplementary Fig. S14: Size of *Bgh* colonies on leaves of *HvRBOHF2* KD plants in two further independent experiments. Length of *Bgh* colonies on the surface of leaves of 17-day-old barley *HvRBOHF2* KD line E08 and the azygous controls. Colony length was sized using the software Leica LAS v4.5. Eighty pustules per line and leaf type were evaluated. Box- plots represent the median (horizontal line) and the interquartile range (box). Whiskers show the minimum and maximum measured values and letters the grouping of data sets according to Games-Howell test at $P = 0.05$.



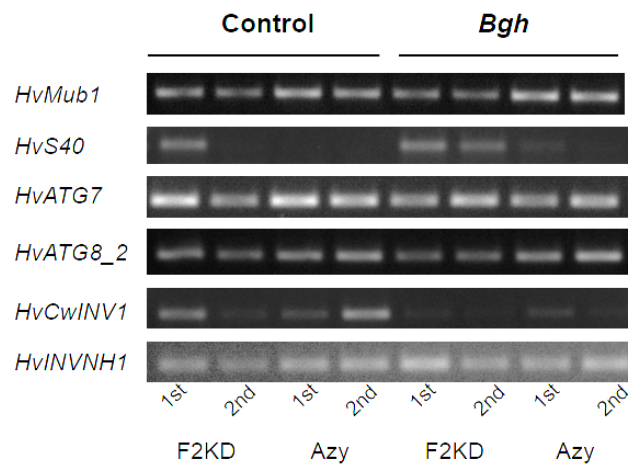
Supplementary Fig. S15: Effect of the silencing of *HvRBOHF2* KD on the progression of the powdery mildew disease in the line E06 in two further independent experiments. (A) Number of developing colonies per leaf area on the surface of leaves of 17-day-old-barley *HvRBOHF2* KD line E06 and the azygous control plants. Plants were infected with *Bgh* and incubated for 96 hours in a climate chamber. Then, the leaves were fixed and prepared for inspection under a stereomicroscope. Data represent the means of four to six leaves per line. Error bars show standard errors of the mean and letters the grouping of data sets according to Tukey's test at $P < 0.05$. (B) Length of *Bgh* colonies on the surface of different leaves of 17 day-old-barley *HvRBOHF2* KD line E06 and the azygous controls. Colony length was sized using the software Leica LAS v4.5. Sixty to eighty pustules per line and leaf type were evaluated. Box-plots represent the median (horizontal line) and the interquartile range (box). Whiskers show the minimum and maximum measured values and letters the grouping of data sets according to Games-Howell test at $P = 0.05$.



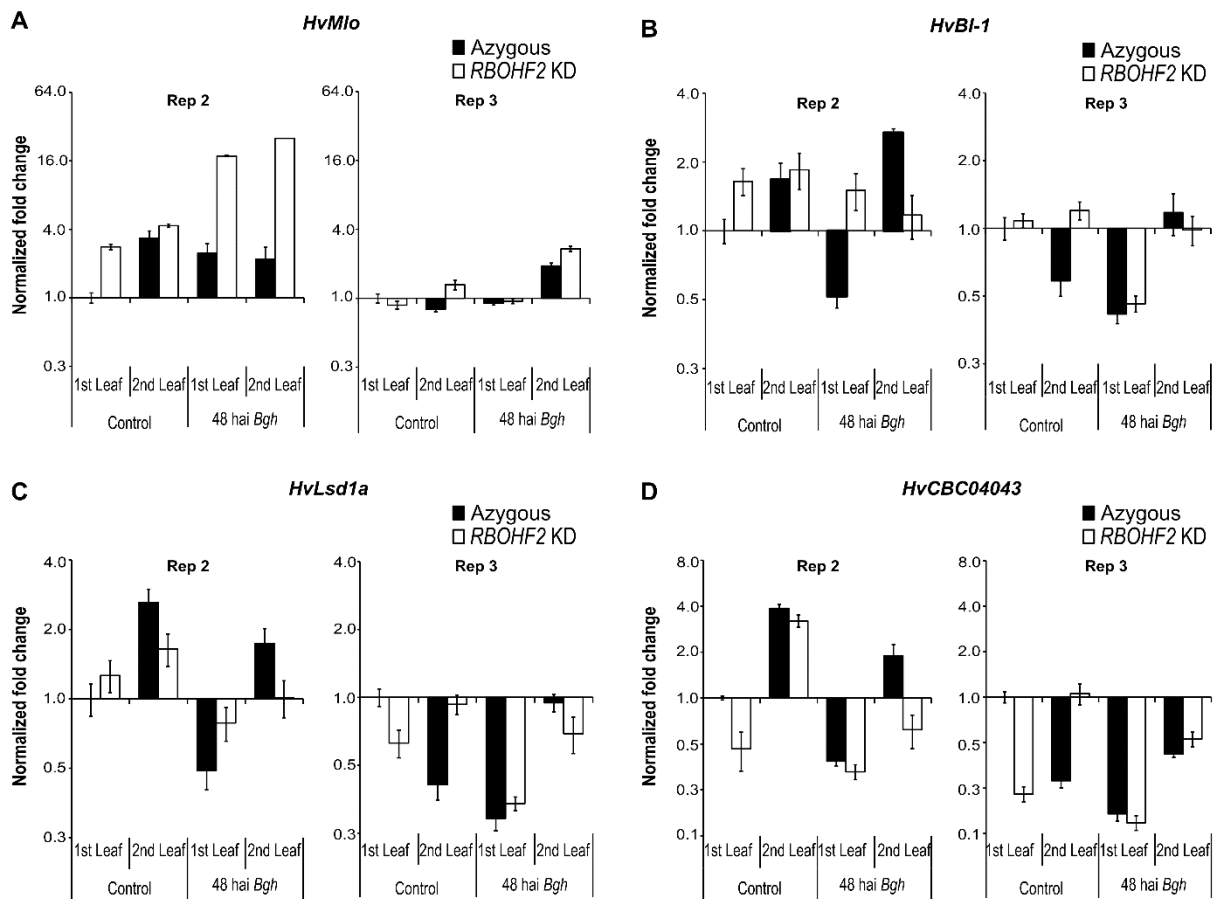
Supplementary Fig. S16: *HvRBOHF* expression in transgenic barley plants in two further independent experiments. Relative expression levels of barley *HvRBOHF1* (A) and *HvRBOHF2* (B) in first and second leaves of 11-day-old *HvRBOHF2* knock-down (KD) line E08 and the azygous control. Total RNA was extracted from a pool of three to four leaves of barley plants 48 hai from non-inoculated or *Bgh*-inoculated leaves. The cDNA was synthesized and afterwards subjected to real-time PCR analysis. Expression of the genes was measured relative to the expression of the reference gene barley MONOUBIQUITIN-LONG-TAIL FUSION 1 (*HvMub1*). Error bars show confidence intervals of the means at P = 0.05 of three technical replicates.



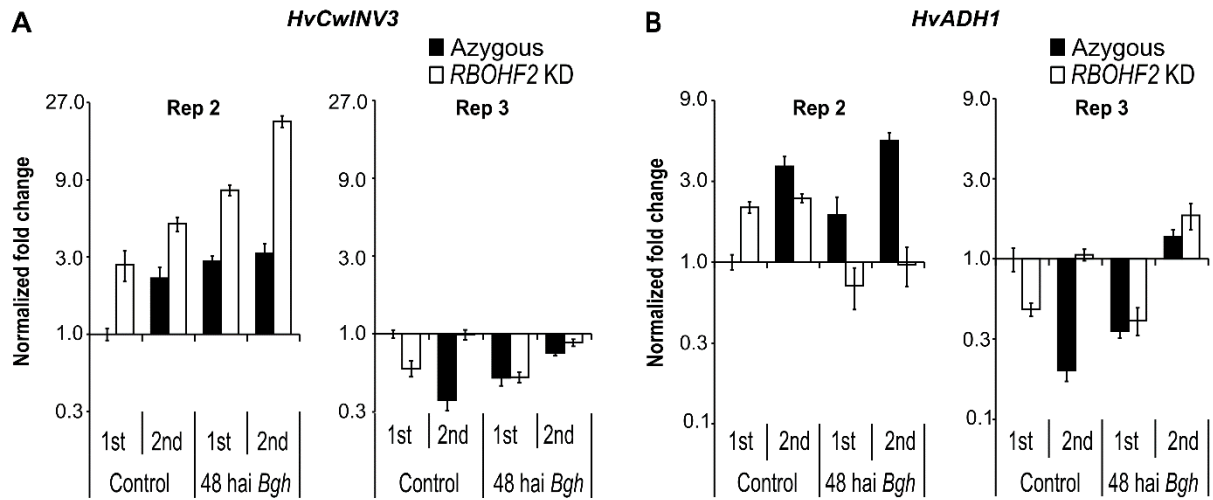
Supplementary Fig. S17: *HvRBOHF2* expression in 17-day-old barley transgenic plants. Relative expression levels of barley *HvRBOHF2* in second and third leaves of 17-day-old *HvRBOHF2* knock-down (KD) line E08 and the azygous control. Total RNA was extracted from a pool of three to four leaves of barley plants 48 hai from non-inoculated or *Bgh*-inoculated leaves. The cDNA was synthesized and afterwards subjected to real-time PCR analysis. Expression of the genes was measured relative to the expression of the reference gene barley MONOUBIQUITIN-LONG-TAIL FUSION 1 (*HvMub1*). Error bars show confidence intervals of the means at $P = 0.05$ of three technical replicates. No RNA of good quality were obtained from second leaves of *HvRBOHF2* KD plants in the first and second replicates.



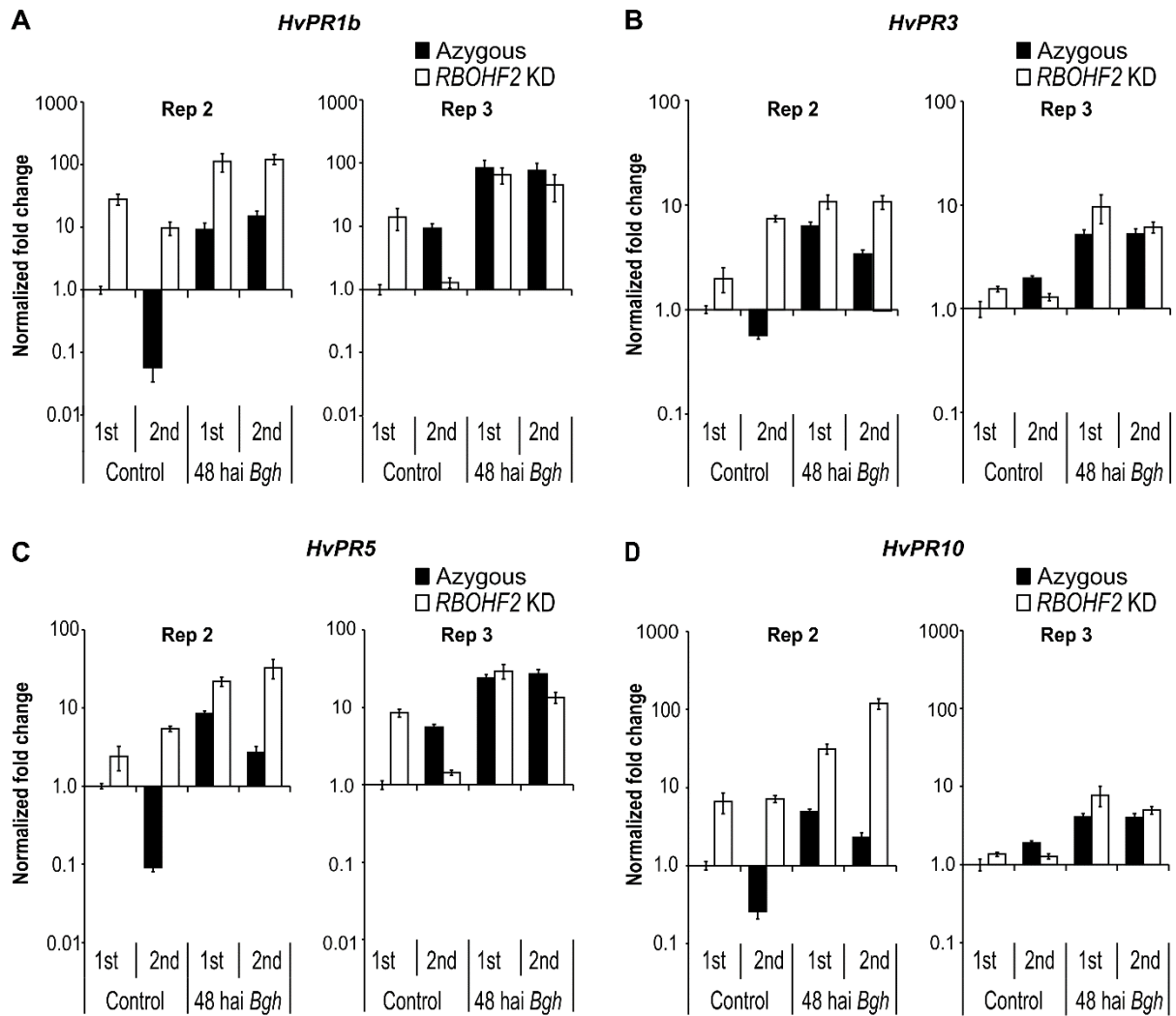
Supplementary Fig. S18: Transcript levels of selected genes in transgenic barley leaves. Total RNA from leaves of 11-days-old seedlings was extracted from a pool of three to four leaves each of azygous (AZ) and *HvRBOHF2* knock down (KD) line E08. Pictures show inverted photographs of ethidium-bromide-stained 1% agarose-gels after electrophoresis of RT-PCR products. The barley MONOUBIQUITIN-LONG-TAIL FUSION 1 (*HvMub1*) gene as used as internal control. The experiments were repeated two times with similar results.



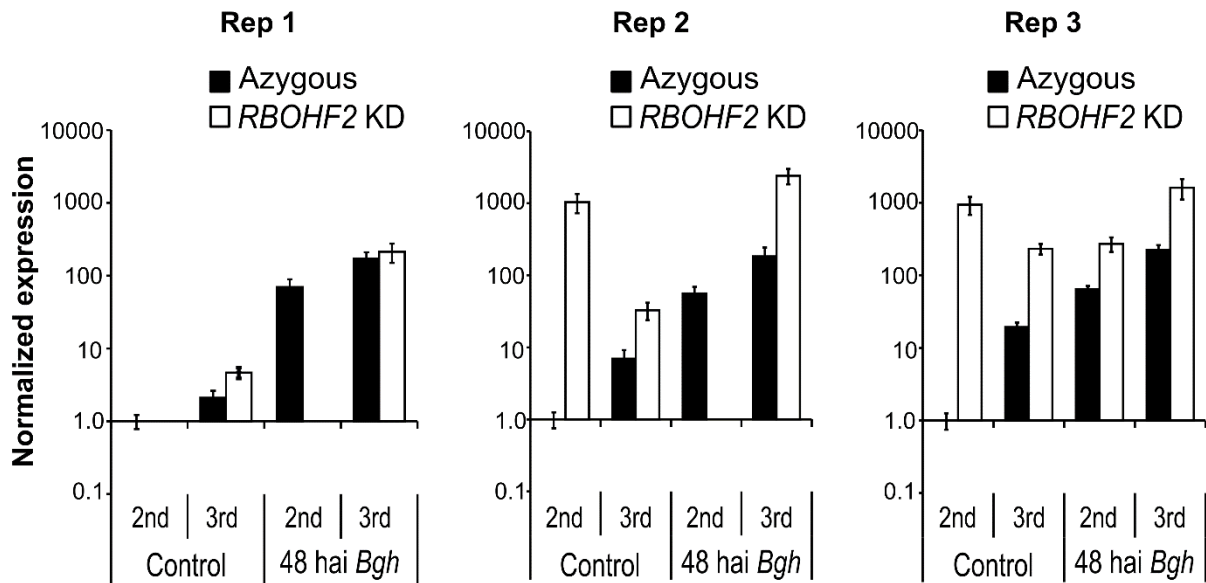
Supplementary Fig. S19: Expression of cell death regulators genes in two further independent experiments. Relative expression levels of barley *HvMlo* (A), *HvBI-1* (B), *HvLSD1a* (C) and *HvCBC04043* (D) in first and second leaves of *HvRBOHF2* KD line E08 and the azygous control. Total RNA was extracted from a pool of three to four leaves of barley plants 48 hai from non-inoculated or *Bgh*-inoculated leaves. The cDNA was synthesized and afterwards subjected to real-time PCR analysis. Expression of the genes was measured relative to the expression of the reference gene barley MONOUBIQUITIN-LONG-TAIL FUSION 1 (*HvMub1*). Error bars show confidence intervals of the means at $P = 0.05$ of three technical replicates.



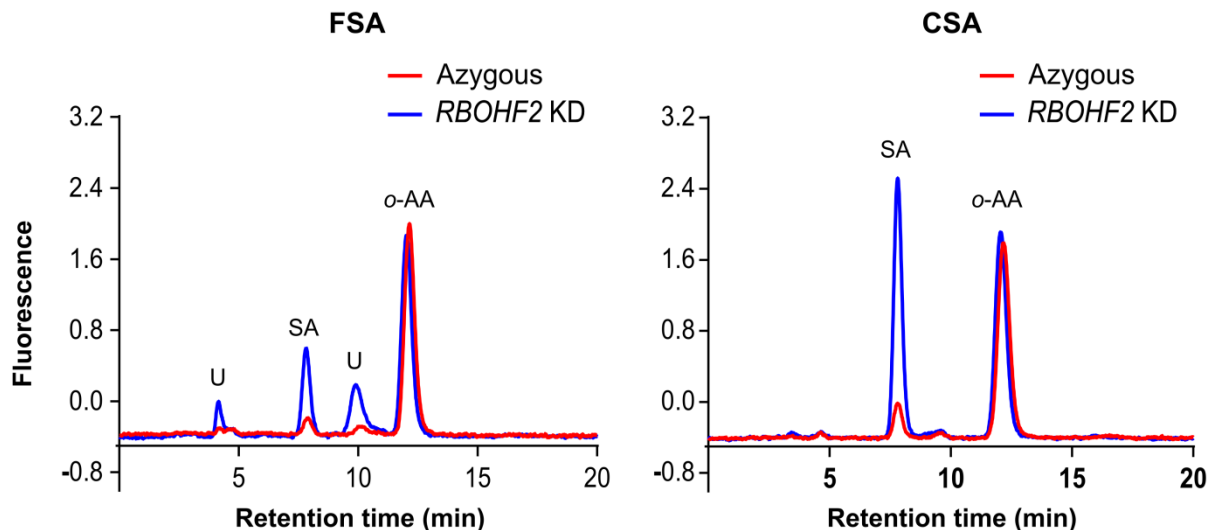
Supplementary Fig. S20: Expression of genes related to carbohydrate catabolism in two further independent experiments. Relative expression levels of barley *HvCwiINV3* (A) and *HvADH1* (B) in first and second leaves of *HvRBOHF2* KD line E08 and the azygous control. Total RNA was extracted from a pool of three to four leaves of barley plants 48 hai from non-inoculated or *Bgh*-inoculated leaves. The cDNA was synthesized and afterwards subjected to real-time PCR analysis. Expression of the genes was measured relative to the expression of the reference gene barley MONOUBIQUITIN-LONG-TAIL FUSION 1 (*HvMub1*). Error bars show confidence intervals of the means at $P = 0.05$ of three technical replicates.



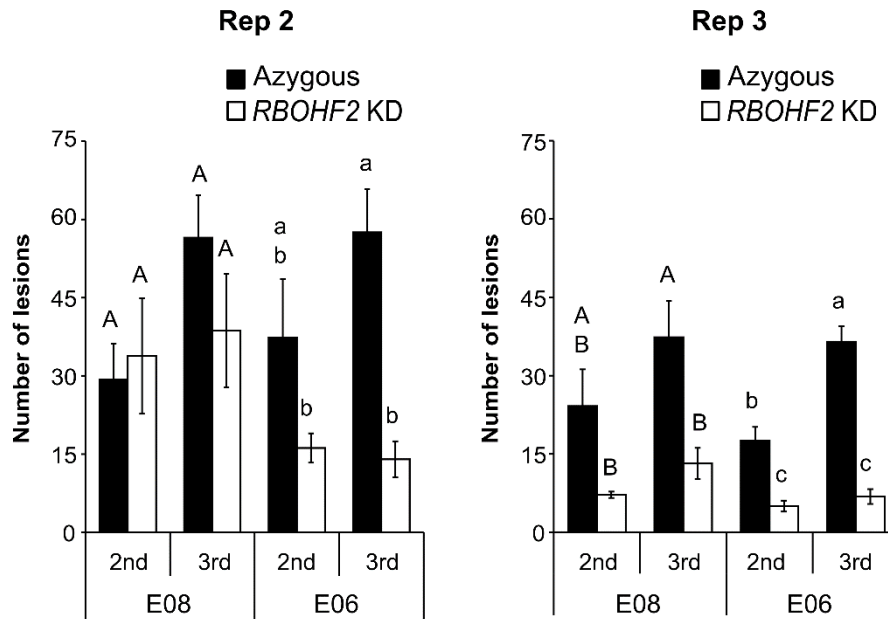
Supplementary Fig. S21: PATHOGENESIS-RELATED (PR) genes expression in two further independent experiments. Relative expression levels of barley *HvPR1b* (A), *HvPR3* (B), *HvPR5* (C) and *HvPR10* (D) in first and second leaves of *HvRBOHF2* KD line E08 and the azygous control. Total RNA was extracted from a pool of three to four leaves of barley plants 48 hai from non-inoculated or *Bgh*-inoculated leaves. The cDNA was synthesized and afterwards subjected to real-time PCR analysis. Expression of the genes was measured relative to the expression of the reference gene barley MONOUBIQUITIN-LONG-TAIL FUSION 1 (*HvMub1*). Error bars show confidence intervals of the means at P = 0.05 of three technical replicates.



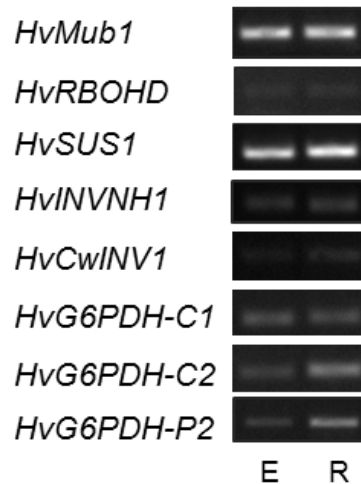
Supplementary Fig. S22: *PR1b* gene expression in 17-day-old barley transgenic plants. Relative expression levels of barley *HvPR1b* in second and third leaves of *HvRBOHF2 KD* line E08 and the azygous control. Total RNA was extracted from a pool of three to four leaves of barley plants 48 hai from non-inoculated or *Bgh*-inoculated leaves. The cDNA was synthesized and afterwards subjected to real-time PCR analysis. Expression of the genes was measured relative to the expression of the reference gene barley MONOUBIQUITIN-LONG-TAIL FUSION 1 (*HvMub1*). Error bars show confidence intervals of the means at $P = 0.05$ of three technical replicates. No RNA of good quality were obtained from second leaves of *HvRBOHF2 KD* plants in the first and second replicates.



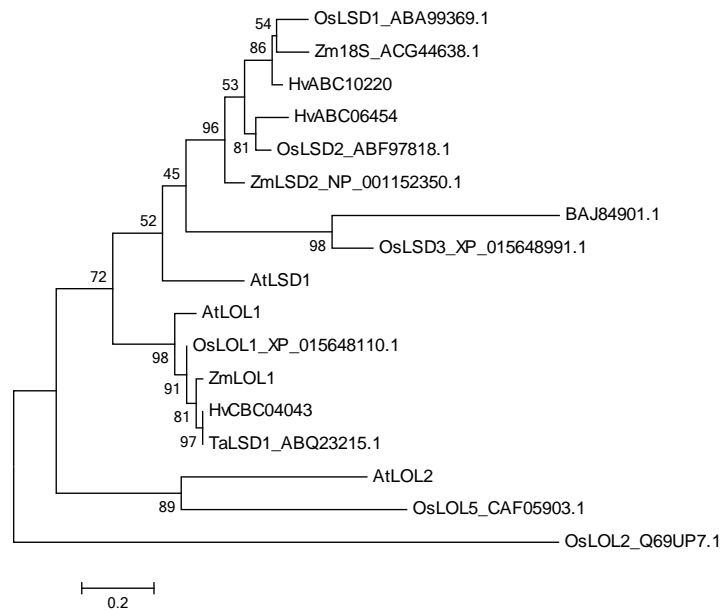
Supplementary Fig. S23: Exemplary HPLC chromatograms of barley first leaf methanol extracts. A) Free and (B) conjugated levels of SA in first leaf of 17-day-old plants of the *HvRBOHF2 KD* line E08 and the azygous control. SA was extracted from a pool of four to five leaves of barley plants 24 hai from non-inoculated or *Bgh*-inoculated leaves. FSA, free salicylic acid; CSA, conjugated salicylic acid; SA, salicylic acid; *o*-AA, *o*-anisic acid; U, unknown.



Supplementary Fig. S24: Effect of the silencing of *HvRBOHF2* in the susceptibility to *B. sorokiniana* in two further experiments. Number of *Bs*-induced lesions per leaf in 17 day-old-barley *HvRBOHF2* KD lines E08 and E06 and the azygous controls. Plants were spray-inoculated with *Bs*, incubated for 96 hours in a climate chamber and individually harvested. Lesions were quantified in fixed leaves under a stereomicroscope. Error bars show standard errors of the mean of six leaves per line. Uppercase letters show the grouping of data sets relative to line E08 and lowercase to line E06 according to Tukey's test at $P = 0.05$.



Supplementary Fig. S25: Tissue-specific gene expression of *HvRBOHD* and genes related to sucrose metabolism. Total RNA was isolated from 9-day-old barley cv. Golden Promise leaves. The abaxial epidermal peels (E) and the remaining leaf tissue (R) were used. The barley MONOUBIQUITIN-LONG-TAIL FUSION 1 (*HvMub1*) gene as used as internal control. Pictures show inverted photographs of ethidium-bromide-stained 1% agarose-gels after electrophoresis of RT-PCR products. The experiment was performed once.



Supplementary Fig. S26: Phylogenetic analysis of plants LSD1-like genes. The full-length amino acid sequences of LSD1-like from Arabidopsis (At), barley, maize (Zm), rice (Os) and wheat (Ta) were aligned with ClustalW (Thompson *et al.*, 1994) using the BLOSUM 30 protein weight matrix with a gap opening penalty of 10 and a gap-extension penalty of 0.05. BAJ84901 represents an additional barley LSD1-like gene found in a BLASTP search at the NCBI GenBank against the *H. vulgare* database using the protein sequences of Arabidopsis AtLSD1. Notable, similar to AtLOL2, the new orthologue displayed two LSD1-like zinc finger motif instead of three and it is a closer homologue of AtLSD1. Evolutionary analyses were conducted in MEGA6 (Tamura *et al.*, 2013) using the Maximum Likelihood method based on the JTT matrix-based model and tested with a bootstrap of 1000 replications.

AtCwINV1	MTK-----EVCSNIGLWLLLLTLLIGNYVVNL-----EAS--HHV----YK-R-LT	37
HvCwINV1	MLOCMSTRP-----	14
BAK07035.1	MLOCMW--NPLWSVGPWLLL-----LLLQL-----AGA---S---IH-GSME	33
ZmCwINV1	---MGTRPRGVVLAPWAVVLV--LALRL-----AGA--SHV---IH-RSLE	37
OsCwINV1	---MG--TRLALAPWLLL-----LLLQL-----AGA--SHV---VH-RSLE	31
HvCwINV3	MLOCMG--TPKWWVVAPLALL-----LLLQL-----AGA--SHD---VR-RSLE	36
Q70AT7.1	-MAQAW---AFLLLPLALALASYASHLLLLPAYITTPLCGGGDGARSFFLCAQAPKDQ---	52
BAK08333.1	MAQSSW---ALFLL-----LALFSSLLVCSSNG--ERVFLYPQ---S---	35
BAJ87518.1	-----AWPCSNGG--PFFFCSQS---S---	17
BAJ93390.1	MAKTNS---SFVSSP-----SSPPIGKPTTIAFVF---SLSSSPLR	35
HvCwINV2	MA-----RLPLA-ACIVAFHLCLLLLPSSSLR	26
β-fructosidases motif		
AtCwINV1	---QSTNTKSPSVNQPYRTGFHFQPPKNWMDPNGPMIYKGIYHLFYQWNPKGAVW----	90
HvCwINV1	RRRRRPLCRLRFSTPSSLTGYHFRPIKNWINDPNAPMYYKGYHLFYQYNPKGAVW----	70
BAK07035.1	AVAPLPSPVNFVTNPLLRTGYHFQPPKNWINDPNGPLYKGYHLFYQYNPRGADW----	89
ZmCwINV1	AEAA-PSVPASIVSPLLRTGYHFQPPMNWINDPNAPLYYKGYHLFYQYNPKGAVW----	92
OsCwINV1	AEQAPSSVPASIVSPLLRTGYHFQPPMNWINDPNGPLYKGYHLFYQYNPKGAVW----	87
HvCwINV3	AEAATPSVPASILSPLLRTGYHFQPPMNWINDPNGPLYKGYHLFYQYNPKGAVW----	92
Q70AT7.1	-----DQDPSASTMYKTAFAHFQPAKNWMDPSGPMYFNGIYHEFYQYNLNGPIF----	102
BAK08333.1	-----QKVSSIVSQRYRTAYHFQPPKNWINDPNGPMYNGIYHEFYQYNPNGSVW----	85
BAJ87518.1	-----TKVPSIVSQRYRTAYHLQPPKNWINDPCGPMYNGIYHEFYQYNPDGSEFNPTS	71
BAJ93390.1	T-MD-----GLEHPRNGRTAYHFQPAKFWQNDPNGPLYHNGMYHFFYQYNPHGATWGD--	87
HvCwINV2	R-LSEAESSLVRHGVGIRPAYHFMPAKNWQNDPNGPMYHNGVYHMFYQYNPLGAMWSP--	83

WSGSAT motif

AtCwINV1	GNIVWAHSTSTDLINWDPHPAIFPSAPFDINGCWSGSATILPNGKPVILYTGIDP-K--	147
HvCwINV1	GNIVWAHVSVRDLINWVALETAIQPSIKSDKYGCWSGSAXILRDGTPAIMYTGIDR-ADI	129
BAK07035.1	VNTLWAHVSVRDLINWNLGLALEPSIRPKDYGVWSGSATILLDGTTPVLVYTGIDR-QDI	148
ZmCwINV1	GNIVWAHVSVRDLINWVALEPAIYPSIPSDKYGCWSGSATILEDGTPAILYTGIDR-ADI	151
OsCwINV1	GNIVWAHVSQDLINWIALEPAIKPDIIPSDQYGCWSGSATILPDGTPAILYTGIDR-PNI	146
HvCwINV3	GNIIWAHVSVRDLINWMALEPAIKPSIPTDQYGVWSGSATILPDGTPAMLYTGIDR-PGT	151
Q70AT7.1	GDIVWGHVSVDLNVNWI GLEPALVRDTPSDIDGCWTGSGV TILPGGKPVIIYTGIDR-N--ID	159
BAK08333.1	GNIVWGHVSVDLINWIPLETAIERDTPSDINGCWTGSGATILPGNRLVIIYTGIDR-D--PE	142
BAJ87518.1	LNIVWGHVSVDLNVNWI TLEPAIEPDPNDIKGCWSGSATIVSGDQPVIIYTGIDR--IE	129
BAJ93390.1	GTLSWGHSVSGDLVNWADVGNALDPTSPFDANGCWSGSATVLPGGRPAIYTGIDR--AN	144
HvCwINV2	GNLSWGHVSVRDLVNWDAALDPTAPFDSDGCWSGSATILPGGIPALYTGIDRINATNK	143

RDP-motif

AtCwINV1	NQQVQNI AEPKNLSDPYLREWKK-PLNPLMAPDAVNGINASSFRDPTTAWLGQDKKWRV	206
HvCwINV1	NYEVQNI AEPKNLSDPYLREWKK-RGNPI IVP-EG-GINATQFRDPTTAWYA-DGHWR	185
BAK07035.1	PYQVQNI AEPKNLSDPYLREWKK-DYNPI IVP-ES-GMNVQFRDPTTAWHI-DGQWR	204
ZmCwINV1	NYQVQV LALPKDASDPLLEWEKPEEYNPVATP-AAGGINATQFRDPTTAWRH-AGHWR	209
OsCwINV1	NYQVQNI AEPKNLSDPYLREWKK-AYNPVATP-EP-GMNATQFRDPTTAWYA-DGHWR	202
HvCwINV3	NYQIQNI AEPKNLSDPYLREWKK-GYNPI IAVP-EA-GMNATQFRDPTTAWHAGDGLWR	208
Q70AT7.1	QHQTQNI AEPKNLSDPYLREWKA-ANNPVL RPD-EPGMNVI EFRDPTTGWIGPDGHWR	217
BAK08333.1	KRQVQNI VVPKNLSDPYLRWTKA-VNNPVIQPV-GPGLNSGQFRDPTTGWIGPDGLWR	200
BAJ87518.1	KHQVQNI ALPKNRSDPYLRWTKA-GNNPVIQSG-VPGLNSGQFRDPTTGWIGPDGLWR	187
BAJ93390.1	RVQVQNV AFAKNPADPDLLEWEKP-DCNPVMPM--PADVTGNFRDPTTEAWRGRDGLWR	201
HvCwINV2	EVQVQNV AEPKNPADPDLLEWEKP-AYNPVIPL--PADVPGDKFRDPTTAWVGRDGLWR	200

:: . * . : : *

acid/base catalyst

AtCwINV1	IIGSKIHR---RGLAITYSKDFLKEKESPELHYDDGSGMWECPDFFPVTRFGSN---G	260
HvCwINV1	LIGALSGA--SRGVAYVRSRDFMRWTRVRKPLHS-APTGMWECPDLYPVTADGRHRHKG	242
BAK07035.1	LVGGEKGS---QQQAYVYRSTDFKHWRRAKHPLHS-AINGMWECLDFFPVLMQGK---KG	257
ZmCwINV1	LVGSVRGA---RGMALVYRSRDFRKTWRAKHPLHSALTGMWECPDFFPVSGPGLQ--AG	264
OsCwINV1	LVGGLKGA--RLGLAYLYRSRDFKTWRAKHPLHS-ALTGMWECPDFFPLQAPGLQ--AG	257
HvCwINV3	LVGGLKPGT-LRGMALYRSRDFKHWRRAKHPLHS-ALTGMWECPDFFPVREP GHP--GG	264
Q70AT7.1	AVGGELN---GYSAAALYKSEDFLNWTKVDHPPYSHNGSNMWECPDFFAAL-PGNN--GG	271
BAK08333.1	AVGAELN---GDSAAALYKSKDFLNWTRVDHPLYSSNSSMWECPDFFAVL-PGNS--GG	254
BAJ87518.1	AVGAELN---GYGAALYKSEDFLNWTRVDHPLYSSNGTRMF ECLDFFPVLP-PGSD--NG	241
BAJ93390.1	GIVAEVGGV---GSLLVYRSADFLRWERNAAPLHASD-VPVLECPDLFPMAPPGVA--EG	255
HvCwINV2	AVAAKVGINGIASTLIYRSKDFRQWKRNAMPLYTSRAAGMVECPDLFPVAEPGVE--EG	258

. * * * * : * : * * * : * *

AtCwINV1	VETSSFGEPEILKHVLIKISLDDTKHDYTYTIGTYDRVKDKFVDPDNG----FKMDGTAPRY	316
HvCwINV1	LDTSV--VSGPRVKHVLKNSL DLR RYDYTYTIGTYDRKTERYVPDNP----AGD-EHHLRY	295
BAK07035.1	LDTY---EHSARVKYVLKSSLEKAR YDYTYTIGTYDNRTESYVPDDL----NGD-YHRLRY	309
ZmCwINV1	LDTSV--A--PGTKYVLKSSL DLT RYDYTYTIGSYDGGKDRYYPDDP----AGDYHHRRY	315
OsCwINV1	LDTSV--V--PSSKYVLKNSL DLT RYDYTYTIGIYKVTERYVPDNP----AGD-YHRLRY	307
HvCwINV3	LDAS--EFGPHYKYVLKNSL DLT RYDYTYTIGTYNNRTERYVPDNP----TGDVYQRLQY	317
Q70AT7.1	LDLSA--AIPQGAHALKMSVD--SVDKYMIGVYDLQRDAFVDPDNP----VDDRRLWLRM	323
BAK08333.1	LDLST--AIPNGAKHVLKMSLD--SCDKYMIGVYDLKSDTFIPDTV----LDDRRLWSRI	306
BAJ87518.1	LDMSS--TIPYGAKHVLKMGNF--FQDVMIGVYDLKRDFAFVDPDIV----LDDSRWLWRI	293
BAJ93390.1	LDVSA---SGAGVLHVLKLTDF A-KEDHYMVGRYDDEADTFVPAEPER--GGDPGNWRR	309
HvCwINV2	RLGTA--SGAVPVRHVLKLSV MNT TVDYAVGRYDDVADTFVPEVDGERSVDDCRRWRF	316

: ** * * * * : : * :

AtCwINV1	DYGKYYASKTFYDPAKRRRILGWWTNESSVEDDVEKGWSGIQTIPRKIWLDRSGKQLIQ	376
HvCwINV1	DYGNFYASKTFYDPAKRRRILGWANESDAAVDDVAKGWAGIQAIPRKVWLDPSGRQLMQ	355
BAK07035.1	DYGKYYASKTFYDPAKQSRVILGWANESDTPDDIAKGWSGIHAIPRKIWLDPGGKQLVQ	369
ZmCwINV1	DYGNYYASKTFYDVERRRVLLGWANESDTPDDKAKGWAGIHAIPRKIWLDPGKQLLQ	375
OsCwINV1	DYGNFYASKTFYDPAKRRRILGWANESDTPYDPAKGWAGIHAIPRKVWLDPSGKQLLQ	367
HvCwINV3	DYGNFYASKTFYDPAKRRRILGWANESDTPVAHNAKGWAGIHAIPRKIWLDPGKQLLQ	377
Q70AT7.1	DYGTFFYASKSFFDSKKGRRIVWGSGETDPSDDLAKGWAGLHTIPRTIWLADGKQLLQ	383
BAK08333.1	DYGNFYASKSFFDSKKGRRIIWGWNTDSSDDVAKGWAGIHAIPRTIWLADIHGKQLLQ	366
BAJ87518.1	DYGNFYASKTFYDPAKRRRILGWANESDTPVAHNAKGWAGIHAIPRTIWLADGKQLLQ	353
BAJ93390.1	DHGHLYASKSFFDGRNRRVLAWVDENDG--GGVARGWAGIQAIPRAIWLADGKRLVQ	367
HvCwINV2	DYGHVYASKSFFDSRKNRRVLAWSASESDNSNDLARGWSGVQIVPRKVWLDGDKQLRQ	376

* * * * * : * * * * : * * * * * : * * * * *

AtCwINV1	WPVREVERLRTKQVKNLRNKVLKSGSRLEVYGVTAQAQADVEVLFKV-----RDLEKADV	430
HvCwINV1	WPVEELEALRGKRPVSIKNRVVKRGEHVEVTGLRTSQADVEVSFEV-----ASIDGAEA	409
BAK07035.1	WPIEEVEQLRRK-SVSVTNKVVKPGDHFVEVKGLETYQADVEVTFKI-----RSLERAEP	422
ZmCwINV1	WPIHEVEKLRGK-AVSVDAKLKPKGDHFVEVTGIATYQADVEVSFELELEAGTSLLEKAEA	434
OsCwINV1	WPIEELETLRGK-SVSVFDKVVKPGEHFQVTGLGTYQADVEVSLEV-----SGLEKAEA	420
HvCwINV3	WPVEELEQLRGK-AVSVGDKVVKPGQHFVEVTGLQSYQSDVEVSFEV-----ASLDKAEAP	430
Q70AT7.1	WPVEEIESLRTNEI-NHQGLELKNKGDLEFIKEIVDAFQADVEIDFEL-----ASIDEAEP	436
BAK08333.1	WPVEEVESLRGNEI-NHQGLELKKGGLEFIKGDADFQADVEIDFEL-----TSIDKADP	419
BAJ87518.1	WPVEEIKSLRRNEI-NHHELELKKGDLEFDIKGIDTLQADVEIDFEL-----ASIHADAP	406
BAJ93390.1	WPIEEIETLRRKRVLQWATEVEAGGRKEIAGIVSSQADVEAVFEI-----PNLEEAEET	421
HvCwINV2	WPIEEIERLRSKRIVGMLGAQVNVAGGVNKIVGV-GAQAADVEAIFEI-----PSLEEAEET	429
	:.*: : ** : :: * .: *:* ::: .: *:	
AtCwINV1	IEPSWT-DPQLICSKMNVSVKSGLPGFGLMVLASKNLEEYTSVYFRIFKARQN----SNK	485
HvCwINV1	LDPALANDAQKLCMRGAHVEGGVGPFGWLVLASSKLEEKTAVFVFRVFKAARNINSTNNK	469
BAK07035.1	FDQAFSDDAQKLCRMKGADKKGGVGPFGWLVLASANLEEKTVVFRVFKDG-----HGK	476
ZmCwINV1	FDPAYDDDAQKLCGVKGADARGGVGPFGWLVLASADLQERTAVFVFRVFRDG-----HGK	488
OsCwINV1	LDPAFGDDAERLCCGAKGADVRGGV-VFGLWVLASAGLEEKTAVFVFRVFKPAG----HGAK	475
HvCwINV3	FDPAYANDAQKLCGMKNADAKGGVGPFGWLVLASADLAEKTAVFVFRVFKDG-----YGK	484
Q70AT7.1	FDPSSLDLPEKHCEAGASVPGGIGPFGLVVLASDNMDEHTVYFRVYKSQ-----EK	489
BAK08333.1	FDPSSLDLPEKHCEAGASVNGGIGPFGLVVLASDNMEEHTAVHFRVYKSE-----QK	472
BAJ87518.1	FDPSSLFDTPQKHCREADASVHGGIGPFGLVVLASDNMEEHTVHFRVYKSQ-----KN	459
BAJ93390.1	LDPKWLQDPKGLSAEMGASGHGGVGPFGLLVLASGDLEHTAVFVFRVFKHD-----GK	474
HvCwINV2	FQPNWLLPEQNLCAEKGASVPGGVPFGLLVMASGDLQEHTAIFFRVFRHD-----QK	482
	:: : : .. : *** : ** : * * : . * : : :	
AtCwINV1	YVVMCSDQSRSSLKEDNDKTTYGAFVDIN--P-HQPLSLRALIDHSVVESFGGKGRACI	542
HvCwINV1	PVVLMCSDPTMSSLNPNLYKPTFAGFVDTDIA--KGI SLRSLIDRSVVESFGAGGRTCI	527
BAK07035.1	PVILMCTDPTMSSLGRDLKPYAGFVNADISS--SGQISLRSLIDHSVVESFGAGGRTCI	535
ZmCwINV1	PKVLMCTDPTKSSLSPLDYKPTFAGFVDADIS--SGKITLRSLLIDRSVVESFGAGGKTCI	546
OsCwINV1	PVVLMCTDPTKSSLSPLDYKPTFAGFVDTDIS--SGKISLRSLIDRSVVESFGAGGKTCI	533
HvCwINV3	PLVLMCSDPTKSSLTPGLYKPTFAGFVDTDIS--SGKISLRSLIDRSVVESFGAGGKTCI	542
Q70AT7.1	YVLMCSDLRRSSLRPGLEKPYAGGFFFDLAK-ERKISLRSLIDRSVVESFGGGRVCI	548
BAK08333.1	YMLLMCSDLRSSLRAGLYTPAYGGFFFDLEK-EKKISLRSLIDRSVVESFGGGRVCI	531
BAJ87518.1	YMLLMCSDLRSSLVTPGLDTPAYGGFFFDLEK-ERKISLRSLIDRSVVESFGGGRVCI	518
BAJ93390.1	YKVLMTDLTRSSRKEGINKPSYGAFLDVDVEK-DRISLRSLIDHTVVESFGDGGRTCM	533
HvCwINV2	YKVLMTDLTRSSGRDKVYKSPYGGFVDIDIEQHGRSISLRSLIDHSVVESFGGGRTCI	542
	:***:* * : . : . * : : :***:* : : . ***** * : * :	
AtCwINV1	TSRVYPKLAIGK--SSHLFAFNYGYQSVLDVNLNNAWSMNSAQIS-----	584
HvCwINV1	LSRVYPTLALGK--NARLHVFNNGKVDIKVSELTAWEMKKPALMNGA-----	572
BAK07035.1	ISRVYPSIAIGK--NAHLHVFNNGDVIDIKVSRLTAWEMESSKMNSV-----	580
ZmCwINV1	LSRVYPSIAVGK--DAHLYVFNNGEVDVTVSGLTAWEMKKPLMNGA-----	590
OsCwINV1	LSRVYPSMAIGD--KAHLYVFNNGEADIKISHLKAWEMKKPLMNGA-----	577
HvCwINV3	LSRVYPSMAIGK--DAHLYVFNNGETDIKVSQKAWEMKKPMMNGA-----	586
Q70AT7.1	TSRVYPAVLAN-VGRAHIYAFNNGNAMVRVQPQLSAWTRKAQVNVVEKGSWAI-----	599
BAK08333.1	MARVYPAVVDG--VAHMYAFNNGSTTVRVQPQLRAWSMRRAQVNVVKGMV-----	578
BAJ87518.1	MARVYPSLVDDHQPLMYAFNNGSATLVRVPRLRAWSMRRAQMSV-----	563
BAJ93390.1	TARVYPEHAATG--SSRLYAFNYGAGAVKSKLEAWELATAAVNGGGAM-----	580
HvCwINV2	TARVYPQHAENK--NSHVVFVNNGTGLVKVSKLEAWRLATAAVNVVHGRLP-----	592
	:*** : . * * * : : * * : : :	

Supplementary Fig. S27: Sequence alignment of CwINV proteins. The full-length amino acid sequences of CwINVs from *Arabidopsis thaliana* (At), barley (Hv), maize (Zm) and rice (Os) were aligned with Clustal Omega (Sievers *et al.*, 2011) using default parameters. Identified conserved features are highlighted and include WMNDPNG (β -fructosidases motif), WSGSAT, FRDP and WECF (acid/base catalyst) motifs. The “catalytic triad” (Asp23/22, Asp149/147 and Glu203/201), indispensable for binding and catalysis (Lammens *et al.*, 2009), is shown in red. Conserved amino acids in the vicinity of the active site of CwINVs are shown in green and include the Asp239 / Asp 242 or Asp239 / Lys242 couple, Trp82 and Ile101 (Van den Ende *et al.*, 2009). Conserved amino acids differing between cell-wall invertases and vacuolar invertases were shown in blue and include Pro in the WECF motif, Gly in the KGWSG motif and Gly in the FNNG motif (Ji *et al.*, 2005).

ACKNOWLEDGEMENTS

Here, I would like to take the opportunity to express my sincere gratitude to all those who encouraged, helped and supported me during this challenging, but rewarding PhD time.

First, I would like to thank the Brazilian government and the National Council for Scientific and Technological Development (Conselho Nacional de Desenvolvimento Científico e Tecnológico [CNPq]) for financial support. I thank also Prof. Olinto Liparini Pereira and Prof. Maria Catarina Megumi Kasuya for all the support and guidance during my studies at Federal University of Viçosa (Brazil) and for the encouragement to do my PhD abroad.

I would like to express my deepest gratitude to Prof. Dr. Ralph Hückelhoven for giving me the opportunity to perform my PhD thesis in Germany. I am very grateful for all support, knowledge sharing and encouragement. Working in his team has benefited me on a professional as well as on a personal level. I really appreciate every little thing I have learnt through all these years.

I wish to thank Prof. Dr. Jörg Durner for taking over as the chairperson and Prof. Dr. Wolfgang Oßwald for taking over as my second reviewer of my thesis examination committee.

Special thanks go to Dr. Reinhard Pröls for the guidance, advice and patience. I am very grateful for his help during my entire PhD. Furthermore, I feel deeply indebted and thankful for the time and effort he put into proofreading my thesis. I also thank Dr. Harald Schempp for the help with the salicylic acid and chlorophyll content measurement and for the nice ROS-chats.

Thanks to all current and former staff members of the chair of Phytopathology for the nice work environment, willingness to help and kindness. My sincere gratitude goes to Angi, Johanna and Carolin for the technical assistance and to Regina and Michael for providing the *Bipolaris* isolate. Also, many thanks to Traudl and Claudia for help with administrative matters and German bureaucracy. I want to thank the PhD candidates and post docs for all the amusing "Stammtische". Besides this, I am very thankful to Lars for the many hours he spent reading and correcting my thesis. I greatly appreciate his advice, encouragement, support and kindness in the last phase of my PhD.

Thank all my dearest friends, especially Cléssio, Deizi and Eduardo for the encouragement, for listening to my problems and helping me with to find solutions and for bringing a bit of Brazil to Germany.

Last but not at least, I would like to thank my family for the love, patience and encouragement during my whole life.

CURRICULUM VITAE**Persönliche Daten**

Name: Denise Pereira Torres
Geburtsdatum: 18. October 1987
Geburtsort: Januária, Brasilien

Studium und Beruf

08/2013 – heute: Doktorandin (CNPq/DAAD-Stipendiatin)
Lehrstuhl für Phytopathologie
Technischen Universität München

02/2011 – 02/2013: Magister Scientiae der Phytopathologie
Lehrstuhl für Phytopathologie
Universidade Federal de Viçosa, Brasilien

05/2006 – 10/2010: Bachelorstudiengang Agrarwissenschaften
Universidade Federal de Viçosa, Brasilien

Schulbildung

2001 – 2003: Sekundarstufe
Centro Federal de Educação Tecnológica de Januária
Januária, Brasilien